Illuminating Epithelial-Stromal Communication Using Engineered Synthetic Matrix Microenvironments

by

Christi Dionne Cook

B.S., Biochemistry
Indiana University, Bloomington (2011)

Submitted to the Department of Biological Engineering in partial fulfillment of the requirements for the degree of

Doctor of Philosophy in Biological Engineering
at the
MASSACHUSETTS INSTITUTE OF TECHNOLOGY

February 2018

Author. . . . . Signature redacted . . . . . .
Department of Biological Engineering
November 17, 2017

Certified by. . . Signature redacted . . . . . .
Linda G. Griffith
S.E.T.I. Professor of Biological and Mechanical Engineering
Thesis Supervisor

Accepted by. . . . . Signature redacted . . . .
Mark Bathe
Chair, Graduate Program Committee

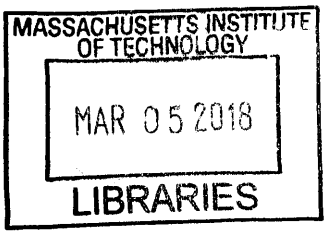

ARCHIVES

The following committee has evaluated this doctoral thesis:

Professor Linda Griffith
Thesis Supervisor
Department of Biological Engineering
Department of Mechanical Engineering
Massachusetts Institute of Technology

Professor Darrell Irvine
Chairman, Thesis Committee
Department of Biological Engineering
Department of Materials Science and Engineering
Massachusetts Institute of Technology

Professor Douglas Lauffenburger
Member, Thesis Committee
Department of Biological Engineering
Department of Biology
Massachusetts Institute of Technology

Professor Kevin Osteen
Member, Thesis Committee
School of Medicine
Vanderbilt University

Illuminating Epithelial-Stromal Communication Using Engineered Synthetic Matrix Microenvironments

by
Christi Dionne Cook

Submitted to the Department of Biological Engineering on November 17, 2017, in partial fulfillment of the requirements for the degree of Doctor of Philosophy in Biological Engineering

Abstract

Mucosal barrier tissues are prominent targets for drugs against infection and chronic inflammatory disorders. One such mucosal barrier tissue, the endometrium, undergoes monthly cyclic remodeling via hormone-mediated growth, immune cell recruitment and proteolytic breakdown. Hormone response disruption has been associated with numerous endometrial pathologies, including endometriosis, adenomyosis, and infertility, which impacts upwards of 10% of women during their reproductive years. Currently, our understanding of endometrial biology is limited by the ability to replicate complex 3D physiology *in vitro*. Our ability to parse disease mechanisms and test efficacy of therapeutic interventions relies on development of reproducible models, adaptable to the limited numbers of cells available from patient biopsies. In this thesis, I address a critical gap in accessible tools to study and control endometrial biology *in vitro* and do so in a manner that can be translated to other epithelial-stromal mucosal tissues.

Using the endometrium as an example mucosal barrier, I first establish design principles for the development of a synthetic, modular extracellular matrix (ECM) hydrogel suitable for 3D functional co-culture of epithelial and stromal cells. This 'one-size-fits-all' matrix features components that can be remodeled by cells and that responds dynamically to sequester local cell-secreted ECM characteristic of each cell type enabling long-term, hormonally responsive co-cultures. Next, I establish methods to expand and cryopreserve primary human endometrial epithelial cells, which maintain barrier and secretory function, further enabling studies using primary cells. Finally, we use data-driven network modeling of secreted proteins to understand how variation in cytokine signaling may alter hormone responsiveness and proteolytic remodeling in primary epithelial-stromal co-cultures. With the ability to create and parse more complex 3D tissue models using primary cells to recapitulate healthy and diseased states, we further enable basic understandings of disease pathologies and subsequent drug discovery efforts aimed at inflammation, wound healing and immune modulation.

Thesis Supervisor: Linda G. Griffith
Title: S.E.T.I. Professor of Biological and Mechanical Engineering

Acknowledgements

I'm thankful for the opportunity I had to develop as a research scientist under the guidance of Prof. Linda Griffith. Her visionary perspectives on the integration of tissue engineering and systems biology have created a truly interdisciplinary and exciting lab environment in which to conduct research. I'm grateful for the opportunity to have TA'd for Prof. Darrell Irvine, my thesis chair. His biomaterials class provided invaluable scientific perspective for my thesis and his professional and practical guidance offered as thesis chair was a constant source of support. I would like to thank Prof. Kevin Osteen and Dr. Kaylon Bruner-Tran for providing invaluable scientific perspective on endometrial biology and phenotypic evaluation of endometrial cells, and of equal importance perspective on work/life balance. Finally, I'm incredibly grateful to Prof. Douglas Lauffenburger for scientific guidance, and most importantly, for his commitment to foster a rigorous, inclusive, and supportive culture in the Biological Engineering Department, which is evident in everything he does.

It is with immense gratitude that I recognize my previous research mentors and teachers, Prof. Peter Ortoleva at Indiana University and Dr. Rasha Hammamieh at USACEHR, who welcomed me into their labs as an undergraduate and provided crucial research experiences that shaped my ultimate decision to pursue a PhD. I'm especially grateful to Peter for providing candid, fatherly advice and encouraging me to apply to MIT. My inspiration to pursue a career in research came as a direct result of the strength, mentorship and passion for knowledge displayed by several former middle and high school math and science teachers, especially including Teresa Cook, Leslie Knight and Holly Harlow.

My time at MIT has been immeasurably shaped by my interactions with Dr. Michael Beste whose example of scientific rigor and thoughtful mentorship, I strive to carry forward in my future endeavors. I'm thankful to the incredibly intelligent, supportive and detail-oriented technicians that I was fortunate enough to work with as part of the DARPA Microphysiological Systems project including Linda Stockdale, Julia Papps, and Martina deGeus; their dedication and input has been instrumental in realizing this thesis research. During my PhD, I've had the opportunity to mentor many incredibly talented, compassionate and intelligent future scientists and physicians including Margaret Guo, Nursen Ogutveren, Evette Ronner, Catherine Roukhadze, and Charlotte Fonta. I'm immensely grateful for these interactions and look forward to following their future successes.

I'm thankful to the numerous lifelong friends and office mates that have made my time at MIT more enjoyable. Specifically, Abby Hill, Caroline Chopko, Shannon Hughes, Jorge Valdez, Allison Claas, Alex Brown, Samantha Strasser, Sepideh Dolatshahi, Elizabeth Proctor, Brian Joughin and numerous other Griffith and Lauffenburger lab members provided both scientific perspective and great memories. I'm grateful to our hard-working lab manager, Hsinhwa Lee, who has been a motherly figure. I'm especially grateful to the BE Communications Lab and Dr. Annelien Zweemer for her encouragement and critical reading of this thesis.

I'm grateful for the patients that agreed to participate through Newton-Wellesley Hospital and the study and surgical staff past and present, including Dr. Keith Isaacson, Dr. Stephanie Morris, Dr. Nicole Doyle, Dr. Amelia Bailey, Dr. Johanna Renggli-Frey, and Emily Prentice that contributed to the collection of primary donor samples.

I thank the NIH Biotechnology Training Program under the guidance of Prof. Dane Wittrup and Darlene Ray for funding, the opportunity to complete an industry internship, and for creating an interdisciplinary and stimulating scientific community. Dr. John Hambor, Dr. Erick Young and Su-Ellen Brown for welcoming me into their lab at Boehringer Ingelheim and providing scientific and career mentorship.

Finally, this thesis is dedicated to my family whose unconditional support made this achievement possible. I'm thankful for my parents allowing me to dream big and always sacrificing to provide the necessary resources for me to succeed. They continue to provide an unwavering example of what it means to be selfless, persistent, and work hard. I'm thankful to my husband, Dylan, and son, Parker, for their limitless love, patience and support to pursue my dreams.

Contents

List of Figures

Chapter 1.

Chapter 2.

Chapter 3.

Chapter 4.

List of Tables

Chapter 2.

Chapter 3.

Chapter 4.

Chapter 1

1 Introduction

While preclinical safety studies have vastly improved predictive drug toxicity outcomes, over half of new drugs currently fail in Phase II clinical trials due to a failure to establish efficacy in patients.[1,2] Although patient genomic and transcriptomic data is increasingly easier and more cost-effective to acquire, it often provides limited insights into potential disease mechanisms for therapeutic target identification. Chronic inflammatory diseases at sites of epithelial barrier mucosal tissues, such as inflammatory bowel diseases, endometriosis, and asthma often arise from complex etiologies involving disruption of numerous cell and protein signaling networks that cannot be explained by simple genetic abnormalities. Additionally, animal models and basic cell line assays often fail to capture the heterogeneous disease presentations and etiologies seen in diverse patient populations. Thus, drug discovery, especially therapeutic target identification and subsequent evaluations of efficacy in chronic inflammatory disorders, is hampered by a lack of predictive early preclinical models that elucidate dysregulated protein-signaling networks.

More physiologic *in vitro* preclinical models that utilize primary human cells or tissues obtained from clinical biopsies offer promise to advance cost-effective, personalized medicine approaches to enable therapeutic target identification, evaluate patient stratification prior to clinical trial initiation and potentially better predict therapeutic efficacy earlier in drug development. Here, we establish design principles for engineering *in vitro* epithelial barrier mucosal tissues to study inflammatory paracrine signaling and matrix remodeling. This is accomplished using an endometrial barrier mucosal model through a) development of a modular synthetic hydrogel matrix to support long-term 3D function of multiple cell types (Chapter 2), b) methods to expand primary epithelial cells from endometrial biopsies *in vitro* (Chapter 3), and c) investigation of cytokine and protease protein signaling networks during inflammation induced matrix remodeling (Chapter 4).

1.1 Endometriosis as a Paradigm for Dysregulated Mucosal Paracrine Signaling

Endometriosis and adenomyosis are gynecological disorders affecting approximately 10% of women arising from the dysregulation of normal endometrial function.[3] Endometriosis is characterized by the growth of uterine stromal and epithelial cells usually at ectopic peritoneal sites including the ovaries, bladder, bowel, and peritoneum resulting in 50% of gynecological cases presenting with pelvic pain and female factor infertility,[4,5] while adenomyosis is characterized by endometrial lesions within the myometrial muscle of the uterus. For endometriosis, the inappropriate endometrial tissue presence has been mainly attributed to dislodged endometrium which is retrogradely menstruated into the peritoneum (Sampson's hypothesis) with some evidence supporting peritoneal metaplasia or lymphatic spreading, although the pathophysiology underlying the attachment, proliferation, and invasion of these cells remains poorly characterized.[3,6] Endometriosis may also arise from aberrant distribution of endometrial cells developmentally or neonatally.[7] This spectrum of plausible etiologies underscores the heterogeneities of the disease and motivates development of patient-specific *in vitro* models for stratification.

Endometriosis is a disease of heterogeneous manifestations, which are classified into four stages ranging from small superficial lesions to sites of multiple adhesions, ovarian cysts and highly invasive rectovaginal involvement.[8] Many patients exhibit a spectrum of lesion types likely spanning disease progression as diagnosis generally occurs decades after initial symptom onset.[3] A kinetic lesion study in a non-human primate model of endometriosis suggests dynamic progression of lesion phenotypes leading to hormone response disruption.[9–11] However, lesion burden and gross pathology, including standard surgical staging criteria, as established by the American Association for Reproductive Medicine, often does not correlate with clinical symptoms warranting further investigation into the molecular and cellular features underlying disease presentation and progression.[12–14]

While nearly all women display retrograde menstruation, only 10% will develop endometriosis. The endometrium has been cited as a possible source of disrupted tissue containing genetic and epigenetic modifications to hormone response elements in endometriosis patients,[15,16] resulting in reduced secretory differentiation of stromal cells

from the endometrium and endometriotic lesions.[17] It has been suggested that differences in progesterone responsiveness leads to dysregulated extracellular matrix interactions, including increased cell adhesion molecules and matrix remodeling enzymes that mediate endometrial cell attachment and invasion.[18] Thus, reduced progesterone response may prime survival and proliferation of endometrial tissue for some women upon retrograde menstruation of these cells into the peritoneum.

A normal physiological response to progesterone during the secretory phase prepares the endometrium for implantation by limiting inflammatory signaling pathways. Stromal produced transforming growth factor β (TGF-β) mediates global suppression of stromal and epithelial matrix metalloproteinase (MMP) expression and coordinates reciprocal increases in the endogenous MMP inhibitors, or tissue inhibitors of metalloproteinases, TIMPs. The endometrium becomes only locally responsive to remodeling at the site of the implanting embryo which secretes interleukin 1, as well as numerous other cytokines and growth factors known to modulate expression of adhesion, extracellular matrix and matrix remodeling proteins.[19,20] Thus, the ability to understand and treat complex inflammatory disorders, like endometriosis and adenomyosis, will require a multifaceted approach to investigate the inherent variability among patients including their dynamic responses to hormones or inflammatory cues. Specifically, models of the barrier mucosa are needed to elucidate abnormal epithelial-stromal interactions that may drive disease initiation and progression.

1.2 Epithelial Barrier Mucosa: Endometrium as a Case Study

Epithelial barrier mucosal tissues including those that line the gastrointestinal, respiratory, and urogenital tracts are responsible for providing a protective physical barrier that selectively interfaces with the surrounding environment. In general, epithelial mucosal tissues consist of a sheet of tightly bonded epithelial cells that resides on top of a protein matrix-rich stroma comprising fibroblasts, blood vessels, and resident immune cells. The epithelium provides a physical barrier responsible for protecting underlying tissues from commensal and pathogenic microbes, mediates secretion of ions and mucous to prevent tissue dehydration, and keeps damaging bodily fluids, such as stomach acid, compartmentalized.[21] In the case of the endometrium, the epithelial mucosa has an

additional role of providing cues to enable blastocyst attachment, survival and invasion leading to placentation and embryo development.[22]

In addition to providing a passive physical barrier, mucosal epithelial tissues mediate dynamic tissue function through active absorption and secretion of key nutrients, gases, proteins and hormones. The epithelium is often organized into glands and folds to maximize surface area and absorptive capacity, and thus provides an attractive location for drug delivery via oral, sublingual, inhaled, nasal, or intrauterine routes. These tissues are also sites of active immune surveillance and peripheral tolerance, and modulate inflammatory responses through secretion of cytokines, chemokines, proteases and growth factors during injury, infection and tissue repair to recruit and mature immune cells.[21,23] When epithelial repair and subsequent signaling becomes disrupted, pathological consequences including chronic infection, fibrosis and inflammatory disorders ensue.

The endometrium is a highly dynamic mucosal barrier within the uterus that contains simple columnar epithelial cells organized into a single layer of luminal and interconnecting glandular structures supported by a highly vascularized stromal compartment. Hormones mediate over 500 cycles of endometrial breakdown, regeneration, and differentiation during the lifetime of a female. A drop in progesterone levels results in a cascade of signaling events that mediate extracellular matrix breakdown, cellular apoptosis and shedding of the surface endometrium leading to menstruation.[24]

Endometrial repair occurs in two phases, a hormone-independent followed by an estrogen-dependent phase. Initial repair is marked by fibrin clotting and rapid luminal reepithelialization and occurs concomitant with menstruation in a hormone independent fashion.[25,26] During the proliferative phase, a rise in estrogen triggers rapid matrix reassembly and stromal proliferation to fully restore the functional endometrium within one week completing scar-free endometrial repair.[24] Following endometrial repair and ovulation, a subsequent increase in progesterone signaling causes stromal cells to differentiate and epithelial glands to take on a tortuous appearance, increasing both surface area and secretory protein production, to support embryo implantation. In the

absence of established pregnancy, progesterone levels drop and protease activity increases leading to menstruation and the cycle begins anew.

The ability to study endometrial mucosal biology, and in particular hormone responsiveness, proteolytic remodeling, and repair has been hampered by a lack of long lived, reproducible *in vitro* models that more faithfully recapitulate the 3D architecture and cellular and matrix compositions important to studying these complex physiologies. I aim to recapitulate a basal endometrial state using methods to expand limited primary patient samples (Chapter 3) to better capture donor heterogeneity from which studies of normal and inflammation induced disruption of hormone mediated cellular communication can be investigated (Chapter 4). While immune cell recruitment, signaling, and maturation along with dynamic angiogenesis of endothelial cells are important mediators of endometrial barrier mucosal remodeling and function, we choose to focus here on first characterizing cytokine induced proteolytic remodeling between endometrial epithelial cells and stromal fibroblasts in co-culture. This simplified co-culture model of the hormonally responsive endometrial mucosa can be expanded in future studies to investigate immune cell recruitment and angiogenesis.

1.3 Endometrial Epithelial and Stromal Co-culture Models

Current primary tissue culture models used to parse endometrial epithelial and stromal communication range in complexity. Some use primary tissue explants, which contain cellular and matrix compositions most related to *in vivo* tissue function, but long-term studies are limited by their short *in vitro* lifespan. Still others utilize isolated individual cell types that are physically separated, often using cell culture inserts, but signal to each other through common media.

Tissue explants have provided valuable insight into the hormonal regulation of matrix metalloproteinases (MMPs). Specifically, stromal and epithelial MMPs 3 and 7 are suppressed in healthy donors in response to progesterone induced TGFβ production by stromal cells, whereas women with endometriosis exhibit reduced progesterone responsiveness and thus maintain higher MMP expression.[27–29] While explants may be the closest surrogate to observing *in vivo* patient behavior, there are practical experimental limitations to their use including 1) difficulties standardizing observations across

conditions due to the unknown cellular compositions, 2) challenges to parse any individual cell types contribution to the signaling environment, and 3) difficulties in performing repeated studies or many experimental conditions due to limited samples obtained from donor biopsy, which cannot be cryopreserved.

Prior work has demonstrated the ability to reproducibly isolate, cryopreserve and culture endometrial stromal and epithelial cells from donor biopsies with high purity, viability, and maintenance of function.[30,31] Isolated cells have been co-cultured by seeding epithelial cells on top of a cell culture insert with (apical) media on top and stromal cells underneath on the bottom of a cell culture plate, which then share a common (basal) media reservoir.[27,28,32,33] This system is advantageous in that it allows for assessment and support of a polarized epithelium, measurement of apically versus basally secreted factors, and separation of cell types for later genetic and biochemical characterization.[32] While the ability to physically separate and culture distinct cell types offers many advantages, including the ability to specifically attribute cellular responses to secreted factors rather than direct cellular interactions, there are practical limitations including non-physiologic dilution effects that often occur in a large shared media volume. Additionally, these models are unable to capture cell-cell interactions and phenotypic behaviors such as 3D tissue remodeling or morphogenesis. In fact, previously it was shown that endometrial stromal protease activity was decreased in 2D cultures compared to cells cultured in a 3D collagen matrix,[34] suggesting that either the cellular matrix directly influences protease activity or that the matrix may contribute to establishing a local signaling environment that concentrates proteolytic remodeling cues.

Natural extracellular matrices have been used to construct a more physiologic representative 3D tissue architecture that overcomes dilution effects and enables cell-cell interactions. Additionally, phenotypes including migration, morphogenesis, and matrix remodeling can be studied. Numerous models have been constructed for myriad endometrial function studies including epithelial polarization, hormone receptor expression, hormone responsiveness, and trophoblast attachment and invasion.[35–39] Often endometrial stromal cells are embedded within a 3D natural ECM hydrogel, such as Collagen I, agarose, or fibrin. Then, epithelial cells are cultured on top, frequently with a thin coating of basement membrane matrix, such as Matrigel.[36–39] Still others have

embedded endometrial explants or both isolated stromal and epithelial cells within fibrin or Matrigel to better recapitulate a glandular endometrial model, with no single natural matrix being representative of the *in vivo* environment of both cell types.[35,40]

While 3D cell culture necessitates use of an extracellular matrix scaffold, the use of natural matrices is limiting for some applications. They contain a complex and often unknown composition of matrix and growth factor molecules, which may influence cellular signaling and phenotypic behaviors. For example, Matrigel, a tumor-derived basement membrane ECM extract secreted by Englebreth-Holm-Swarm mouse sarcoma, contains TGFβ, which has been shown to suppress MMP expression and thus may not be ideal for studying protease regulation in the endometrium.[28,41] Additionally, these matrices are often derived from animal sources and exhibit batch-to-batch variation, with researchers often prescreening batches for desired function or protein content, limiting reproducibility. Furthermore, cells rapidly remodel natural matrices either leading to matrix breakdown and degradation, or in the case of Collagen I significant contraction more closely mimicking wound matrix.[42] Thus, a highly defined, reproducible matrix scaffold, as introduced in Chapter 2, is desirable for 3D tissue model development.

1.4 Engineered Synthetic Extracellular Matrix for Epithelial-Stromal Co-culture

The ability to establish a matrix scaffold that supports attachment and function of distinct cell types while permitting cell-mediated remodeling is desired. When designing a matrix environment to support an epithelial barrier overlying stroma, it is important to consider the local tissue architecture. Epithelial and stromal cells occupy spatially distinct, but adjacent microenvironments *in vivo*. A sparse, porous matrix surrounds stromal cells with the bulk comprising threadlike fibrils of collagen and fibronectin. This is in contrast to epithelial cells that reside on top of a densely packed sheet-like structure, or basement membrane (BM) comprising laminin, collagen IV, and proteoglycan-rich matrix proteins.

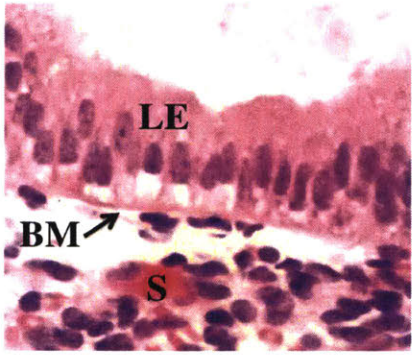

Figure 1-1. Early secretory endometrium photomicrograph of H&E staining showing luminal epithelium (LE) on top of a dense basement membrane (BM) matrix, which separates the epithelium from the underlying stroma (S).[84]

The basement membrane (BM) serves to filter and concentrate paracrine-signaling molecules at the basal surface, anchors the luminal epithelium (LE) to the underlying stromal (S) compartment, and creates a barrier to prevent cellular migration into the stroma (Fig. 1-1).[43] Thus, the matrix reinforces spatial heterogeneities that may contribute to distinct local signaling microenvironments.

Synthetic polymers, that can be crosslinked to form hydrogel matrices, offer a blank slate from which modular design and biofunctionality can be introduced for various applications. Hydrogels have supported diverse healthy and disease cell culture models including 3D organoids, vascular network formation, cancer spheroids and stromal fibrosis.[44–48] Specifically, polyethylene glycol (PEG) provides a relatively blank, bio-inert polymer scaffold from which we can add bioactive cues to instruct cellular phenotypes such as adhesion, differentiation and polarization.[49–59] While a PEG backbone provides mechanical and biophysical stimuli, which can be modulated via changes in polymer and crosslinker concentration, other key proteins from the extracellular matrix must be incorporated to mediate cellular responses including attachment, migration, and cell-secreted matrix accumulation.

Approaches to modifying PEG gels with adhesion peptides that bind cell surface integrin receptors are now well established and usually involve fibronectin derived amino acid sequences,[53,60,61] peptide domains from other ECM proteins,[55,58,62,63] or even whole proteins.[44,53,61,64–66] One gap in the field is the almost universal focus on a modest library of integrin-engaging sequences, with relatively little exploration into how these cues drive subsequent cellular remodeling of the microenvironment. Little is known, for example, about how cell-produced ECM accumulates in the local microenvironment. Thus, a major premise of this thesis is the exploration of hydrogel properties and peptide cues that mediate cell attachment and local matrix secretion and accumulation. Cell-secreted matrix proteins engage adhesion receptors and initiate downstream intracellular kinase activity to promote cell survival, proliferation, differentiation, matrix assembly and migration.[67] More importantly individual motifs from matrix proteins do not provide enough signaling complexity; so establishing environments that secure cell-secreted matrices might more faithfully recapitulate *in vivo* ECM architecture and cellular signaling.

If we consider first cellular adhesive interactions; two distinct general approaches are to modify the hydrogel with adhesion peptides or allow for deposition of cell-secreted matrix (Fig. 1-2). During isolation of primary endometrial cells, the ECM is degraded to isolate the stroma from the epithelia.[30] Thus, when encapsulating endometrial cells in a synthetic matrix, incorporation of adhesion peptides is likely necessary as primary cells are particularly sensitive to anoikis, or apoptosis in response to loss of ECM interactions.[68] Furthermore, integrin engagement is crucial to modulating cellular matrix secretion and assembly.[69–71] The capture of cell-secreted ECM is favorable to solely providing direct integrin engaging sequences because allowing natural ECM formation provides 1) multivalent interactions that are challenging to artificially recreate, 2) establishment of growth factor gradients, and 3) selective diffusion and mechanical tension for fibril formation. Additionally, the use of ECM derived peptide binding sites provides a mechanism by which sequestration of secreted peptides mimic *in vivo* capture so as not to disrupt important cell signaling motifs.[72–74]

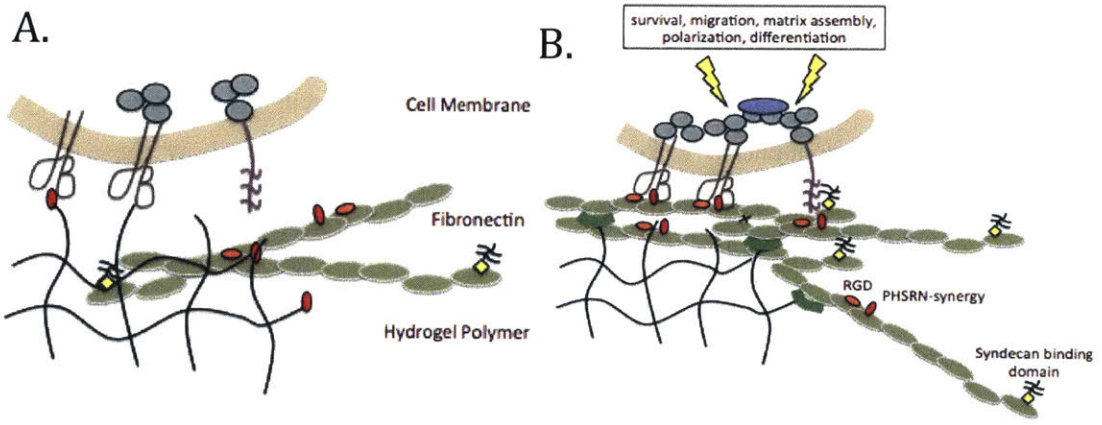

Figure 1-2. Hydrogel functionalization strategies for fibronectin signaling by (A) directly engaging cell adhesion receptors by addition of amino acid sequences (RGD and PHSRN) derived from fibronectin that bind cellular integrin receptors or (B) capture of cell-secreted fibronectin matrix to mediate fibril assembly.

Thus, the goal of this work is to design highly defined, synthetic hydrogel environments that are biofunctionalized to engage cellular adhesion receptors *and* that are locally responsive to cell-secreted extracellular matrix proteins and proteases. Additionally, these matrices can be dissolved on-demand using a previously established method incorporating a crosslink that contains the substrate for the bacterial transpeptidase enzyme, Sortase A.[59] This allows selective cleavage of hydrogel crosslinks and gel dissolution while preserving cell-secreted proteins intact for further analysis. We anticipate these matrices will further enable development of 3D culture microenvironments to better understand hormonally driven paracrine signaling and proteolytic remodeling events for normal and diseased states of barrier mucosal tissues.

1.5 Data-Driven Protein Network Modeling of Endometrial Mucosal Inflammation

Inflammatory conditions arising from innate immune defects, infection, wounding or environmental toxicant exposures, have been shown to disrupt the normal progestational differentiation response leading to enhanced MMP expression and establishment of ectopic endometrial growth in a murine model of endometriosis.[75–80] There are a variety of pathological agents that could lead to the same clinical disease presentation enabling multiple underlying etiologies to converge on the same tissue-level phenotype. Of importance, this means that the molecular changes, and thus effective therapeutic interventions, may vary significantly depending on disease pathophysiology.

In the case of endometriosis, hormone therapy is often used as a first-line treatment, but this treatment is inappropriate for infertility patients. Furthermore, of the women receiving medical treatment for endometriosis-associated pain—including surgery, GnRH agonists or progestin therapy—11-19% reported no pain relief at all, 5-59% continued to have pain at the end of treatment, and an additional 5-9% discontinued treatment due to adverse events or lack of efficacy.[81] This varied response rate, especially to hormonal therapies, warrants further investigation into the underlying molecular mechanisms affecting hormone responsiveness.

Previously, discordance was found between clinical disease presentation and molecular protein signaling networks that modulate the local immune environment. An unbiased approach was used to classify endometriosis and control donors based on

inflammatory cytokine profiles measured in their peritoneal fluid. A consensus signature of 13 cytokines was correlated with more severe disease, but not specifically informative of any particular clinical feature such as pain, infertility or endometriosis staging.[13] Furthermore, no single cytokine was significantly predictive of disease versus control donors suggesting that changes associated with endometriosis are likely multifactorial involving alterations of protein networks that may be missed with univariate analyses. Taken together, a better understanding of inflammatory cytokine signaling and how it may contribute to hormone response disruption would greatly enhance our understanding of endometriosis development.

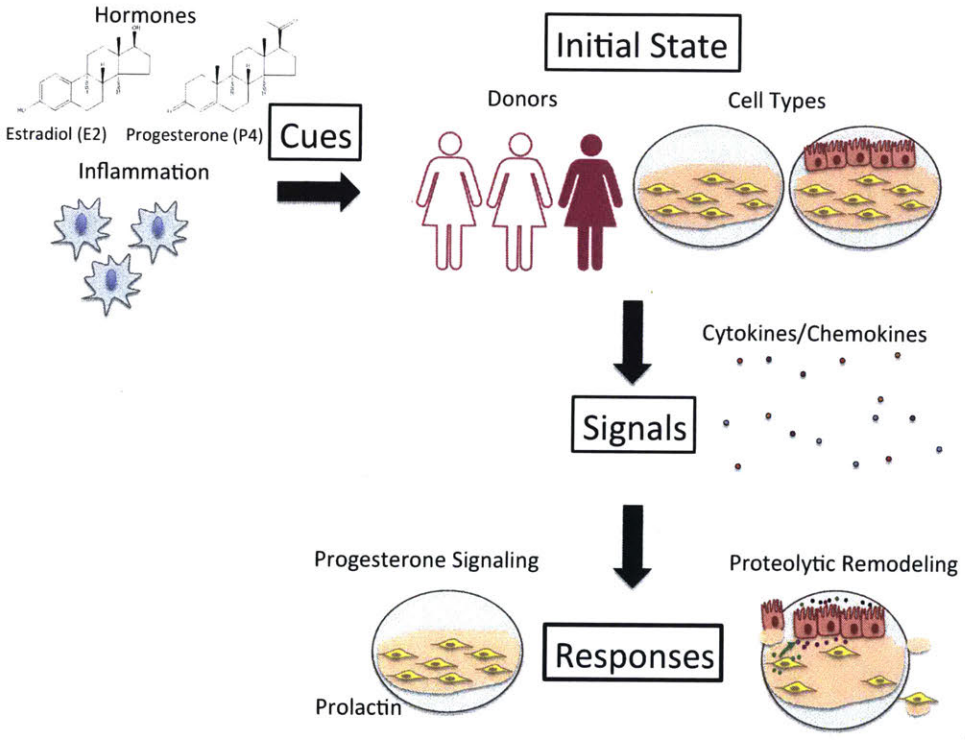

Figure 1-3. Cues, signals, and responses in endometrial cultures. Clinical donors or variation in cell culture composition establish initial states that can differentially respond to ***cues***, including hormone treatments or inflammatory stimuli. Cultures respond by production of cytokine ***signals*** that affect cellular ***responses*** related to endometrial function including progesterone signaling and proteolytic remodeling.

In order to address the complexities of endometrial pathophysiology, we begin by establishing a framework that includes both tissue engineering and multivariate data analyses to parse intercellular cytokine signaling in epithelial-stromal cultures. We employ a 'cue-signal-response' paradigm whereby inherent donor variation and cell culture composition establish an initial state that we can dynamically perturb via cues, including hormone treatment or inflammation induction, which subsequently influence signaling through changes in cytokine production.[82,83] Varying cytokine signals ultimately influence cellular responses such as proteolytic remodeling and progesterone differentiation. This framework allows us to parse how a given cue impacts downstream cellular responses and generates further hypotheses for subsequent mechanistic testing. The studies presented in this thesis will serve as a foundation for future considerations including 1) design principles for development of complex 3D *in vitro* model systems, 2) appropriate selection of cell types (i.e., sources, donors, and primaries versus cell lines), and 3) computational techniques to capture key disease physiology to hopefully enable novel target identification for therapeutic drug development.

1.6 Overall Objectives

Specifically, we aim to improve upon current 3D endometrial co-culture models to study hormonal paracrine signaling through the design of highly defined, synthetic matrices that are locally responsive to both epithelial and stromal cells. Our understanding of endometrial biology, and the ability to parse disease mechanisms and test efficacy of therapeutic interventions, is limited by the ability to replicate complex 3D physiology *in vitro*, especially in a reproducible manner, adaptable to the limited numbers of cells available from patient biopsies. This thesis addresses a critical gap in accessible tools to study and control endometrial biology *in vitro* and does so in a manner that can rapidly be translated to other epithelial-stromal barrier mucosal tissues. This is pursued by 1) development and characterization of a locally adaptable synthetic hydrogel matrix to support formation of an endometrial barrier mucosal model, 2) methods to expand and cryopreserve primary human endometrial epithelial cells and 3) data-driven network modeling of secreted proteins to understand how cytokine signaling influences proteolytic remodeling in epithelial-stromal co-cultures.

1.7 References

1. Arrowsmith J, Miller P. Trial Watch: Phase II and Phase III attrition rates 2011–2012. *Nat Rev Drug Discov.* 2013;12(8):569-569.
2. Cook D, Brown D, Alexander R, et al. Lessons learned from the fate of AstraZeneca's drug pipeline: a five-dimensional framework. *Nat Rev Drug Discov.* 2014;13(6):419-431.
3. Giudice LC. Clinical practice. Endometriosis. *N Engl J Med.* 2010;362(25):2389-2398.
4. Goldstein DP, DeCholnoky C, Emans SJ, Leventhal JM. Laparoscopy in the diagnosis and management of pelvic pain in adolescents. *J Reprod Med.* 1980;24(6):251-256.
5. Eskenazi B, Warner ML. Epidemiology of endometriosis. *Obstet Gynecol Clin North Am.* 1997;24(2):235-258.
6. Sampson JA. Metastatic or Embolic Endometriosis, due to the Menstrual Dissemination of Endometrial Tissue into the Venous Circulation. *Am J Pathol.* 1927;3:93-110.43.
7. Burney RO, Giudice LC. Pathogenesis and pathophysiology of endometriosis. *Fertil Steril.* 2012;98(3):511-519. doi:10.1016/j.fertnstert.2012.06.029.
8. Adamson GD. Endometriosis classification: an update. *Curr Opin Obstet Gynecol.* 2011;23:213-220.
9. Afshar Y, Hastings J, Roqueiro D, Jeong J-W, Giudice LC, Fazleabas AT. Changes in eutopic endometrial gene expression during the progression of experimental endometriosis in the baboon, Papio anubis. *Biol Reprod.* 2013;88(2):44.
10. Harirchian P, Gashaw I, Lipskind ST, et al. Lesion kinetics in a non-human primate model of endometriosis. *Hum Reprod.* 2012;27(8):2341-2351.
11. Leconte M, Nicco C, Ngô C, et al. The mTOR/AKT inhibitor temsirolimus prevents deep infiltrating endometriosis in mice. *Am J Pathol.* 2011;179(2):880-889.
12. American Society for Reproductive. Revised American Society for Reproductive Medicine classification of endometriosis: 1996. *Fertil Steril.* 1997;67(5):817-821.
13. Beste MT, Pfaffle-Doyle N, Prentice EA, et al. Molecular Network Analysis of Endometriosis Reveals a Role for c-Jun-Regulated Macrophage Activation. *Sci Transl Med.* 2014;6(222):222ra16-222ra16.
14. Miller MA, Meyer AS, Beste MT, et al. ADAM-10 and -17 regulate endometriotic cell migration via concerted ligand and receptor shedding feedback on kinase signaling. *Proc Natl Acad Sci U S A.* 2013;110(22):E2074-83.
15. Bulun SE. Endometriosis. *N Engl J Med.* 2009;360(3):268-279.
16. Bruner-Tran KL, Resuehr D, Ding T, Lucas JA, Osteen KG. The Role of Endocrine Disruptors in the Epigenetics of Reproductive Disease and Dysfunction: Potential Relevance to Humans. *Curr Obstet Gynecol Rep.* 2012;1(3):116-123.
17. Klemmt PAB, Carver JG, Kennedy SH, Koninckx PR, Mardon HJ. Stromal cells

from endometriotic lesions and endometrium from women with endometriosis have reduced decidualization capacity. *Fertil Steril.* 2006;85(3):564-572.
18. Bruner-Tran KL, Herington JL, Duleba AJ, Taylor HS, Osteen KG. Medical management of endometriosis: emerging evidence linking inflammation to disease pathophysiology. *Minerva Ginecol.* 2013;65(2):199-213.
19. Lessey BA, Damjanovich L, Coutifaris C, Castelbaum A, Albelda SM, Buck CA. Integrin adhesion molecules in the human endometrium. Correlation with the normal and abnormal menstrual cycle. *J Clin Invest.* 1992;90(1):188-195.
20. Osteen KG, Bruner-Tran KL, Ong D, Eisenberg E. Paracrine mediators of endometrial matrix metalloproteinase expression: potential targets for progestin-based treatment of endometriosis. *Ann N Y Acad Sci.* 2002;955:139-46-8, 396-406.
21. France MM, Turner JR. The mucosal barrier at a glance. *J Cell Sci.* 2017;130(2):307-314.
22. Dimitriadis E. Cytokines, chemokines and growth factors in endometrium related to implantation. *Hum Reprod Update.* 2005;11(6):613-630.
23. Maybin JA, Critchley HOD, Jabbour HN. Inflammatory pathways in endometrial disorders. *Mol Cell Endocrinol.* 2011;335(1):42-51.
24. Maybin JA, Critchley HOD. Menstrual physiology: implications for endometrial pathology and beyond. *Hum Reprod Update.* 2015;21(6):748-761.
25. Garry R, Hart R, Karthigasu KA, Burke C. A re-appraisal of the morphological changes within the endometrium during menstruation: a hysteroscopic, histological and scanning electron microscopic study. *Hum Reprod.* 2009;24(6):1393-1401.
26. Garry R, Hart R, Karthigasu K, Burke C. Structural changes in endometrial basal glands during menstruation. *BJOG An Int J Obstet Gynaecol.* 2010;117(10):1175-1185.
27. Osteen KG, Rodgers WH, Gaire M, Hargrove JT, Gorstein F, Matrisian LM. Stromal-epithelial interaction mediates steroidal regulation of metalloproteinase expression in human endometrium. *Proc Natl Acad Sci U S A.* 1994;91(21):10129-10133.
28. Bruner KL, Rodgers WH, Gold LI, et al. Transforming growth factor beta mediates the progesterone suppression of an epithelial metalloproteinase by adjacent stroma in the human endometrium. *Proc Natl Acad Sci U S A.* 1995;92(16):7362-7366.
29. Bruner-Tran KL, Webster-Clair D, Osteen KG. Experimental endometriosis: the nude mouse as a xenographic host. *Ann N Y Acad Sci.* 2002;955:328-39-2, 396-406.
30. Osteen KG, Hill GA, Hargrove JT, Gorstein F. Development of a method to isolate and culture highly purified populations of stromal and epithelial cells from human endometrial biopsy specimens. *Fertil Steril.* 1989;52(6):965-972.
31. Chen JC, Hoffman JR, Arora R, et al. Cryopreservation and recovery of human endometrial epithelial cells with high viability, purity, and functional fidelity. *Fertil Steril.* 2016;105(2):501-10.e1.
32. Chen JC, Erikson DW, Piltonen TT, et al. Coculturing human endometrial

epithelial cells and stromal fibroblasts alters cell-specific gene expression and cytokine production. *Fertil Steril.* 2013;100(4):1132-1143.
33. Igarashi TM, Bruner-Tran KL, Yeaman GR, et al. Reduced expression of progesterone receptor-B in the endometrium of women with endometriosis and in cocultures of endometrial cells exposed to 2,3,7,8-tetrachlorodibenzo-p-dioxin. *Fertil Steril.* 2005;84(1):67-74.
34. Schutte SC, Taylor RN. A tissue-engineered human endometrial stroma that responds to cues for secretory differentiation, decidualization, and menstruation. *Fertil Steril.* 2012;97:997-1003.
35. Arnold JT, Lessey BA, Seppälä M, Kaufman DG. Effect of normal endometrial stroma on growth and differentiation in Ishikawa endometrial adenocarcinoma cells. *Cancer Res.* 2002;62(1):79-88.
36. Bentin-Ley U, Pedersen B, Lindenberg S, Larsen JF, Hamberger L, Horn T. Isolation and culture of human endometrial cells in a three-dimensional culture system. *J Reprod Fertil.* 1994;101(2):327-332.
37. Meng C-X, Andersson KL, Bentin-Ley U, Gemzell-Danielsson K, Lalitkumar PGL. Effect of levonorgestrel and mifepristone on endometrial receptivity markers in a three-dimensional human endometrial cell culture model. *Fertil Steril.* 2009;91(1):256-264.
38. Wang H, Bocca S, Anderson S, et al. Sex steroids regulate epithelial-stromal cell cross talk and trophoblast attachment invasion in a three-dimensional human endometrial culture system. *Tissue Eng Part C Methods.* 2013;19(9):676-687.
39. Bartel C, Tichy A, Schoenkypl S, Aurich C, Walter I. Effects of steroid hormones on differentiated glandular epithelial and stromal cells in a three dimensional cell culture model of the canine endometrium. *BMC Vet Res.* 2013;9:86.
40. Prechapanich J, Kajihara T, Fujita K, et al. Effect of a dienogest for an experimental three-dimensional endometrial culture model for endometriosis. *Med Mol Morphol.* 2014;47(4):189-195.
41. Vukicevic S, Kleinman HK, Luyten FP, Roberts AB, Roche NS, Reddi AH. Identification of multiple active growth factors in basement membrane Matrigel suggests caution in interpretation of cellular activity related to extracellular matrix components. *Exp Cell Res.* 1992;202(1):1-8.
42. Tsuno A, Nasu K, Yuge A, Matsumoto H, Nishida M, Narahara H. Decidualization attenuates the contractility of eutopic and ectopic endometrial stromal cells: implications for hormone therapy of endometriosis. *J Clin Endocrinol Metab.* 2009;94(7):2516-2523.
43. Yurchenco PD. Basement membranes: cell scaffoldings and signaling platforms. *Cold Spring Harb Perspect Biol.* 2011;3(2):1-28.
44. Gjorevski N, Sachs N, Manfrin A, et al. Designer matrices for intestinal stem cell and organoid culture. *Nature.* 2016;539(7630):560-564.
45. Zanotelli MR, Ardalani H, Zhang J, et al. Stable engineered vascular networks from human induced pluripotent stem cell-derived endothelial cells cultured in synthetic hydrogels. *Acta Biomater.* 2016;35:32-41.
46. Moon JJ, Saik JE, Poché RA, et al. Biomimetic hydrogels with pro-angiogenic properties. *Biomaterials.* 2010;31(14):3840-3847.

47. Tokuda EY, Jones CE, Anseth KS. PEG–peptide hydrogels reveal differential effects of matrix microenvironmental cues on melanoma drug sensitivity. *Integr Biol.* 2017;9(1):76-87.
48. Matsuzaki S, Canis M, Pouly J-L, Darcha C. Soft matrices inhibit cell proliferation and inactivate the fibrotic phenotype of deep endometriotic stromal cells in vitro. *Hum Reprod.* 2016;31(3):541-553.
49. Rizzi SC, Ehrbar M, Halstenberg S, et al. Recombinant protein-co-PEG networks as cell-adhesive and proteolytically degradable hydrogel matrixes. Part II: biofunctional characteristics. *Biomacromolecules.* 2006;7(11):3019-3029.
50. Lutolf MP, Lauer-Fields JL, Schmoekel HG, et al. Synthetic matrix metalloproteinase-sensitive hydrogels for the conduction of tissue regeneration: engineering cell-invasion characteristics. *Proc Natl Acad Sci U S A.* 2003;100(9):5413-5418.
51. Patterson J, Hubbell JA. Enhanced proteolytic degradation of molecularly engineered PEG hydrogels in response to MMP-1 and MMP-2. *Biomaterials.* 2010;31(30):7836-7845.
52. Bott K, Upton Z, Schrobback K, et al. The effect of matrix characteristics on fibroblast proliferation in 3D gels. *Biomaterials.* 2010;31(32):8454-8464.
53. Cambria E, Renggli K, Ahrens CC, et al. Covalent Modification of Synthetic Hydrogels with Bioactive Proteins via Sortase-Mediated Ligation. *Biomacromolecules.* 2015;16(8):2316-2326.
54. Raza A, Ki CS, Lin C-C. The influence of matrix properties on growth and morphogenesis of human pancreatic ductal epithelial cells in 3D. *Biomaterials.* 2013;34(21):5117-5127.
55. Weiss MS, Bernabé BP, Shikanov A, et al. The impact of adhesion peptides within hydrogels on the phenotype and signaling of normal and cancerous mammary epithelial cells. *Biomaterials.* 2012;33(13):3548-3559.
56. Reyes CD, Petrie TA, García AJ. Mixed extracellular matrix ligands synergistically modulate integrin adhesion and signaling. *J Cell Physiol.* 2008;217(2):450-458.
57. Gill BJ, Gibbons DL, Roudsari LC, et al. A synthetic matrix with independently tunable biochemistry and mechanical properties to study epithelial morphogenesis and EMT in a lung adenocarcinoma model. *Cancer Res.* 2012;72(22):6013-6023.
58. Gould ST, Anseth KS. Role of cell-matrix interactions on VIC phenotype and tissue deposition in 3D PEG hydrogels. *J Tissue Eng Regen Med.* 2016;10(10):E443-E453.
59. Valdez J, Cook CD, Ahrens CC, et al. On-demand dissolution of modular, synthetic extracellular matrix reveals local epithelial-stromal communication networks. *Biomaterials.* 2017;130:90-103.
60. Hersel U, Dahmen C, Kessler H. RGD modified polymers: biomaterials for stimulated cell adhesion and beyond. *Biomaterials.* 2003;24(24):4385-4415.
61. Zhang C, Hekmatfer S, Karuri NW. A comparative study of polyethylene glycol hydrogels derivatized with the RGD peptide and the cell-binding domain of fibronectin. *J Biomed Mater Res A.* April 2013.

62. Weber LM, Hayda KN, Haskins K, Anseth KS. The effects of cell-matrix interactions on encapsulated beta-cell function within hydrogels functionalized with matrix-derived adhesive peptides. *Biomaterials.* 2007;28(19):3004-3011.
63. García JR, Clark AY, García AJ. Integrin-specific hydrogels functionalized with VEGF for vascularization and bone regeneration of critical-size bone defects. *J Biomed Mater Res Part A.* 2016;104(4):889-900.
64. Martino MM, Briquez PS, Ranga A, Lutolf MP, Hubbell JA. Heparin-binding domain of fibrin(ogen) binds growth factors and promotes tissue repair when incorporated within a synthetic matrix. *Proc Natl Acad Sci.* 2013;110(12):4563-4568.
65. Roch A, Giger S, Girotra M, et al. Single-cell analyses identify bioengineered niches for enhanced maintenance of hematopoietic stem cells. *Nat Commun.* 2017;8(1):221.
66. Gjorevski N, Lutolf MP. Synthesis and characterization of well-defined hydrogel matrices and their application to intestinal stem cell and organoid culture. *Nat Protoc.* 2017;12(11):2263-2274.
67. Zhang J, Yang PL, Gray NS. Targeting cancer with small molecule kinase inhibitors. *Nat Rev Cancer.* 2009;9(1):28-39.
68. Bertrand K. Survival of exfoliated epithelial cells: a delicate balance between anoikis and apoptosis. *J Biomed Biotechnol.* 2011;2011:534139.
69. Sechler JL, Corbett SA, Schwarzbauer JE. Modulatory roles for integrin activation and the synergy site of fibronectin during matrix assembly. *Mol Biol Cell.* 1997;8(12):2563-2573.
70. Hamill KJ, Kligys K, Hopkinson SB, Jones JCR. Laminin deposition in the extracellular matrix: a complex picture emerges. *J Cell Sci.* 2009;122(Pt 24):4409-4417.
71. Tzu J, Marinkovich MP. Bridging structure with function: structural, regulatory, and developmental role of laminins. *Int J Biochem Cell Biol.* 2008;40(2):199-214.
72. Johnson G, Moore SW. Identification of a structural site on acetylcholinesterase that promotes neurite outgrowth and binds laminin-1 and collagen IV. *Biochem Biophys Res Commun.* 2004;319(2):448-455.
73. Chiang TM, Kang AH. A synthetic peptide derived from the sequence of a type I collagen receptor inhibits type I collagen-mediated platelet aggregation. *J Clin Invest.* 1997;100(8):2079-2084.
74. Gao X, Groves MJ. Fibronectin-binding peptides. I. Isolation and characterization of two unique fibronectin-binding peptides from gelatin. *Eur J Pharm Biopharm.* 1998;45(3):275-284.
75. Bruner-Tran KL, Eisenberg E, Yeaman GR, Anderson TA, McBean J, Osteen KG. Steroid and Cytokine Regulation of Matrix Metalloproteinase Expression in Endometriosis and the Establishment of Experimental Endometriosis in Nude Mice. *J Clin Endocrinol Metab.* 2002;87(10):4782-4791.
76. Bruner-Tran KL, Yeaman GR, Crispens MA, Igarashi TM, Osteen KG. Dioxin may promote inflammation-related development of endometriosis. *Fertil Steril.* 2008;89(5):1287-1298.

77. Stocks MM, Crispens MA, Ding T, Mokshagundam S, Bruner-Tran KL, Osteen KG. Therapeutically Targeting the Inflammasome Product in a Chimeric Model of Endometriosis-Related Surgical Adhesions. *Reprod Sci.* 2017;24(8):1121-1128.
78. Herington JL, Crispens MA, Carvalho-Macedo AC, et al. Development and prevention of postsurgical adhesions in a chimeric mouse model of experimental endometriosis. *Fertil Steril.* 2011;95(4):1295-1301.e1.
79. Bruner-Tran KL, Carvalho-Macedo AC, Duleba AJ, Crispens MA, Osteen KG. Experimental endometriosis in immunocompromised mice after adoptive transfer of human leukocytes. *Fertil Steril.* 2010;93(8):2519-2524.
80. Azuma Y, Taniguchi F, Nakamura K, et al. Lipopolysaccharide promotes the development of murine endometriosis-like lesions via the nuclear factor-kappa B pathway. *Am J Reprod Immunol.* 2017;77(4):e12631.
81. Becker CM, Gattrell WT, Gude K, Singh SS. Reevaluating response and failure of medical treatment of endometriosis: a systematic review. *Fertil Steril.* 2017;108(1):125-136.
82. Cosgrove BD, Griffith LG, Lauffenburger DA. Fusing Tissue Engineering and Systems Biology Toward Fulfilling Their Promise. *Cell Mol Bioeng.* 2008;1(1):33-41.
83. JANES K, LAUFFENBURGER D. A biological approach to computational models of proteomic networks. *Curr Opin Chem Biol.* 2006;10(1):73-80.
84. Ong M. Early secretory endometrium. http://www.ganfyd.org/index.php?title=File:Endometrium_secretory_early.jpg. Published 2015. Accessed August 20, 2017.

Chapter 2

2 Synthetic Extracellular Matrix Microenvironments Enable Functional 3D Endometrial Epithelial and Stromal Co-culture

Contributions: Linda Stockdale and Julia Papps contributed technical assistance performing hydrogel experiments and biochemical assays. Julia Papps contributed to primary sample collection, isolation, and culture. Hongkun He performed AFM to characterize hydrogel mechanical properties. This chapter appears, in part, as a manuscript published in *Integrative Biology*.[1]

Mucosal barrier tissues, comprising a layer of tightly-bonded epithelial cells in intimate molecular communication with an underlying matrix-rich stroma containing fibroblasts and immune cells, are prominent targets for drugs against infection, chronic inflammation, and other disease processes. Although human *in vitro* models of such barriers are needed for mechanistic studies and drug development, differences in extracellular matrix (ECM) needs of epithelial and stromal cells hinder efforts to create such models. Here, using the endometrium as an example mucosal barrier, we describe a synthetic, modular ECM hydrogel suitable for 3D functional co-culture, featuring components that can be remodeled by cells and that respond dynamically to sequester local cell-secreted ECM characteristic of each cell type. The synthetic hydrogel combines peptides with off-the-shelf reagents and is thus accessible to cell biology labs. Specifically, we first identified a single peptide as suitable for initial attachment of both endometrial epithelial and stromal cells using a 2D semi-empirical screen. Then, using a co-culture system of epithelial cells cultured on top of gel-encapsulated stromal cells, we show that inclusion of ECM-binding peptides in the hydrogel, along with the integrin-binding peptide, leads to enhanced accumulation of basement membrane beneath the epithelial layer and more fibrillar collagen matrix assembly by stromal cells over two weeks in culture. Importantly, endometrial co-cultures composed of either cell lines or primary cells displayed hormone-mediated differentiation as assessed by morphological changes and secretory protein production. In summary, we define a "one-size-fits-all" synthetic ECM that enables long-term, physiologically responsive co-cultures of epithelial and stromal cells in a mucosal barrier format.

2.1 Introduction

Mucosal barrier tissues, including the digestive, respiratory and urogenital tracts, comprise a polarized, mucus-secreting epithelium that resides on top of an extracellular matrix (ECM)-rich stroma containing fibroblasts and immune cells. These barriers are the sites of complex paracrine communication events that govern tissue homeostasis, including host-microbiome interactions, as well as, response to environmental insults, injury, and infection. Perturbations of barrier function are associated with both acute and chronic diseases, including Crohn's disease, susceptibility to HIV infection, infertility, and many more.[2–6] The tremendous need to understand mucosal barrier function and assess efficacy of therapies directed at mucosal barrier diseases is driving development of both new animal models and new methods to culture human tissues to capture complex *in vivo* physiology *in vitro*. Here, using the endometrium as a model system, we establish a workflow for engineering a modular synthetic ECM scaffold that supports a functionally viable *in vitro* epithelial barrier co-culture for at least two weeks.

Several *in vitro* culture approaches have been used to analyze barrier epithelial-stromal interactions and discern integrated epithelial-stromal phenotypic responses to perturbations. At one extreme, human tissue explants can maintain crucial phenotypic functions in culture for at least days and in some cases weeks.[7,8] However, human tissue explants are not widely available, exhibit significant donor variability, cannot be readily cryopreserved for repeated studies, and require specialized culture apparatus for analysis of vectorial production of cell products. Physiologic tissue mimics created from primary cells isolated from tissues, or from cell lines, offer potential advantages of reproducibility within and between labs, and control over cell composition. Transwell-type membrane cultures are widely used, as they foster a well-polarized and well-differentiated epithelial layer that communicates with stroma plated on the underside of the semi-permeable membrane or on the bottom of the culture dish.[9–13] While this approach allows analysis of apical and basal compartments separately, it potentially distorts physiological interactions by physically separating cells and diluting paracrine signals. These latter limitations can arguably be overcome, and a more physiological 3D environment for stromal cells created, by encapsulating stromal cells within a hydrogel ECM and plating the epithelial cells on top to engineer a better representation of *in vivo* tissue architecture.

Epithelia and stroma experience different ECM environments *in vivo*. Hence, defining an appropriate ECM hydrogel for engineering mucosal barrier tissues for extended *in vitro* culture and function is an ongoing challenge. In epithelial monocultures, the basement membrane extract Matrigel™ is commonly used,[14,15] whereas type I collagen gels or fibrin gels are used as representative microenvironments for stromal cells,[16–18] with no single composition ideal for both cell types in co-culture. Further, although these and other natural ECM gels are readily available commercially, they exhibit substantial inherent batch-to-batch variability, variations in growth factor composition depending on preparation method, limited opportunity to tailor matrix degradation or signaling properties, and are difficult to microfabricate for organs-on-chips type applications.[19] In contrast, synthetic ECM can be built up in modular fashion from individual well-defined components to control crosslinking, signaling, degradation, cell adhesion, permeability, and mechanical properties in a systematic manner.[20–29] The design principles for how to tailor synthetic ECM for specific applications are still emerging, and suitable design principles for construction of a "one-size-fits-all" synthetic ECM for 3D co-culture of epithelial and stromal cells have not yet been developed.

Here, using the human endometrium as a model mucosal epithelial barrier and the well-established platform of peptide-modified PEG hydrogels crosslinked by Michael-type addition reaction,[20,21] we explore both the canonical modular synthetic ECM parameter space (crosslink density, degradation properties, adhesion ligand motifs and concentration) and identify a new design element—localized stabilization of cell-secreted matrix—that leads to phenotypically appropriate 3D tissues that are hormonally responsive over two weeks in culture. This approach incorporates features that allow initial peptide cues provided by the synthetic ECM to foster culture establishment, with additional matrix-responsive elements to reinforce cell remodeling of the microenvironment toward a tissue-appropriate architecture. A workflow for the establishment of epithelial barrier models was developed for an endometrial model, in which we (1) identified an appropriate attachment environment for stromal and epithelial cells, (2) tuned matrix remodeling by modulating extent of crosslinking and inclusion of matrix-binding peptides, (3) analyzed cell viability and function, and (4) replicated known hormone-mediated cell communication.

2.2 Results and Discussion

2.2.1 Synthetic hydrogel matrix biological properties

A 2-D attachment screen identifies PHSRN-K-RGD as a suitable ligand for initial attachment of both epithelial and stromal cells

Epithelial and stromal cell phenotypes *in vitro* are sensitive to both the biochemical and biophysical properties of integrin ligands that mediate cell attachment.[30–35] In order to identify peptides that foster the greatest degree of cell-matrix interactions in the initial stages of culture, we assessed attachment of stromal and epithelial cells to the surface of peptide-modified polyethylene glycol (PEG) hydrogels. Epithelial cells or stromal cells were seeded in serum-containing medium onto the surfaces of hydrogels synthesized by crosslinking 8-arm peptide-functionalized PEG macromers with a dithiol matrix metalloproteinase (MMP)-sensitive peptide crosslinker as shown schematically in Figure 2-1A. A panel of four peptide sequences derived from ECM proteins found in the endometrium and offering a range of published integrin specificities (see Methods for full sequences), was tested: fibronectin(FN)-derived *RGD*, recognized by $\alpha_v\beta_3$ and weakly by other integrins; a synthetic branched peptide, *PHSRN-K-RGD*, mimicking the FN-III 9-10 domain binding sites recognized by integrins $\alpha_5\beta_1$ and $\alpha_3\beta_1$;[31,32,36] a collagen I-derived peptide, *GFOGER*, reported to engage integrin $\alpha_2\beta_1$ and others; [37,38] and *Lam-5* a peptide derived from the basement membrane protein laminin 5 that reportedly engages integrin $\alpha_3\beta_1$.[39] Each peptide was included at various nominal concentrations (0, 0.25, 0.5, and 1.0 mM) during crosslinking, resulting in final concentrations in the hydrogel of about half these initial values (0, 0.12, 0.23, and 0.47 mM) after post-crosslink equilibrium swelling.

As expected, neither stromal nor epithelial cells showed significant attachment to gels lacking adhesion peptides (Fig. 2-1B). The FN-derived peptides *RGD* and *PHSRN-K-RGD* conferred a statistically significant attachment advantage over *GFOGER* and *Lam-5* peptides at all concentrations tested for tHESCs, and at the highest peptide concentration, *PHSRN-K-RGD* enhanced attachment of tHESCs significantly compared to all other peptides. *PHSRN-K-RGD* showed enhanced attachment for Ishikawa epithelial cells at nominal concentrations of 0.5 and 1 mM, and we have previously found

that *PHSRN-K-RGD* also provides an adequate adhesion environment for attachment of primary endometrial epithelial cells to 2D PEG hydrogels.[24]

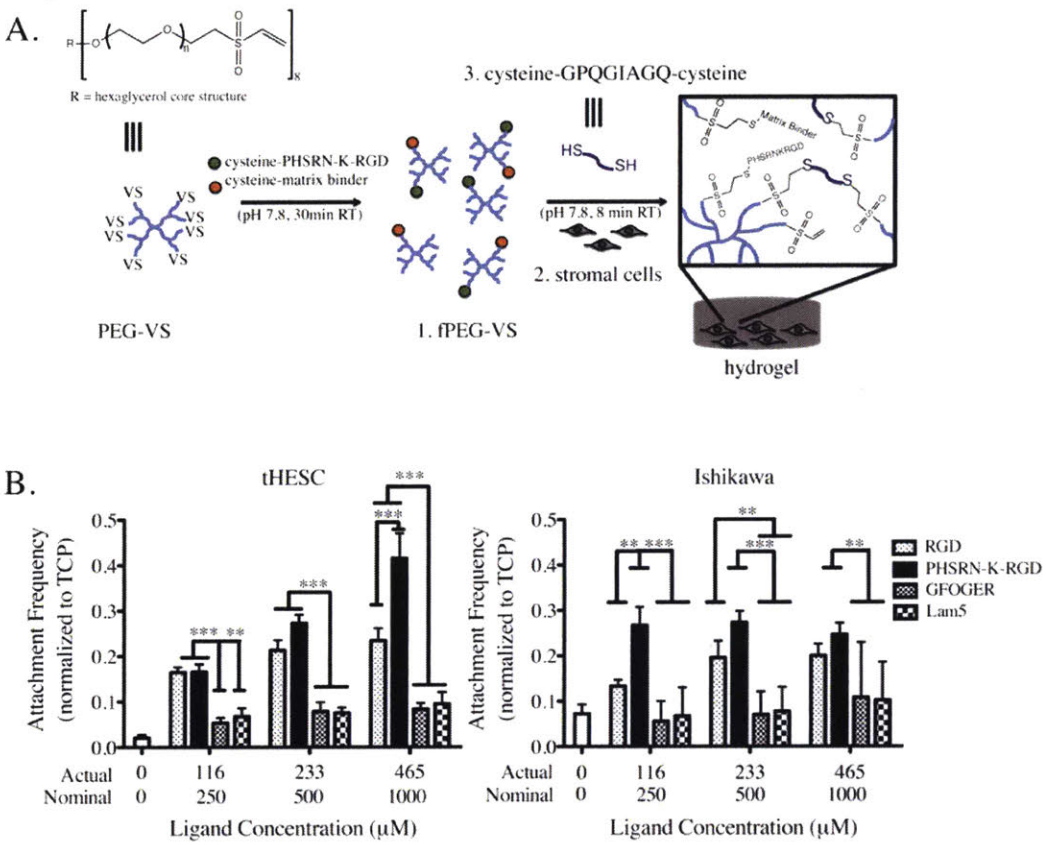

Figure 2-1. Attachment of endometrial stromal and epithelial cells to a panel of integrin ligands identifies PHSRN-K-RGD as the preferred ligand for both cell types. (A) Peptide modified hydrogels were synthesized via Michael-type addition of fPEG macromers to dithiol peptide crosslinkers at pH 7.8; for attachment studies, stromal cells were seeded onto the gels whereas for later studies they were encapsulated as shown. (B) Ishikawa epithelial cells and tHESCs seeded onto a library of integrin engaging peptide sequences showed significantly greater attachment to RGD-containing ligands, with PHSRN-K-RGD showing enhanced attachment over RGD alone; mean ± SEM, N= 3 biological replicates with N=3 technical replicates in each. Statistical significance was assessed by 2-way ANOVA with Bonferroni Posttests, where *P < 0.05, **P < 0.01, and ***P < 0.001.

Identification of the fibronectin-derived peptide sequence, *PHSRN-K-RGD*, as suitable for endometrial cell attachment is conceivable as the endometrial stroma contains fibronectin during all stages of the menstrual cycle and increases in expression in response to progesterone-mediated differentiation during the days prior to menstruation.[40,41] The dynamics of fibronectin expression in the endometrium correspond with dynamic endometrial epithelial and stromal cell expression of fibronectin-binding integrins,[41,42] and a lack of endometrial fibronectin following ovulation has been observed in infertile women.[43] Hence, we selected *PHSRN-K-RGD* as the primary attachment peptide for further studies, as it supports both stromal and epithelial matrix engagement in the early stages of culture.

Primary human endometrial stromal cells encapsulated in peptide-modified PEG gels exhibit functional viability

Following identification of a fibronectin-derived peptide, *PHSRN-K-RGD*, that supports initial attachment of both endometrial epithelial and stromal cells to a synthetic PEG hydrogel ECM, we next evaluated the functional hormone-responsive phenotypic behavior of primary human endometrial stromal cells when encapsulated within 3D hydrogels. Specifically, hydrogels (comprising 5 wt% fPEG-VS and 40% crosslinked) contained the attachment peptide *PHSRN-K-RGD* (0.5 mM nominal concentration) and two additional peptides intended to capture local cell-secreted ECM. Matrix-binding peptides were designed to capture fibronectin (*FN-binder*, 0.25 mM) produced by endometrial stromal fibroblasts throughout the cycle [40,43] and both laminin and type IV collagen basement membrane proteins (*BM-binder*, 0.25 mM) that are normally produced by the epithelium during all menstrual cycle stages and locally produced and accumulated in the pericellular region of hormonally responsive fibroblasts in the stroma.[40,43,44]

Primary patient endometrial stromal cells (ESCs) from three different donors in the proliferative phase of the menstrual cycle were encapsulated within PEG hydrogels and assessed for the ability to undergo functional secretory differentiation (decidualization) in response to hormonal cues 0.5 mM cAMP and 1 μM medroxyprogesterone acetate (MPA) as described previously.[45,46] These decidualization cues were added at the start of the culture and in each medium replacement. By day 9, ESCs in control cultures (no stimulation) showed elongated and spindle-shaped

morphologies while ESCs stimulated with decidualization cues showed plump, rounded morphologies characteristic of a decidualization phenotype (Fig. 2-2A). While cytoplasmic shape changes were observed by phase contrast imaging, no difference in nuclear shape was found between control and cAMP/MPA stimulated primary cells (See Appendix Fig. 2A1) as has been previously described for an endometrial stromal cell line cultured in 3D collagen gels under decidualization conditions.[16]

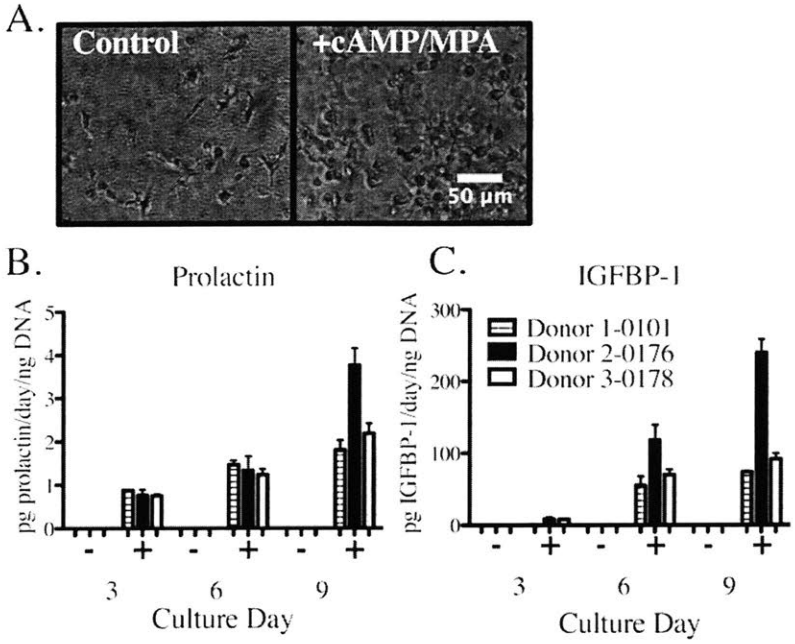

Figure 2-2. Primary human endometrial stromal cells encapsulated in synthetic ECM exhibit appropriate phenotypic responses to hormonal stimulation. (A) Proliferative phase endometrial stromal cells (ESCs) encapsulated (50,000 cells in 12 uL gel) in synthetic ECM hydrogel (nominal composition: 0.5 mM PHSRN-K-RGD, 0.25 mM FN-binder, 0.25 mM BM-binder). Control cultures (left panel) demonstrate matrix remodeling and elongation, whereas hormone-stimulated cells (+ right panel) exhibit morphological changes associated with decidualization (plumping). Primary endometrial stromal cells from 3 different donors (designated as "0101", "0176", and "0178" in the bar graphs) showed a functionally appropriate increase in (B) prolactin and (C) IGFBP-1 following hormonal stimulation on days 0, 3 and 6 of culture.

Secreted proteins IGFBP-1 and prolactin increased in stimulated conditions on days 3, 6 and 9 (after being stimulated on days 0, 3, and 6) of culture as compared to unstimulated ESCs, which did not secrete decidual proteins above the assay detection limits (Fig. 2-2B). Primary stromal cells were both viable and capable of hormone-mediated differentiation when encapsulated within PEG hydrogels, suggesting these cells would be capable of dynamic hormonal paracrine interactions when co-cultured with endometrial epithelial cells.

2.2.2 Biological and physical properties govern matrix remodeling

Epithelial monolayer morphology and stromal cell remodeling are influenced by crosslink density in long-term epithelial-stromal co-cultures

After establishing that primary endometrial stromal cells maintained a hormone responsive phenotype when encapsulated in 3D hydrogels, we explored the phenotypic effects of varying hydrogel crosslinking density on the establishment and evolution of relevant co-culture characteristics using cell lines as an initial model system. Co-culture features over the first two weeks, including epithelial barrier formation and encapsulated stromal cell remodeling, were investigated. For a given macromer composition and weight percent, synthetic ECM mechanical properties (including bulk stiffness and nano-scale ligand biophysical presentation), permeability, and topology are governed by the extent of crosslinking. The extent of crosslinking also governs the ease with which cells can remodel the synthetic ECM as the crosslinker can be cleaved by cell-associated proteinases. Hence, we varied crosslink density as the independent variable, recognizing the resulting epithelial monolayer and encapsulated stromal cell behaviors represent a convolution of responses to the properties affected by the crosslink density.

We formed gels by first reacting 8-arm PEG-VS macromers with adhesion and matrix binding peptides with a stoichiometry to yield an average of 0.7 peptides/PEG macromer (10% modification, 2:1:1 *PHSRN-K-RGD:FN-binder:BM-binder*, nominal 1 mM total). PEG macromers were combined with various concentrations of dithiol peptide crosslinker resulting in 40-70% of total macromer arms crosslinked. The hydrogels were crosslinked with *MMP-CL* peptide, containing the substrate GPQGIAGQ, which is reportedly cleaved by MMP2 and MMP9, allowing remodeling by cellular proteinases.[22,47,48] We selected a substrate with intermediate cleavage kinetics from among those reported in the literature,[22] aiming to achieve gradual remodeling and replacement by cell-produced ECM over two weeks. The post-swelling total peptide concentration ranged from 0.5 mM (40% crosslinked resulted in 2.2 swollen/initial volume) to 0.7 mM (70% crosslinked resulted in 1.5 swollen/initial volume).

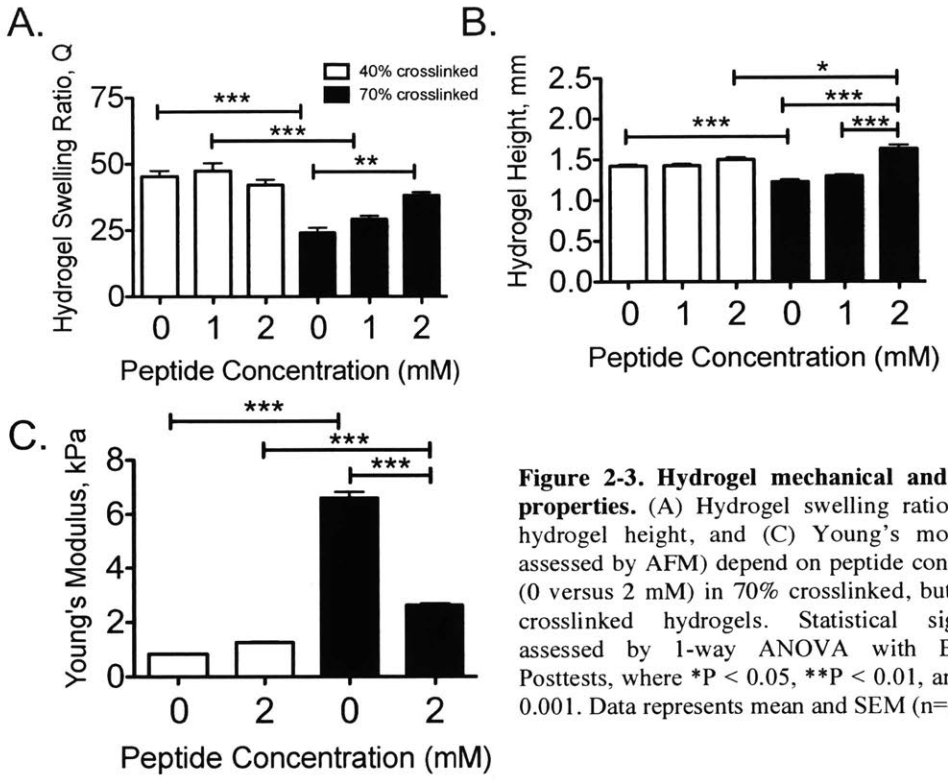

Figure 2-3. Hydrogel mechanical and swelling properties. (A) Hydrogel swelling ratio (Q), (B) hydrogel height, and (C) Young's modulus (as assessed by AFM) depend on peptide concentration (0 versus 2 mM) in 70% crosslinked, but not 40% crosslinked hydrogels. Statistical significance assessed by 1-way ANOVA with Bonferroni Posttests, where *P < 0.05, **P < 0.01, and ***P < 0.001. Data represents mean and SEM (n=6-8).

Hydrogel physical properties, including swelling ratio (Q), post-swelling height, and Young's modulus were evaluated for 40% and 70% crosslinked hydrogels comprising 0, 1, or 2 mM total peptides (2:1:1 ratio *PHSRN-K-RGD:FN-binder:BM-binder*) (Fig. 2-3). Given that hydrogel peptide functionalization occurs at the same sites as crosslinking, it was not surprising that for 70% crosslinked hydrogels, significant differences in swelling (Q, 24±2 versus 38±1), gel height (1.23±0.03 versus 1.63±0.05 mm) and Young's modulus (6.6±0.2 versus 2.6±0.1 kPa) were observed between 0 and 2 mM peptide addition. As expected, 70% crosslinked hydrogels displayed both increased swelling and gel heights and reduced Young's modulus upon addition of 2 mM, but not 1 mM, of peptide. The physical property changes associated with addition of 0 or 2 mM adhesion peptide in a 40% crosslinked hydrogel were insignificant given that the calculated molarity of free vinyl sulfones, after accounting for peptide crosslinker addition, are able to fully accommodate the 2 mM of adhesion peptide with 5.8 mM available for 5 wt% gel 40% crosslinked versus only 2.9 mM for 5 wt% gel 70%

crosslinked. Thus, for subsequent studies pertaining to cell phenotype differences in response to hydrogel crosslinking variations, 1 mM peptide functionalization was chosen to ensure complete crosslinking.

Epithelial monolayer formation on top of the hydrogel was investigated as chemical, mechanical, and topological features of the underlying substrate are known to influence the initiation and progression of an epithelial monolayer.[49–51] Gel formation including stromal cell encapsulation, was carried out during a centrifugation step to eliminate the meniscus, as we found that gel curvature compromised the epithelial barrier integrity, resulting in patchy areas near edges of high curvature as reported for other epithelia.[49,52] These denuded areas were not observed on flat gels or on gel-free culture inserts (Fig. 2-4A). All gel crosslinker conditions resulted in a confluent epithelial layer by day 4 after initially seeding 7.5 X 10^4 Ishikawa cells (Fig. 2-4B). However, by day 12, defects (holes) were observed in epithelial layers cultured on the most highly crosslinked gels, and complete delamination was observed at 70% crosslinking. Few monolayer defects developed for the 40% crosslinker condition after two weeks in co-culture.

Next, we evaluated the ability of encapsulated stromal fibroblasts to elongate and migrate within the hydrogel over two weeks in co-culture. Stromal fibroblasts, which were displaced to regions of the gel near the membrane during initial gel formation and centrifugation, remained rounded at days 7 and 14 in the 70% crosslink condition, unless they were in direct contact with the membrane (Fig. 2-4C). In contrast, stromal fibroblasts encapsulated in the 40% crosslinked gels and co-cultured with an Ishikawa epithelial monolayer appeared to migrate toward the epithelial layer from their initial position close to the membrane, as they were present in the middle of the gel at days 7 and 14 and showed enhanced elongation near the epithelial layer (Fig. 2-4C). The epithelial layer produces cytokines that may stimulate such migration, including PDGF-BB (See Chapter 4).[53,54] One explanation for the failure of cells to elongate and migrate in the 70% crosslink condition is that the cells must cleave a greater number of crosslinks, and are kinetically trapped, but an additional plausible explanation is that the dense crosslinks also obscure access to the adhesion ligands, and may prevent the integrin clustering required to gain sufficient signaling and traction for motility.[55–57]

Additional insight into the evolution of the encapsulated stromal cell behavior is revealed by examination of the thickness of the stromal layer, as the thickness represents a balance of both gel swelling due to crosslink cleavage and gel contraction due to cells depositing new matrix. Phase images of the epithelial layer and the culture insert membrane were used as boundaries to measure the in situ gel height. Measurements were the average of three locations across the diameter of the hydrogel over three weeks in cultures. Scans in the focal plane of the epithelial layer of each culture showed variation of (~30 um in height) evolving after the first week, due to formation of dome-like structures in the epithelium that spanned ~100 um in width. Hydrogels heights of ~450 μm and ~475 μm were consistently observed for the 70% and 40% crosslinked gels, respectively (data not shown). Stromal cells encapsulated in collagen gels often shrink substantially in dimension during culture due to matrix compaction,[17,23,58] whereas synthetic gels typically swell upon cleavage of crosslinks.[59] Even though the encapsulated cell concentration (nominally 4 x 10^6 cells/cm^3) was at least twice the value commonly reported for encapsulated stromal cultures,[17,58,60] gels did not change dimensions significantly. We therefore examined additional phenotypic behaviors, including matrix accumulation, using the 40% crosslink condition as it permitted epithelial barrier formation and fibroblast proteolytic remodeling and migration to occur.

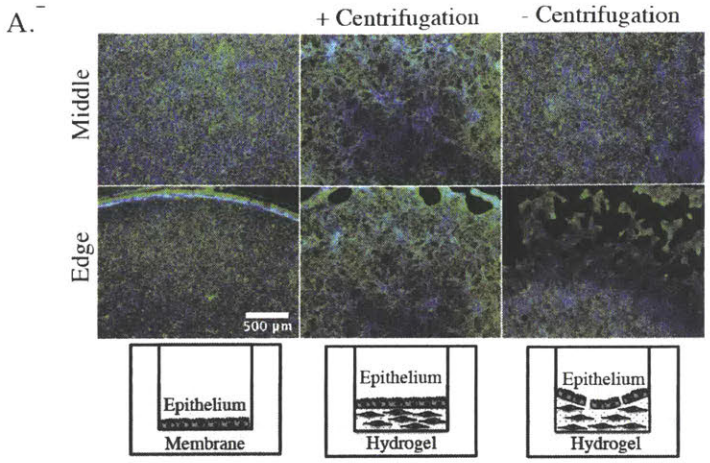

Figure 2-4. Systematic variation of crosslink density in synthetic hydrogels alters epithelial monolayer integrity and fibroblast matrix remodeling. (A) Epithelial cells plated directly onto the Transwell membrane (left) or onto encapsulated stromal cell layers that were either centrifuged to remove meniscus (middle) or static (right) were cultured for 7 days, then fixed and stained for the epithelial marker CK-18 (green) and for nuclei with DAPI (blue). Schematics below illustrate the approximate cross sectional geometry of each culture configuration.

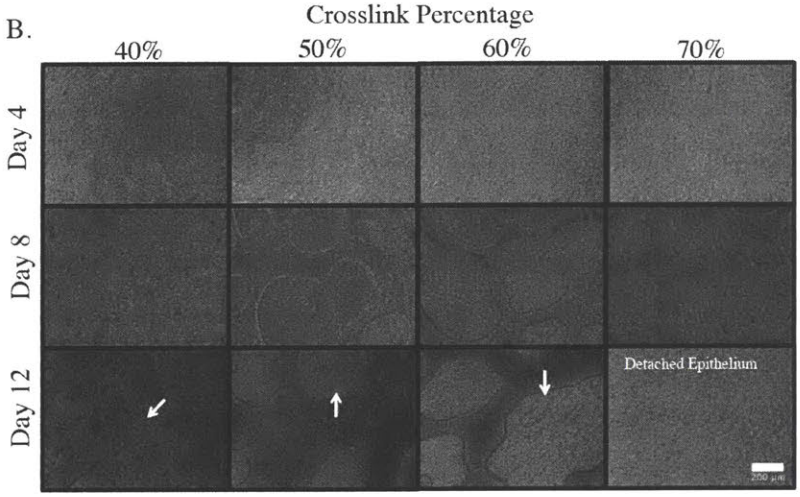

(B) Phase contrast images of Ishikawa epithelial sheet formation on top of hydrogels containing encapsulated tHESCs, illustrating enhanced monolayer integrity for lower thiol:VS crosslinking ratios (40%) after 12 days in co-culture; higher crosslinker ratios resulted in larger hole formation in the sheet and eventual delamination in the 70% condition by day 12.

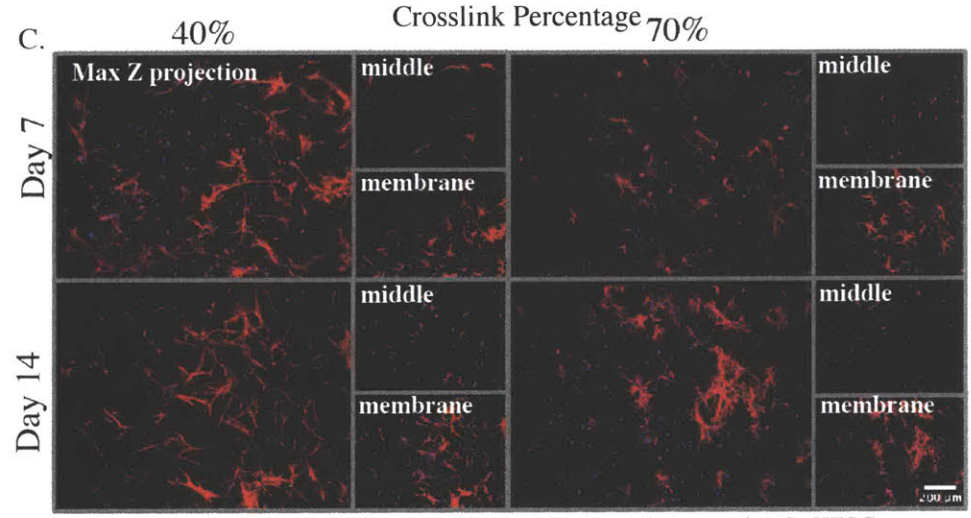

(C) Confocal maximum intensity Z-projection images of encapsulated tHESCs grown in co-culture showed elongated fibroblasts throughout the 3D gel volume for lower crosslinking percentages (40% versus 70%) over 7 and 14 days in co-culture. In comparison, the 70% crosslinking condition showed rounded cells in the middle of the hydrogel at both 7 and 14 days, with elongated cells present only at the membrane interface. Phalloidin (red) stain for F-actin with DAPI (blue) nuclear stain. Images shown are the maximum Z projection through the entire hydrogel (~200 μm mounted), and individual z-slices showing the middle (100 um above the gel-membrane interface) and 10 μm above the gel/membrane interface for each condition (smaller images). Hydrogels contained 0.5 mM *PHSRN-K-RGD*, 0.25 mM *FN-binder*, and 0.25 mM *BM-binder*.

Matrix-binding peptides enhance deposition of Ishikawa epithelial-secreted ECM

The initial establishment and subsequent evolution of cell-matrix interactions may be influenced by different peptides within the synthetic ECM. After identifying peptides that mediate initial cell attachment, *PHSRN-K-RGD*, and crosslinker conditions that allow cell protease remodeling of the microenvironment, we investigated how inclusion of peptides with affinity to matrix proteins influences deposition and organization of local cell-produced ECM. Cell-secreted ECM anchors cells to their microenvironments and regulates myriad cell functions from survival to differentiation.[61–63] The basement membrane, a specialized ECM enriched in laminin, type IV collagen, and various heparan sulfate proteoglycans, underlies the epithelial layer and separates epithelial and stromal compartments.[62] Although epithelial cells produce basement membrane proteins at their basolateral surfaces in culture, PEG gels tend to resist protein adsorption, and thus ECM produced by cells may disperse into the culture medium and fail to accumulate to significant levels. We speculated that inclusion of small peptides that bind to ECM proteins might foster more robust ECM deposition in a locally responsive manner – i.e., accumulation of basement membrane proteins by epithelial cells and a stromal matrix (fibronectin evolving to fibrillar collagen) by stromal cells.

To test the effects of *FN-binder* (fibronectin) and *BM-binder* (collagen IV and laminin) on ECM accumulation, we reconsidered the constraint on total peptide concentration in light of the results from Fig 2-4, which show that the 40% crosslinking condition is preferable for morphogenesis of stroma and stable retention of the epithelial layer in co-cultures of endometrial cell lines. The total combined concentration of functional peptides (i.e., *PHSRN-K-RGD*, *FN-binder*, and *BM-binder*) in the gel is constrained by the common VS-thiol chemistry used for both crosslinking and functionalization (Fig. 2-3). Near-complete reaction of the 8 pendant VS-groups on the PEG macromers is required to achieve 70% crosslinking for a total nominal functional peptide concentration of 1 mM, which affords only 0.5 mM *PHSRN-K-RGD* integrin-binding peptide, a concentration below the 1 mM associated with enhanced attachment of stromal cells in the 2D studies (Fig. 2-1B). We therefore chose a nominal 2 mM total peptide concentration (1 mM *PHSRN-K-RGD*, 0.5 mM *FN-binder*, 0.5 mM *BM-binder*) to further enhance interactions with stromal cells for future studies involving longer-term

cultures and more detailed investigations of phenotypes. Indeed, this gel formulation resulted in culture morphologies characterized by fewer and smaller defects in the epithelial layer over more than two weeks, and redistribution of a significant fraction of stromal cells from the near-membrane region into the gel near the epithelium (Fig. 2-5A).

Having verified that the 2 mM total peptide concentration resulted in enhanced morphological phenotypes, we then examined whether *BM-binder* influenced ECM accumulation and other properties of the epithelial layer by immunostaining constructs at the one week time point after a confluent monolayer was achieved. Epithelial cells (Ishikawa) attached, proliferated, and formed an epithelial sheet when seeded at 2.3 x 10^5 cells/cm^2 in all conditions with or without matrix binders as evidenced by immunostaining for CK-18, which anchors hemidesmosomes and actin structures to the underlying basement membrane (Fig. 2-5B). However, in the absence of *BM-binder* (i.e., in gels containing no matrix binders, or just *FN-binder*), accumulation of basement membrane (as assessed by collagen IV immunostaining) by the epithelial layer after one week of co-culture was very sparse, even in the presence of *FN-binder* (Fig. 2-5B). This is consistent with known properties of basement membrane assembly, which proceeds independent of fibronectin.[64,65] In contrast, abundant collagen IV immunostaining was observed beneath epithelial cells when *BM-binder* was included in the gels used for co-culture (Fig. 2-5B). Furthermore, collagen IV matrix patterning appears similar to cytoskeletal protein CK-18 organization suggesting that matrix binders may also contribute to the structural organization of the epithelial layer rather than simple accumulation of basement membrane matrix.

The images in Fig. 2-5B represent a shallow composite z-stack (30 μm) as the surface of the epithelial layer undergoes morphogenesis in the first week to create small domes and valleys; hence, the composite image includes some regions of closely-associated fibroblasts, which also stain positive for pericellular collagen IV. Individual z-planes of the Fig. 2-5B projection image illustrate that there is abundant collagen IV staining associated with long thin fibroblasts (Fig. 2-5C, arrows) that have migrated and are closely associated with the epithelial layer in all of the tested conditions. Fibroblasts were visualized in the same plane as Ishikawa nuclei in many instances.

A.

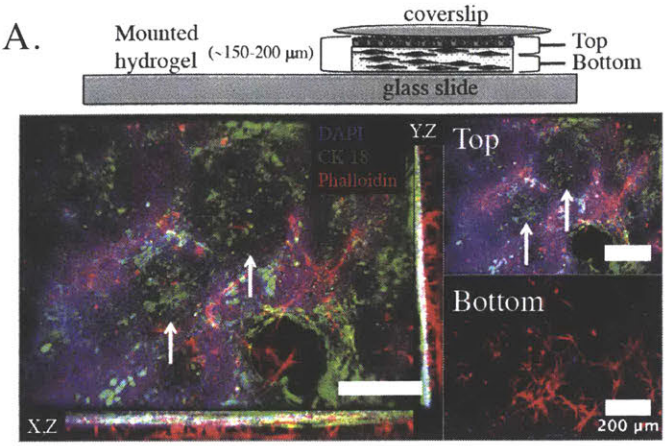
coverslip
Mounted hydrogel
(~150-200 μm)
Top
Bottom
glass slide
DAPI
CK 18
Phalloidin
YZ
XZ
Top
Bottom
200 μm

B.

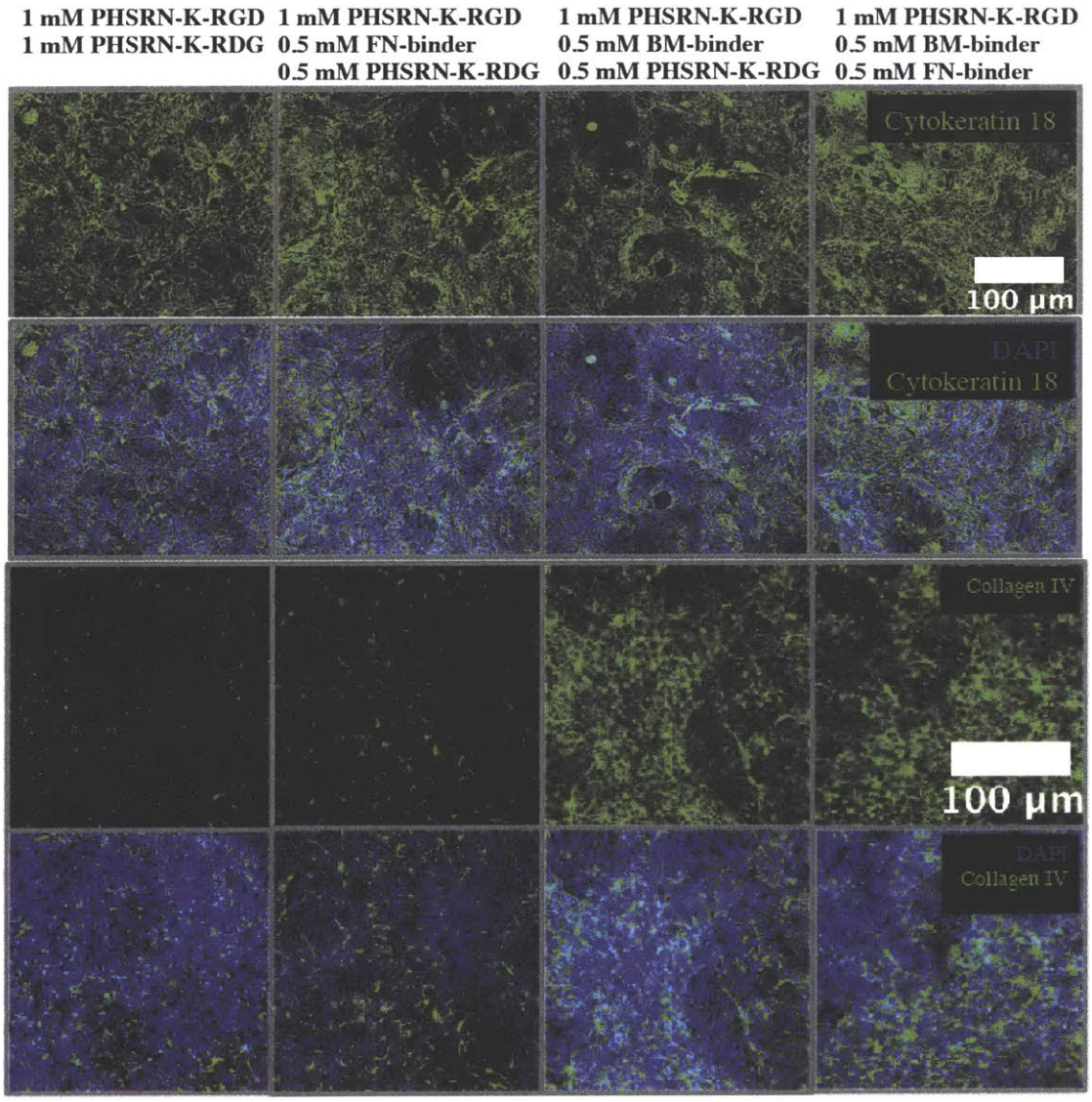
1 mM PHSRN-K-RGD
1 mM PHSRN-K-RDG
1 mM PHSRN-K-RGD
0.5 mM FN-binder
0.5 mM PHSRN-K-RDG
1 mM PHSRN-K-RGD
0.5 mM BM-binder
0.5 mM PHSRN-K-RDG
1 mM PHSRN-K-RGD
0.5 mM BM-binder
0.5 mM FN-binder
Cytokeratin 18
100 μm
DAPI
Cytokeratin 18
Collagen IV
100 μm
DAPI
Collagen IV

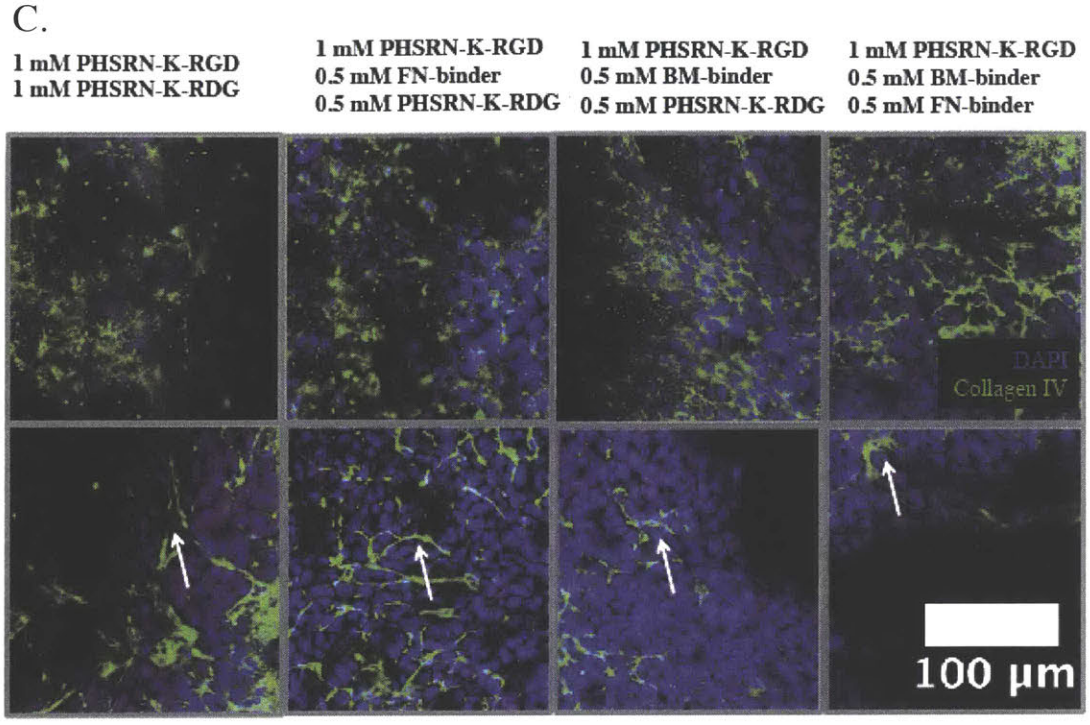

Figure 2-5. Enhanced epithelial extracellular matrix deposition and organization by incorporation of matrix-binding peptides for collagen IV/laminin. (A) 3D confocal reconstruction of a co-culture fixed and stained at day 25 shows encapsulated tHESCs distributed throughout the hydrogel with a mostly defect-free contiguous layer of Ishikawa cells on top displaying topological domes (arrows); maximum intensity Z-projection (~150 µm) of entire coverslip mounted hydrogel as schematically presented above, Ishikawa epithelial cells and underlying tHESCs (top) and tHESCs only (bottom), where epithelial cells are stained for CK-18 (green), F-actin stained with phalloidin shows stromal cells (red), and nuclei with DAPI (blue). (B) Confocal maximum Z projections (30 µm) of epithelial sheet phenotype +/- matrix-binding peptides after 7 days in co-culture shows Cytokeratin-18 (green, top panels) and organized collagen IV (green, bottom panels) when *BM-binder* is present. (C) Collagen IV (green) staining at the top of the epithelial layer (top images) and 15 µm below (bottom images) for conditions +/- matrix-binding peptides after 7 days and DAPI-stained nuclei (blue)). Single Z-planes show that the epithelial layer has organized, cell-associated collagen IV when BM-binder is present (top images) and fibroblasts that have migrated to the base of the Ishikawa layer show collagen IV staining in all conditions (arrows). Hydrogels contained 1 mM *PHSRN-K-RGD*, +/- 0.5 mM *FN-binder*, and +/- 0.5 mM *BM-binder* for a total of 2 mM peptide. *PHSRN-K-RDG* (scrambled) was used in place of missing matrix-binding peptides to correct for differences in total peptide concentration to reduce mechanical property differences among conditions.

Migration and intimate association of stromal fibroblasts with epithelia is consistent with other heterotypic cell culture systems where pericellular fibroblasts may become locally activated contributing to matrix production of collagens and fibronectin immediately surrounding adjacent epithelia.[66,67] The presence of collagen IV in the stromal layer is expected as endometrial fibroblasts, like fibroblasts from many other tissues, produce collagen IV.[44] However, collagen IV immunostaining in the stromal layer was strongly visible only in the upper region of the co-culture, near the epithelial

cells, and was faint in the deeper regions of the stroma (data not shown), suggesting that collagen IV in the pericellular region of the fibroblasts may derive primarily from interactions with epithelia. In normal human endometrium, collagen IV immunostaining is localized to the basement membrane except during hormone differentiation where decidual cells (stromal fibroblasts that undergo differentiation in response to hormones) secrete basement membrane proteins locally around themselves, including collagen IV and laminin.[40,43,68,69] Since we used the tumor-derived Ishikawa epithelial cells and the human immortalized stromal cells, the appearance of collagen IV staining in the stromal layer near the epithelia may arise from the transformed nature of these cells, or it may reflect that the early stages of culture are similar to a wound-healing phase where provisional matrix is deposited as a transition to regenerated normal tissue structure.[70] Our goal in these screening studies was to determine if the matrix-binding peptides could locally influence matrix accumulation, and indeed, enhanced collagen IV accumulation and organization was observed when matrix-binding peptide, *BM-binder,* was present.

Matrix-binding peptides enhance accumulation of stromal-secreted ECM

Having established that *BM-binder* and *FN-binder* peptides in combination dramatically enhanced accumulation of collagen IV at the basal surface of the epithelial layer, we investigated the influence of these peptides on the accumulation and properties of ECM secreted by stromal cells encapsulated in the gel beneath the epithelial layer. Both cell-produced and plasma-derived fibronectin are major components of provisional stromal wound-healing matrices that are ultimately remodeled to collagen-rich ECM that replaces the fibronectin-rich scaffold.[70] Fibronectin binds collagens and other ECM molecules to facilitate this evolution of ECM architecture.[65] We included *FN-binder* in the gel to facilitate the natural stromal ECM evolutionary process, speculating that stabilization of FN secreted by stromal cells immediately after encapsulation would provide a foundational ECM for further matrix deposition and remodeling.

Fibronectin accumulated in all conditions after two weeks with no discernible differences at the level of immunostaining (Fig. 2-6A), which is not surprising as the gel encapsulating the stromal cells likely hinders diffusion of fibronectin away from the pericellular region and immunostaining does not reveal subtle differences in ECM

organization, or presence of other cell-produced ECM molecules that might bind to FN to create a more fully assembled ECM. In order to further probe ECM composition and structure, we live-imaged the stromal layer with two-photon second harmonic imaging to visualize fibrillar collagens (i.e., collagens I-III and others, excluding the non-fibrillar collagen IV).[71,72] A cell associated second harmonic signal was observed in the presence of matrix-binding peptides, especially the *FN-binder*, but was absent without matrix stabilizing peptides (Fig. 2-6B). The signal was greatly enhanced when both matrix binders were present, indicative of organized structural matrix assembly.

Further quantification of collagen matrix proteins was assessed by measurement of hydroxyproline, an analog of the amino acid proline that is post-translationally hydroxylated, and is found in abundance in collagen matrix proteins. Collagen content was increased in all conditions with matrix binders present, and was greatest in the condition with both *FN* and *BM-binder* likely due to enhanced stabilization of various collagens, including both fibrillar collagens and collagen type IV (Fig. 2-6C). In particular, a 1.3-, 1.1- and 1.5-fold increase in hydroxyproline content (when normalized to total DNA per condition) was associated with the presence of *BM-binder* alone, *FN-binder* alone, or *BM-binder* + *FN-binder*, respectively when compared to *PHSRN-K-RGD* alone. *BM-binder* resulted in statistically significant increases in hydrogel hydroxyproline content, which is likely due in part to the stabilization of collagen IV basement membrane matrix at the hydrogel epithelial barrier interface. These differences in matrix deposition were observed in conditions that are likely less than optimal overall for matrix deposition, as cells were maintained in a standard culture medium containing 0.01 mM ascorbate in the basal compartment, rather than in conditions that boost collagen production by supplementing with additional ascorbate to compensate for oxidation and depletion.[73,74] Further, softer matrices are less conducive to accumulation of fibrillar collagen compared to stiffer environments.[75] Fine tuning these environmental parameters, along with carrying out studies with primary cells, may reveal further differences in how the combination of matrix-binding peptides influences evolution of cell-secreted ECM.

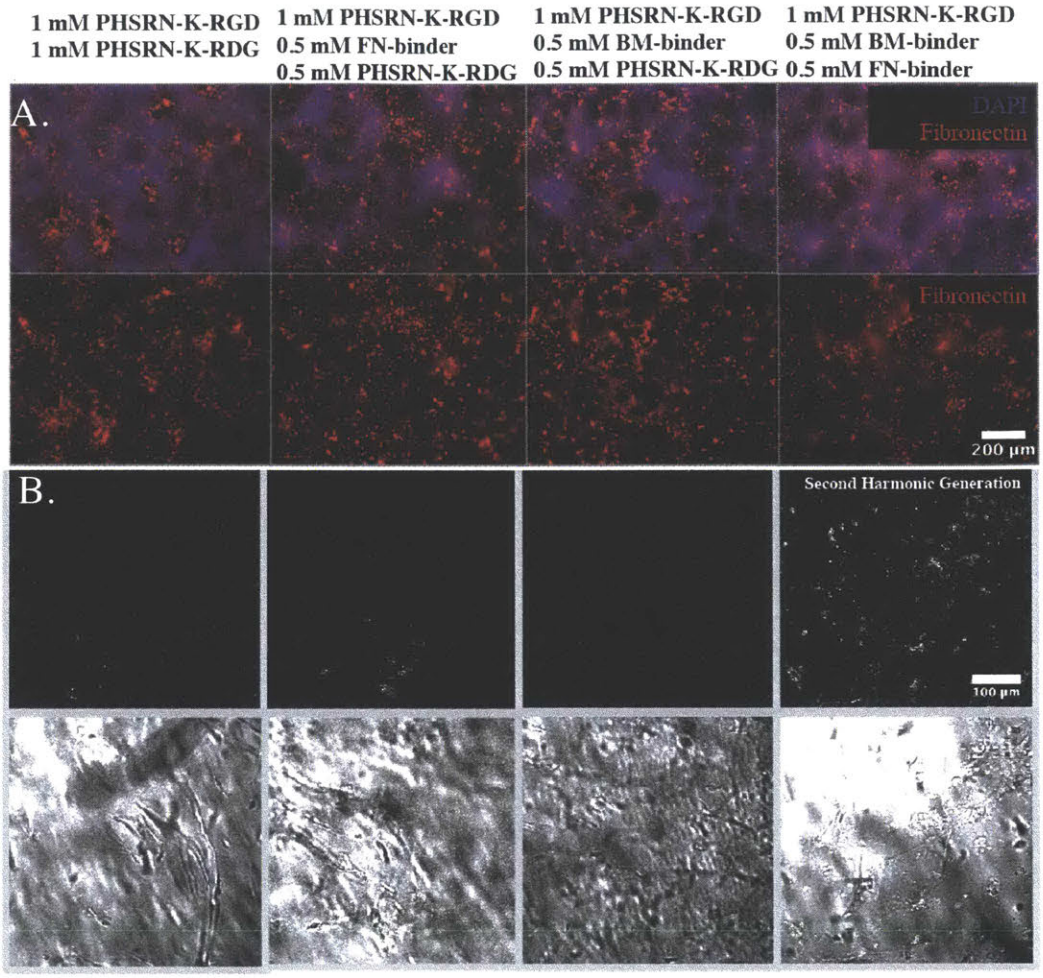

Figure 2-6. Enhanced stromal extracellular matrix accumulation by incorporation of matrix-binding peptides for fibronectin and collagen IV/laminin. (A) Immunofluorescence images on day 16 of co-culture showing fibronectin (red) accumulation of encapsulated stromal cells (DAPI-stained nuclei (blue)) occurs in all conditions with *PHSRN-K-RGD*. (B) Second harmonic imaging shows fibrillar collagen matrix deposition (white) in conditions with *FN-binder* after 14 days of culture, with significant enhancement in the presence of both *FN-binder* and *BM-binder* but no apparent deposition with *BM-binder* alone (top panel is a maximum Z projection of 250 μm for unfixed hydrogels imaged while hydrated on a coverslip) and the bottom panel shows a phase image (from a single z plane to illustrate the presence of stromal cells in all conditions) merged with the second harmonic signal. (C) Hydroxyproline assay to quantify total collagen content shows increases for co-cultures at day 14 with *BM-binding* peptide or both matrix-binding peptides when compared to adhesion *PHSRN-K-RGD* peptide alone where statistical significance is indicated as *$P < 0.05$, **$P < 0.01$, and ***$P < 0.001$ for one-sample, two-tailed t-tests on the log transformed fold-changes. Hydrogels contained 1 mM *PHSRN-K-RGD*, +/- 0.5 mM *FN-binder*, and +/- 0.5 mM *BM-binder* for a total of 2 mM peptide. *PHSRN-K-RDG* (scrambled) was used in place of missing matrix-binding peptides to correct for differences in total peptide concentration to reduce mechanical property differences among conditions.

2.2.3 Co-culture viability and hormone responsiveness

In vitro endometrial cell line co-cultures are proliferative and hormone responsive for at least 2 weeks

Having established a synthetic ECM composition that fosters desirable morphologies and matrix accumulation, we then examined the proliferative and hormone responsive phenotypes of these cultures. The cultures were maintained in low serum conditions starting on day 3 (1% FBS in apical medium; 0% serum in basal medium); nevertheless, Ishikawa epithelial cells exhibited robust and sustained proliferation throughout the culture period (34.7 ± 2.5% and 34.5 ± 1.9% of nuclei stained positive for EdU after 4-hour incorporation on days 7 and 14, respectively; Fig 2-7A). This proliferation of Ishikawa cells in low serum is consistent with other reports.[76,77] Stromal cells (tHESCs) encapsulated in the 3D synthetic ECM similarly showed sustained, though less pronounced, proliferation (18.9 ± 4.0% and 19.3 ± 1.9% of cells incorporated EdU over 4 hours on days 7 and 14, respectively), with proliferative cells distributed throughout all regions of the hydrogel. This stromal proliferation rate is consistent with observations of ~3-fold increase in DNA content when dermal fibroblasts were encapsulated in RGD-modified PEG gels and cultured for two weeks.[23]

We initially seeded 1.25 X 10^5 total cells (7.5 X 10^4 Ishikawa and 5 X 10^4 tHESC), corresponding to ~ 1 μg of total DNA. The increase to ~2 μg of total DNA present at days 12 and 24 of co-culture represents roughly one population doubling of the cells that were initially seeded. Interestingly, despite the observed sustained DNA synthesis, the total DNA content of the cultures (i.e., combined epithelial and stromal cells) showed insignificant change from day 12 to day 24 (Fig. 2-7B), suggesting cells are being lost from the cultures at the same rate as they are being produced. AlamarBlue assay additionally showed initial increases in metabolic activity, mainly observed in the apical media, likely due to proliferation and increased cell numbers in early culture stages (Fig. 2-7C). Metabolic activity peaks when dynamic morphogenesis of the epithelial layer begins ~week 2 before declining to a basal rate similar to that observed at 1 week in culture, and basal levels persisted through culture week 4.

The most likely mechanism of cell loss is through continuous dynamic morphogenesis of the epithelial layer involving groups of cells that form domes and then

detach either by terminal differentiation and apoptosis or by budding off as clumps that float in the apical medium, leaving a defect in the monolayer. Epithelial barriers are known to undergo dynamic growth, differentiation and morphogenic processes to replace terminally differentiated cells which are thought to comprise locally formed domes.[12,77,78] Domes and valleys in the epithelial monolayer were observed after the cells reached confluence (around one week of co-culture), and these morphological features persisted during the remaining culture weeks.

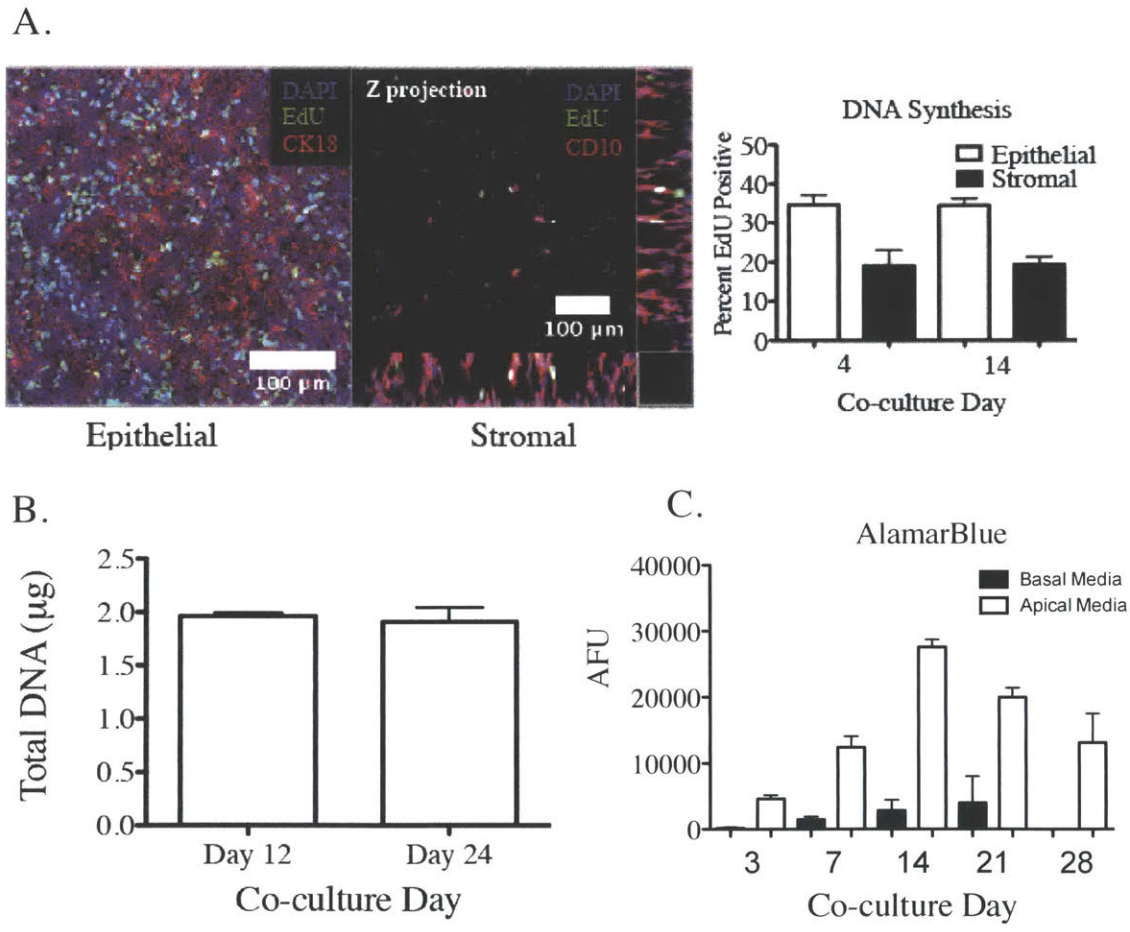

Figure 2-7. Endometrial tHESC stromal and Ishikawa epithelial cell co-cultures are proliferative and metabolically active for more than 2 weeks. (A) Representative images (left) and quantification of images (right) analyzing DNA synthesis for stromal and epithelial cells on days 4 and 14 of co-culture using EdU incorporation (green) to assess DNA synthesis and DAPI (blue) to stain all nuclei; CK18 (epithelial) or CD10 (stromal) stains in red allow quantification of each cell type individually. (B) Total DNA in co-culture does not change between co-culture days 12 and 24 (where n=2 and 6 hydrogels analyzed on days 12 and 24, respectively). (C) AlamarBlue metabolic assay was performed on the apical and basolateral side of Transwell co-cultures on days 3, 7, 14, 21 and 28 of culture (n=3 hydrogels quantified per condition).

Previous culture models showed epithelial differentiation, including monolayer morphogenesis and dome formation, is enhanced by increasing media serum content or culturing in the presence of fibroblasts.[52,77,79] Thus, we investigated the effect of serum content (low-1% versus high-10%) and fibroblast presence on the frequency and size of epithelial domes that formed in the monolayer over 3 weeks in culture. While dome frequency was slightly increased in co-culture at day 5, compared to Ishikawa monocultures alone, later dome frequency did not depend on either serum composition or the presence of endometrial stromal cells (Fig. 2-8A). Although previous research using Ishikawa cells showed serum media levels >1% are necessary for dome formation (within 48hr), our results suggested that lower serum levels also support dome formation, but that the domes only become visible after longer culture periods >5 days.[77] Dome frequency remained fairly constant from day 5 through day 26 in culture, whereas average dome size increased in all conditions (Fig. 2-8B). The presence of 10% serum significantly increased dome size in co-cultures compared to monocultures beyond 17 days, and resulted in comparable dome sizes observed in 1% FBS conditions in mono- or co-cultures. These results agree with previous literature where lower serum levels result in larger, more stable dome formation.[77] It is possible that having stromal cells in culture provides a protective mechanism against serum-induced dome collapse/cell loss either by neutralization of serum factors leading to terminal differentiation or secretion of factors that enhance dome stability.

Visualization of both intact domes (arrows) and a subsequent barrier defect are representative of features observed after 3 weeks in co-culture (Fig. 2-5A, day 25 of co-culture). The domes appear to be the result of epithelia detaching from the hydrogel surface and extending into the apical media as evidenced by the lack of nuclei in contact with the hydrogel surface underneath these raised structures. Additionally, we observed that over the course of a couple days, some dome regions collapsed resulting in holes or defects in the monolayer with visible cell debris present within. This is consistent with cell death in response to loss of cell-matrix interactions. We observed that domes were more likely to remain intact, without progression to a barrier defect, in conditions with less crosslinking (40% versus 70%) or higher adhesion ligand density (2 mM versus 1

mM total nominal peptide), possibly suggesting that ligand accessibility and integrin clustering ability may be important for maintenance of epithelial layer integrity.

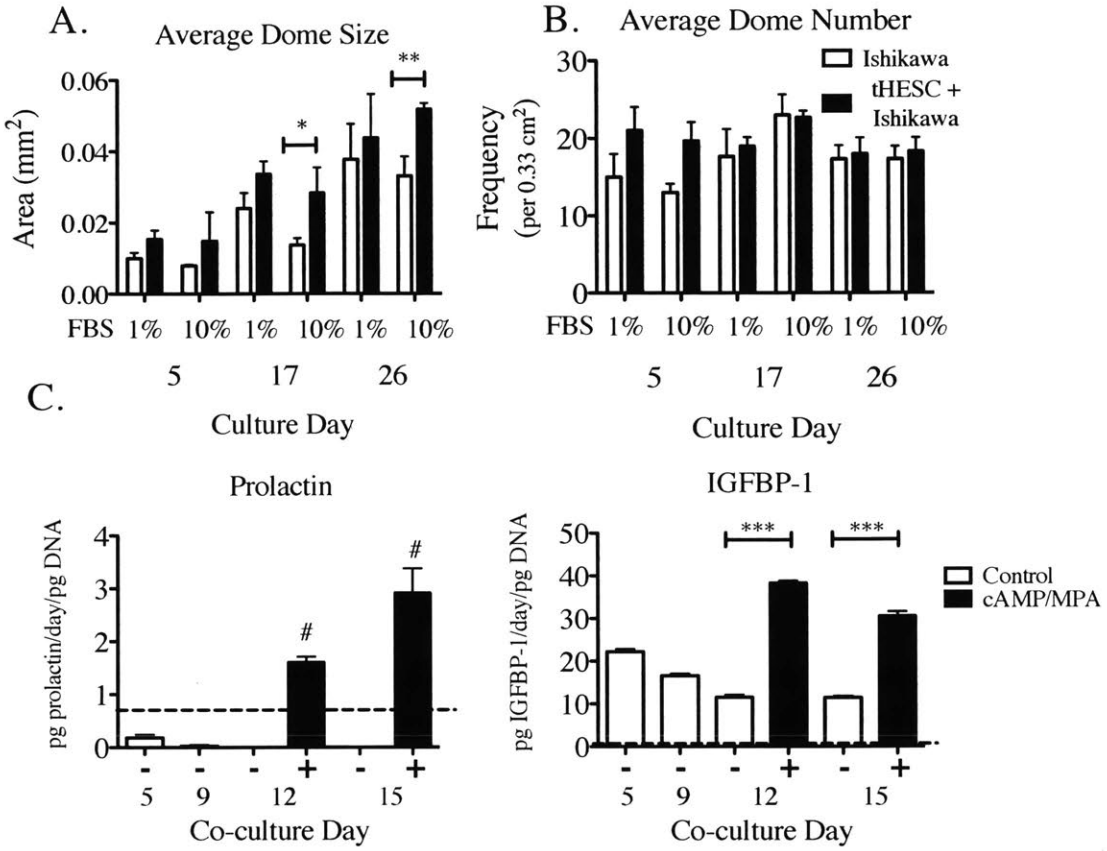

Figure 2-8. Endometrial epithelial layers undergo morphogenesis and co-cultures remain hormone responsive for at least 2 weeks. Dynamic epithelial layer morphogenesis as assessed by dome formation was influenced by fibroblasts in co-culture, but not affected by 1% versus 10% serum- supplemented media. At days 17 and 26, epithelial dome (A) size but not (B) frequency was significantly increased for co-cultures in 10% media versus epithelial cells in monoculture where *P < 0.05, **P < 0.01, and ***P < 0.001 for 2-way ANOVA with Bonferroni correction. (C) Co-cultures undergo hormone-mediated decidualization in response to 0.5 mM 8-Br-cAMP and 1 μM MPA stimulation on days 9 and 12 of co-culture by statistically significant increases in secretory protein production (measured apically) of IGFBP-1 and prolactin on days 12 and 15 of co-culture. Statistical significance, *P < 0.05, **P < 0.01, and ***P < 0.001 for two-tailed t-tests comparing unstimulated to stimulated cultures or # P < 0.05 for one sample t-test different than detection limit of assay (dotted line represents 3 standard deviations above the blank mean). Hydrogels contained 1 mM *PHSRN-K-RGD*, 0.5 mM *FN-binder*, and 0.5 mM *BM-binder*

Finally, the cultures remained hormone-responsive, as assessed by the response to decidualization cues 0.5 mM 8-Br-cAMP and 1 μM medroxyprogesterone acetate (MPA). When these were added on days 9 and 12, they elicited significant increases in secretion of IGFBP-1 and prolactin measured on days 12 and 15 (Fig. 2-8C). The decidualization response is marked by secretory protein production of IGFBP-1 and prolactin by endometrial stromal cells in response to decidualizing cues including progestogens (MPA, progesterone) and cAMP.[16,46,80] As previously reported for other culture configurations, where co-stimulation with cAMP sensitized stromal cells to MPA induced decidual protein production,[46] no stimulation by estradiol was required prior to addition of decidualization cues in order to elicit production of decidual proteins prolactin and IGFBP-1 in this 3D in vitro model system. The establishment of this long-term co-culture system may enable future studies of how endometrial phenotype is regulated throughout an entire menstrual hormonal cycle, comparing primary cells from healthy and diseased patients, for example.

Primary 3D endometrial stromal and epithelial co-cultures are proliferative and respond to decidualization cues

While cell line models may provide reproducibility and some tissue specific function for some applications, primary cells offer the ability to elucidate differences in cytokine and growth factor cell-cell communication networks that may arise from normal biological heterogeneity in healthy women, and are needed to construct models of disease mechanisms in samples from diseased patients. We therefore evaluated the ability of the synthetic matrix (1 mM *PHSRN-K-RGD*, 0.5 mM *BM-binder*, and 0.5 mM *FN-binder*, 40% crosslinked) to support proliferation and hormone responsiveness of primary endometrial cells (isolated from proliferative biopsies) over two weeks in co-culture.

Since a single standard biopsy typically yields only 0.2-2 X 10^6 primary epithelial cells from proliferative phase endometrium, we investigated a range of seeding densities based on a benchmark of 10^5 cells/insert (3 x 10^5 cells/cm^2) for forming a monolayer of epithelium on transwells.[12] Cells were maintained for at most one week in culture prior to establishment of between 4-12 co-cultures per donor (see Methods). Epithelial monolayers formed for one donor (Fig. 2-9A) when epithelial cells were seeded at 7.5 X

10^4 cells per culture insert (2.3 X 10^5cells/cm^2) resulting in 430 μm^2 per cell, or 21 μm center-to center spacing. Lower seeding densities were ineffective: epithelial cells from two additional donors, seeded at 5 X 10^4 cells/insert (1.5 X 10^5cells/cm^2), resulted in initial incomplete coverage of the hydrogel surface and a patchy appearance throughout the entire two-week culture period, despite some evidence of proliferation (see below).

Three different donor co-cultures were assessed for the ability to respond to decidualization cues. The primary donor with epithelial cells seeded at 7.5 X 10^4 cells per insert and co-cultured for 2 weeks with stromal cells showed dramatic morphological responses to decidualization cues added at days 9 and 12 (Fig. 2-9A). CK18 and actin staining were both diffusely-localized in the absence of cAMP and MPA, but revealed a classic epithelioid layer morphology in the presence of hormones, with actin ringing the perimeter of cells (Fig. 2-9A). Although both conditions appear to have a contiguous cell layer revealed by actin staining, the CK18 staining in these images was not uniformly contiguous across the surface in the same regions, even when the actin stain was associated with an epithelioid morphology (Fig. 2-9A). Confirmation of the nature of the cells that appear to be CK18- in these images would require additional staining to rule out decidual cells (differentiated stromal fibroblasts). Concomitant with morphological changes, decidualization cues added on days 9 and 12 of culture resulted in significant increases in prolactin and IGFBP-1 protein levels on days 12 and 15 of culture (Fig. 2-9B). These studies establish the potential of this culture system to respond to physiological cues, and provide a foundation for future investigations of a range of physiological stimuli and responses involved in dynamic behavior of the endometrium.[81]

Additionally, DNA synthesis was assessed for two subsequent donors on day 15 of co-culture resulting in 7.8 ± 3.2% and 8.3 ± 1.6% EdU positive epithelial cells (CK18+) and 10.3 ± 3.1% and 15.5 ± 1.6% EdU positive stromal cells (CK18-) after EdU incorporation for 24 hour. Results are the average of a hormone stimulated and a control co-culture for each donor (Fig. 2-9C). Greater than 60% of CK18- cells were found encapsulated within the hydrogel (as opposed to spread on the culture insert membrane) after 15 days for both donors. Of those CK18- cells present on the membrane, 4.9 ± 0.3% and 5.6 ± 3.2% were EdU positive, indicating that most of the CK18- cells that were EdU positive were encapsulated within the hydrogel.

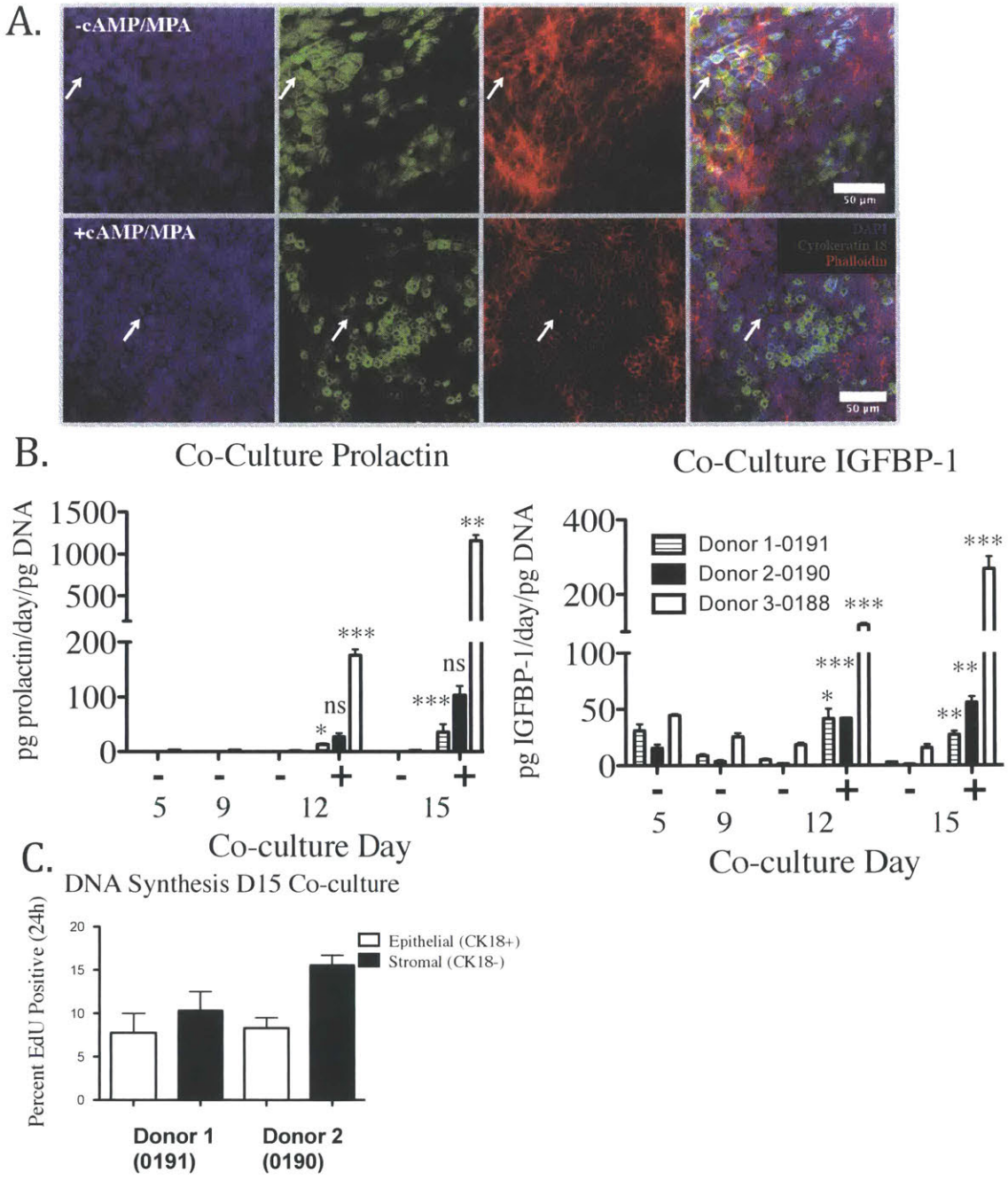

Figure 2-9. Primary proliferative phase endometrial stromal and epithelial cells in co-culture show proliferation and hormone-mediated decidualization. (A) Immunofluorescence images of epithelial layer with mitotic nuclei (arrows) show hormone responsive morphology after 15 days in co-culture (CK18 (green) epithelial cells, phalloidin (red) stains all cells, and DAPI stained nuclei (blue)). (B) Decidual protein (IGFBP-1 and prolactin) production is significantly higher on days 12 and 15 of co-culture in response to 0.5 mM 8-Br-cAMP and 1 µM MPA stimulation on days 9 and 12, n = 4-12 for each donor. (C) Primary co-culture viability was assessed by DNA synthesis on day 15 of co-culture during a 24 h period. Statistical significance is indicated as *P < 0.05, **P < 0.01, and ***P < 0.001 for one-tailed t-tests comparing unstimulated to stimulated co-cultures on days 12 and 15. Hydrogels contained 1 mM *PHSRN-K-RGD*, 0.5 mM *FN-binder*, and 0.5 mM *BM-binder*.

2.3 Materials and Methods

2.3.1 Materials and cell culture

Materials

PEG macromers (40 kDa, 8-arm) functionalized with vinyl sulfone (PEG-VS) were obtained from JenKem Technology (Beijing). All peptides were custom synthesized and purified (>95%) by Boston Open Labs (Cambridge, MA). Peptides used in these studies include the following: "*MMP-CL*," a dithiol crosslinking peptide containing a matrix metalloproteinase (MMP)-sensitive substrate, (Ac)GCRD-GPQGIAGQ-DRCG(Am);[22] "*RGD*," a fibronectin (FN)-derived adhesion peptide containing the canonical RGD motif from the 10th FN type III domain NH_2-GCRE-RGDSP(Am);[21] "*PHSRN-K-RGD*," a fibronectin-derived adhesion peptide containing both the RGD motif and the PHSRN synergy site from the 9th FN Type III repeat in a branched configuration to mimic features of the biophysical presentation in FN, (Ac)PHSRNGGGK-GGGERCG(Ac)-GGRGDSPY(Am);[24,36] "*PHSRN-K-RDG*," a scrambled control sequence where the RGD motif was scrambled reducing integrin binding; (Ac)PHSRNGGGK-GGGERCG(Ac)-GGRDGSPY(Am); "*GFOGER*," a collagen I-derived adhesion peptide, NH_2-GGYGGGPG$(GPP)_5$GFOGER$(GPP)_5$GPC(Am),[38] "*Lam-5*," a laminin 5-derived adhesion peptide, NH_2-GCRG-PPFLMLLKGSTR(Am) (Lam5);[39] "*FN-binder*," a peptide with affinity for FN, (Ac)GCRE-TLQPVYEYMVGV(Am);[82] and "*BM-binder*," a peptide with affinity for basement membrane proteins type IV collagen and laminin, NH_2-GCRE-ISAFLGIPFAEPPMGPRRFLPPEPKKP(Am).[83] For reactions, peptides were reconstituted in Milli-Q water (Millipore) at a concentration of 10 mM for adhesion and matrix binding peptides and 45 mM for *MMP-CL*. All other reagents and supplies were obtained as indicated in subsequent sections.

Cell culture

Ishikawa human endometrial adenocarcinoma cells (Sigma-Aldrich),[84,85] hTERT-immortalized human endometrial stromal cells (tHESCs) (ATCC),[86] and primary isolated endometrial stromal and epithelial cells were routinely cultured in a humidified atmosphere at 37°C and 5% CO_2 in phenol red-free DMEM/F12 (mixture of Dulbecco's Modified Eagle's Medium and Ham's F-12 (Gibco) media) supplemented with 1%

penicillin/streptomycin (Gibco) and 10% *v/v* dextran/charcoal treated fetal bovine serum (Atlanta Biologicals) (DMEM/F12/FBS). Epithelial cells were split 1:4 and stromal cells were split 1:2 once they reached 70-80% confluencey, and medium was replaced every 2-3 days. Following reports of possible contamination of endometrial cell lines by HeLa or other lines,[87] STR profiling analysis (Genetic Resources Core Facility, Johns Hopkins School of Medicine, Institute of Genetic Medicine) was used to confirm the fidelity of the tHESCs and Ishikawa cell lines against known cell databanks. Cell lines were routinely used prior to passage 10 and primary cells prior to passage 4.

Primary Endometrial Cell Isolation and Expansion

Purified endometrial glandular epithelium and stromal fibroblasts were isolated from proliferative phase eutopic endometrial biopsies using established protocols as described by Osteen and co-workers[88] with some modifications (Appendix). Pipelle biopsies (2 or 3 biopsies per donor) were obtained from women undergoing laparoscopic surgery for non-malignant gynecologic indications. All participants provided informed consent in accordance with a protocol approved by the Partners Human Research Committee and the Massachusetts Institute of Technology Committee on the Use of Humans as Experimental Subjects. Study enrollment was limited to pre-menopausal women with regular cycles (26-35 days) and excluded patients with an irregular or ambiguous cycle history or a history of hormone use in the prior 3 months. All specimens were from the menstrual/proliferative phase (day 1-14) according to the donor's menstrual history (Appendix Table 2A1). A standardized questionnaire was used to document clinical data.

Stromal cells were expanded in culture by seeding initial isolates (typical yield 1-5 x 10^6 cells per patient) into a T-25 or T-75 flask (Falcon) at a cell density of 2-5 x 10^4 cells/cm^2 in 4 mL or 8 mL of DMEM/F12/FBS, respectively. Cultures were grown to 80% confluencey then subcultured 1:2. Stocks were frozen at passage 2 in DMEM/F12/FBS 10% v/v DMSO (Sigma) with typical yields of 5 x 10^6 cells per patient, and 5 x 10^5 cells/vial. Freshly isolated epithelial cell glands were seeded as glandular fragments at an overall density of 0.2-2 x 10^6 cells per T-75 flask (Falcon). Epithelial cell density was confirmed prior to seeding by trypsinization and counting a portion of the glandular fraction. Stromal cells were maintained for up to two weeks prior to

cryopreservation. For primary co-cultures, epithelial and stromal cells were used within one week of being freshly isolated. Primary endometrial cells from six different donors in the proliferative phase were used for these studies.

2.3.2 Hydrogel formation

Michael-type polymerized PEG hydrogels (5 wt/wt%) were fabricated using 40 kDa 8-arm PEG-VS functionalized with cell adhesion and matrix-binding peptides. Peptide-functionalized PEG macromers, "fPEG-VS," were synthesized by incubating peptides with PEG-VS in 1x PBS, 1M HEPES (pH 7.8) buffer for 30 minutes to create macromers with 20% of the -VS groups functionalized with peptide (2 mM final concentration), with greater than 99% peptide incorporation, as assessed by Ellman's reaction, occurring after 30 minutes. The fPEG-VS solution was crosslinked with *MMP-CL*, adjusted to pH 7.8 with 1M NaOH just prior to addition, in a 0.4 thiol:VS ratio (unless otherwise noted). The concentration of free cysteine thiols was quantified utilizing Ellman's reagent (Sigma). Data about ambient temperature effect on hydrogel gelation time (Appendix Table 2A2).

2D attachment studies

Attachment was assessed for tHESCs and Ishikawa cells plated on PEG hydrogels (synthesized as described above) functionalized with adhesion peptides (*RGD*, *PHSRN-K-RGD*, *GFOGER*, or *Lam5*) at nominal concentrations of 0.25, 0.5, or 1.0 mM. The final gel solution was pipetted into 96-well angiogenesis plates (IBIDI) at 10 μL per well. Gelation proceeded for 15 minutes. Gels were then incubated in 70 μL of serum-free DMEM/F12 medium supplemented with 1% penicillin/streptomycin (DMEM/F12) overnight (5% CO2, 95% air, 37 °C), where they swelled ~2-fold in volume as measured by an increase in hydrogel mass. Cells were seeded at 4 x 10^5 cells/cm^2 in full-serum medium (DMEM/F12/FBS) at 50 μL per well. After a 6 h attachment period, wells were rinsed 2X with PBS, fixed in 4% paraformaldehyde for 30 minutes at room temperature and stained with DAPI. Wells were imaged using a Leica DMI 6000 microscope and Oasis Surveyor software. Images were binarized, and DAPI-stained cell nuclei were counted using ImageJ64 software. Attachment values were normalized to cell attachment in wells without a hydrogel.

3D stromal encapsulation

Hydrogels were fabricated on top of the membrane of Transwell inserts (Corning #3470, 6.5 mm diameter, 0.4 um pores, 0.33 cm^2 culture area, polyester) using Michael-type reaction chemistry. For these experiments, fPEG-VS macromers were prepared by reacting 8-arm PEG-VS (1.4 mM) with free thiols (-SH) on adhesion and/or matrix stabilization peptides in 1x PBS with 1 M HEPES (pH 7.8) for 30 minutes. Immediately after the functionalization reaction, the fPEG-VS macromer (average 6.4 free -VS groups per macromer) solution was mixed with a cell suspension (4.2 x 10^7 cells/mL in serum-free DMEM/F12, 1% penicillin/streptomycin). fPEG-VS macromers were then reacted with the cysteine thiol (-SH) groups on the bifunctional *MMP-CL* crosslinker in volumetric ratios of 8.6:1:0.4 fPEG-VS:cells:*MMP-CL* to yield a final crosslinking solution comprising 4.2 X 10^6 cell/mL (~50,000 cells in 12 μL), 2 mM total adhesion/matrix binding peptide, 1.2 mM total fPEG-VS macromers (5 wt%), and 1.9 mM crosslinking peptide *MMP-CL* in PBS, 1 M HEPES buffer (pH 7.8). Nominal peptide concentrations in the final gel were 1 mM *PHSRN-K-RGD*, 0.5 mM *FN-binder* and 0.5 mM *BM-binder* unless otherwise noted.

Hydrogel gelation, as determined by the point at which the solution could no longer be pipetted, occurred approximately 8 minutes (pH 7.8) after crosslinker addition, but varied between 8-12 minutes depending on the specific hydrogel formulation. The hydrogel solution was pipetted for 2 minutes to keep stromal cells in suspension, allowed to sit in tube for 3-7 minutes (where wait time = gelation time – 5 minutes), was transferred to inserts (12 μL/insert), manually spread with a pipette tip, then was centrifuged for 4 minutes at (330 RCF in an Eppendorf centrifuge 5810) to ensure gelation occurred in the middle of centrifugation creating a flat, meniscus-free hydrogel on top of the cell culture inserts. Plates were then incubated an additional 10 minutes at RT to allow crosslinking to proceed to completion. After gelation was complete, DMEM/F12/FBS was added to the apical (top) (100 μL) and basolateral (bottom) (600 μL) sides of the Transwell to achieve hydrostatic equilibrium. Cultures were maintained in a humidified incubator at 37 °C, 95% air, 5% CO_2.

Endometrial epithelial cell cultures on synthetic hydrogels with encapsulated stroma

Endometrial epithelial cells were seeded on top of gel-encapsulated stromal cells 24 h after initiation of stromal cultures. Ishikawa cells were harvested via trypsinization, resuspended in DMEM/F12/FBS, and seeded at a density of 75,000 cells/Transwell (225,000 cells/cm^2). Primary epithelial cells were harvested via trypsinization and seeded at 50,000-75,000 cells/Transwell (150,000-225,000 cells/cm^2). Apical medium was changed 24 hr after seeding to remove non-adherent epithelial cells. On day 3 of co-culture, medium was changed to maintenance media comprising DMEM/F12 supplemented with 1% DC-FBS, 1% penicillin/streptomycin, and 2% Cell Maintenance Supplement (Cocktail B) (LifeTechnologies CM4000) on the apical side (100 μL) and Williams E Medium (LifeTechnologies A1217601) supplemented with 1% penicillin/streptomycin, 4% Cell Maintenance Supplement (Cocktail B) (LifeTechnologies CM4000) and 100 nM hydrocortisone (Sigma 50-23-7) on the basolateral side (600 μL), with changes every 2-3 days thereafter.

Hormone-mediated decidualization of epithelial and stromal co-cultures and primary encapsulated endometrial stromal cells

Endometrial co-culture decidualization was assessed by stimulation with 0.5 mM 8-bromoadenosine 3′,5′-cyclic monophosphate (Sigma B5386) and 1 μM medroxyprogesterone 17-acetate (MPA) (Sigma M1629) in the apical and basal medium starting on days 9 and 12 of co-culture, respectively, according to common protocols previously described.[45,46] Apical medium (100 μL) was collected on days 5, 7, 9, 12, and 15 of co-culture and stored at -80 °C until analyzed by ELISA for proteins IGFBP-1 (R&D systems DY871) and prolactin (R&D systems DY682), indicative of secretory differentiation. Protocols provided by the manufacturer were adapted to allow ELISAs to be performed in a 384-well plate (ThermoFisher 464718) to minimize medium (sample) volume needed (see below). For primary patient endometrial stromal cell (ESCs) monocultures, cells were incubated with hormone-containing media on days 0, 3, and 6 of culture, and apical conditioned media (100 μL) samples were collected on days 3, 6 and 9 of culture. Reported values are the mean of 3-6 (apical samples) biological replicates (different gels) minus mean concentration of no-cell gel controls.

2.3.3 Hydrogel physical properties

Hydrogels were cross-linked as outlined above in the specific geometry of being sandwiched between two hydrophobic glass slides which had been treated with Rain-X Original Glass Treatment, rinsed with water, and separated with 1 mm spacer slides on either side. Hydrogels made from 20μL precursor solution, were swollen overnight in 2 mL 1X PBS at 37°C. Hydrogels were equilibrated to room temperature and removed from PBS immediately prior to measurements.

Hydrogel swelling ratio

For each hydrogel, the volumetric swelling ratio was estimated as the ratio of precursor volume to swollen gel mass and was used to calculate final peptide concentrations in the swollen hydrogel. Hydrogel height was measured with calipers and gels were then placed on tared glass slides and dehydrated for 48 h at 60°C. The mass swelling ratio, Q, is reported as the ratio of swollen mass to dry mass, each mass less the assumed mass of salt from PBS (10.7 mg/mL in liquid fraction) for n=6 hydrogels.

Atomic force microscopy

The elastic modulus of the hydrogels was measured using a commercial scanning probe microscope (Molecular Force Probe 3D, Asylum Research, Santa Barbara, CA). Force spectroscopy measurements were taken with two different types of functionalized cantilevers. The tip was modified with a 5μm diameter silicon oxide particle (Novascan Technologies, Ames, IA). The nominal spring constants of the PS and SiO2 cantilever was 0.07 N/m and 0.12 N/m. All hydrogels (20 μL precursor solution) were imaged in PBS at 25°C. Five force displacement curve measurements at 8 random and disperse locations were acquired for each gel. The quantitative elastic modulus (E) was extracted from the force displacement data using the Hertz model for a spherical tip.

$$E = \frac{3}{4}\frac{(1-\nu^2)F}{\sqrt{R}\delta^{\frac{3}{2}}}$$

Where F= applied force, R= radius of particle, δ= indentation depth, and ν= Poisson's ratio, which was assumed to be 0.5 for all hydrogels. IGOR Pro data analysis software (WaveMetrics, Lake Oswego, OR) was used to analyze all force curves.

2.3.4 Biochemical assays

DNA synthesis assay

Click-iT EdU Alexa Fluor 488 kit (Life Technologies) was used to quantify cells actively synthesizing DNA. On days 4 or 14 of co-culture, hydrogels were incubated with 10 μM of 5-ethynyl-2′-deoxyuridine (EdU) for 4 h for tHESC and Ishikawa cultures (or on day 15 for 24 h for primary co-cultures) at 37 °C, 95% air, 5% CO_2. Cells were fixed with 4% formaldehyde in 1X PHEM buffer and MQ for 1 h at RT. Cells were washed twice with 3% BSA in PBS and permeabilized with 0.5% Triton X-100 in PBS for 20 min at RT while shaking. Click-iT reaction cocktail was prepared as described by the manufacturer and 100 μL per well was added apically and 400 μL per well added basally. Cells were incubated for 30 min at RT protected from light while shaking. After cells were washed once with 3% BSA in PBS and once with PBS, they were incubated with DAPI diluted 1:1000 in PBS for 30 min at RT protected from light. Cells were stained with anti-Cytokeratin 18 or anti-CD10 as indicated below, washed twice with PBS and imaged using a Leica DMI 6000 microscope and Oasis Surveyor software. Total number of DAPI nuclei and total number of EdU nuclei were counted using ImageJ64 software. The percentage of cells synthesizing DNA was computed as the ratio of EdU positive cells divided by the total number of DAPI counterstained cells. Reported values are the mean of at least 3 ROIs for two technical replicates per condition.

Hydroxyproline assay for collagen quantification

The hydroxyproline content, indicative of collagen content, of a Transwell hydrogel was measured using the Hydroxyproline Assay Kit (Sigma MAK008). Briefly, 2-3 gels from each culture condition were combined and hydrolyzed in 100 μL 12 M HCl at 120°C in a heat block for 3 h. Hydroxyproline standards were prepared according to the manufacturer's protocol. The hydrolyzed sample was transferred to the 96-well plate with standards and incubated at 60°C to evaporate to dryness. The plate was allowed to come

to RT after overnight incubation and 100 µL of chloramine T/oxidation Buffer was added to each well and incubated at RT for 5 min followed by incubation with 100 µL/well 4-(dimethylamino)benzaldehyde (DMAB) for 90 minutes at 60°C. Absorbance was measured using a plate reader at 560 nm. Eight-point linear standard curves were used to calculate concentrations and reported values are the mean fold change of hydroxyproline content of 4 experiments normalized to total DNA content per condition where 2-3 hydrogels were pooled per condition per experiment. Values with matrix binding peptides were normalized within each experiment to the *PHSRN-K-RGD* only condition.

Cell lysis and DNA quantification

Transwell hydrogels were prepared for lysing by rinsing twice with warm 1x PBS (100 uL apical, 600 uL basal). Apical and basal PBS were removed and 100 uL of RIPA buffer (Pierce Thermo 89900) (25 mM Tris•HCl pH 7.6, 150mM NaCl, 1% NP-40, 1% sodium deoxycholate, 0.1% SDS) supplemented with 1% phenylmethanesulfonyl fluoride (PMSF) (Sigma 93482) and 1% Protease Inhibitor Cocktail (Sigma P8340) was added apically to each Transwell hydrogel. The hydrogel was scraped with a pipet tip, then the plate was shaken on a plate shaker for 15 min at 4 °C. The lysate and gel were transferred to a tube and vortexed. Lysates were clarified by centrifugation at 16K rcf for 15 min at 4 °C. Supernatant was transferred to a new tube and frozen at -80 °C with a lysis buffer blank until further use.

The Quant-IT PicoGreen dsDNA Kit (Life Technologies P7589) was used to measure dsDNA in lysed endometrial co-cultures and used to normalize other metrics (IGFBP-1, prolactin, and hydroxyproline) to estimated cell populations. Lysates and RIPA buffer blank were diluted 20-fold in 1X TE Buffer. Samples and standards (50 µL) were incubated, protected from light, in 50 µL of detection reagent (diluted 1:200 in 1X TE buffer) for 5 min at RT. Fluorescence was measured in a plate reader at 480 nm excitation and 520 nm emission. Sample dsDNA concentration was the average of technical duplicates determined from the standard curve and multiplied by the dilution factor after subtraction of a no cell hydrogel blank.

AlamarBlue metabolic assay

AlamarBlue assay was performed according to manufacturers recommendation. Briefly, cellular metabolic activity was monitored by conversion of resazurin to resorufin in the apical and basolateral media of Transwell co-cultures on days 3, 7, 14, 21 and 28 of culture. AlamarBlue reagent was added to culture media (1 part AB dye:10 culture media). Media was prewarmed, then 100 ul was added apically and 600 ul added basally and cultures incubated for 30 min at 37 °C with 5% CO_2. Subsequently, 100 ul of apical and basal media was transferred to a black, clear-bottom 96-well plate (Thermofischer M33089). Fluorescence was measured in a plate reader at 570 nm excitation and 585 nm emission. Metabolic activity was the average of biological replicates (n=3) minus subtraction of a no cell hydrogel blank.

ELISAs for IGFBP-1 and prolactin

Briefly, plates were coated with capture antibody (23 µL) overnight at 4 °C at concentration of 4.0 µg/mL and 0.8 µg/mL for IGFBP-1 and prolactin, respectively. Wells were rinsed three times with 0.1% Tween-20 in PBS wash buffer then blocked in 46 µL 5% Tween-20 in PBS for IGFBP-1 and 1% BSA in PBS for prolactin for 1 h at RT. Wells were again rinsed three times in wash buffer, then 23 µL of sample or standard was added and incubated overnight at 4 °C. Plates were rinsed three times with wash buffer then incubated with 23 µL detection antibody at 400 ng/mL in blocking buffer for prolactin and in blocking buffer plus 2% goat serum for IGFBP-1 for 2 h at RT. Wells were rinsed three times in wash buffer, then incubated with 23 µL streptavidin-HRP (1:200) in blocking buffer for 20 minutes at RT. HRP substrate solution (23 µL) was added until color developed followed by addition of 11.5 µL of 2N H_2SO_4 to stop the reaction. Absorbance values were immediately read at 450 nm and 540 nm. Absorbance values 450 nm were corrected by subtracting absorbance values at 540 nm to account for discrepancies in the plate. Eight-point standard curves plus blanks (apical medium) were included for quantification. For each protein, 4-parameter logistic curves were fit to the standards, including blanks (Cardillo G. (2012) Four parameters logistic regression - There and back again, http://www.mathworks.com/matlabcentral/fileexchange/38122). Curves were used to calculate concentrations for each sample replicate.

2.3.5 Immunofluorescence and microscopy

Samples were fixed in 4% paraformaldehyde PHEM buffer (Electron Microscopy Sciences) for 1 h, permeabilized in 0.2% TritonX-100 in PBS (Sigma) for 30 min, and blocked for 1 h in 1% BSA (Sigma), 5% normal donkey serum (Electron Microscopy Sciences) PBS at room temperature. Hydrogels were incubated with primary antibodies (1:100, except anti-Cytokeratin 18 1:250) and rhodamine phalloidin (1:1000) (Life Technologies) overnight while rocking at 4°C, rinsed with blocking buffer 3 times (5 min each while rocking at RT), followed by secondary staining with AlexaFluor488 or AlexaFluor568-conjugated donkey anti-rabbit and anti-mouse IgG (1:500) (Invitrogen) rocking overnight at 4°C. Cell nuclei were counterstained with DAPI (1:1000) (Life Technologies) for 15 min at RT. Finally, hydrogels were rinsed 3 times with 1x PBS (5 min each) and rocked overnight prior to mounting using Prolong Gold Antifade (Life Technologies P36935) on glass coverslips. Primary mouse antibodies included RPE conjugated anti-CD10 (Dako, SS2/36) anti-Fibronectin (Millipore FBN11, Ab-3, Calbiochem CP70), anti-Collagen I (Millipore MAB3391), and primary rabbit antibodies included anti-Collagen IV (Abcam ab6586), and anti-Cytokeratin 18 (Abcam ab52948).

Phase images were acquired using a Leica DMI 6000 microscope and Oasis Surveyor software for unfixed hydrogels in culture inserts. Confocal images were acquired using a Nikon Spinning Disk or the Nikon A1R Ultrafast Spectral Scanning Microscope and Nikon NIS Elements acquisition software on fixed and coverslip-mounted hydrogels. Fibrillar collagen was detected by second harmonic generation microscopy using an Olympus FV1000 Multiphoton Laser Scanning Confocal Microscope and Olympus acquisition software on unfixed hydrated hydrogels, gently cut away from culture inserts and placed on coverslips. Second harmonic channel was background-corrected by subtraction of autofluorescence signal at 488 nm. For epithelial dome quantification, images were acquired using a Nikon D600 DSLR camera attached to an inverted tissue culture microscope (Nikon Diaphot, Japan). Images were processed using Capture NX2 software to enhance contrast and manually identify domes prior to quantification of dome numbers and sizes using Fiji-ImageJ.

2.3.6 Statistical analysis

Data are expressed as average ± standard error of the mean (SEM). Statistical analysis was performed using GraphPad Prism v.5 for Mac OS X. Unpaired t-tests assuming unequal variances and two-way ANOVAs with appropriate post-tests were performed as indicated in the results. Statistical significance was defined as * $p < 0.05$, ** $p < 0.01$, *** $p < 0.001$.

2.4 Conclusions

Creation of 3D barrier epithelial tissue mimics from donor epithelial and stromal cells requires a 'one-size-fits-all' extracellular matrix that allows for stromal cell remodeling and epithelial polarization, is permissive to matrix deposition and assembly, and fosters characteristic tissue phenotypic responses to external perturbations. Here, using the endometrium as an example mucosal barrier tissue, we define a modular synthetic ECM based on readily-available PEG macromers and synthetic peptides that fosters physiologically responsive co-cultures of epithelial and stromal fibroblast cells for several weeks. The essential design features of this modular synthetic ECM include an adhesion peptide that engages both stromal and epithelial cells, peptides that bind to and stabilize the ECM produced by each cell type in a locally-responsive fashion, and a crosslinker that is susceptible to cell-mediated cleavage to enable remodeling and evolution of tissue structure. The modular nature of the synthetic ECM, its ease of fabrication, and the delineation of design principles involved in implementing its use for new applications, together provide a foundation for its adaption for widespread application in mucosal barrier tissue engineering.

2.5 References

1. Cook, C. D. *et al.* Local remodeling of synthetic extracellular matrix microenvironments by co-cultured endometrial epithelial and stromal cells enables long-term dynamic physiological function. *Integr. Biol. (Camb).* **9,** 271–289 (2017).
2. Kim, H. J., Li, H., Collins, J. J. & Ingber, D. E. Contributions of microbiome and mechanical deformation to intestinal bacterial overgrowth and inflammation in a human gut-on-a-chip. *Proc. Natl. Acad. Sci.* **113,** E7–E15 (2016).
3. Wira, C. R., Fahey, J. V., Rodriguez-Garcia, M., Shen, Z. & Patel, M. V. Regulation of Mucosal Immunity in the Female Reproductive Tract: The Role of Sex Hormones in Immune Protection Against Sexually Transmitted Pathogens. *Am. J. Reprod. Immunol.* **72,** 236–258 (2014).
4. Bruner-Tran, K. L. *et al.* Exposure to the environmental endocrine disruptor TCDD and human reproductive dysfunction: Translating lessons from murine models. *Reprod. Toxicol.* (2016). doi:10.1016/j.reprotox.2016.07.007
5. Fitzgerald, H. C., Salamonsen, L. A., Rombauts, L. J. R., Vollenhoven, B. J. & Edgell, T. A. The proliferative phase underpins endometrial development: Altered cytokine profiles in uterine lavage fluid of women with idiopathic infertility. *Cytokine* **88,** 12–19 (2016).
6. Salamonsen, L. A., Evans, J., Nguyen, H. P. T. & Edgell, T. A. The Microenvironment of Human Implantation: Determinant of Reproductive Success. *Am. J. Reprod. Immunol.* **75,** 218–225 (2016).
7. Osteen, K. G. *et al.* Stromal-epithelial interaction mediates steroidal regulation of metalloproteinase expression in human endometrium. *Proc. Natl. Acad. Sci. U. S. A.* **91,** 10129–10133 (1994).
8. Bruner, K. L. *et al.* Transforming growth factor beta mediates the progesterone suppression of an epithelial metalloproteinase by adjacent stroma in the human endometrium. *Proc. Natl. Acad. Sci. U. S. A.* **92,** 7362–6 (1995).
9. Pierro, E. *et al.* Stromal-epithelial interactions modulate estrogen responsiveness in normal human endometrium. *Biol. Reprod.* **64,** 831–8 (2001).
10. Igarashi, T. M. *et al.* Reduced expression of progesterone receptor-B in the endometrium of women with endometriosis and in cocultures of endometrial cells exposed to 2,3,7,8-tetrachlorodibenzo-p-dioxin. *Fertil. Steril.* **84,** 67–74 (2005).
11. Bläuer, M., Heinonen, P. K., Martikainen, P. M., Tomás, E. & Ylikomi, T. A novel organotypic culture model for normal human endometrium: regulation of epithelial cell proliferation by estradiol and medroxyprogesterone acetate. *Hum. Reprod. Oxford Engl.* **20,** 864–871 (2005).
12. Chen, J. C. *et al.* Coculturing human endometrial epithelial cells and stromal fibroblasts alters cell-specific gene expression and cytokine production. *Fertil. Steril.* **100,** 1132–43 (2013).
13. Kim, M. R. *et al.* Progesterone-dependent release of transforming growth factor-beta1 from epithelial cells enhances the endometrial decidualization by turning on the Smad signalling in stromal cells. *Mol. Hum. Reprod.* **11,** 801–8 (2005).
14. Kleinman, H. K. *et al.* Isolation and characterization of type IV procollagen, laminin, and heparan sulfate proteoglycan from the EHS sarcoma. *Biochemistry* **21,** 6188–93 (1982).

15. Kleinman, H. K. & Martin, G. R. Matrigel: basement membrane matrix with biological activity. *Semin. Cancer Biol.* **15,** 378–86 (2005).
16. Schutte, S. C. & Taylor, R. N. A tissue-engineered human endometrial stroma that responds to cues for secretory differentiation, decidualization, and menstruation. *Fertil. Steril.* **97,** 997–1003 (2012).
17. Schutte, S. C., James, C. O., Sidell, N. & Taylor, R. N. Tissue-engineered endometrial model for the study of cell-cell interactions. *Reprod. Sci.* **22,** 308–15 (2015).
18. Wang, H. *et al.* Sex steroids regulate epithelial-stromal cell cross talk and trophoblast attachment invasion in a three-dimensional human endometrial culture system. *Tissue Eng. Part C. Methods* **19,** 676–87 (2013).
19. Vukicevic, S. *et al.* Identification of multiple active growth factors in basement membrane Matrigel suggests caution in interpretation of cellular activity related to extracellular matrix components. *Exp. Cell Res.* **202,** 1–8 (1992).
20. Rizzi, S. C. & Hubbell, J. A. Recombinant Protein- *co* -PEG Networks as Cell-Adhesive and Proteolytically Degradable Hydrogel Matrixes. Part I: Development and Physicochemical Characteristics. *Biomacromolecules* **6,** 1226–1238 (2005).
21. Lutolf, M. P. *et al.* Synthetic matrix metalloproteinase-sensitive hydrogels for the conduction of tissue regeneration: engineering cell-invasion characteristics. *Proc. Natl. Acad. Sci. U. S. A.* **100,** 5413–8 (2003).
22. Patterson, J. & Hubbell, J. A. Enhanced proteolytic degradation of molecularly engineered PEG hydrogels in response to MMP-1 and MMP-2. *Biomaterials* **31,** 7836–45 (2010).
23. Bott, K. *et al.* The effect of matrix characteristics on fibroblast proliferation in 3D gels. *Biomaterials* **31,** 8454–64 (2010).
24. Cambria, E. *et al.* Covalent Modification of Synthetic Hydrogels with Bioactive Proteins via Sortase-Mediated Ligation. *Biomacromolecules* **16,** 2316–26 (2015).
25. Raza, A., Ki, C. S. & Lin, C.-C. The influence of matrix properties on growth and morphogenesis of human pancreatic ductal epithelial cells in 3D. *Biomaterials* **34,** 5117–27 (2013).
26. Weiss, M. S. *et al.* The impact of adhesion peptides within hydrogels on the phenotype and signaling of normal and cancerous mammary epithelial cells. *Biomaterials* **33,** 3548–59 (2012).
27. Reyes, C. D., Petrie, T. A. & García, A. J. Mixed extracellular matrix ligands synergistically modulate integrin adhesion and signaling. *J. Cell. Physiol.* **217,** 450–458 (2008).
28. Gill, B. J. *et al.* A synthetic matrix with independently tunable biochemistry and mechanical properties to study epithelial morphogenesis and EMT in a lung adenocarcinoma model. *Cancer Res.* **72,** 6013–23 (2012).
29. Gould, S. T. & Anseth, K. S. Role of cell-matrix interactions on VIC phenotype and tissue deposition in 3D PEG hydrogels. *J. Tissue Eng. Regen. Med.* **10,** E443–E453 (2016).
30. Bachman, H., Nicosia, J., Dysart, M. & Barker, T. H. Utilizing Fibronectin Integrin-Binding Specificity to Control Cellular Responses. *Adv. wound care* **4,** 501–511 (2015).
31. Brown, A. C., Rowe, J. A. & Barker, T. H. Guiding epithelial cell phenotypes with

engineered integrin-specific recombinant fibronectin fragments. *Tissue Eng Part A* **17,** 139–150 (2011).

32. Brown, A. C., Dysart, M. M., Clarke, K. C., Stabenfeldt, S. E. & Barker, T. H. Integrin a3b1 binding to fibronectin is dependent on the ninth type III repeat. *J. Biol. Chem.* **290,** 25534–25547 (2015).
33. Bochen, A. *et al.* Biselectivity of isoDGR peptides for fibronectin binding integrin subtypes α5β1 and αvβ6: conformational control through flanking amino acids. *J. Med. Chem.* **56,** 1509–19 (2013).
34. Maheshwari, G., Brown, G., Lauffenburger, D. A., Wells, A. & Griffith, L. G. Cell adhesion and motility depend on nanoscale RGD clustering. *J. Cell Sci.* **113 (Pt 1,** 1677–86 (2000).
35. Cavalcanti-Adam, E. A. *et al.* Lateral spacing of integrin ligands influences cell spreading and focal adhesion assembly. *Eur. J. Cell Biol.* **85,** 219–24 (2006).
36. Kuhlman, W., Taniguchi, I., Griffith, L. G. & Mayes, A. M. Interplay between PEO tether length and ligand spacing governs cell spreading on RGD-modified PMMA-g-PEO comb copolymers. *Biomacromolecules* **8,** 3206–13 (2007).
37. Herr, A. B. & Farndale, R. W. Structural insights into the interactions between platelet receptors and fibrillar collagen. *J. Biol. Chem.* **284,** 19781–19785 (2009).
38. Wojtowicz, A. M. *et al.* Coating of biomaterial scaffolds with the collagen-mimetic peptide GFOGER for bone defect repair. *Biomaterials* **31,** 2574–2582 (2010).
39. Kim, J.-M., Park, W. H. & Min, B.-M. The PPFLMLLKGSTR motif in globular domain 3 of the human laminin-5 alpha3 chain is crucial for integrin alpha3beta1 binding and cell adhesion. *Exp. Cell Res.* **304,** 317–27 (2005).
40. Aplin, J. D., Charlton, A. K. & Ayad, S. An immunohistochemical study of human endometrial extracellular matrix during the menstrual cycle and first trimester of pregnancy. *Cell Tissue Res.* **253,** 231–40 (1988).
41. Evans, J., Kaitu'u-Lino, T. & Salamonsen, L. A. Extracellular matrix dynamics in scar-free endometrial repair: perspectives from mouse in vivo and human in vitro studies. *Biol. Reprod.* **85,** 511–23 (2011).
42. Lessey, B. A. *et al.* Integrin adhesion molecules in the human endometrium. Correlation with the normal and abnormal menstrual cycle. *J. Clin. Invest.* **90,** 188–95 (1992).
43. Bilalis, D. A., Klentzeris, L. D. & Fleming, S. Immunohistochemical localization of extracellular matrix proteins in luteal phase endometrium of fertile and infertile patients. *Hum. Reprod.* **11,** 2713–8 (1996).
44. Tanaka, T., Wang, C. & Umesaki, N. Autocrine/paracrine regulation of human endometrial stromal remodeling by laminin and type IV collagen. *Int. J. Mol. Med.* **22,** 581–7 (2008).
45. Brosens, J. J., Hayashi, N. & White, J. O. Progesterone receptor regulates decidual prolactin expression in differentiating human endometrial stromal cells. *Endocrinology* **140,** 4809–20 (1999).
46. Gellersen, B. & Brosens, J. Cyclic AMP and progesterone receptor cross-talk in human endometrium: a decidualizing affair. *J. Endocrinol.* **178,** 357–72 (2003).
47. Nagase, H. & Fields, G. B. Human matrix metalloproteinase specificity studies using collagen sequence-based synthetic peptides. *Biopolymers* **40,** 399–416

(1996).
48. Turk, B. E., Huang, L. L., Piro, E. T. & Cantley, L. C. Determination of protease cleavage site motifs using mixture-based oriented peptide libraries. *Nat. Biotechnol.* **19,** 661–667 (2001).
49. Broaders, K. E., Cerchiari, A. E. & Gartner, Z. J. Coupling between apical tension and basal adhesion allow epithelia to collectively sense and respond to substrate topography over long distances. *Integr. Biol. (Camb).* **7,** 1611–21 (2015).
50. Widdicombe, J. H., Sachs, L. A. & Finkbeiner, W. E. Effects of growth surface on differentiation of cultures of human tracheal epithelium. *Vitr. Cell. Dev. Biol. - Anim.* **39,** 51 (2003).
51. Markowski, M. C., Brown, A. C. & Barker, T. H. Directing epithelial to mesenchymal transition through engineered microenvironments displaying orthogonal adhesive and mechanical cues. *J. Biomed. Mater. Res. - Part A* **100 A,** 2119–2127 (2012).
52. Arnold, J. T. Endometrial stromal cells regulate epithelial cell growth in vitro: a new co-culture model. *Hum. Reprod.* **16,** 836–845 (2001).
53. Gentilini, D. *et al.* PI3K/Akt and ERK1/2 signalling pathways are involved in endometrial cell migration induced by 17beta-estradiol and growth factors. *Mol. Hum. Reprod.* **13,** 317–322 (2007).
54. Weimar, C. H. E., Macklon, N. S., Post Uiterweer, E. D., Brosens, J. J. & Gellersen, B. The motile and invasive capacity of human endometrial stromal cells: Implications for normal and impaired reproductive function. *Hum. Reprod. Update* **19,** 542–557 (2013).
55. Li, Z. *et al.* Perfusion culture enhanced human endometrial stromal cell growth in alginate-multivalent integrin α5β1 ligand scaffolds. *J. Biomed. Mater. Res. A* **99,** 211–20 (2011).
56. Kyburz, K. A. & Anseth, K. S. Three-dimensional hMSC motility within peptide-functionalized PEG-based hydrogels of varying adhesivity and crosslinking density. *Acta Biomater.* **9,** 6381–92 (2013).
57. Singh, S. P., Schwartz, M. P., Lee, J. Y., Fairbanks, B. D. & Anseth, K. S. A peptide functionalized poly(ethylene glycol) (PEG) hydrogel for investigating the influence of biochemical and biophysical matrix properties on tumor cell migration. *Biomater. Sci.* **2,** 1024–1034 (2014).
58. Bentin-Ley, U. *et al.* Isolation and culture of human endometrial cells in a three-dimensional culture system. *J. Reprod. Fertil.* **101,** 327–32 (1994).
59. Rizzi, S. C. *et al.* Recombinant protein-co-PEG networks as cell-adhesive and proteolytically degradable hydrogel matrixes. Part II: biofunctional characteristics. *Biomacromolecules* **7,** 3019–29 (2006).
60. Park, D. W. *et al.* A well-defined in vitro three-dimensional culture of human endometrium and its applicability to endometrial cancer invasion. *Cancer Lett.* **195,** 185–92 (2003).
61. Hynes, R. O. The extracellular matrix: not just pretty fibrils. *Sci. New York NY* **326,** 1216–9 (2009).
62. Yurchenco, P. D. Basement membranes: cell scaffoldings and signaling platforms. *Cold Spring Harb. Perspect. Biol.* **3,** 1–28 (2011).
63. Mouw, J. K., Ou, G. & Weaver, V. M. Extracellular matrix assembly: a multiscale

deconstruction. *Nat. Rev. Mol. Cell Biol.* **15,** 771–85 (2014).
64. Yurchenco, P. D. & Patton, B. L. Developmental and pathogenic mechanisms of basement membrane assembly. *Curr. Pharm. Des.* **15,** 1277–94 (2009).
65. Singh, P., Carraher, C. & Schwarzbauer, J. E. Assembly of Fibronectin Extracellular Matrix. *Annu. Rev. Cell Dev. Biol.* **26,** 397–419 (2010).
66. Coulson-Thomas, V. J. *et al.* Colorectal cancer desmoplastic reaction up-regulates collagen synthesis and restricts cancer cell invasion. *Cell Tissue Res.* **346,** 223–36 (2011).
67. Betz, P. *et al.* Time-dependent pericellular expression of collagen type IV, laminin, and heparan sulfate proteoglycan in myofibroblasts. *Int. J. Legal Med.* **105,** 169–72 (1992).
68. Giannelli, G. *et al.* Endometriosis is characterized by an impaired localization of laminin-5 and alpha3beta1 integrin receptor. *Int. J. Gynecol. Cancer* **17,** 242–7
69. Määttä, M. *et al.* Distribution of basement membrane anchoring molecules in normal and transformed endometrium: altered expression of laminin gamma2 chain and collagen type XVII in endometrial adenocarcinomas. *J. Mol. Histol.* **35,** 715–22 (2004).
70. Stoffels, J. M. J., Zhao, C. & Baron, W. Fibronectin in tissue regeneration: Timely disassembly of the scaffold is necessary to complete the build. *Cell. Mol. Life Sci.* **70,** 4243–4253 (2013).
71. Sung, K. E. *et al.* Transition to invasion in breast cancer: a microfluidic in vitro model enables examination of spatial and temporal effects. *Integr. Biol. (Camb).* **3,** 439–50 (2011).
72. Güç, E., Fankhauser, M., Lund, A. W., Swartz, M. A. & Kilarski, W. W. Long-term intravital immunofluorescence imaging of tissue matrix components with epifluorescence and two-photon microscopy. *J. Vis. Exp.* (2014). doi:10.3791/51388
73. Schwarz, R. I., Mandell, R. B. & Bissell, M. J. Ascorbate induction of collagen synthesis as a means for elucidating a mechanism of quantitative control of tissue-specific function. *Mol. Cell. Biol.* **1,** 843–53 (1981).
74. Michels, A. J. & Frei, B. Myths, artifacts, and fatal flaws: identifying limitations and opportunities in vitamin C research. *Nutrients* **5,** 5161–92 (2013).
75. Matsuzaki, S., Canis, M., Pouly, J.-L. & Darcha, C. Soft matrices inhibit cell proliferation and inactivate the fibrotic phenotype of deep endometriotic stromal cells in vitro. *Hum. Reprod.* **31,** 541–53 (2016).
76. Holinka, C. F. *et al.* Proliferation and responsiveness to estrogen of human endometrial cancer cells under serum-free culture conditions. *Cancer Res.* **49,** 3297–301 (1989).
77. Fleming, H. Differentiation in human endometrial cells in monolayer culture: dependence on a factor in fetal bovine serum. *J. Cell. Biochem.* **57,** 262–70 (1995).
78. Chang, Y.-H. *et al.* Activation of caspase-8 and Erk-1/2 in domes regulates cell death induced by confluence in MDCK cells. *J. Cell. Physiol.* **211,** 174–82 (2007).
79. Arnold, J. T., Lessey, B. A., Seppälä, M. & Kaufman, D. G. Effect of normal endometrial stroma on growth and differentiation in Ishikawa endometrial adenocarcinoma cells. *Cancer Res.* **62,** 79–88 (2002).
80. Aghajanova, L., Hamilton, A., Kwintkiewicz, J., Vo, K. C. & Giudice, L. C.

Steroidogenic Enzyme and Key Decidualization Marker Dysregulation in Endometrial Stromal Cells from Women with Versus Without Endometriosis1. *Biol. Reprod.* **80,** 105–114 (2009).
81. Yu, J. *et al.* Endometrial Stromal Decidualization Responds Reversibly to Hormone Stimulation and Withdrawal. *Endocrinology* **157,** 2432–2446 (2016).
82. Gao, X. & Groves, M. J. Fibronectin-binding peptides. I. Isolation and characterization of two unique fibronectin-binding peptides from gelatin. *Eur. J. Pharm. Biopharm.* **45,** 275–84 (1998).
83. Johnson, G. & Moore, S. W. Identification of a structural site on acetylcholinesterase that promotes neurite outgrowth and binds laminin-1 and collagen IV. *Biochem. Biophys. Res. Commun.* **319,** 448–55 (2004).
84. Nishida, M., Kasahara, K., Kaneko, M., Iwasaki, H. & Hayashi, K. [Establishment of a new human endometrial adenocarcinoma cell line, Ishikawa cells, containing estrogen and progesterone receptors]. *Nihon Sanka Fujinka Gakkai Zasshi* **37,** 1103–11 (1985).
85. Lessey, B. A. *et al.* Luminal and glandular endometrial epithelium express integrins differentially throughout the menstrual cycle: implications for implantation, contraception, and infertility. *Am. J. Reprod. Immunol.* **35,** 195–204 (1996).
86. Krikun, G. *et al.* A novel immortalized human endometrial stromal cell line with normal progestational response. *Endocrinology* **145,** 2291–6 (2004).
87. Korch, C. *et al.* DNA profiling analysis of endometrial and ovarian cell lines reveals misidentification, redundancy and contamination. *Gynecol. Oncol.* **127,** 241–248 (2012).
88. Osteen, K. G., Hill, G. A., Hargrove, J. T. & Gorstein, F. Development of a method to isolate and culture highly purified populations of stromal and epithelial cells from human endometrial biopsy specimens. *Fertil. Steril.* **52,** 965–72 (1989).

2.6 Appendix

Primary endometrial epithelial and stromal cell isolation and purification

Primary endometrial epithelial and stromal cell biopsies were dissociated and cells purified as described by Osteen and coworkers[88] with some modifications. Biopsy specimens were collected using a pipelle and immediately placed in 10 mL of ice-cold 1:1 mixture of Dulbecco's Modified Eagle's Medium and Ham's F-12 (Gibco) supplemented with 1% penicillin/streptomycin (Gibco) and 10% *v/v* dextran/charcoal treated fetal bovine serum (Atlanta Biologicals) (DMEM/F12/FBS) and transported on ice. The tissue was washed twice by centrifugation at 400xg in DMEM/F12 and dissected into small pieces (1-2 mm^3). Tissue pieces were incubated for 1h at 37°C in DMEM/F12 supplemented with 0.5% collagenase Type IV (Worthington Biochemical Corporation LS004188), 0.02% DNAase (Sigma-Aldrich DN25) and 2% chicken serum (Sigma-Aldrich C5405) and vortexed every 30 min. As a result of this first dissociation, stromal cells are present as single cells while epithelial cells remain aggregated. The cell suspension was then filtered twice through a 70 μm membrane filter (Falcon 352350) in order to separate the stromal cells from the epithelial cell clumps. The latter were collected on the surface of the filters and washed by centrifugation with sterile PBS. The stromal fraction flow through was further purified by two rounds of differential sedimentation at unit gravity as follows. Stromal cell were washed twice by centrifugation at 400xg for 5min and resuspended in 10 mL of DMEM/F12/FBS. After the second centrifugation, stromal cells were resuspended in 2 mL DMEM/F12/FBS and layered slowly drop by drop over 10 mL of DMEM/F12/FBS in a sterile 15 mL conical tube, and the tube was incubated in an upright position at 37°C for 30 min. The top 8 mL of sedimentation medium were collected, centrifuged at 400xg for 5min and resuspended in 2 mL DMEM/F12/FBS, and the sedimentation step was repeated for an additional 30 minutes. The top 8 mL of sedimentation medium was collected, filtered through a 40 μm membrane filter (Falcon 352340), and stromal cells were counted and seeded at 2-5 x 10^4 cells/cm^2 in DMEM/F12/FBS. The medium was replaced the following day and every 2-3 days thereafter until further use.

Further dissociation of the epithelial aggregates was achieved by incubation with an enzyme mixture supplemented with 0.5% collagenase, 0.1% hyaluronidase (Sigma-

Aldrich H3506), 0.1% pronase (Sigma-Aldrich P5147), 0.02% DNAase and 2% chicken serum in PBS for 15-20 min at 37°C in a water bath. The cell preparation was filtered through a 70 μm membrane filter in order to get rid of the remaining stromal cells that were released during this digestion and epithelial cell clumps were collected again and further digested with fresh enzyme mixture for 30-45 min at 37°C. This final digestion resulted in small epithelial cell clumps of 50-100 cells that were purified by differential sedimentation at unit gravity as follows. Cells were centrifuged and resuspended in 2 mL DMEM/F12/FBS. Cells were layered slowly over 10 mL of DMEM/F12/FBS in a sterile 15 mL conical tube and the tube was incubated in an upright position at 37°C for 30 min. The top 10 mL of sedimentation medium were discarded and the sedimentation step was repeated with the bottom 2 mL. The top 10 mL of sedimentation medium were discarded again and 5 mL of DMEM/F12/FBS were added. Final purification was achieved by selective attachment of any remaining stromal cells to plastic substrate as follows. Cells were seeded in a 75 cm^2 tissue culture flask and incubated at 37°C, 95% air, 5% CO2 for 1h in DMEM/F12/FBS. Non-attached epithelial cells were collected and cultured in DMEM/F12/FBS at a density of 3 X 10^5 cells/mL for 2-3 days. After this plating period, medium was changed every other day for 2-3 days until further use.

Appendix Figures and Tables

Figure 2A1: Nuclear shape index of decidualized cells in hydrogels does not distinguish between control and cAMP/MPA stimulated primary endometrial stromal cells cultured in 3D. DAPI-stained nuclei were imaged and quantified using ImageJ software to quantify the nuclear shape index (NSI), where NSI = 4π x area / perimeter^2 for at least 50 nuclei counted per each ROI (n=3). A shape index of 1 indicates a perfect circle, whereas a shape index of 0 indicates a straight line.

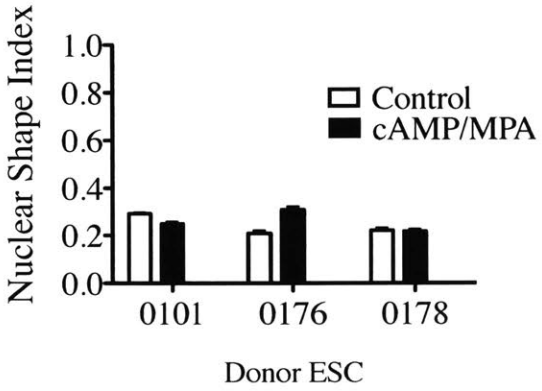

Table 2A1: Primary endometrial biopsy donor data.

Donor	Age	Cycle Day	Diagnoses
0101	31	5	unilateral ovarian cyst
0176	27	7	left salpingitis
0178	20	4	bilateral ovarian cyst
0188	41	12	adenomyosis
0190	49	7	leiomyoma
0191	33	14	bilateral, paratubal cyst

Table 2A2: Hydrogel gelation time dependence on temperature.

The gelation time was measured at various temperatures while making a hydrogel as follows: 5 w/w% 40 kDa PEG vinyl sulfone hydrogel, that was 40% crosslinked, comprising 1 mM PHSRN-K-RGD, 0.5 mM BM-binder, and 0.5 mM FN-binder.

Temperature	Location	Gelation Time
4°C	Thermal Shaker	51 min
8°C	Thermal Shaker	34 min
12°C	Cold Water Bath	31 min
17.3°C	Lab Bench	20 min
17.3°C	Lab Bench	18 min
21.6°C	Thermal Shaker	17 min
21.6°C	Thermal Shaker	17 min
22.6°C	Lab Bench	13.5 min
30°C	Water Bath	14 min
37°C	Thermal Shaker	9 min

Chapter 3

3 Experimental Methods for *in vitro* Human Endometrial Epithelial Expansion, Cryopreservation, and Culture

Contributions: Julia Papps contributed to protocol development for epithelial expansion. Julia Papps and Evette Ronner contributed to primary sample collection, isolation, and culture.

Diseases involving molecular reprogramming of uterine epithelial cells are numerous including cancers and several chronic inflammatory disorders such as infertility, adenomyosis, and endometriosis. Epithelial cells are of interest because of their highly diverse functional roles in governing normal tissue homeostasis. Epithelial secretory and barrier functions range from enabling embryo implantation in the uterus to lubrication and immune signaling at mucosal surfaces to prevent infections from entering the body. Unlike mesenchymal lineage cells, such as fibroblasts and myofibroblasts, epithelial cells undergo rapid senescence and subsequent crisis *in vitro* unless they are transformed or acquire genetic mutations. In order to study secretory, metabolic, and barrier functions of healthy and diseased epithelial tissue systems, *in vitro* expansion methods are needed to increase the limited numbers of cells obtained from primary uterine biopsies.

Here we show utility of a method to expand and cryopreserve primary human endometrial epithelial cells for later use in epithelial-stromal co-culture studies. Conditional reprogramming of primary endometrial epithelial cells using a mitotically arrested fibroblast feeder layer and a small molecule inhibitor to Rho-associated kinase (Y-27632) enabled an average of 12 population doublings in 8 out of 9 donors. Expanded cells were immunopositive for epithelial cell markers cytokeratin-18 and epithelial cell adhesion molecule. Additionally, expanded cells remained functional post-expansion and -cryopreservation retaining characteristic cytokine and protease production along with barrier function, as measured by transepithelial electrical resistance. With new methods to expand and cryopreserve epithelial cells for later culture, we overcome sample limitations, increasing sample sizes for statistical analysis. Additionally, we can perform repeated studies on the same samples and match patient specific stromal and epithelial cells for future co-culture studies.

3.1 Introduction

In vitro studies of endometrial cell co-cultures responding to hormonal or inflammatory stimuli can potentially illuminate mechanisms governing uterine pathologies ranging from endometrial receptivity and implantation biology to diseases such as endometriosis.[1–9] Inflammation is hypothesized to contribute to a reduced progestational response possibly leading to ectopic endometrial invasion and growth following menstruation. Although endometrial cell lines may recapitulate some aspects of cellular morphology and signaling, they differ substantially from primary cells in the compendium of growth factors and cytokines produced (Chapter 2).[10] Primary cells offer greater fidelity of phenotype and the opportunity to study patient heterogeneity and biological disease mechanisms.[10] Primary endometrial stromal cell monocultures can be readily expanded and retain many physiologically-appropriate responses to cyclical hormone stimulation over several populations *in vitro*.[11] However, endometrial epithelial cell cultures are difficult to expand and maintain in culture often requiring paracrine signaling factors from the underlying stromal compartment for most physiological responses to cyclic hormones.[1,12–14] Additionally, epithelial cells have finite lifespans and often display limited regenerative capacities as they undergo maturation to a functional differentiation phenotype. Hence, there are significant barriers to experimental studies with primary cultured epithelial cells, and we aim to develop robust primary epithelial expansion and cryopreservation protocols to enable further *in vitro* studies.

The endometrial epithelium consists of a single sheet of interconnecting glands that opens up into a central luminal space. Glandular models of epithelial cells grown in 3D, including organoids, allow understanding of the morphogenic processes that drive gland formation allowing many independent events (organoid glands) to be studied within the same culture.[3,15–17] Additionally, the enclosed luminal space enables concentration of signaling molecules, although access to the luminal space and characterization of barrier function are technically challenging to interrogate. Barrier models, often involving epithelial cells seeded as a single layer in 2D on a culture insert, are useful for drug absorption, paracrine signaling and functional barrier studies as they allow easy access to both the luminal and basolateral compartments but may distort physiological signaling due to basal media dilution effects.[1,2,18] Methods to expand

primary epithelial cells in 3D-glandular and 2D-barrier formats have been developed for numerous epithelial tissues of interest including the breast, lung and gastrointestinal tract,[19–23] but endometrial epithelial cryopreservation and expansion efforts have only recently been explored.[15,16,24]

The endometrium displays a unique capacity to regenerate monthly, undergoing rapid, scar-free wound repair following menstrual tissue breakdown. However, the cells responsible for repopulating the endometrium are still as yet to be identified.[25,26] Numerous other epithelial tissue-specific stem cells have been identified, but definitive endometrial stem cell markers remain to be elucidated, hindering current endometrial epithelial expansion efforts.[27,28] The endometrial functionalis contains the luminal epithelium and is hormone responsive. Progesterone mediates functionalis differentiation, priming the cells for blastocyst implantation by limiting proteolytic remodeling during the luteal phase.[1] Conversely, the deeper basalis endometrium is not responsive to cyclic hormones and is thus preserved through menstruation. Although mice do not menstruate, DNA label-retaining studies in mice have suggested that epithelial progenitor cells may reside at the bases of glands located in the basalis region and are partly responsible for endometrial regeneration in the functionalis region.[29] Thus, the ability to expand endometrial epithelial progenitor cells would enable future *in vitro* studies of human endometrial function including cell growth, wound healing and hormonal regulation important to normal and pathological endometrial conditions including endometriosis, adenomyosis and infertility.

Despite the lack of a definitive endometrial epithelial stem cell compartment, we expect that they may behave like other primary epithelial stem cells where culture expansion methods have already been established.[20–23,30,31] Additionally, we recognize that primary endometrial epithelial cells may pose their own unique challenges to culture expansion (e.g., they may be dependent on hormones like estradiol or tissue specific signals for growth). However, previous studies have indicated that initial reepithelialization occurs simultaneously with menstruation in the absence of steroid hormones, suggesting stem cell growth may be prompted locally by stromal niche or wound factors similarly observed in other epithelial tissues that experience damage.[32]

Two general approaches to epithelial expansion exist, and both rely on the

presence of stromal factors for which producer cell lines have recently become commercially available.[30,33] The first method, known as conditional reprogramming, involves coaxing mature isolated primary epithelial cells to enter a stem-like state. This is achieved by culturing cells with a small molecule inhibitor to Rho-associated kinase (ROCK), Y-27632, either on top of irradiated 3T3-J2 murine feeder fibroblast cells or in the presence of feeder cell-conditioned media.[21–23,33,34] Specifically, studies with primary keratinocytes showed an increase in proliferation and a decrease in genes associated with terminal differentiation when ROCK was inhibited by Y-27632.[35] Additionally, when primary prostate epithelial cells were cultured on 3T3-J2 feeder cells, irrespective of ROCK inhibition, telomerase reverse transcriptase (hTERT) gene expression increased 20-fold.[21] hTERT is responsible for extending telomere length and promoting self-renewal while preventing cellular senescence. Although the exact mechanisms of cellular reprogramming are not entirely understood, evidence in primary cells suggests both feeder cells and ROCK inhibition are necessary for long-term reprogramming.[21-23]Additionally, cellular reprogramming is temporary, with mucosal epithelial cells reverting back to a differentiated state, including formation of tight junctions and expression of cilia and mucus, upon removal of feeder cells and ROCK inhibitor.[22]

A second recently developed method involves generating epithelial stem cell organoids.[15,16] Isolated primary epithelial cells are cultured in a 3D matrix, often Matrigel, in the presence of WNT3A-, Noggin-, and R-spondin-supplemented medium.[20,30] For human epithelial cells, addition of small molecule inhibitors against ROCK and TGFβ signaling were also necessary to prevent differentiation and sustain expansion.[20,31] This method selectively expands epithelial progenitor cells in a WNT-dependent manner. WNT signaling, which likely comes from the underlying stroma in the stem cell niche, is enhanced through R-spondin binding to leucine-rich repeat-containing G-protein-coupled receptors, LGRs. The presence of R-spondin leads to sequestration of proteins that contribute to WNT-receptor, frizzled, endocytosis and turnover. Thus, the presence of R-spondin serves to prolong WNT signaling. LGR receptors have been identified as enriched in label-retaining epithelial progenitor populations and may represent a marker of adult stem cells.[36,37] Specifically, endometrial LGR-4, -5, and -7 expression has been previously established.[16,28,38,39] Recent work suggests nearly half of endometrial LGR-5+

cells, which comprise ~1% of the total endometrial cells, also display hematopoietic lineage markers, suggesting further studies are necessary to determine the lineage and source of cells expressing LGR5+ within the endometrium.[28]

Currently, primary endometrial biopsies yield low cell counts usually between $1x10^5$–$5x10^6$ epithelial cells per donor depending on menstrual cycle phase and endometrial thickness during collection. In accordance with previously established endometrial cultures, we are generally only able to establish 6–24 Transwell cultures for *in vitro* experiments.[40] Additionally, these cells display low viability post-cryopreservation and undergo rapid *in vitro* senescence upon culture (generating <3 population doublings), which prevents long-term studies unless they are genetically transformed.[24,41] Given the important role of epithelial cell signaling at mucosal barriers, and the desire to develop *in vitro* models that include epithelial cells, we aim to establish robust expansion of non-transformed cells and cryopreservation methods to overcome current sample limitations.

Here we show that conditional reprogramming improves expansion of primary endometrial epithelial cells isolated from endometrial pipelle biopsies and cultured using an irradiated feeder cell layer and a small molecule inhibitor against ROCK. Expansion was observed in 8 out of 9 donors enabling an average of 12 population doublings (generating ~1 x 10^7 cells per donor). Cells could be cryopreserved and retained epithelial markers and function. Expanded cells were immunopositive for epithelial cell markers cytokeratin-18 and epithelial cell adhesion molecule. Upon removal of ROCK inhibitor, cells displayed barrier function as observed by high transepithelial electrical resistance and tight junction formation by zona occludens staining. Finally expanded primaries retained heterogeneous endometrial epithelial cytokine and protease expression not observed in a standard endometrial cell line, Ishikawa cells. Thus, conditional reprogramming offers a robust method to expand primary endometrial epithelial cells, enabling future studies of endometrial immune barrier mucosal biology *in vitro*.

3.2 Results and Discussion

3.2.1 Conditionally reprogramming primary epithelial cells requires 3T3-J2 feeder cells and ROCK inhibition

Methods to conditionally reprogram primary epithelial cells using feeder cells and a small molecule inhibitor to Rho-associated kinase (ROCK) signaling (Y-27632) were adapted for expansion of endometrial epithelial cells (Fig. 3-1).[21–23] Specifically, 3T3-J2 murine embryonic fibroblast feeder cells were harvested via trypsinization at 80% confluency and gamma-irradiated (30 Gy) to induce mitotic arrest. Irradiated cells were seeded at 4×10^4 cells/cm^2 (or 5×10^4 cells/cm^2 if previously cryopreserved–see below) 24–48 hours prior to initiation of epithelial cell culture. Primary endometrial epithelial cells (Fig. 3-1, white arrows) were seeded at 5×10^3 cells/cm^2 onto previously prepared feeder layers in conditional reprogramming media. Visible growth of small epithelial colonies occurred by day 3, with larger colonies comprising hundreds of cells observed by day 6 in culture. Epithelial colonies were subcultured by trypsinization after 4-7 days (80% confluence) and reseeded onto fresh feeder cell layers for up to 10 passages. In order to establish robust protocols for epithelial expansion, we first investigated methods to prepare irradiated 3T3-J2 feeder cell layers.

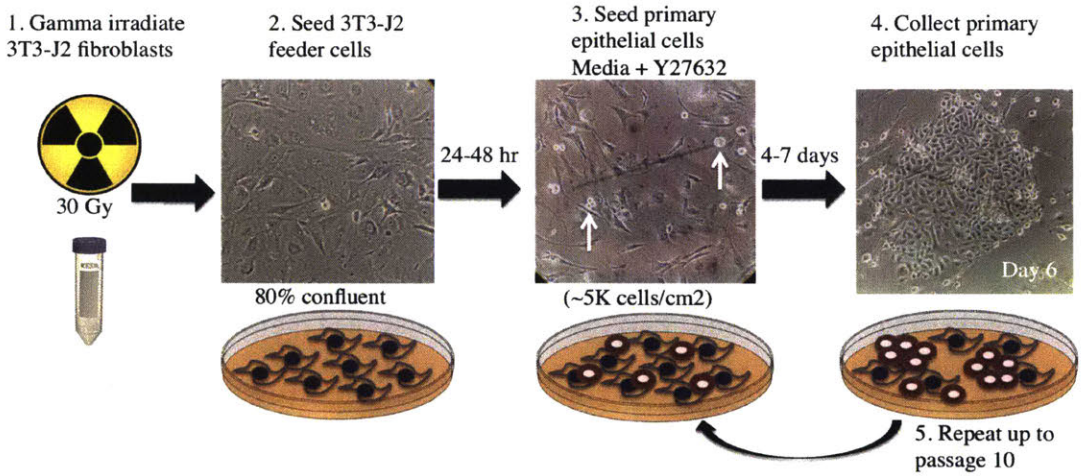

Figure 3-1. Conditionally reprogramming endometrial epithelial cells requires irradiated 3T3-J2 feeder cells and ROCK inhibition. Schematic of conditional reprogramming method where primary endometrial epithelial cells are culture-expanded after seeding single epithelial cells (white arrows) at 5 x 10^3 cells/cm^2 on top of irradiated 3T3-J2 cells (4 x 10^4 cells/cm^2) seeded 24–48 hours in advance at 80% confluence. Epithelial cells are grown in media containing 10 μM ROCK inhibitor (Y-27632) resulting in rapid epithelial colony growth over 4–7 days. Epithelial cells are subsequently harvested by trypsinization and passaged onto previously prepared 3T3-J2 feeder cells up to 10 passages.

3T3-J2 fibroblast feeder cell preparation, irradiation and cryopreservation

The goal of these initial studies was to establish a protocol that enabled efficient production of fibroblast feeder cell stocks, which could be irradiated and cryopreserved in advance for future use. This allowed for the needed flexibility to have irradiated feeder stocks ready on demand, rather than timing feeder cell seeding, growth, and irradiation prior to every epithelial passage (every 4-7 days).

Epithelial cell growth was shown to be dependent on soluble factors secreted by mitotically arrested 3T3-J2 feeder cells.[33,34] Chemical (mitomycin C) or gamma radiation exposure induces DNA damage resulting in mitotic arrest of feeder cells to prevent overgrowth during epithelial culture.[33,42,43] We hypothesized that to provide feeder layer longevity, with ideal media-conditioning properties, that feeder cells should be exposed to a radiation dosage that adequately arrests growth but does not impact cell viability.

Due to variation in suggested irradiation protocols,[23,44] we investigated the effect of a high (8000 rad, 80 Gy) and a low (3000 rad, 30 Gy) dose of gamma radiation (Cobolt-60 source) on feeder cell viability and growth. Irradiated feeder cell viability was assessed 30 minutes after irradiation prior to seeding (Appendix Fig. 3A1). Only feeder cells that received the higher radiation dosage (8000 rad) showed a decrease in viability (75% versus pre-irradiation viability of 89%) after 30 minutes. Following irradiation, cells were seeded at a density of 4×10^4 cells/cm^2 in a 6-well plate to assess cell morphology and growth (Appendix Fig. 3A1). After 3 days and after one week in 3T3-J2 growth media, cells were trypsinized and counted. Neither the high nor the low radiation exposed cells exhibited increases in cell counts, suggesting that 3000 rad was sufficient to induce mitotic arrest and prevent proliferation. Additionally, although no visible morphological differences were observed between the high and low dose radiation conditions, the higher radiation dosage resulted in a lower viability after one week (67% for 8000 rad versus 83% for 3000 rad). After confirming that 3000 rad was sufficient to mitotically arrest 3T3-J2 cells under growth conditions while maintaining higher viability than cells irradiated with 8000 rad, we investigated how cryopreservation affected feeder cell viability.

Feeder cell activity declines over multiple passages and after overgrowth necessitating cryopreservation to limit the need for unnecessary subculture.[23] However, we noticed that cryopreservation of irradiated 3T3-J2 feeder cells resulted in slightly lower viability post-thaw compared to never-frozen cells (80% versus 90%). Previously established protocols suggested that increasing serum during cryopreservation enhances post-thaw viability of murine embryonic feeder cells.[23,45] Thus, to investigate whether bovine calf serum (BCS) content during cryopreservation enhanced feeder cell viability, we froze irradiated 3T3-J2 cells for 5 days in either DMEM/BCS with 10% *v/v* DMSO or 90% BCS with 10% *v/v* DMSO.

Although initial viability post-thaw was slightly higher for cells frozen in BCS/DMSO (87% viability in 90% serum versus 82% viability in 10% serum), cryopreservation serum content did not affect long-term viability or morphology (Appendix Fig. 3A2). Therefore, we chose to use DMEM/BCS with 10% DMSO moving forward since it was a more economical choice. To account for the reduced viability, feeder cells were seeded at a higher density post-thaw at 5 x 10^4 cells/cm^2, rather than 4 x 10^4 cells/cm^2 when feeder layers were prepared from cells already in culture. After identifying irradiation and cryopreservation methods to prepare feeder layers, we investigated feeder layer morphology and evolution during conditional reprogramming.

3T3-J2 feeder cells show detachment and displacement by epithelial cells during conditional reprogramming

Since feeder cell-secreted factors are critical to epithelial expansion and epithelial cells must be grown in specialized media, we first assessed irradiated feeder cell longevity in epithelial reprogramming media in the absence of epithelial cells. Feeder cells where cultured in conditional reprogramming F-media with and without Y-27632 ROCK inhibition (Appendix Fig. 3A3). In media containing Y-27632 (10 μM), feeder fibroblasts exhibited morphological changes marked by the presence of rounded cell bodies and long, thin membrane protrusions (Fig. 3A3). These dramatic morphological changes did not occur in F-media alone or when irradiated feeders were kept in 3T3-J2 culture media (DMEM supplemented with 10% BCS). Although F-media with ROCK inhibition induced cytoplasmic changes that were unfavorable to fibroblast spreading and attachment, viability remained high (~83%) (Fig. 3A3). Despite maintenance of high

viability in F-media with Y-27632, only 30% of cells initially seeded remained in culture after 4 days compared to 40% of cells in F-media without Y-27632. Thus, we concluded that ROCK inhibition does not impact feeder viability, but may be useful in allowing epithelial cells to more easily push feeder cells away during colony expansion.

Next, we investigated feeder layer morphology in the presence of primary epithelial cells. Irradiated feeder cell layers exhibited a reproducible progression from near complete coverage of the culture flask to detachment resulting in only ~10-20% coverage after 5–7 days in culture (Fig. 3-2). Prepared feeder cells initially seeded in DMEM/BCS spread and covered the entire culture dish (Fig. 3-2A). Following addition of epithelial cells in F-media with ROCK inhibitor, feeder cell morphology changed from flat to spindly cells (Fig. 3-2B). Epithelial cell colony growth resulted in feeder cells detaching and aggregating around the edges of the expanding epithelial colonies (Fig. 3-2B-C, arrows). Once epithelial colonies grew to 70–80% confluence (usually after 5–7 days), few feeder cells remained.

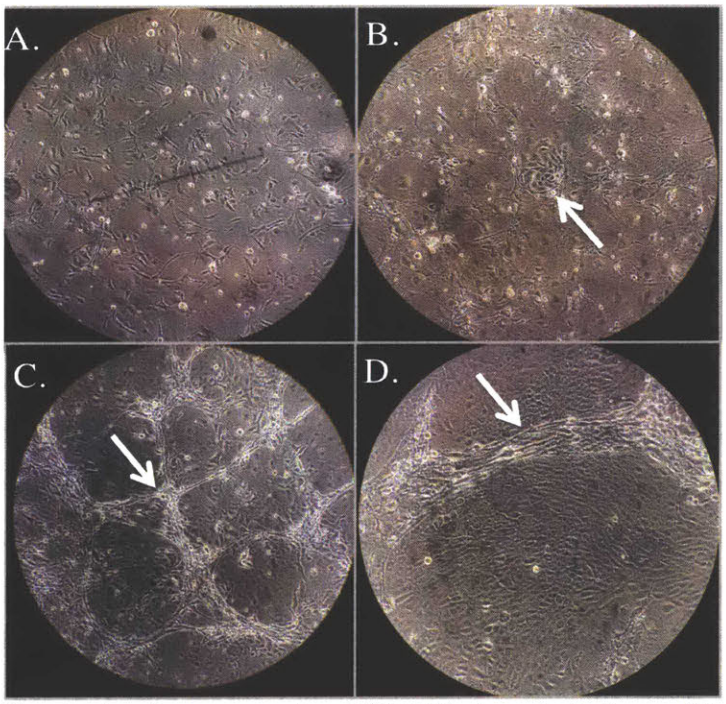

Figure 3-2. Phenotypic culture progression of 3T3-J2 feeder cells during conditional reprogramming. (A) 3T3-J2 cells ($5x10^4$ cells/cm^2) initially cover 80% of the culture flask. (B) After 2-3 days, small visible epithelial colonies begin displacing feeder cells (arrow). (C) By 5-7 days, large epithelial colonies push surrounding feeder cells to accumulate near the expanding edges (arrow). (D) When cultures become too confluent, epithelial colonies become large enough to merge with neighboring colonies further displacing feeder cells (arrow).

An example of an overly confluent culture shows adjacent epithelial colonies nearly touching, separated only by a detaching feeder cell rope (Fig. 3-2D, arrow). We observed that if epithelial cells become overly confluent or feeder cells become too sparse prior to passaging, then epithelial cells will undergo terminal differentiation resulting in rapid loss of growth potential in subsequent passages. After assessing that conditional reprogramming media resulted in feeder cell detachment over time, we next assessed growth and viability of primary endometrial fibroblasts, which were not mitotically arrested, but could be present as contaminating cells in isolated epithelial glands.

3.2.2 Conditional reprogramming diminishes primary stromal cell expansion

Endometrial stromal cells show reduced viability and growth in F-media with Y-27632

Endometrial stromal fibroblast cells typically comprise less than 5% of the isolated epithelial gland fraction obtained from an endometrial biopsy.[46] Despite the low abundance of contaminating stromal cells, we have observed that under standard culture conditions in DMEM/F12 media supplemented with 10% FBS (DMEM/F12/FBS) stromal fibroblasts will outcompete epithelial cells in culture (data not shown). Thus, it is important to limit stromal fibroblast growth to allow epithelial expansion.

In order to evaluate how endometrial stromal cells behave under conditional reprogramming, we seeded CellTracker green dye-labeled primary stromal cells (ESC) (n=2) and TERT-immortalized human endometrial stromal cells (tHESCs) in F-media plus Y-27632 and DMEM/F12/FBS with and without feeder cells (Fig. 3-3A, primary ESC shown, tHESC not shown). Stromal cells appeared brighter and less spread with long, thin protrusions and prominent cell bodies in the presence of F-media plus Y-27632 as compared to DMEM/F12/FBS. ROCK inhibition is known to induce intermediate filament and microtubule reorganization leading to cytoskeletal changes and extended cell processes.[47] Changes in cell morphology were visualized in both endometrial stromal cells and irradiated feeder fibroblasts when seeded in F-media plus Y-27632 but not in DMEM/F12/FBS (Fig. 3-3A).

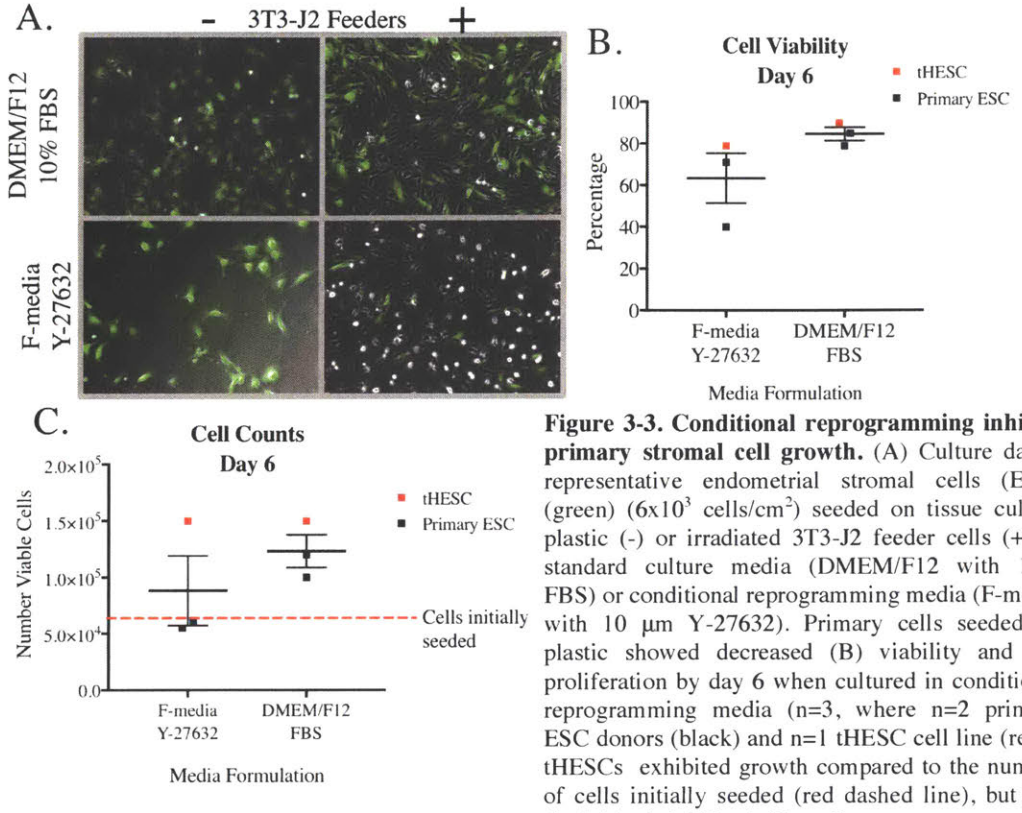

Figure 3-3. Conditional reprogramming inhibits primary stromal cell growth. (A) Culture day 2 representative endometrial stromal cells (ESC) (green) ($6x10^3$ cells/cm^2) seeded on tissue culture plastic (-) or irradiated 3T3-J2 feeder cells (+) in standard culture media (DMEM/F12 with 10% FBS) or conditional reprogramming media (F-media with 10 μm Y-27632). Primary cells seeded on plastic showed decreased (B) viability and (C) proliferation by day 6 when cultured in conditional reprogramming media (n=3, where n=2 primary ESC donors (black) and n=1 tHESC cell line (red)). tHESCs exhibited growth compared to the number of cells initially seeded (red dashed line), but had diminished viability in F-media.

Dye-labeled cells appeared brighter in F-media (with or without feeder cells) compared to in DMEM/F12/FBS suggesting cells proliferated less in F-media as cell dye becomes diluted upon proliferation. Quantification of primary stromal cells seeded on plastic after 6 days in F-media plus Y-27632 confirmed reduced viability and growth (Fig. 3-3B&C, black data points), compared to stromal cells seeded in traditional growth media, DMEM/F12/FBS. While primary cells in F-media did not proliferate over 6 days, tHESCs increased in numbers two-fold, but displayed decreased viability (79% in F-media versus 90% in DMEM/F12/FBS) (Fig. 3-3B&C, red data points). This suggests that hTERT-induced immortalization was beneficial for overcoming conditional reprogramming to allow growth. Our results were in agreement with previous studies showing primary skin fibroblasts had reduced proliferation when cultured on irradiated 3T3-J2 feeder fibroblasts in F-media plus Y27632.[33] After verifying that primary endometrial stromal fibroblast growth was hindered during conditional reprogramming, we evaluated primary epithelial cell expansion using 3T3-J2 feeders.

3.2.3 Conditional reprogramming promotes primary epithelial cell expansion

Conditional reprogramming requires 3T3-J2 feeder cells and maintains epithelial colony morphology

To investigate culture expansion of primary endometrial epithelial cells, we first compared commercially available medium to conditional reprogramming methods. Commercially available epithelial cells (n=2 donors) were grown in either commercially recommended culture medium (ReproLife) with and without feeder cells or conditional reprogramming F-media with and without feeder cells (Fig. 3-4A). Cells were acquired at passage 3 and grown to passage 10. Both donors failed to expand beyond 3 population doublings when cultured in F-media without 3T3-J2 feeder cells suggesting feeder cell factors are crucial for epithelial cell growth in F-media. However, ReproLife media supported growth with or without feeder cells, which may be due to added media supplements like bovine pituitary extract (BPE). BPE is known to contain growth factors and antioxidants that enhance primary epithelial cell proliferation.[48,49]

Primary endometrial epithelial cells showed comparable growth (~10 population doublings) in commercially available media (ReproLife) and during conditional reprogramming with feeder cells in F-media (Fig. 3-4B). However, conditionally reprogrammed cultures maintained epithelial cell cuboidal morphology during expansion, whereas cells in ReproLife media became elongated, losing cell-cell contacts and adopting a mesenchymal appearance after passage 6 (Fig. 3-4A). Because epithelial morphology was maintained under conditional reprogramming, we next investigated expansion efficiency of the conditional reprogramming method with additional donors sourced from frozen endometrial epithelial cells and freshly isolated endometrial pipelle biopsies.

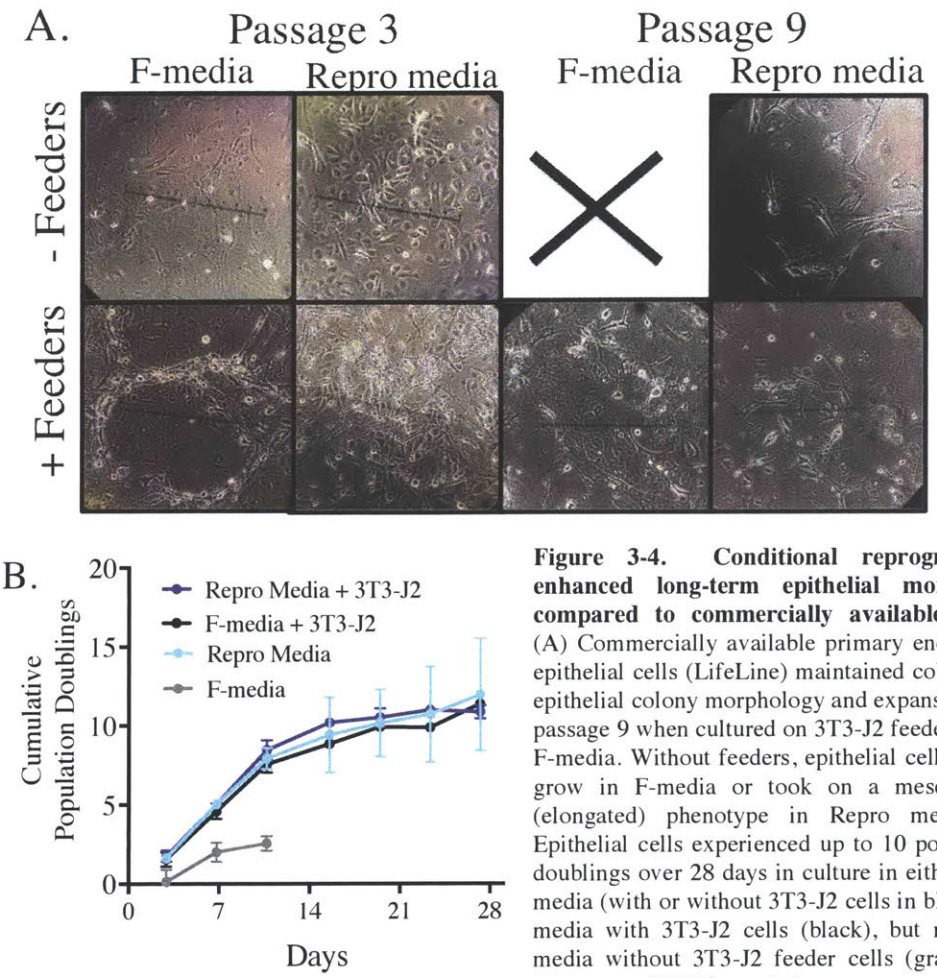

Figure 3-4. Conditional reprogramming enhanced long-term epithelial morphology compared to commercially available media. (A) Commercially available primary endometrial epithelial cells (LifeLine) maintained cobblestone epithelial colony morphology and expansion up to passage 9 when cultured on 3T3-J2 feeder cells in F-media. Without feeders, epithelial cells did not grow in F-media or took on a mesenchymal (elongated) phenotype in Repro media. (B) Epithelial cells experienced up to 10 populations doublings over 28 days in culture in either Repro media (with or without 3T3-J2 cells in blue) or F-media with 3T3-J2 cells (black), but not in F-media without 3T3-J2 feeder cells (gray). Data are mean ± SEM for n=2 donors.

Conditional reprogramming promotes transient endometrial epithelial expansion

Additional primary endometrial epithelial cells (n=7 donors) were acquired from pipelle biopsies and isolated using methods adapted from previously established protocols[46] as outlined in 2.3.1 and Chapter 2 Appendix. Cells cultured under conditional reprogramming methods resulted in 89% (8 out of 9 donors) expanding at least 5 population doublings and 67% (6 out of 9 donors) expanding greater than 10 population doublings (Table 3-1). Of the 8 donors that expanded at least 5 population doublings, donors exhibited an average of 12 population doublings and attained 8 passages corresponding to 32 days in culture before showing signs of cellular senescence, as observed by cells becoming large and fried egg-shaped with abundant cytoplasmic area. Cell growth as indicated by calculated population doublings >1 was observed on average

around passage 3 corresponding to 14 days after culture initiation, with most gains in cell doublings occurring between passages 4–7 (typically between 20–45 days in culture) (Fig. 3-5A).

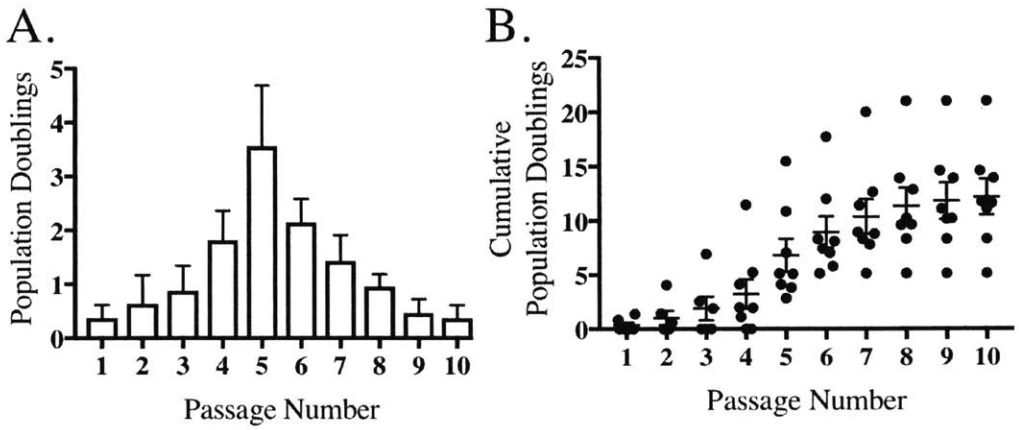

Figure 3-5. Conditional reprogramming enhances primary epithelial cell survival and growth. Primary endometrial epithelial cells were cultured on 3T3-J2 feeder cells in F-media with Y-27632 up to passage 10. (A) Average number of population doublings per culture passage shows cell growth was greatest between passages 4-7, with peak doubling efficiency at passage 5. (B) Cumulative number of population doublings per culture passage shows on average a lag phase between passages 1-3, followed by rapid growth during passages 3-7, and a slowing of growth after passage 7. Data presented are average ± SEM for n=8 donors.

The observed delay in initial cell doubling may suggest that conditional reprogramming takes time, resulting in an initial lag time before cells become proliferative (Fig. 3-5B). Alternatively, the culture growth lag could be explained by outgrowth occurring in a subset of cells that are selected for during conditional reprogramming. We observed that only some cells initially attached and rapidly formed colonies whereas numerous other cells remained floating in the media. This supports that conditional reprogramming likely promotes growth of some, but not all, cells initially seeded and may select for a subset of cells. It is possible that some terminally differentiated cells cannot be reprogrammed to a proliferative state and thus will die off over the first few passages of culture, while other less differentiated cells may exhibit immediate growth. The net result is cell growth that offset cell death over the first few passages resulting in an apparent lag phase before growth was observed.

This growth pattern is indicative of a transit amplifying population. During tissue regeneration or growth, stem cells, which proliferate slowly, are thought to give rise to a population of transit amplifying cells that are capable of multiple rounds of rapid proliferation prior to terminal differentiation.[27] We observed a subset of cells were capable of rapid proliferation for 3–4 passages prior to becoming senescent (Fig. 3-5). Indeed, recent studies confirmed rapid induction of transit amplifying cell markers in conditionally reprogrammed prostate cells.[50] However, unlike our results, these cells were capable of over 70 population doublings over 90 days in culture, suggesting additional maintenance of a long-term progenitor population during culture. Taken together, these results suggest that conditional reprogramming may result in a stem-like state where culture expansion is highly dependent on the stage of adult stem cell commitment.

Previous studies that used conditional reprogramming to expand primary ectocervical epithelial cells did not find evidence to support selection of a subpopulation of cells.[22] Specifically, after 2 days under conditional reprogramming, epithelial cells exhibited rapid induction of adult stem cell markers, including CD44, integrin α6, and p63 transcription factor, which persisted over 11 passages, but not embryonic or induced pluripotent stem cell markers.[22] In addition, conditional reprogramming of mammary, prostate, lung, and liver cells showed greater than 50 population doublings with cells exhibiting proliferation over 100 days in culture.[21] Despite our ability to improve current expansion efforts for endometrial epithelial cells, we were unable to achieve the same results of near infinite expansion potential reported for some epithelial tissues. However, similar to colon and pancreas epithelia, we were able to achieve population doublings greater than 3-fold the current standard for endometrial epithelial cells under conditional reprogramming culture conditions.[21,23] Endometrial epithelial cells may require additional factors beyond 3T3-J2 feeder cells and ROCK inhibition to further increase expansion efficiency. Additionally, we may not be culturing the appropriate progenitor cell population; however, future exploration of the stromal cell compartment should be explored for endometrial regeneration.[25,26,51]

Recently published modifications to the conditional reprogramming protocol suggest methods must be adapted to support expansion of some tissues, including colon and pancreas.[23] Specifically, colon epithelial cells exhibited enhanced growth when

plated on collagen-coated flasks with feeder-conditioned media, rather than directly on irradiated feeder cells. Furthermore, colon cells required lower oxygen concentrations (2% O_2 rather than 5%) and media supplementation with R-spondin (1 μg/mL).[23] Interestingly, recent work showing expansion of endometrial epithelial organoids revealed R-spondin, i.e., WNT pathway activation, as necessary to promote long-term culture.[16] Thus, future studies should investigate whether endometrial epithelial cells, like colon cells, require additional factors, including R-spondin, to maintain a stem cell population and overcome cellular crises during expansion.

Given the highly proliferative nature of endometrial epithelial cells in response to estrogen, label-retaining studies have thus far failed to establish definitive epithelial stem cell markers and localization within the endometrium.[29,52] Additionally, some evidence suggests that the cycling endometrium, including the epithelium, may be in part repopulated from recruited (i.e., non-uterine) bone marrow-derived mesenchymal stem cells.[53] Thus, it is worth noting that our results do not rule out the possibility that there exists a mesenchymal stem cell that may give rise to more differentiated lineage-specific progenitor cells, i.e., epithelial and stromal progenitors that are capable of only a finite number of expansions. Conditional reprogramming may select for these more differentiated progenitor populations in the endometrium, preventing long-term expansion beyond ~10 population doublings *in vitro*.

Conditional reprogramming expansion is feasible for heterogeneous clinical donors

Given that some donor heterogeneity was observed with expansion and the eventual goal of studying both healthy and pathological conditions, we wanted to assess whether clinical characteristics such as donor age, menstrual cycle phase, and diagnosis (benign gynecologic conditions) influenced expansion potential (Table 3-1).

All acquired donors were premenopausal, with 7 out of 9 donors exhibiting regular menstrual cycles, without intermenstrual bleeding, and no history of hormone use in the 3 months prior to collection (clinical data was unavailable for n=2 Lifeline donors). Donors ranged in age from 25 to 45, including 4 proliferative phase and 3 luteal phase samples as confirmed by histology (Table 3-1). All donors under the age of 40 exhibited greater than 10 population doublings, while donors above 40 ranged from no expansion

to greater than 20 population doublings. Because there exists heterogeneity in the age of onset of menopause, which is preceded by changes in hormone levels and declining ovarian reserves prior to amenorrhea, we cannot rule out that age, especially variations in perimenopausal hormone changes, may result in inconsistent cell expansion in donors over 40 years of age.[54,55]

The endometrium is a unique tissue where declining progesterone levels leads to an irreversible cascade resulting in protease expression and tissue breakdown.[56] Furthermore, endometrial growth is known to be estrogen-dependent with endometrial regression and thinning occurring post-menopause when estradiol levels are low.[57] However, epithelial cell regeneration is known to occur independently of progesterone and estradiol during the menstrual phase,[32] and given our desire to control hormone levels in endometrial cell cultures, we initiated expansion in defined hormone conditions, i.e., dextran-charcoal (DC) stripped serum to remove hormones and phenol red-free media, as phenol red has been shown to act as a weak estrogenic compound.[58] Previous conditional reprogramming methods have used both regular serum and phenol red-containing media.[23] In pilot studies (n=2 donors), we did not find that using regular FBS increased growth compared to DC stripped serum (data not shown). Thus, further experiments are necessary to determine the potential role of hormone signaling during endometrial epithelial survival and expansion, and to determine the impact, if any, of hormone supplementation and phenol red on maintaining long-term reprogramming expansion of primary epithelial cells.

There were no other obvious donor characteristics or clinical diagnoses that correlated with donor expansion potential, suggesting conditional reprogramming could be applied to isolated cells acquired during any cycle phase and could be used to generate cells from both healthy donors and donors exhibiting pathological diagnoses including myomas, endometriosis or adenomyosis. Additionally, cells could be expanded from either freshly acquired or previously frozen cells. Future studies are needed to assess whether this approach is useful for expansion of post-menopausal or hormone-treated donor cells. After determining that conditional reprogramming was a generalizable method with promise for expanding cells from both follicular and luteal menstrual cycle

phases, we assessed progression of epithelial phenotypes from initial culture through culture senescence.

Table 3-1. Primary endometrial epithelial donor data

Donor #	Fresh/ Frozen	Highest Passage	Population Doublings	Cycle Phase	Age	Diagnoses
160	Frozen	10	14	luteal	34	myoma
193	Fresh	8	14	proliferative	38	adeno/endo(IV)
197	Fresh	9	11	luteal	35	myoma/adeno
196	Fresh	3	<1	proliferative	45	myoma/adeno/ endo(I)
203	Fresh	7	8	luteal	43	myoma/adeno/ endo(I)
208	Fresh	10	21	proliferative	42	myoma
209	Fresh	6	5	proliferative	42	endo(IV)
LifeLine (03839)	Frozen	10	11	unknown	33	unknown
LifeLine (05263)	Frozen	10	11.5	unknown	25	unknown

Endometrial epithelial cell morphology is influenced by culture passage

Endometrial epithelial cells showed a predictable culture progression of morphologies starting from initial culture through passage 10 (Fig. 3-6). Isolated epithelial cell aggregates (comprising ~20-200 cells) cultured from either previously isolated and frozen (n=3) or freshly isolated (n=6) biopsies were seeded on feeder cells (Fig. 3-6A, arrow). As expected, colony forming efficiency of seeded cells was initially low since many of the seeded cells were assumed to be fully differentiated and thus would be expected to exhibit limited self-renewal. After the first 2-3 passages, cell death declined and a proliferative cell population marked by small cobblestone epithelial cells with visible cell-cell contacts persisted for the next 4-5 passages (Fig. 3-6B, arrow). Around passage 7-8 (10-12 population doublings), often cell growth rapidly declined and morphology shifted. Epithelial cells tended to become large and fried egg-shaped with abundant cytoplasmic areas indicative of a senescent phenotype (Fig. 3-6C, arrow). Additionally, cells with numerous vacuoles or colonies of elongated cells without defined cell borders were observed (Fig. 3-6D, arrow).

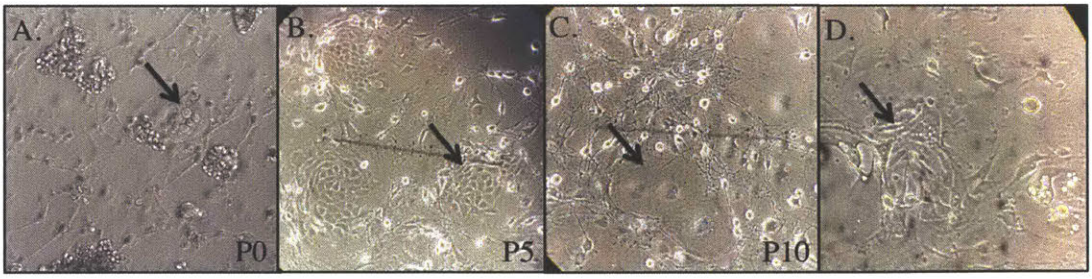

Figure 3-6. Phenotypic culture progression of epithelial cells during conditional reprogramming. (A) Following isolation at passage 0, epithelial glands attach to 3T3-J2 feeder layers. (B) Epithelial colonies exhibit prototypical cobblestone morphology during culture passages up to 7. At later passages (8–10), epithelial morphologies shift to frequently include (C) large, cytoplasmic cells indicative of senescence and (D) cells with abundant vacuoles or mesenchymal-like colonies with elongated cells without defined borders (arrow).

Population doubling time was shortest for cells between passages 4–7 with longer population doubling times observed for initial and later passages. Interestingly, cryopreserved cells from commercial donors were acquired at passage 3 and exhibited the most robust growth during passages 4–8, in agreement with the freshly isolated glands that we observed in culture. Additionally, prototypical epithelial cuboidal cellular morphology was routinely maintained up to 7 populations doublings (~5–8 passages), suggesting that these cells may be useful in future experiments investigating primary endometrial epithelial cell function. While previous studies have shown conditionally reprogrammed cells remained karyotypically stable,[21] future investigation of expanded cells is needed to rule out genetic drift. After confirming that conditional reprogramming methods could reproducibly expand primary endometrial epithelial cells, routinely yielding 10^7 cells prior to passage 6, we investigated the cellular markers, function, and protein secretion of the expanded cells.

3.2.4 Conditionally reprogrammed cells display epithelial markers and functional phenotypes

Flow cytometry reveals expanded cells are of epithelial origin

First, to confirm that conditionally reprogrammed cells were of epithelial origin, we evaluated expression of epithelial cell markers cytokeratin 18 (CK18) and epithelial cell adhesion molecule (EpCAM). Epithelial cells cryopreserved at passage 0 and passage 9 post-expansion were compared against donor matched stromal cells (passage 2) (Fig. 3-7). The isolated epithelial fraction at passage 0 showed heterogeneity with small populations (representing ~5%) that were negative for epithelial cell markers CK18 and EpCAM, but positive for stromal marker vimentin. In line with previous studies, our results suggested minimal stromal cell contamination after initial isolation.[46] However, after expansion, epithelial cells at passage 9 showed a single uniform population with a narrower distribution that was positive for epithelial markers and negative for vimentin. This confirmed our previous result showing conditional reprogramming hinders primary stromal growth while promoting epithelial expansion. After verifying that expanded cells were epithelial, we next investigated whether epithelial cells retained barrier function and characteristic protein secretion post-expansion.

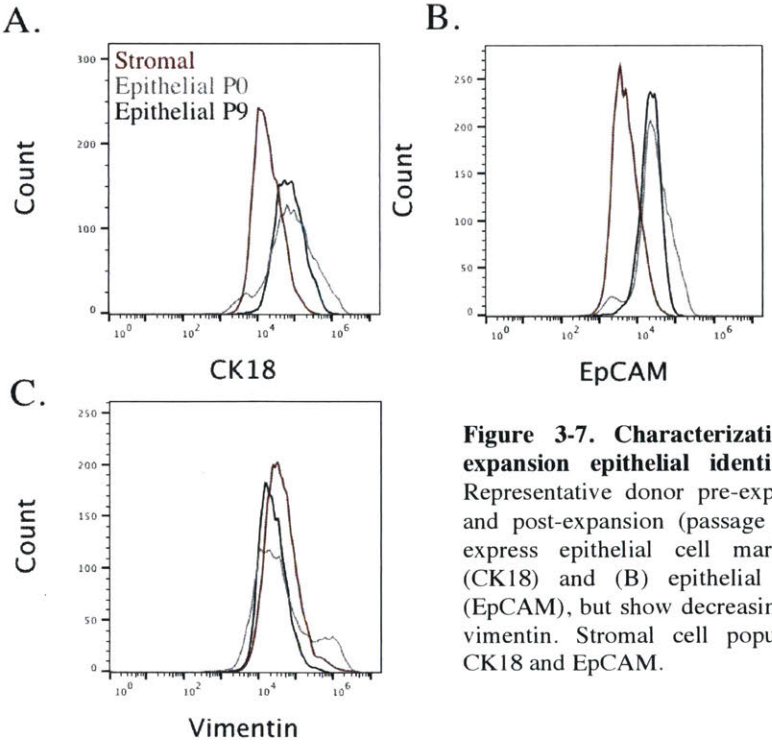

Figure 3-7. Characterization of pre- and post-expansion epithelial identity by flow cytometry. Representative donor pre-expansion (passage 0, gray) and post-expansion (passage 9, black) epithelial cells express epithelial cell markers (A) cytokeratin-18 (CK18) and (B) epithelial cell adhesion molecule (EpCAM), but show decreasing (C) stromal cell marker vimentin. Stromal cell population was negative for CK18 and EpCAM.

Conditionally reprogrammed cells display epithelial barrier function

We next wanted to assess whether the expanded and cryopreserved epithelial cells were capable of forming a cell monolayer with barrier function. A defining characteristic of epithelial cells is the ability to form cell-cell contacts with neighboring cells to create an integrated barrier that selectively allows passage of ions and proteins while preventing passage of infectious agents into the underlying stroma. Transepithelial electrical resistance (TEER) is a measurement of how easily current flows across an epithelial monolayer and is used to monitor barrier integrity.[59] High TEER values are associated with increased barrier function including monolayer confluence and formation of tight cellular junctions.

Three expanded primary donors (passage 4 or 5) or the endometrial adenocarcinoma Ishikawa cell line were seeded on cell culture inserts in F-media with 10 μM Y-27632 for 3 days ($2x10^5$ cells/insert or $6x10^5$ cells/cm^2). After three days, cells were switched to differentiation F-media (without Y-27632, higher calcium and lower EGF) to induce monolayer differentiation. TEER was assessed on days 2 and 8 following induction of differentiation (Fig. 3-8A).

For endometrial epithelial cultures, typical TEER values have been reported to be 350-1000 ohms x cm^2.[24,40,60] Of note, the two donors collected from the luteal phase (0160 and 0203) both exhibited TEER values above 1000 ohms x cm^2 on day 8 whereas the proliferative phase donor (0208) was ~500 ohms x cm^2. Uterine epithelial cultures exposed to estrogen have been previously shown to exhibit lower TEER values compared to cells exposed to progesterone.[60] Thus, further investigation of additional expanded donor cells is needed to see if maintenance of hormone responsive TEER differences are preserved through expansion or can be induced post-expansion. Additionally, while the primary epithelial cells displayed high TEER values suggestive of barrier function, the adenocarcinoma endometrial epithelial Ishikawa cell line failed to achieve appreciable TEER (~14 ohms x cm^2) even after 8 days in differentiation media.

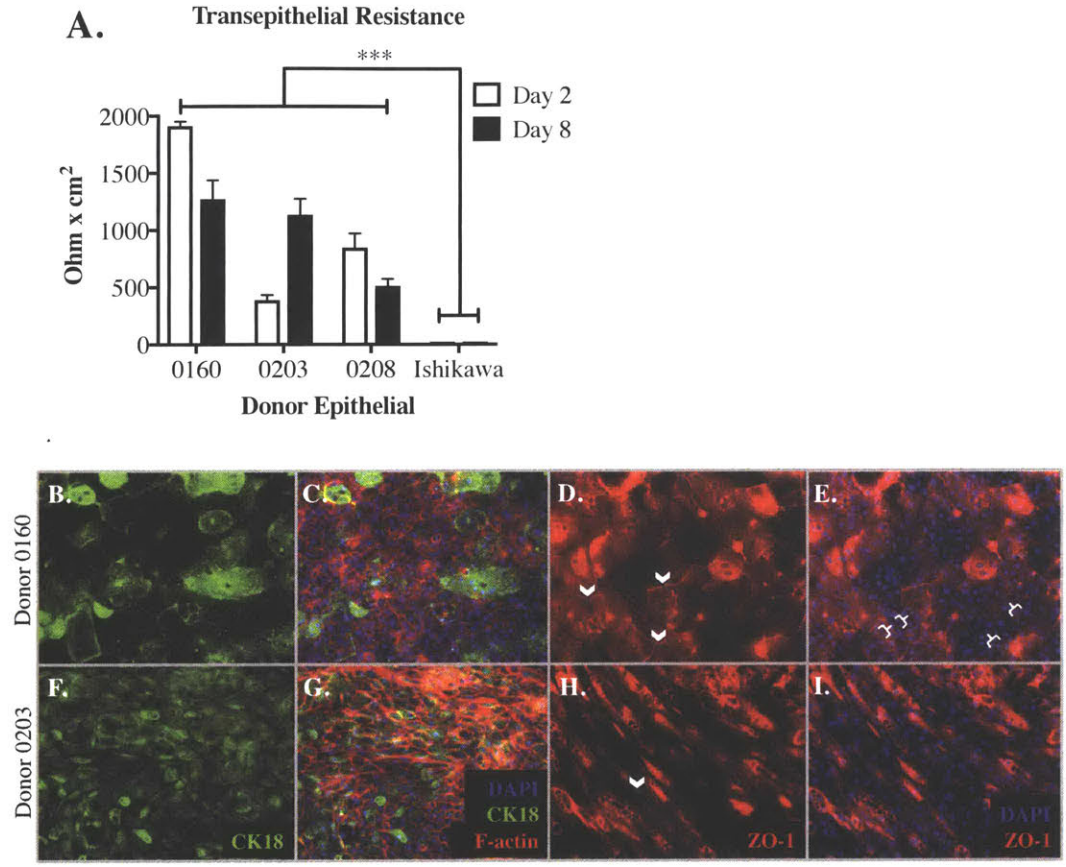

Figure 3-8. Primary expanded epithelial cells display barrier function by increased electrical resistance and tight junction formation. (A) Transepithelial electrical resistance (TEER), indicative of a functional epithelial barrier, is significantly higher in primary expanded epithelial cells (Passage 4 or 5) than in the Ishikawa epithelial cell line. Immunostaining shows expanded cells stain for epithelial marker (B),(F) cytokeratin 18 (CK18) (green). (C),(G) All cells display defined F-actin (red) cell-cell borders with only some cells staining for CK18 (green). (D) Tight junction protein zona occludens 1 (ZO-1, red) shows defined localization at cell-cell borders (white arrows) correlating with high TEER (>1000 ohm x cm^2), (H) with a more diffuse cytoplasmic ZO-1 localization when cultures displayed lower TEER values (<500 ohm x cm^2). (E) Mitotic events (white brackets) were observed in donor 0160, (I) but not in donor 0203. Cell nuclei are stained with DAPI (blue).

Following 8 days of differentiation, expanded epithelial cultures generally displayed two phenotypes. The first contained two layers of cells (observed in n=2 donors, 0160 and 0208). The lower layer, closest to the insert membrane, was generally more regular in appearance with F-actin staining revealing cell boundaries associated with each nuclei and overall round cobblestone morphology (Fig. 3-8 C). The top layer was sparser with fewer nuclei, but had prominent cytokeratin 18 staining not observed in the bottom cell layer with defined tight junction (ZO-1) staining (Fig. 3.8 B-D, white arrows). Additionally, mitotic events were only observed in the lower layer of cells (Fig. 3-8 E). This morphology more closely mimicked a pseudostratified appearance with a more proliferative less differentiated basal cell layer.

On the other hand, Donor 0203 showed a more characteristic secretory phenotype with cells forming a single cytokeratin 18 positive layer with prominent vacuolization and the absence of mitotic events (Fig. 3-8 F-I). Cells also showed less tight junction formation (ZO-1 localization to cell-cell borders) and thus had lower TEER compared to the donors with more ZO-1 localization (Fig. 3-8 A,H). After confirming epithelial marker immunostaining and barrier function of expanded cells, we next compared secretion of cytokines and proteases between expanded primary epithelial cells and the Ishikawa cell line model.

Cytokine and protease secretion in conditionally reprogrammed cells

In order to assess whether expanded epithelial cells may be suitable for future paracrine signaling studies, cytokine and proteases were measured in expanded and cryopreserved primary cells and the Ishikawa cell line model. Unsupervised hierarchical clustering analysis of secreted cytokine and matrix metalloproteinases (MMPs) showed expanded primary epithelial cells (n=5 donors) appeared more similar in their protein secretion profiles compared to the endometrial epithelial adenocarcinoma Ishikawa cell line (Fig. 3-9A). Additionally, within the expanded primary cell cluster, further clustering revealed heterogeneity amongst the primaries that was evident even after expansion (Fig. 3-9A). For example, the commercially available donors, LL03839 and LL05236, appeared more similar to one another forming their own cluster which may mean cell source, including isolation protocol or initial culture media, may have impacts on cytokine and MMP

secretion that are present even after expansion. This suggests that conditional reprogramming does not yield a uniform cell population and may even preserve donor heterogeneity that may be of interest. Future studies with additional donors are needed to assess whether the heterogeneity is of biological significance or correlated with particular clinical characteristics.

Primary cells secreted a higher abundance of most measured analytes compared with the Ishikawa cell line. Ishikawa cells secreted 25 of 36 measured cytokines and MMPs at or below levels observed in all of the expanded primary donors (Fig. 3-9B). Only 3 cytokines, FGFb, IL12p70 and VEGF showed heterogeneous secretion in primary cells compared to Ishikawa cells. Neither Ishikawa nor primary expanded epithelial cells secreted detectible IL7, IL13, IL15, IL17A, or MMP8. Secreted levels of IL2 and IL5 were consistent between all donors and the Ishikawa cell line, while IL10 was the only analyte produced in higher abundance by Ishikawa cells compared to all primary donors.

Additionally, our cytokine secretion results are in agreement with previous studies looking at freshly isolated and cultured endometrial epithelial cells where cells secreted measureable levels of IL8, IL6, G-CSF, GM-CSF, TNFa, and MIP1b, but cells did not produce detectible IL4 or IL17.[24,40] One notable difference was the abundance of MCP1 in freshly isolated cells, which we detected at much lower levels in the expanded cells. This may be due to loss of immune cells during expansion that may contribute to MCP1 secretion. Overall, Ishikawa cells poorly represented endometrial barrier and protein secretion, while expanded primary epithelial cells retained expected functional characteristics post-expansion and cryopreservation suggesting they may be useful for further *in vitro* studies of endometrial pathobiology.

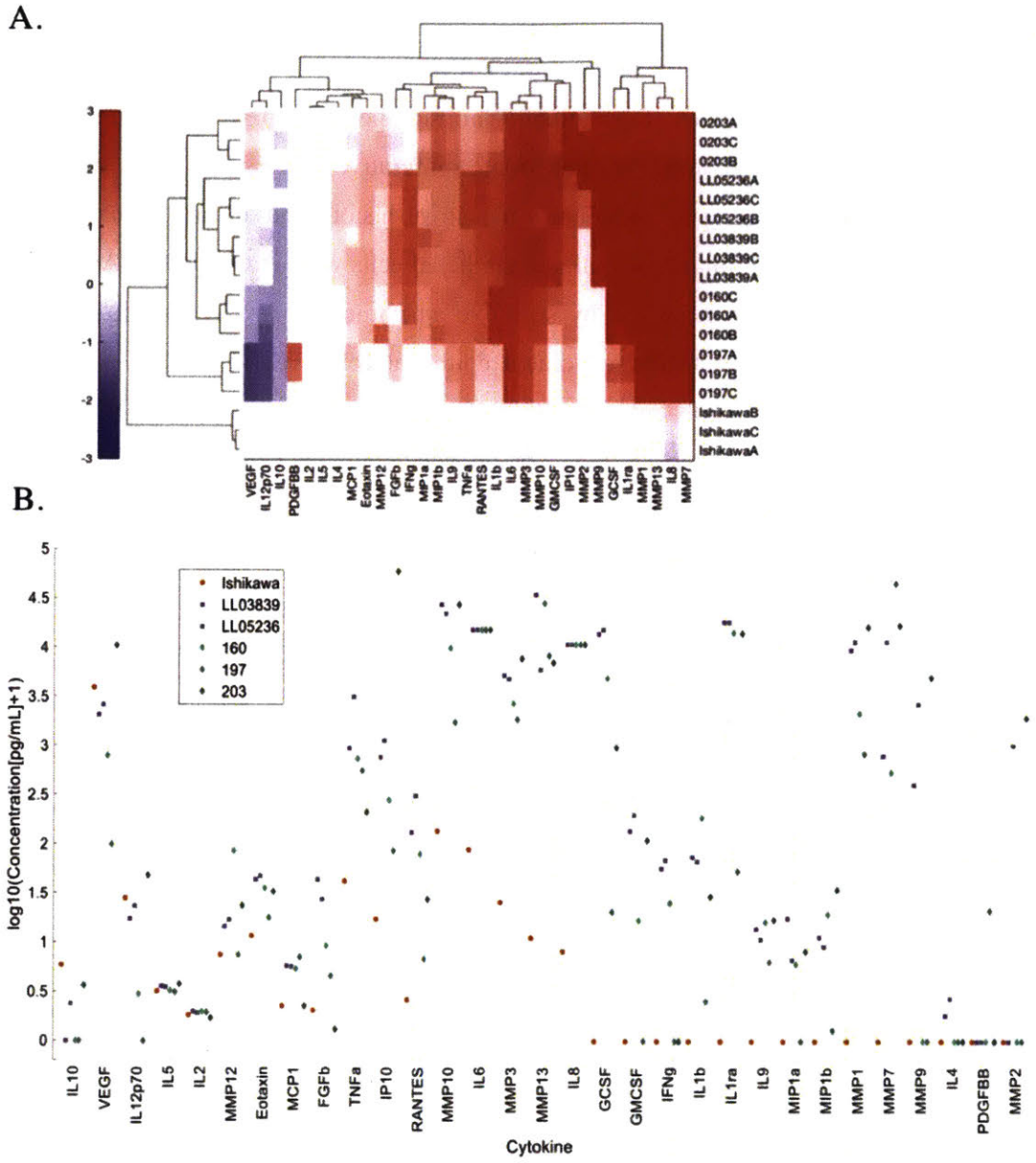

Figure 3-9. Primary epithelial cells exhibit higher and more heterogeneous post-expansion secretion of MMPs and cytokines compared to Ishikawa cells. (A) Unsupervised hierarchical clustering analysis of secreted cytokine and MMPs (48 h conditioned media) reveals heterogeneity in primary expanded donor epithelial cells that appear more similar to one another compared to the endometrial adenocarcinoma cell line, Ishikawa. (B) In general, Ishikawa cells secrete levels of cytokines and MMPs at or below primary donor cells for 25 of 36 measured analytes with only IL-10 secreted in higher abundance by Ishikawa cells compared to all primary donors (n=5 donors, n=3 replicates).

3.3 Materials and Methods

3.3.1 Primary endometrial cell isolation and culture

Endometrial biopsy specimens (three pipelle biopsies per donor) were acquired as in 2.3.1. All specimens were from the menstrual/proliferative phase (day 1-14) or luteal phase (day 15-30) according to the donor's menstrual history and/or histological dating (Appendix Table 3A1). Primary stromal and epithelial cells were isolated as in Appendix 2.6. Final purification was achieved by selective attachment of any remaining stromal cells to plastic substrate as follows: Isolated epithelial cells were seeded in a 75 cm^2 tissue culture flask and incubated at 37°C, 95% air, 5% CO2 for 1h in DMEM/F12 supplemented with 5% FBS and 1% P/S. Non-attached epithelial cells were collected and cultured in subsequent conditional reprogramming or cryopreserved as glandular fragments in F-media supplemented with 10% *v/v* DMSO for later analysis or expansion. Additional already isolated primary epithelial cells (passage 3) (Lifeline Cell Technology, FC-0078, Frederick, MD) were culture expanded in fully supplemented ReproLife media (Lifeline Cell Technology, LL-0068) with 1% P/S at an initial density of $2x10^4$ cells/cm^2 after thawing. Subsequently, once cells reached 80% confluence, cells were passaged at a density of $5x10^3$ cells/cm^2 and cultured or cryopreserved at passage 4 in ReproLife media with 10% *v/v* DMSO until further use. All cells were grown in a humidified incubator at 5% CO2 and 37°C.

3.3.2 Conditional reprogramming expansion

Cell culture reagents

Primary endometrial epithelial cells were expanded in F growth media (F-media) comprising DMEM/F12 (3:1 mixture of Dulbecco's Modified Eagle's Medium and Ham's F-12 (Gibco) phenol-red free media), 5% *v/v* dextran/charcoal treated fetal bovine serum (DC-FBS) (Atlanta Biologicals), 25 ng/mL hydrocortisone (Sigma H0888), 5 μg/mL insulin (Sigma I9278), 10 ng/ml EGF (PeproTech AF-100-15), 10 μM Y-27632 (Tocris 1254), 8.4 ng/mL cholera toxin (Sigma C8052), and 1% penicillin/streptomycin (P/S) (Gibco, 15140). 3T3-J2 embryonic mouse fibroblast cells (Kerafast EF3003, Boston, MA) were cultured in DMEM/BCS comprising DMEM (Thermofisher

21063029) supplemented with 10% *v/v* iron-supplemented bovine calf serum BCS (GE Healthcare/Hyclone SH30072.03) and 1% P/S unless otherwise noted.

Murine 3T3-J2 feeder cell expansion, irradiation and preparation

3T3-J2 cells were initially seeded in accordance to manufacturer's guidelines at 1.3 x 10^4 cells/cm^2 in a 75 cm flask in 20 mL of DMEM/BCS without centrifugation to remove DMSO. Cells were passaged at 60–80% confluence and reseeded at a density of 3.5-5 x 10^3 cells/cm^2 during subculture. Cells were cryopreserved in DMEM/BCS containing 10% *v/v* sterile DMSO or irradiated for use as feeders prior to passage 15.

After reaching 80% confluency, 3T3-J2 cells were prepared for irradiation in DMEM/BCS media as follows. Cells were trypsinized, collected into a 50 mL conical tube and resuspended in fresh DMEM/BCS at 1x10^6 cells/mL. Cells were immediately irradiated (3000 rad or 30 Gy, unless otherwise noted) using a Cobalt-60 Irradiator (Gammacell 220 Excel). After irradiation, cells were either cryopreserved in DMEM/BCS with 10% *v/v* DMSO at 4 x 10^6 cells/mL and stored in LN_2 or reseeded at 4 x 10^4 cells/cm^2 in DMEM/BCS usually 24-48 hours prior to epithelial seeding.

Stromal cell culture on 3T3-J2 murine feeder fibroblasts

Primary endometrial stromal cells (passage 2) and tert-immortalized human endometrial stromal cells (passage 9) were CMFDA dye-labeled (1 μM) (ThermoFisher C2925) for 30 minutes at room temperature in PBS. Cells were centrifuged and resuspended in DMEM/F12 10% DC-FBS or F-media and seeded at 6x10^3 cells/cm^2 in a six well plate with and without 3T3-J2 feeder cells. Stromal cells were imaged on day 2 and counted on day 6 of culture to assess viability and proliferation.

Epithelial expansion on 3T3-J2 murine feeder fibroblasts

Primary epithelial cells were expanded according to previously established methods for conditionally reprogramming primary epithelial cells.[21] Briefly, isolated epithelial glandular fragments, or single cells from trypsinized glandular fragments, were initially seeded and subsequently passaged onto irradiated 3T3-J2 feeder cells prepared preferably 24-48 h in advance (although 2 h was found to be acceptable when time did not permit 24 h). Epithelial cells were seeded at a density of 3-7 x 10^3 cells/cm^2 together with feeder

cells seeded at a density of 4-5.5 x 10^4 cells/cm^2 in F-media unless otherwise noted. Epithelial cells were passaged onto a new feeder layer once they reached 75% confluence (4-7 days), and medium was replaced every 2 days thereafter.

Endometrial epithelial subculture and cryopreservation

Epithelial cells were separated from feeder cells during passaging using differential trypsinization as previously described.[21] Briefly, co-cultures were washed with 1X PBS and subsequently incubated with room temperature 0.05% trypsin-EDTA (Sigma Life Sciences, T4174) (3 mL in 75 cm flask) for 1-1.5 min until feeder cells began to detach as confirmed by microscopy. Subsequently, cultures were gently tapped and detached feeder cells were removed by aspiration. Epithelial cells were rinsed with 1 X PBS to remove additional feeders and incubated with pre-warmed 37°C 0.05% trypsin (3 mL in 75 cm flask) for 5–15 min until epithelial cells detached as determined by close monitoring by microscopy every 5 minutes. Trypsin was neutralized with DMEM/F12 supplemented with 10% *v/v* DC-FBS and 1% P/S, and single cells were counted, centrifuged at 500g for 5 min and then resuspended in F-media for passaging onto a fresh feeder layer. Expanded primary epithelial cells were cryopreserved prior to passage 10 in F-media with 10% *v/v* DMSO for subsequent characterization or expansion.

3.3.3 Expanded epithelial cell characterization

Flow Cytometry

Pre-expanded (passage 0, n=2 donors) and post-expanded (passages 6-9, n=5 donors) epithelial samples were thawed and fixed in 3.7% paraformaldehyde for 10 min at room temperature. After washing with 1% BSA/PBS, cells were permeabilized with 0.1% Triton-X/1% BSA in 1X PBS for 10 minutes, and then subsequently pelleted and resuspended in 1% BSA/PBS for 15 minutes. Cells were stained with the following pre-conjugated primary antibodies (1:100 dilution in 1% BSA/PBS): Ms anti Cytokeratin-18 FITC (abcam C-04 ab52459), Ms anti-EpCAM PerCP/Cy5.5 (abcam VU-1D9 ab157319), Ms anti-vimentin FITC (abcam RV202 ab128507), or isotype controls (Ms IgG1 FITC, abcam B11/6 ab91356) (Ms IgG1 PerCP/Cy5.5, BD Biosciences MOPC-21 552834), and then incubated for 30 minutes. Cells were rinsed 2X in 1% BSA/PBS prior

to flow cytometry analysis. At least 10^4 events were acquired for each condition using an Accuri C6 (BD Biosciences) and data was analyzed using FlowJo software v10.2 on a Mac OS X.

Transepithelial Electrical Resistance

Ishikawa adenocarcinoma cell line (passage 8) and primary expanded epithelial cells (n=3 donors, passage 4 or 5) were thawed and seeded at $2x10^5$ cells on a cell culture insert (Corning #3470, 6.5 mm diameter, 0.4 um pores, 0.33 cm^2 culture area, polyester) in F-media. After 3 days, cells were switched to higher calcium differentiation media comprising F-media with the following alterations (without Y-27632, added 1 mM $CaCl_2$ and lower EGF 0.5 ng/mL). Epithelial barrier function was assessed on days 2 and 8 of differentiation by measuring transepithelial electrical resistance using an Ohm meter (EVOM2 World Precision Instruments). Briefly, pre-warmed media was replaced apically (100 µL) and culture inserts were placed into an Ohm chamber (ENDOHM-6) containing 1 mL of pre-warmed differentiation F-media (or HBSS++) on a hot plate set to 40 °C. Resistance measurements are the average of 3 culture insert measurements background corrected using the resistance measured for a cell-free culture insert.

Immunofluorescence

Samples were fixed in a 4% paraformaldehyde PHEM buffer (Electron Microscopy Sciences) for 10 min, permeabilized in 0.1% TritonX-100 in PBS (Sigma) for 10 min, and blocked for 30 min in 1% BSA (Sigma), 5% normal donkey serum (Electron Microscopy Sciences) PBS at room temperature (RT). Culture inserts were incubated with primary antibodies (1:100) and rhodamine phalloidin (1:1000) (Life Technologies) for 2 h at room temperature, rinsed with 1% BSA/PBS 3 times, followed by secondary staining with AlexaFluor488 or AlexaFluor568-conjugated donkey anti-rabbit IgG (1:500) (Invitrogen) for 1 h rocking at RT. Cell nuclei were counterstained with DAPI (1:1000) (Life Technologies) for 10 min at RT. Finally, inserts were rinsed 3 times with 1x PBS and mounted using Prolong Gold Antifade (Life Technologies P36935) on glass slides. Primary antibodies included mouse anti-EpCAM PerCP/Cy5.5 (abcam VU-1D9 ab157319); primary rabbit antibodies included anti-Cytokeratin 18 (abcam ab52948) and

anti-zona occludens 1 (Thermo Fisher Scientific 40-2300). Isotype control included Ms IgG1 PerCP/Cy5.5, (BD Biosciences MOPC-21 552834). Phase contrast images were taken with an iPhone 6 (Apple) through the objective of an inverted tissue culture microscope (Nikon Diaphot, Japan). Wide field fluorescent images were acquired using a Leica DMI 6000 microscope and Oasis Surveyor software.

Cytokine and Protease Luminex Analysis

Primary expanded epithelial cells (n=5 donors, passages 5-7) or Ishikawa adenocarcinoma cells (passage 6) were thawed and seeded at 1 x 10^5 cells/insert (3 x 10^5 cells/cm^2) (Corning #3470) in 100 µl apical and 600 µl basal DMEM/F12 supplemented with 1% DC-FBS, 1% penicillin/streptomycin, and 2% Cell Maintenance Supplement (Cocktail B) (LifeTechnologies CM4000). 48 h-conditioned media (apical) was collected, clarified by centrifugation, and stored at -80 °C until further analysis.

Cytokines and matrix metalloproteinases (MMPs) in 48- hour conditioned apical medium from day 2 during the culture period were measured by Luminex assay using the magnetic Human Cytokine 27-plex (BioRad M500KCAF0Y) and MMP 9-plex (BioRad 171AM001M) on a Bio-Plex 3D Suspension Array System. Protocols provided by the manufacturer were adapted to allow the assay to be performed in a 384-well plate to avoid introducing batch effects. Ten-point standard curves plus blanks were included for quantification.

For each cytokine and protease, 5-parameter logistic curves were fit to the standards, excluding the blanks (Cardillo G. (2012) Five parameters logistic regression - There and back again, http://www.mathworks.com/matlabcentral/fileexchange/38043). Fit curves were used to calculate concentrations for each sample replicate. Median fluorescence intensities (MFI) for the samples below the lower asymptote or above the upper asymptote of the fit curve were imputed to be either the MFI of the minimum asymptote or 99% of the MFI of the maximum asymptote, respectively. Reported values are the mean of 3 technical replicates. Concentrations that fell above the highest standard but below the maximum asymptote (due to incomplete coverage of the quantifiable range by the standard curve) are reported as greater than the concentration of the highest standard.

Data processing of cytokine and protease measurements was performed as follows: computed analyte concentrations were log transformed to obtain $[analyte]_{log}$, where $[analyte]_{log} = log([analyte] + 1)$. It was necessary to add 1 to all computed analyte concentrations in order to log transform concentrations that were below the assay detection limit. Unsupervised hierarchical cluster analysis was performed on log-transformed fold changes of each replicate normalized to the mean concentration secreted by the Ishikawa cell line as follows, $[analyte]_{log} - log([mean\ Ishikawa\ analyte] + 1)$. Cluster analysis was performed in MATLAB_R2016a (MathWorks, Natick, MA) where clustergram distance is represented as the Euclidean distance and the linkage is the average.

3.4 Conclusions

In summary, conditional reprogramming using feeder fibroblast cells and ROCK inhibition holds promise for expanding primary endometrial epithelial cells for future *in vitro* studies of the endometrial mucosal barrier. Expanded cells are of epithelial origin and display enhanced post-expansion barrier and immune signaling functions that are more representative of patient heterogeneity compared to a standard endometrial cell line model (Ishikawa). Since reprogrammed cells may represent an adult stem cell state observed in adult cycling tissue, expanded cells may provide clues as to the normal tissue repair mechanisms following menstruation. We determined that stromal feeder fibroblast factors were necessary to promote endometrial epithelial expansion. Thus, future co-culture studies with primary endometrial stromal and epithelial cell should be explored to better understand the factors governing normal and pathological epithelial repair in the endometrium. In particular, stromal-epithelial crosstalk may contribute to diseases such as endometriosis (growth and invasion of endometrial stromal and epithelial lesions at ectopic locations), Asherman's (where the endometrium becomes fibrotic and is replaced by stromal scar tissue) or adenomyosis (where epithelial cells inappropriately invade and proliferate into the uterine myometrial muscle layer).

3.5 References

1. Osteen, K. G. *et al.* Stromal-epithelial interaction mediates steroidal regulation of metalloproteinase expression in human endometrium. *Proc. Natl. Acad. Sci. U. S. A.* **91,** 10129–10133 (1994).
2. Bruner, K. L. *et al.* Transforming growth factor beta mediates the progesterone suppression of an epithelial metalloproteinase by adjacent stroma in the human endometrium. *Proc. Natl. Acad. Sci. U. S. A.* **92,** 7362–6 (1995).
3. Bläuer, M., Heinonen, P. K., Martikainen, P. M., Tomás, E. & Ylikomi, T. A novel organotypic culture model for normal human endometrium: regulation of epithelial cell proliferation by estradiol and medroxyprogesterone acetate. *Hum. Reprod. Oxford Engl.* **20,** 864–871 (2005).
4. Meng, C.-X., Andersson, K. L., Bentin-Ley, U., Gemzell-Danielsson, K. & Lalitkumar, P. G. L. Effect of levonorgestrel and mifepristone on endometrial receptivity markers in a three-dimensional human endometrial cell culture model. *Fertil. Steril.* **91,** 256–64 (2009).
5. Evron, A., Goldman, S. & Shalev, E. Effect of primary human endometrial stromal cells on epithelial cell receptivity and protein expression is dependent on menstrual cycle stage. *Hum. Reprod.* **26,** 176–90 (2011).
6. Wang, H. *et al.* Sex steroids regulate epithelial-stromal cell cross talk and trophoblast attachment invasion in a three-dimensional human endometrial culture system. *Tissue Eng. Part C. Methods* **19,** 676–87 (2013).
7. Prechapanich, J. *et al.* Effect of a dienogest for an experimental three-dimensional endometrial culture model for endometriosis. *Med. Mol. Morphol.* **47,** 189–95 (2014).
8. Schutte, S. C., James, C. O., Sidell, N. & Taylor, R. N. Tissue-engineered endometrial model for the study of cell-cell interactions. *Reprod. Sci.* **22,** 308–15 (2015).
9. Gnecco, J. S. *et al.* Compartmentalized Culture of Perivascular Stroma and Endothelial Cells in a Microfluidic Model of the Human Endometrium. *Ann. Biomed. Eng.* (2017). doi:10.1007/s10439-017-1797-5
10. Cook, C. D. *et al.* Local remodeling of synthetic extracellular matrix microenvironments by co-cultured endometrial epithelial and stromal cells enables long-term dynamic physiological function. *Integr. Biol. (Camb).* **9,** 271–289 (2017).
11. Klemmt, P. A. B., Carver, J. G., Kennedy, S. H., Koninckx, P. R. & Mardon, H. J. Stromal cells from endometriotic lesions and endometrium from women with endometriosis have reduced decidualization capacity. *Fertil. Steril.* **85,** 564–72 (2006).
12. Chobotova, K. *et al.* Heparin-binding epidermal growth factor and its receptors mediate decidualization and potentiate survival of human endometrial stromal cells. *J. Clin. Endocrinol. Metab.* **90,** 913–9 (2005).
13. Cooke, P. S. *et al.* Stromal estrogen receptors mediate mitogenic effects of estradiol on uterine epithelium. *Proc. Natl. Acad. Sci. U. S. A.* **94,** 6535–40 (1997).
14. Pierro, E. *et al.* Stromal-epithelial interactions modulate estrogen responsiveness in normal human endometrium. *Biol. Reprod.* **64,** 831–8 (2001).
15. Turco, M. Y. *et al.* Long-term, hormone-responsive organoid cultures of human

endometrium in a chemically defined medium. *Nat. Cell Biol.* **19,** 568–577 (2017).
16. Boretto, M. *et al.* Development of organoids from mouse and human endometrium showing endometrial epithelium physiology and long-term expandability. *Development* **144,** 1775–1786 (2017).
17. Buck, V. U., Gellersen, B., Leube, R. E. & Classen-Linke, I. Interaction of human trophoblast cells with gland-like endometrial spheroids: a model system for trophoblast invasion. *Hum. Reprod.* **30,** 906–16 (2015).
18. Chen, J. C. *et al.* Coculturing human endometrial epithelial cells and stromal fibroblasts alters cell-specific gene expression and cytokine production. *Fertil. Steril.* **100,** 1132–43 (2013).
19. Jardé, T. *et al.* Wnt and Neuregulin1/ErbB signalling extends 3D culture of hormone responsive mammary organoids. *Nat. Commun.* **7,** 13207 (2016).
20. Sato, T. *et al.* Long-term expansion of epithelial organoids from human colon, adenoma, adenocarcinoma, and Barrett's epithelium. *Gastroenterology* **141,** 1762–72 (2011).
21. Liu, X. *et al.* ROCK Inhibitor and Feeder Cells Induce the Conditional Reprogramming of Epithelial Cells. *Am. J. Pathol.* **180,** 599–607 (2012).
22. Suprynowicz, F. A. *et al.* Conditionally reprogrammed cells represent a stem-like state of adult epithelial cells. *Proc. Natl. Acad. Sci.* **109,** 20035–20040 (2012).
23. Liu, X. *et al.* Conditional reprogramming and long-term expansion of normal and tumor cells from human biospecimens. *Nat. Protoc.* **12,** 439–451 (2017).
24. Chen, J. C. *et al.* Cryopreservation and recovery of human endometrial epithelial cells with high viability, purity, and functional fidelity. *Fertil. Steril.* **105,** 501–10.e1 (2016).
25. Garry, R., Hart, R., Karthigasu, K. A. & Burke, C. A re-appraisal of the morphological changes within the endometrium during menstruation: a hysteroscopic, histological and scanning electron microscopic study. *Hum. Reprod.* **24,** 1393–1401 (2009).
26. Garry, R., Hart, R., Karthigasu, K. & Burke, C. Structural changes in endometrial basal glands during menstruation. *BJOG An Int. J. Obstet. Gynaecol.* **117,** 1175–1185 (2010).
27. Chan, R. W. S., Schwab, K. E. & Gargett, C. E. Clonogenicity of human endometrial epithelial and stromal cells. *Biol. Reprod.* **70,** 1738–1750 (2004).
28. Cervelló, I. *et al.* Leucine-rich repeat-containing G-protein-coupled receptor 5-positive cells in the endometrial stem cell niche. *Fertil. Steril.* **107,** 510–519.e3 (2017).
29. Chan, R. W. S. & Gargett, C. E. Identification of label-retaining cells in mouse endometrium. *Stem Cells* **24,** 1529–38 (2006).
30. Miyoshi, H. & Stappenbeck, T. S. In vitro expansion and genetic modification of gastrointestinal stem cells in spheroid culture. *Nat. Protoc.* **8,** 2471–82 (2013).
31. VanDussen, K. L. *et al.* Development of an enhanced human gastrointestinal epithelial culture system to facilitate patient-based assays. *Gut* **64,** 911–20 (2015).
32. Ludwig, H. & Spornitz, U. M. Microarchitecture of the human endometrium by scanning electron microscopy: menstrual desquamation and remodeling. *Ann. N. Y. Acad. Sci.* **622,** 28–46 (1991).
33. Rheinwald, J. G. & Green, H. Serial cultivation of strains of human epidermal

keratinocytes: the formation of keratinizing colonies from single cells. *Cell* **6,** 331–43 (1975).
34. Palechor-Ceron, N. *et al.* Radiation induces diffusible feeder cell factor(s) that cooperate with ROCK inhibitor to conditionally reprogram and immortalize epithelial cells. *Am. J. Pathol.* **183,** 1862–70 (2013).
35. McMullan, R. *et al.* Keratinocyte differentiation is regulated by the Rho and ROCK signaling pathway. *Curr. Biol.* **13,** 2185–9 (2003).
36. Barker, N. & Clevers, H. Leucine-Rich Repeat-Containing G-Protein-Coupled Receptors as Markers of Adult Stem Cells. *Gastroenterology* **138,** 1681–1696 (2010).
37. Barker, N., Tan, S. & Clevers, H. Lgr proteins in epithelial stem cell biology. *Development* **140,** 2484–2494 (2013).
38. Gil-Sanchis, C. *et al.* Leucine-rich repeat-containing G-protein-coupled receptor 5 (Lgr5) as a putative human endometrial stem cell marker. *Mol. Hum. Reprod.* **19,** 407–14 (2013).
39. Krusche, C. A., Kroll, T., Beier, H. M. & Classen-Linke, I. Expression of leucine-rich repeat-containing G-protein-coupled receptors in the human cyclic endometrium. *Fertil. Steril.* **87,** 1428–37 (2007).
40. Fahey, J. V. Secretion of cytokines and chemokines by polarized human epithelial cells from the female reproductive tract. *Hum. Reprod.* **20,** 1439–1446 (2005).
41. Kyo, S. *et al.* Successful immortalization of endometrial glandular cells with normal structural and functional characteristics. *Am. J. Pathol.* **163,** 2259–69 (2003).
42. Allen-Hoffmann, B. L. & Rheinwald, J. G. Polycyclic aromatic hydrocarbon mutagenesis of human epidermal keratinocytes in culture. *Proc. Natl. Acad. Sci. U. S. A.* **81,** 7802–6 (1984).
43. Llames, S., García-Pérez, E., Meana, Á., Larcher, F. & del Río, M. Feeder Layer Cell Actions and Applications. *Tissue Eng. Part B Rev.* **21,** 345–353 (2015).
44. Alitalo, K. *et al.* Extracellular matrix proteins of human epidermal keratinocytes and feeder 3T3 cells. *J. Cell Biol.* **94,** 497–505 (1982).
45. McElroy, S. L. & Reijo Pera, R. A. Preparation of Mouse Embryonic Fibroblast Feeder Cells for Human Embryonic Stem Cell Culture. *Cold Spring Harb. Protoc.* **2008,** pdb.prot5041-prot5041 (2008).
46. Osteen, K. G., Hill, G. A., Hargrove, J. T. & Gorstein, F. Development of a method to isolate and culture highly purified populations of stromal and epithelial cells from human endometrial biopsy specimens. *Fertil. Steril.* **52,** 965–72 (1989).
47. Hirose, M. *et al.* Molecular dissection of the Rho-associated protein kinase (p160ROCK)-regulated neurite remodeling in neuroblastoma N1E-115 cells. *J. Cell Biol.* **141,** 1625–36 (1998).
48. Hammond, S. L., Ham, R. G. & Stampfer, M. R. Serum-free growth of human mammary epithelial cells: rapid clonal growth in defined medium and extended serial passage with pituitary extract. *Proc. Natl. Acad. Sci. U. S. A.* **81,** 5435–9 (1984).
49. Kent, K. D. & Bomser, J. A. Bovine pituitary extract provides remarkable protection against oxidative stress in human prostate epithelial cells. *In Vitro Cell. Dev. Biol. Anim.* **39,** 388–94

50. Timofeeva, O. A. *et al.* Conditionally reprogrammed normal and primary tumor prostate epithelial cells: a novel patient-derived cell model for studies of human prostate cancer. *Oncotarget* (2016). doi:10.18632/oncotarget.13937
51. Fayazi, M., Salehnia, M. & Ziaei, S. In-vitro construction of endometrial-like epithelium using CD146 + mesenchymal cells derived from human endometrium. *Reprod. Biomed. Online* **35,** 241–252 (2017).
52. Gargett, C. E., Schwab, K. E. & Deane, J. A. Endometrial stem/progenitor cells: the first 10 years. *Hum. Reprod. Update* dmv051 (2015). doi:10.1093/humupd/dmv051
53. Taylor, H. S. Endometrial cells derived from donor stem cells in bone marrow transplant recipients. *JAMA* **292,** 81–5 (2004).
54. Treloar, A. E. Menstrual cyclicity and the pre-menopause. *Maturitas* **3,** 249–264 (1981).
55. Freeman, E. W. *et al.* Follicular phase hormone levels and menstrual bleeding status in the approach to menopause. *Fertil. Steril.* **83,** 383–392 (2005).
56. Slayden, O. D. & Brenner, R. M. A critical period of progesterone withdrawal precedes menstruation in macaques. *Reprod. Biol. Endocrinol.* **4 Suppl 1,** S6 (2006).
57. Andolf, E., Dahlander, K. & Aspenberg, P. Ultrasonic thickness of the endometrium correlated to body weight in asymptomatic postmenopausal women. *Obstet. Gynecol.* **82,** 936–40 (1993).
58. Berthois, Y., Katzenellenbogen, J. A. & Katzenellenbogen, B. S. Phenol red in tissue culture media is a weak estrogen: implications concerning the study of estrogen-responsive cells in culture. *Proc. Natl. Acad. Sci. U. S. A.* **83,** 2496–500 (1986).
59. Powell, D. W. Barrier function of epithelia. *Am. J. Physiol.* **241,** G275-88 (1981).
60. Wira, C. R. *et al.* Sex Hormone Regulation of Innate Immunity in the Female Reproductive Tract: The Role of Epithelial Cells in Balancing Reproductive Potential with Protection against Sexually Transmitted Pathogens. *Am. J. Reprod. Immunol.* **63,** 544–565 (2010).

3.6 Appendix

A.

Gamma Radiation Exposure	Initial Viability	30 min Viability Cell Counts	Day 3 Viability Cell Counts	Day 7 Viability Cell Counts
3000 rad (30 Gy)	89%	89% $3.8x10^5$	83% $3.4x10^5$	83% $3.4x10^5$
8000 rad (80 Gy)	89%	75% $3.8x10^5$	80% $3.4x10^5$	67% $3.8x10^5$

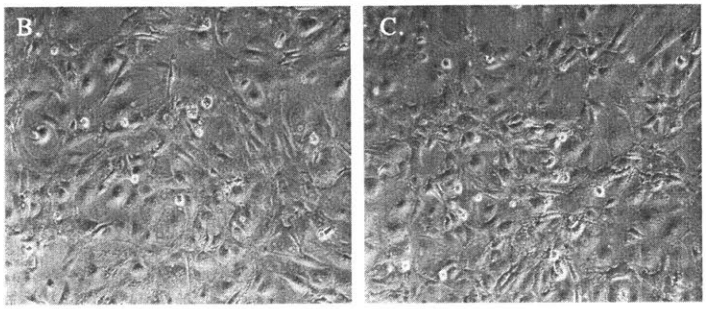

Figure 3A1. Gamma irradiation dosage affects initial and long-term viability of 3T3-J2 feeder cells. 3T3-J2 murine embryonic fibroblast cells were exposed to either 3000 or 8000 rad of gamma irradiation and plated at a density of $4x10^5$ cells/cm^2 in a 6-well plate in DMEM supplemented with 10% BCS. (A) Cell viability and counts were recorded post-irradiation at 30 min prior to seeding and 3 days and 7 days post-seeding. Cell viability decreased both initially and long-term in the 8000 rad condition compared to 3000 rad exposure. Phase images of irradiated 3T3-J2 feeder cells exposed to (B) 3000 rad or (C) 8000 rad after 7 days of culture reveal similar culture morphologies.

A.

Cryopreservation Media	Post-thaw Viability	Day 4 Viability
DMEM/ 10% BCS / 10% DMSO	82%	66%
90% BCS/ 10% DMSO	87%	68%

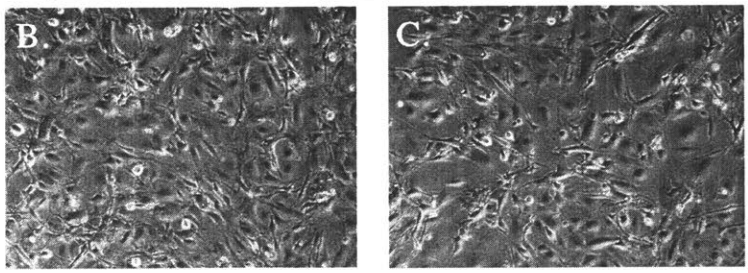

Figure 3A2. Increased serum during cryopreservation does not improve long-term 3T3-J2 feeder cell viability post-thaw. 3T3-J2 murine embryonic fibroblast cells were cryopreserved in either DMEM 10% BCS with 10% *v/v* DMSO or 90% BCS with 10% *v/v* DMSO. After 5 days cells were thawed and plated at a density of $4x10^5$ cells/cm^2 in a 6-well plate for 4 days in DMEM supplemented with 10% BCS. (A) Cell viability initially was slightly lower for cells frozen in (B) DMEM 10% BCS versus cells frozen in (C) 90% BCS, but viability and morphology were similar by day 4 of culture.

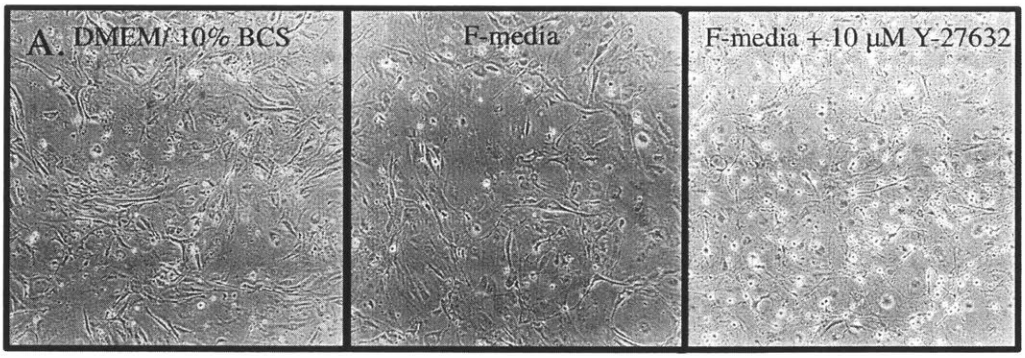

B.

Feeder Media	Day 4 Cell Counts ($1x10^6$ seeded)	Day 4 Viability
DMEM/ 10% BCS	$3.4x10^5$	80%
F-media	$4.1x10^5$	86%
F-media + 10 μM Y-27632	$3.1x10^5$	83%

Figure 3A3. 3T3-J2 feeder cells are viable but detach during conditional reprogramming culture. (A) Phase contrast images on day 4 show flat, attached feeder cell morphology in DMEM/10% BCS or F-media. However, cells exhibited rounded cell bodies and long-thin membrane protrusions in F-media + 10 μM Y-27632. (B) Despite morphological changes in F-media + 10 μM Y-27632, cells retained high viability. However, fewer cells remain in culture suggesting higher cell detachment (30% with Y-27632 versus 40% without Y-27632 of cell initially seeded remain in culture on day 4).

Chapter 4

4 Endometrial Remodeling is Governed by Epithelial-Stromal Cytokine and Protease Crosstalk

Contributions: Linda Stockdale and Julia Papps contributed technical assistance performing hydrogel experiments and biochemical assays. Julia Papps contributed to primary sample collection, isolation, and culture. Abby Hill, Alex Brown, and Samantha Dale Strasser contributed to Luminex assays and data analysis. Sections 4.2.1 and 4.2.2 appear, in part, as a manuscript published in *Integrative Biology*.[1]

Local intercellular communication loops between epithelial and stromal cells are important to endometrial function, as signaling in the local microenvironment results in hormone-responsive differentiation of the stroma enabling blastocyst implantation. The mechanisms by which the endometrium maintains integrity during the secretory phase, while also permitting local inflammation and proteolytic remodeling during implantation, are as yet to be elucidated, especially the contribution of epithelial cells to stromal cell cytokine and protease production.

The advent of more complex *in vitro* epithelial barrier culture models exhibiting spatially representative tissue architecture with an epithelial barrier overlying a 3D stroma, is advantageous for studies of disease pathology and drug discovery. By co-culturing epithelia and stroma in close physical proximity, 3D culture models foster more physiologic cell-cell communication loops than are typically possible in traditional Transwell membrane-insert models, where factors produced by one cell type must diffuse long distances to the second cell type and are diluted by culture medium. Whereas cell-produced signaling proteins can be difficult to recover from Matrigel or similar gels, encapsulation of the stromal cells in a synthetic extracellular matrix (ECM) that can be dissolved on-demand by the bacterial transpeptidase, SortaseA (SrtA), allows release of local cell-produced signaling proteins from the ECM for subsequent immunoassays.

In this chapter, we use primary endometrial cell mono- and co-cultures to parse directional, dynamic intercellular protein signaling networks in the local hydrogel microenvironment and in the surrounding culture media using data-driven modeling techniques. Principal component analysis illuminated how the different cell types, perturbations such as hormones or inflammation, and clinically relevant primary donor

pathologies influence variations in cytokine production. Finally, using partial least squares regression we identify an example of how an epithelial-produced cytokine can induce protease expression in stromal cells by showing that adding exogenous IL-1 to stromal monocultures recapitulates enhanced cytokine and protease concentrations observed in epithelial-stromal co-cultures. The ability to create mucosal models using primary cells to recapitulate healthy and diseased states will further enable basic understandings of disease pathologies and subsequent drug discovery efforts aimed at inflammation, wound healing and immune modulation.

4.1 Introduction

There is growing appreciation for the active role of stromal cells in modulating both tissue homeostasis and disease pathologies ranging from wound healing, cancer progression, immune modulation, and hormone responsiveness.[2–6] Importantly, changes to endometrial stromal cell progesterone responsiveness due to inflammation, epigenetic changes, or toxicant exposure have been implicated in the establishment of endometrial pathologies including endometriosis and adenomyosis.[7–11] Despite insight into factors important for stromal cell hormone response, development of complex chronic inflammatory disorders, such as endometriosis, likely involve multiple cell types and dysregulated protein signaling networks that are not easily replicated by a single cell type or in small animal models.[12–14] Thus, more complex human *in vitro* models that capture intercellular communication, via secreted factors and direct cell-cell interactions, which mediate signaling between stromal cells and immune or epithelial cells are needed for mechanistic studies of disease pathophysiology and drug discovery.

In the endometrium, epithelial-stromal cell interactions have a unique role in regulating hormone responsiveness, tissue remodeling and endometrial function.[11,15–18] Previous studies have shown stromal secreted factors, including transforming growth factor beta (TGF-β), are produced in response to progesterone. These factors modulate epithelial behavior, including suppressing protease expression during the secretory phase to allow implantation.[15,16] Conversely, epithelial-produced cytokines and chemokines, such as interleukin 1 (IL-1), enhance stromal cell protease expression and reduce stromal cell progesterone responsiveness. Furthermore, enhanced IL-1 signaling leads to matrix metalloproteinase (MMP) expression and tissue remodeling, phenomena associated with pathological disorders including endometriosis and abnormal uterine bleeding.[11,17]

While several previous studies have used conditioned medium to glean insight into how factors produced by one cell type modulate behavior of a second cell type in cancer progression and proteolytic remodeling,[5,17] these studies preclude direct cell-cell interactions and fail to capture the dynamic reciprocal communication including cellular feedback that occurs in the local tissue microenvironment. Furthermore, others have used Transwell-type membrane culture inserts to culture multiple cell types with a shared medium reservoir, an arrangement which dilutes cellular communication compared to

juxtaposition of the two cell types.[7,15,16,19] The analysis of complex intercellular protein communication has been limited in part by the lack of suitable cell culture tools necessary to construct and parse dynamic signaling in complex 3D microtissues *in vitro*.

Here, I address this gap. Specifically, I describe how the epithelial-stromal co-culture model developed in Chapter 2 can be extended to analyze protein communication networks within the local microenvironment without dilution effects, due to direct juxtaposition of epithelial cells with stromal cells encapsulated in a synthetic hydrogel ECM that can be dissolved to recover local proteins in the gel. This approach builds on a new method our lab developed to dissolve synthetic ECM incorporating the LPXTG motif, a substrate for a the bacterial transpeptidase Sortase A (SrtA), into the peptide crosslinks previously described.[20] Addition of SrtA and soluble peptide GGG, a second substrate for SrtA, effects rapid and gentle dissolution of gels, leaving most proteins intact due to the relative lack of LPXTG motifs in mammalian proteins.[20] This technology enables recovery of intact cytokines within the local hydrogel for comparison with cytokines measured in the surrounding culture medium outside the gel.

The compendium of measurements made in different compartments, with different cells present, at different time points, and under different conditions (e.g., hormones, inflammation) enable use of data-driven models to parse multivariate intercellular protein communication during homeostasis and inflammation. We identify cytokines within apical media or hydrogel microenvironments that underlie dynamic differences in hormone responses and matrix metalloproteinase production among primary donors. An outline of how the experimental and computational approaches are described and combined in Chapter 4 is provided in Table 4-1.

First, using cell lines cultured in a baseline medium (no temporal hormonal variations), the culture model described in Chapter 2 was extended to parse the relative contributions of epithelial cells and stromal cells to cytokine production, and to show that cytokine production measured in the apical compartment was relatively invariant between days 7 and 14. Subsequently, the apical cytokine production behavior of primary co-cultured epithelial and stromal cells from 3 different donors was compared to that of co-cultured cell lines at day 7 of culture, revealing dramatically more abundant production of most cytokines by primary cells from all donors, even with significant donor-to-donor

variation. Primary co-cultures also responded differently to decidualization cues than cell liens, increasing production of several cytokines, whereas co-cultured cell lines generally suppressed cytokine production.

Principal component analysis (PCA) of primary cell culture cytokine production in stromal monocultures versus epithelial-stromal co-cultures revealed that variation arose primarily from cell composition rather than donor heterogeneity or hormone treatments. Additionally, correlation analysis was used to assess how culture setup (monoculture v co-culture) influenced cytokine levels measured in the hydrogel versus the surrounding culture media. Stromal monocultures exhibited highly correlated cytokine measurements (22 out of 26 correlated), whereas epithelial barrier co-cultures showed lower correlation (13 out of 26 correlated) suggesting our model captures expected spatial heterogeneity in co-culture cytokine secretion.

Finally, using partial least squares regression we identify the IL-1 family (IL-1β and IL-1ra) as being predictive for both identifying hormone responsiveness and proteolytic remodeling within endometrial cultures. We show how IL-1β, which is produced more abundantly in co-culture compared to stromal monoculture, can induce an inflamed state in stromal monocultures when added exogenously, resulting in increased cytokine secretion and protease remodeling. These findings motivate use of more complex *in vitro* models to study cellular crosstalk at mucosal barriers. Taken together, these studies provide a framework for how to construct and parse complex *in vitro* 3D co-culture models to understand how inflammatory cytokine signaling impacts hormone responsiveness and proteolytic matrix remodeling in the endometrium. In general, we demonstrate the ability to measure dynamic, directional intercellular protein signaling networks that underlie primary donor variability and anticipate that such models will yield molecular insight into mucosal barrier disease pathophysiology, which can be exploited for therapeutic discovery.

Table 4-1. Chapter 4 experimental outline.

Results Section	Cell Type	Culture Configuration	Hormone Treatment	Measurement Location	Proteins Measured	Conditions (comparing cytokines)
4.2.1	Cell lines	stromal monoculture, epithelial monoculture & epithelial-stromal co-culture	cAMP/MPA	apical medium	cytokines	day 7 v. day 15 hormone response monoculture v. co-culture
4.2.2	Cell lines & Primary (n=3 donors)	epithelial-stromal co-culture	cAMP/MPA	apical & basal media	cytokines	primary v. cell lines primary hormone response apical v. basal media
4.2.3	Primary (n=3 donors)	stromal monoculture & epithelial-stromal co-culture	E2/P4	apical medium & hydrogel	cytokines	apical media v. hydrogel monoculture v. co-culture
4.2.4 & 4.2.5	Primary (n=3 donors)	stromal monoculture & epithelial-stromal co-culture	E2/P4	apical medium & hydrogel	cytokines	PCA inflamed v. uninflamed media v. hydrogel correlation
4.2.6 & 4.2.7	Primary (n=3 donors)	stromal monoculture & epithelial-stromal co-culture	E2/P4	apical medium & hydrogel	cytokines MMPs prolactin	PLSR analysis cytokines v. MMP3 or prolactin

Abbreviations are as follows: 8-Br-cAMP second messenger (cAMP), medroxyprogesterone acetate (MPA), estradiol (E2), progesterone (P4), matrix metalloproteinases (MMPs), principal component analysis (PCA), partial least squares regression (PLSR)

4.2 Results and Discussion

4.2.1 Apical cytokine and growth factor environment of co-cultures is relatively stable from week 1 to 2 of co-culture, and is conditioned primarily by epithelial cells

The hormonally-modulated immune and growth factor signaling milieu contributes to important for cyclic remodeling of the endometrium and has been implicated in numerous endometrial pathologies.[13,21] In order to establish protocols and a benchmark data set for multiplex measurement of cytokines during long-term (2+ weeks) culture of primary cells, we first evaluated production of 27 cytokines, chemokines, and growth factors in mono- and co-cultures of the commonly-used Ishikawa endometrial epithelial cells with h-TERT immortalized endometrial stromal fibroblasts (see Ch. 2 and references for details of the cells lines and cultures).[22,23]

First, we assessed the cytokine environment, as measured by 48 hour conditioned medium collected on days 7 and 15 of co-culture, to establish how significantly the concentrations of cytokines in the apical medium varies during the 2 week culture period (Fig. 4-1A). We found that most cytokines changed less than 2-fold (dashed lines), with most exceptions also having high replicate variability (PDGF-BB, VEGF, Eotaxin). The only cytokine that was consistently increased on day 15 vs. day 7 was MCP-1, which is produced primarily by the stromal cells, and may require time to diffuse through the gel and pass through the epithelial barrier before accumulating in the apical medium. It is unlikely that this increased value of MCP-1 arises solely from an increase in stromal cell number, as similar increases were not observed for several other cytokines that were later determined to be produced primarily by stromal cells. MCP-1 binds to collagen I,[24] which is produced by stromal cells and accumulates in the extracellular environment of the stromal compartment (Ch. 2),[1] hence it is plausible to speculate that MCP-1 exhibits a transient build-up due to binding ECM, and is released more abundantly after binding sites are saturated. DNA synthesis rates were similar on days 4 and 14, and we observed dynamic dome formation within the epithelial layer, which may have resulted in cell growth and loss that offset yielding similar apical media cytokine production at 1 and 2 weeks of culture (Ch. 2).

Given the singular significant increase in MCP-1, a cytokine that could be produced by epithelial or stromal cells, we sought to parse the relative contributions of stromal and epithelial cells to apical cytokine production. Thus, we compared the apical cytokine concentrations of stromal (tHESC) and epithelial (Ishikawa) monocultures to concentrations of apical cytokines in co-cultures, all at day 15 (Fig. 4-1B and Appendix Table 4A1). Among the 27 cytokines measured for cell lines on day 15, eight cytokines (TNF-α, RANTES, MIP-1α, IL-5, IL-1β, G-CSF, and FGF basic) were below the limit of detection for both single cell lines, although one (MIP-1α) was detectable, albeit at very low levels, in co-culture. Another 11 cytokines (VEGF, PDGF-BB, MIP-1β, IL-9, IL-7, IL-4, IL-17A, IL-13, IL-12p70, IL-10, and GM-CSF) were below the detection limit in stromal cultures alone, but produced abundantly and at similar levels in Ishikawa alone and co-cultures, suggesting that these are produced almost exclusively by Ishikawa epithelial cells in a stromal-independent manner under these hormone and media culture conditions.

Three cytokines (IL-15, MCP-1, and Eotaxin) were produced at higher levels by tHESCs than by Ishikawa cells. One of these, MCP-1, was produced abundantly by stromal cells but was almost undetectable in Ishikawa monoculture, and present in co-culture at greatly reduced (15%) levels compared to stromal mono-culture, suggesting this cytokine is produced by stroma and its access to the apical compartment may be restricted by the epithelial barrier, or that it is consumed by the epithelia. IL-6 and IL-2 were produced at slightly higher levels by epithelial cells than stromal cells in monoculture, with little effect of co-culture. IP-10, IL-1ra, and IFNγ were produced at dramatically higher levels by epithelial cells than stromal cells.

Comparison of the absolute concentrations of cytokines that accumulate over 48 hr for the different combinations of cells (mono-cultures of each cell type vs co-cultures) gives some insights into which cell types may be predominant producers of a particular cytokine, but a more quantitative interpretation and translation to other culture conditions requires consideration of the relative cell numbers present in each condition, as well as measurement of consumption rates. These cultures were initiated with 75,000 epithelial cells and 50,000 stromal cells, both of which were found to proliferate at moderate rates via a DNA synthesis assay (Chap. 2). Cell numbers were not measured as a function of

time in these studies, precluding precise specific rates to be discerned. However, approximate rates can be estimated and thus these data are valuable for future experimental design.

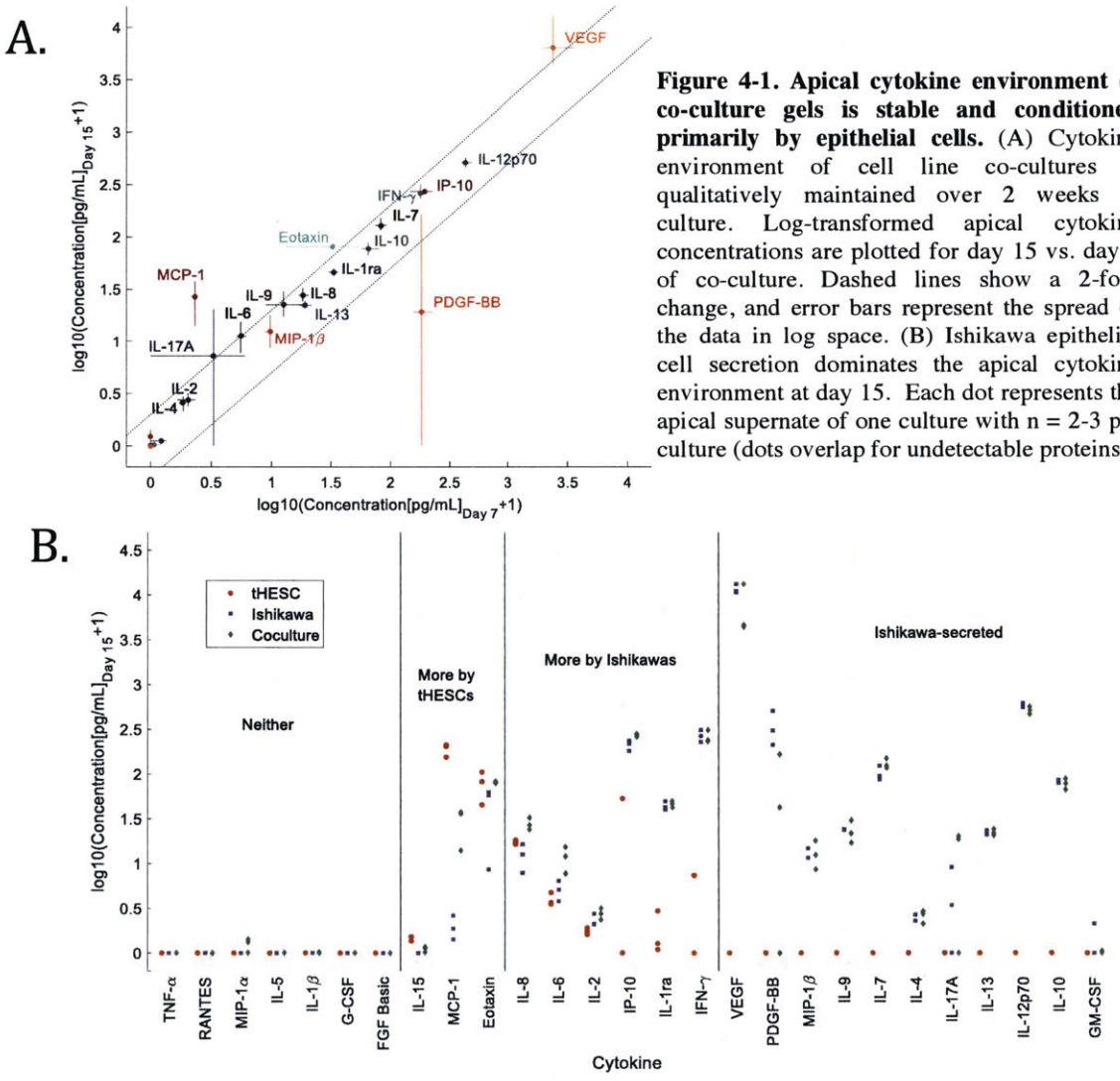

Figure 4-1. Apical cytokine environment of co-culture gels is stable and conditioned primarily by epithelial cells. (A) Cytokine environment of cell line co-cultures is qualitatively maintained over 2 weeks in culture. Log-transformed apical cytokine concentrations are plotted for day 15 vs. day 7 of co-culture. Dashed lines show a 2-fold change, and error bars represent the spread of the data in log space. (B) Ishikawa epithelial cell secretion dominates the apical cytokine environment at day 15. Each dot represents the apical supernate of one culture with n = 2-3 per culture (dots overlap for undetectable proteins).

4.2.2 Primary co-cultures exhibit more diverse and abundant cytokine signaling networks compared to cell line co-cultures

Although endometrial cell lines are a reproducible cell source that may recapitulate some facets of endometrial function, they may not represent the phenotypes observed in primary donor cultures, nor do they reflect donor-to-donor variation. Applications of endometrial models include studies of embryo implantation, microbiome dysregulation, and effects of inflammation and exposure to environmental chemicals on endometrial function – applications where complex cell-cell communication networks regulate tissue response.[7,11,25–28] Hence, we investigated the cytokine and growth factor production by primary endometrial stromal and epithelial cells from 3 different donors compared to each other and to cell lines after 1 week of co-culture (Fig. 4-2A and Appendix Table 4A2; cytokines are ordered by median fold change of each primary cell culture over the cell lines).

Overall, the primary co-cultures appeared more similar to one another than to the cell lines and had a higher level of most secreted factors compared to the Ishikawa and tHESCs. Twenty of 27 cytokines were increased in primary cells compared to the tHESC and Ishikawa cell lines. Six cytokines were not detectable in cell line co-cultures, but were detectable in at least some of the primary co-cultures (GM-CSF, IL-1β, IL-1ra, FGF basic, IL-2, and IL-5). Only 4 showed a decrease (IL-13, IL-12p70, VEGF, and PDGF-BB) and 3 similar levels (IL-7, IL-10, and IL-9). It is unlikely that the increased abundance of cytokines and growth factors in the primary cultures arises from differences in total cell numbers in the culture, as these cultures generally have lower total DNA counts.

These differentially-produced cytokines play diverse roles in the essential functions of the endometrium, from regulating immunity at the maternal-fetal interface during the time of implantation and beyond, to governing breakdown of tissue during menstruation. As one example, VEGF and IP-10, which are expressed in opposite patterns for cell line versus primary co-cultures (VEGF is lower, and IP-10 much higher, in primary cells) play opposing roles in angiogenesis, with VEGF inducing and IP-10 opposing.[29] Cultured in the same microenvironment, cell lines exhibit a cytokine signature of a rapidly growing tissue fostering angiogenesis while the primary cells

exhibit a phenotype of a more mature tissue. Our findings are consistent with previous reports of abundant production of VEGF by Ishikawa cells cultured in a 3D collagen-GAG matrix.[30]

We also compared our measurements to previously published values for 14 of the same cytokines secreted by co-cultures of primary endometrial stromal and epithelial and, despite different time points and culture protocols, found similar trends in relative cytokine levels.[9] Possibly due to the shorter time point or media dilution effects in Chen et al., several cytokines detectable in our samples were not detected there (RANTES, IFNγ, IL-1β, IL-2, IL-5, and IL-10), but of the cytokines detectable in both studies, values reported by Chen et al. varied between 1% (TNFα) and 60% (MIP-1α) of those found here, with a median of 17%. Given the different cell culture times, cell numbers, and volume of apical medium, and assuming a constant secretion rate per cell, we would expect the values in Chen et al., to be about 20% of those we observed.

Primary co-cultures exhibit hormonally responsive cytokine secretion

Finally, we examined how cytokine and growth factor production was influenced by decidualization cues, 0.5 mM 8-Br-cAMP and 1 μM medroxy progesterone acetate (MPA) in primary cells from 3 different donors. Progestogens are known to influence immune signaling in the endometrium during the secretory phase in preparation for embryo implantation especially modulating the maternal-fetal environment to induce immunotolerance.[31] Among the 27 factors assayed, IL-15 and IL-10 levels were most prominently enhanced in all three proliferative phase co-cultures in response to decidualization cues (Fig. 4-2B and Appendix Table 4A3; statistically significant in one donor). An increase in endometrial IL-15 mRNA during the secretory phase has been observed *in vivo*, indicating that this model system is able to reproduce aspects of *in vivo* cytokine behavior in response to hormones.[32]

In addition, progesterone has been demonstrated to modulate IL-10 response to LPS-stimulation, as a model of infection[33] and low levels of endometrial IL-10 are observed in women with recurrent spontaneous abortion.[34] Interestingly, in our data, levels of baseline IL-10 varied widely across subjects, suggesting that the ability to follow cells from the same subject over time is critical to understanding hormone-

responsive cytokine behavior. Additional cytokines (Eotaxin and MIP-1β) showed donor-specific variability in response to hormone treatment (Appendix Table 4A3). Here, we demonstrate the ability to elucidate intercellular cytokine signaling in response to decidualization cues and donor specific variation in immune signaling *in vitro* using a fully synthetic extracellular matrix to establish long-term primary cell co-cultures.

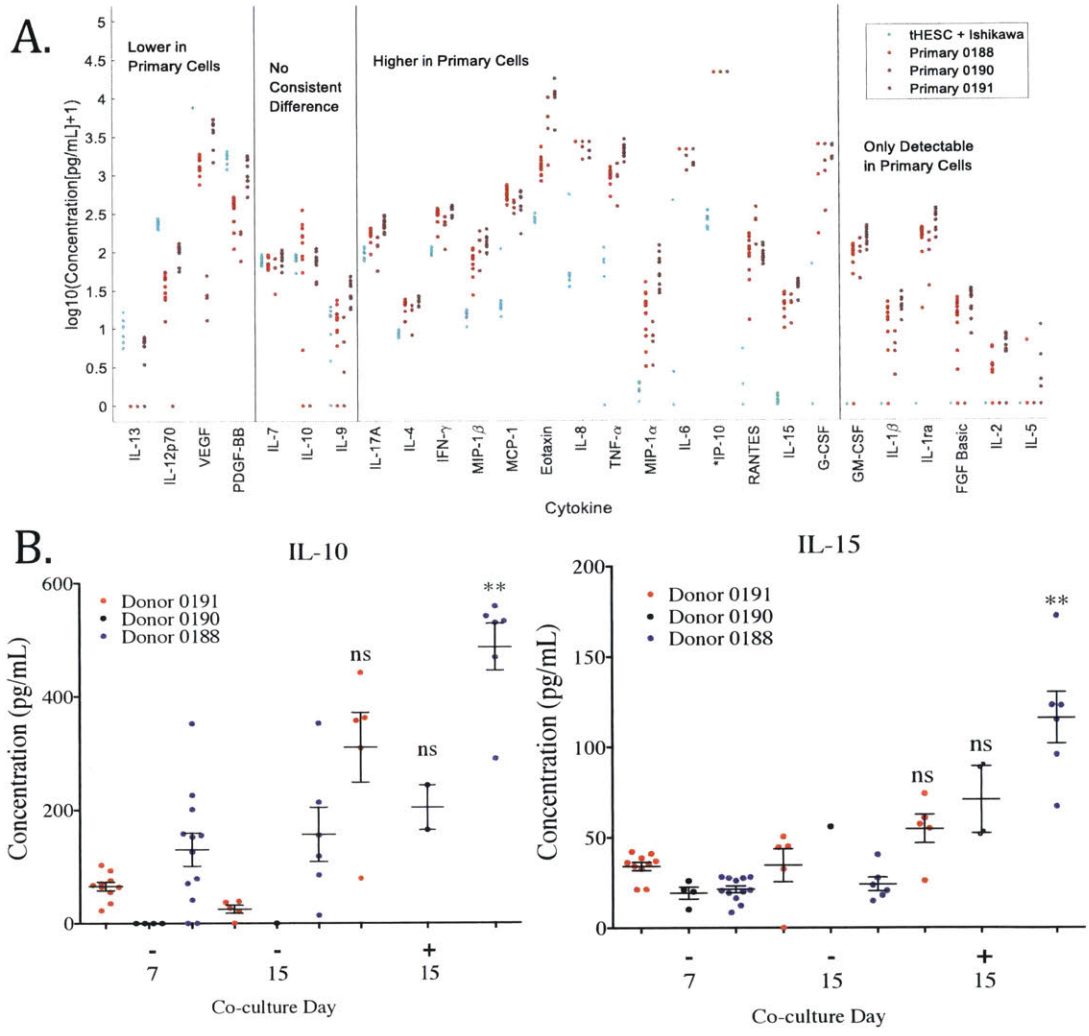

Figure 4-2. Primary endometrial cell co-cultures produce more abundant cytokines and growth factors than endometrial cell lines and exhibit hormone-responsive cytokine production. (A) Twenty (of 27 total assayed) cytokines and growth factors were produced more abundantly in primary cells than cell lines, with 6 of those only detectable in primary cell cultures; each dot represents a single culture apical supernate measurement on day 7 of co-culture. (B) IL-10 and IL-15 cytokine levels were consistently elevated upon decidualization for all donor co-cultures and statistically significantly elevated for at least one proliferative phase donor. Statistical significance is indicated as *P < 0.05, **P < 0.01, and ***P < 0.001 for two-tailed t-tests with Benjamini-Hochberg multiple hypothesis correction for cytokine analysis. Bars represent the mean and SEM.

Decidualized cell line co-cultures show significantly decreased cytokine production

Interestingly, the behavior of the cell line co-cultures to decidualization cues contrasted sharply with the behavior of the primary cells, where most cytokines were relatively unchanged and some were increased in production. Using the same decidualization protocol as described above, we observed that in the apical media of cell line co-cultures, 20 of 27 measured cytokines were produced at significantly lower levels in response to decidualizing cues. Although levels of IL-2, IL-10 and IP-10 trended higher, these did not reach statistical significance (Fig. 4-3, Appendix Table 4A4). This suggests an overall immune suppressive phenotype; i.e., decidualization attenuates production of inflammatory cytokines and chemokines in tHESC and Ishikawa cell line co-cultures, unlike behavior in primary cells.

In summary, these data demonstrate that the synthetic ECM culture environment enables analysis of intercellular cytokine signaling in response to decidualization cues and donor specific variation in immune signaling *in vitro* over time scales relevant for menstrual cycle variation. Further, these data underscore the profound differences in phenotypes between primary cells and the most commonly used endometrial cell line models.

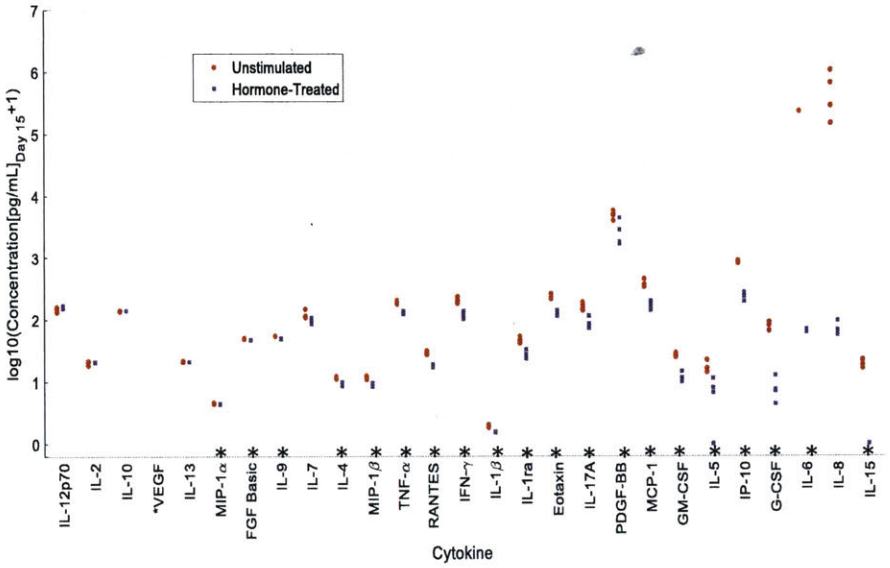

Figure 4-3. Decidualized co-cultures of cell lines exhibit significantly lower cytokine secretion compared to unstimulated cultures. Cytokine levels were consistently decreased (20 out of 27 analytes were significantly decreased) upon decidualization with 0.5 mM 8-Br-cAMP and 1 μM MPA in Ishikawa and tHESC co-cultures. Statistical significance is indicated as * for $P < 0.05$ for two-tailed t-tests with Benjamini-Hochberg multiple hypothesis correction for cytokine analysis. Each dot represents the apical supernate of one culture with n = 4 stimulated and unstimulated cultures (dots overlap for undetectable proteins). (VEGF concentration was too high to quantify).

4.2.3 Analysis of polarized cytokine secretion is improved by measuring local cytokines inside the 3D synthetic hydrogel, compared to measurements on media

Context for cytokine measurements in epithelial-stromal co-cultures: quantitative values of cytokines in apical versus basal compartments in cell culture insert models

Up to this point, we investigated accumulation of cell-produced proteins in the apical media. One challenge with analysis of polarized cytokine secretion using traditional cell culture inserts is illustrated in Fig. 4-4A. The basal compartment media volume (typically 600 μL) is generally 6-fold higher volume than the apical media compartment (typically 100 μL), resulting in a relative ~6-fold dilution in the basal compartment compared to the apical compartment (presuming hypothetical comparable production rates on both sides), to concentration values that are below the detection limits for some cytokines.

These challenges are partially illuminated by comparing the number of detectable cytokines in monocultures of stromal cells compared to co-cultures (Fig 4-1B). Several cytokines were undetectable in the apical media for tHESC monocultures suggesting that either these factors were not produced by the stromal cell line, they accumulated within the hydrogel, or they are present below the assay detection limit (Fig. 4-1B). Although cytokine concentrations in the basal media were not measured in those monoculture experiments, it is reasonable to presume that they would be approximately 6-fold lower there than in the apical compartment–pushing even more analytes into the undetectable range–as the stromal cells are distributed throughout the hydrogel, resulting in approximately equal driving force for efflux of cytokines from both sides of the gel.

A comparison of cytokine concentrations measured in the apical and basal compartments of the co-cultured cell lines offer additional illumination of the dilution effects (Fig. 4-4B). While 14 cytokines were detected at greater than 10 pg/mL in the apical media (a level that is considered above the limit of detection for most cytokines in the Luminex assay), only 10 cytokines were detected above 10 pg/mL in basal media. Of those 14 apical-enriched factors, only 7 of them were also detected above 10 pg/mL in the basal media. Conversely, there were only 3 factors present at greater than 10 pg/mL in the basal compartment, and not in the apical compartment. This could mean that apical cytokine production occurs in a polarized manner with more accumulation occurring

apically, or that the larger basal media volume limits detection of some cytokines that are otherwise detected apically.

Although we found that primary co-cultures secrete greater cytokine concentrations compared to cell lines into the apical media (Fig. 4-2A), and thus fewer cytokines may be susceptible to falling below detection limits due to basal compartment dilution effects, simple dilution effects are not the only concern in parsing cytokine communication by measuring the culture media. An additional challenge in analysis of 3D co-cultures is that the apical and basal compartments are likely enriched in epithelial- and stromal-produced factors, respectively, due to the transport and reaction (consumption) barriers of each tissue region to the factors produced by the other. One reason for this may be the nature of cytokine signaling whereby paracrine and autocrine loops often create feedback signaling that further enhances cytokine secretion.

Notably, several cytokines we found robustly present in the apical media for primary hydrogel co-cultures, including RANTES, IFNγ, IL-1β, IL-2, IL-5, and IL-10, were undetectable in a previous endometrial co-culture study (Chen et al.) in which primary epithelial and stromal cells were separated by a large medium reservoir (1 mL) and the number of epithelial cells was almost an order of magnitude lower and apical medium volumes greater (Fig. 4-2A).[19] These investigators seeded 10^5 epithelial cells on a 24-well sized insert in 200 uL of media apically and collected medium at 12.5 hr, whereas we seeded $7.5\text{-}10^5$ epithelial cells on a 24-well sized insert in 100 uL of media apically and collected conditioned medium after 48 hr. While levels of IL-1β, IL-2, and IL-5 were ~10 pg/mL in our culture (near the limit of detection) and thus, if produced at comparable rates in their model, would have not risen to the level of detection in their model, other factors (RANTES, IFNγ, and IL-10) not detected in the Chen *et al.* model were present at greater than 10-fold the limit of detection in our cultures, hence would be expected to present close to the detection limit if the epithelial biology was similar in each case. These factors may be detectible in our culture model due to more favorable (concentrated) cell:medium ratios, stromal cell production, or because factors from the stromal cells stimulated their production by epithelial cells.

A.

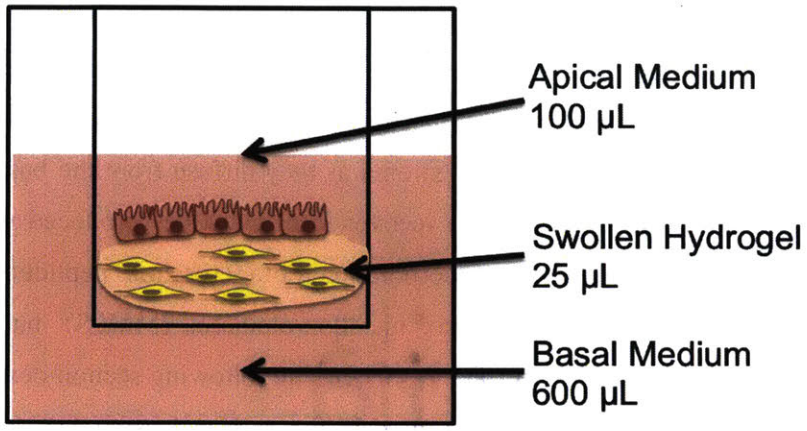

B.

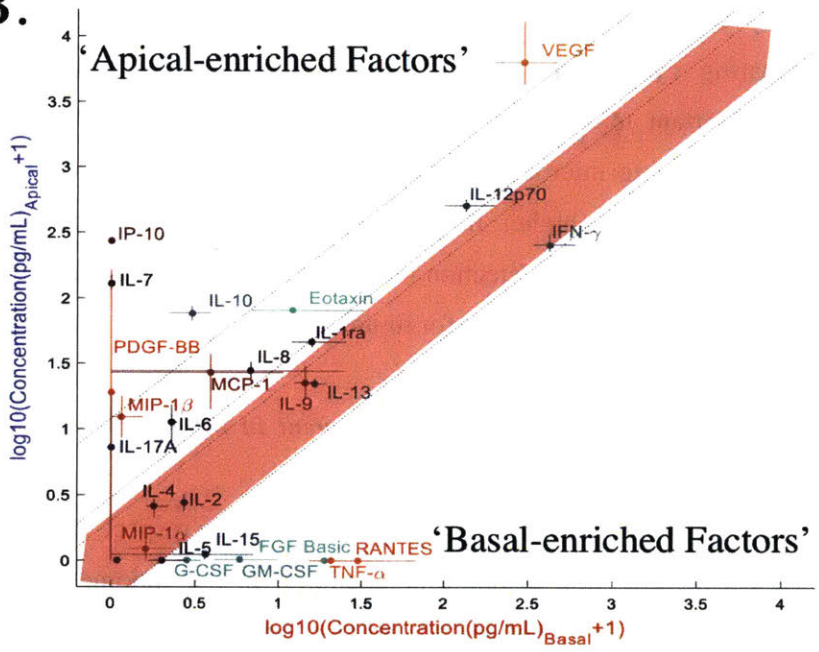

Figure. 4-4 Cytokine detection in apical media allows detection of more cytokines than in basal media. (A) Schematic of a membrane tissue culture insert showing compartment volumes; apical media (100 µL), swollen hydrogel (25 µL) and basal media (600 µL). (B) Log-transformed cell line (Ishikawa and tHESC) co-culture cytokine concentrations are plotted for day 15 apical (100 ul) vs. basal (600 ul) media (48 h conditioned media). Dashed lines (pink region) show a 2-fold change containing cytokines that are present in equal concentrations in the apical and basal medium as would be expected if free diffusion occurred between apical and basal media compartments. Dashed lines (clear region) represent 6-fold change to correct for basal media volume and error bars represent the spread of the data in log space. Overall, cytokines above the pink region are secreted in higher abundance in the apical media, 'apical-enriched factors', whereas cytokines below the pink region are secreted in higher abundance in basal media, 'basal-enriched factors'.

Measurement of cytokine concentrations in the local microenvironment within the hydrogel would offer additional insights into stromal-epithelial communication, as measurement of the total cytokines within the hydrogel would capture epithelial-produced molecules that are consumed by stroma as they diffuse from the basal side of the epithelial cells toward the hydrogel to recover local cytokines produced within the hydrogel.[20] This is achieved through incorporation of a crosslink peptide that is a substrate for not only cell-produced matrix metalloproteinases (MMPS), but also the enzymatic bacterial transpeptidase, Sortase A (*SrtA*). The following section describes the magnitude of cytokine concentrations measured in the hydrogel using *SrtA* to recover cytokines from primary co-cultures, compared to the apical compartment. Follow on studies directly comparing cytokines within the hydrogel versus the basal media compartment will be important to ascertain whether basal media cytokine levels are informative of the local signaling microenvironment inside the hydrogel. Specifically, since overall cytokine secretion is higher in primary cells compared to cell lines, understanding whether dilution prevents detection of some cytokines in the larger basal media, but not the hydrogel, will be informative for future studies.

Cytokine portioning between local pericellular environment in the hydrogel and the culture supernate in monocultures

Epithelial barriers are well-known to be highly polarized with respect to myriad functions, including growth factor and cytokine production.[35] In the endometrium, the apical surface produces mucus, immunological mediators, and factors that regulate embryo implantation. The basal side of the endometrial epithelial barrier communicates with the underlying stroma in a reciprocal fashion, in a manner more complex than most epithelial barriers as communication is regulated by hormones that act differentially on the epithelial and stromal cells.

Methods such as immunohistochemistry, in situ hybridization, and targeted inhibition of specific pathways have all yielded some insights into this reciprocal signaling,[15,16,36,37] but these approaches are limited to a few measurements on targeted pathways. New proteomic approaches employing specific labels for each cell type are emerging to parse epithelial-stromal interactions in a highly multiplexed fashion,[5] but

these approaches are inherently restricted due to experimental difficulty. As an intermediate step in parsing contributions from each cell type without specific labeling of the cell of origin, we investigated the global cytokine concentrations in the local stromal microenvironment, in comparison to the apical microenvironment, as a means of discerning communication trends.

In order to establish baseline behaviors for how cytokines partition between the hydrogel and the culture medium, we first examined stromal cell monocultures, which would presumably produce factors in an unpolarized fashion, allowing insights into how various factors partition between the matrix and the culture medium. For these initial experiments, 50,000-75,000 primary human endometrial stromal cells were encapsulated in 12 uL of hydrogel maintained on a cell culture insert, and cultured for 15 days in hormone containing media representing proliferative or secretory cycle phases (1 nM estradiol or 1 nM estradiol and 100 nM progesterone present in apical and basal media- see methods for hormone stimulation timing) with 2/3 apical and basal media changed every 2 days.

Cytokine measurements were conducted on collected apical media (~100 ul aspirate volume) or *SrtA*-dissolved hydrogels (~100 uL volume, following dissolution of ~25 uL swollen hydrogels with ~75 uL dissolution solution; see Appendix Tables 4A5-10, which include raw hydrogel data before correction for the 4-fold dilution due to the dissolution process). All data were plotted as actual local concentrations, correcting for the dilution of hydrogels (i.e., plots show hydrogel data from Tables 4A5-10 multiplied by 4).

Some cytokines - FGF basic, G-CSF, IL-17A, IL-1ra, and MIP-1β - partition so strongly into the gel that they are barely or not detectable in the supernate media (Fig. 4-5B). Another set of cytokines–IL-5, IL-9, IL-13, and IL15–partition into the gel (i.e., are at higher concentration in the gel than in the supernate) but are also robustly detectable in the supernate. Notably, while previous studies showed *SrtA* dissolution rendered IL-15 undetectable,[20] we did not observe any difference in IL-15 detection in standard curves or samples exposed to *SrtA* and GGG. We speculate that this discrepancy may arise from differences in the samples: recombinant protein standards were used in the prior study,[20] while culture samples analyzed here might contain soluble IL-15 receptor, which binds

with high affinity to IL-15 and may protect it from *SrtA*-mediated degradation.[38] A third set of cytokines–Eotaxin, IL-10, IL12p70, IL-4, IP-10, MCP-1, TNFα, and VEGF–show no evidence of partitioning; i.e., are present in the gel and in the supernate at comparable concentrations. A final set–IFNγ, IL-6, IL-7, IL-8, and RANTES– are detected mostly or only in the supernate and not in the gel. This latter set of cytokines are likely near the detection limit in the 4-fold diluted hydrogel samples; i.e., the amounts measured in the culture medium supernate are only slightly more than 4 times the detection limit. Thus, these data reflect measurement sensitivity limits rather than true biological differences.

These partitioning results show some consistency with previous results for tHESC endometrial stromal cells co-encapsulated with Ishikawa endometrial epithelial acini, where partitioning was measured within 24 hr of encapsulation for basal conditions and again 24 hr after stimulation by IL-1β.[20] In that study, relatively few cytokines (FGF basic, IFNγ, IL-6, IL-8, IL-10, IL12p70, IL-7, VEGF) were detected in both the gel and the supernate media under basal conditions, and all except for IFNγ, IL-6, and IL-8 – which were barely above detection limit in the supernate – exhibited significant partitioning into the gel, perhaps due to the relatively short time period measurements were made after encapsulation (i.e., cytokines were still accumulating and had not yet diffused out of the gel substantially).[20] A much broader array were observed after IL-1β stimulation, with many partitioning very strongly in the gel: IL-4, IL-13, IL-2, TGF-β2, IL12p70, IL-7, FGFb, GM-CSF, IL-10, IL-9, RANTES, IFNγ, MCP-1, IL-6, and G-CSF. Those that showed modest or insignificant partitioning include: IL-7, TGF-β1, Eotaxin, IL-17, IL-1ra, PDGF-BB, TNF-α, and IL-8.

Many of the strongly-partitioning molecules, such as FGF basic, bind to matrix and thus the partitioning results for such molecules are not surprising.[39] Of those that strongly partition but are not known to have high affinity for ECM, some may be higher due to kinetic effects (diffusion-limited transport into the supernatant medium), or bind to cell surfaces and are released during dissolution of the gel. The time period between medium changes in this study was twice as long as the previous study (48 vs 24 hr), and cells had been encapsulated for 15 days rather than just 24-48 hr – protocol conditions that would both favor a greater equilibrium between gel and media – thus it is not surprising that fewer molecules partition in this study. One notable protocol difference

from previous studies, is that we did not add sortase, GGG, and PEG to the apical media measurements, so some differences in absolute levels may occur due to slight differences in background of the components in the samples, as is typical for multiplex immunobead assays. We prepared cytokine standard curves with and without *SrtA* and GGG, and would expect that if these factors influence cytokine detection than this would be accounted for.

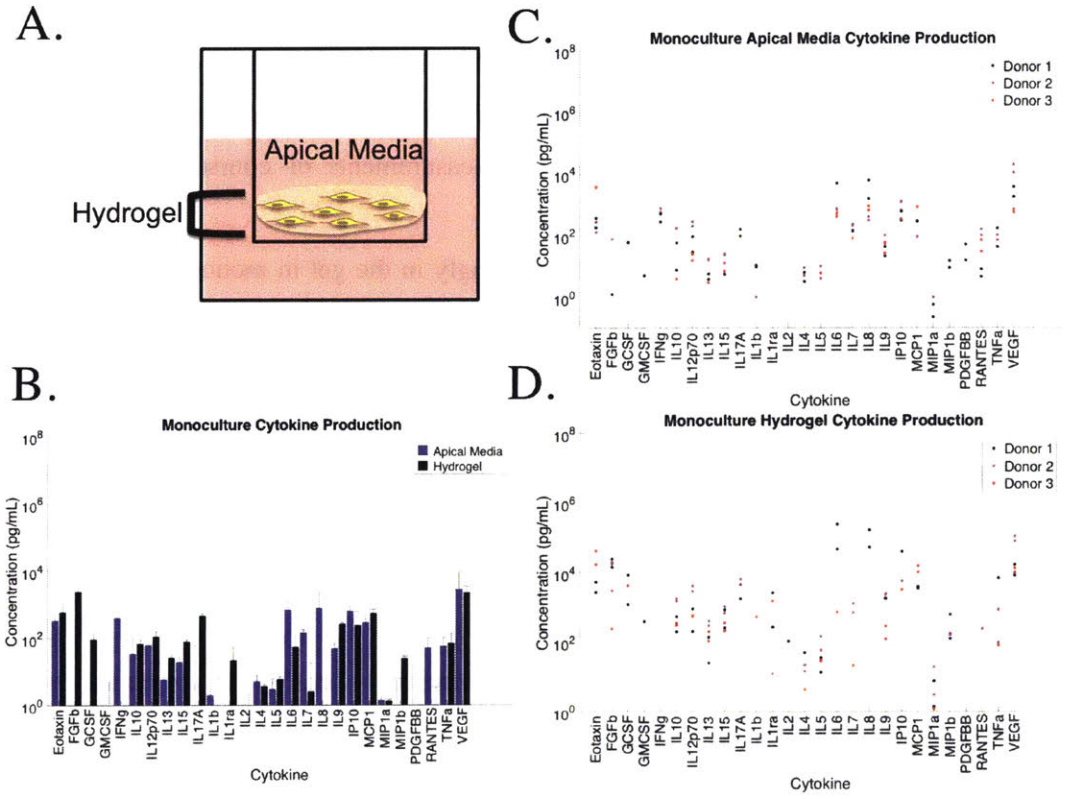

Figure 4-5. Cytokine production in apical media and hydrogel for stromal monoculture. (A) Schematic of stromal monoculture showing the cytokine measurement locations, apical media and hydrogel. (B) Day 15 median cytokine concentration (pg/mL) (48 hr) in the apical media (blue) and hydrogel (black). Data shown are the median and median absolute deviation for 3 donors (including both proliferative and secretory hormone conditions). Individual donor data are represented in dot plots for cytokines measured in the (C) apical media and (D) hydrogel. Each of the two dots per donor represents the mean of 2-3 biological replicates under proliferative or secretory hormone stimulation. Plot (B) represents the median across all donors and hormone conditions with biological replicates represented in plots (C) and (D).

Cytokine distribution in apical media and in local gel microenvironment in primary co-cultures of epithelial and stromal cells

After establishing the baseline partitioning behavior in stromal monocultures, where the production of cytokines and growth factors is not polarized and therefore the apical compartment should reflect an approximate equilibrium with the cell-encapsulated hydrogel, we next examined the distribution of cytokines in co-cultures. Interpretation of data from co-cultures is inherently more complex than monocultures due to the known polarized production of molecules by epithelial cells. The apical measurements are expected to be dominated by molecules produced by the apical side of epithelial cells, while the basal compartment in the gel represents a convolution of molecules produced basally by epithelia and also by stroma. All measurements of course represent net concentrations of production minus consumption.

Of the 5 cytokines shown to partition strongly in the gel in monoculture, four of those same cytokines, FGF basic, G-CSF, IL-17A, and IL-1ra were present in higher abundance in the gel in co-culture. This may suggest that stromal cells are likely the main producers of these cytokines. Additionally, in co-culture, but not monoculture, cytokines GM-CSF, IL-13, IL-15, IL-6 and IL-8 were present at higher levels in the gel (Fig. 4-6B). Most cytokines including Eotaxin, IFN-γ, IL-10, IL12p70, IL-2, IL-4, IL-5, IL-9, IP-10, MCP-1, MIP-1α, MIP-1β, RANTES, TNFα, VEGF were present at similar levels in the hydrogel versus media in co-culture, with only cytokines IL-1β, IL-7, and PDGF-BB present higher in the media, likely due to measurement sensitivity associated with dilution of hydrogel samples during dissolution.

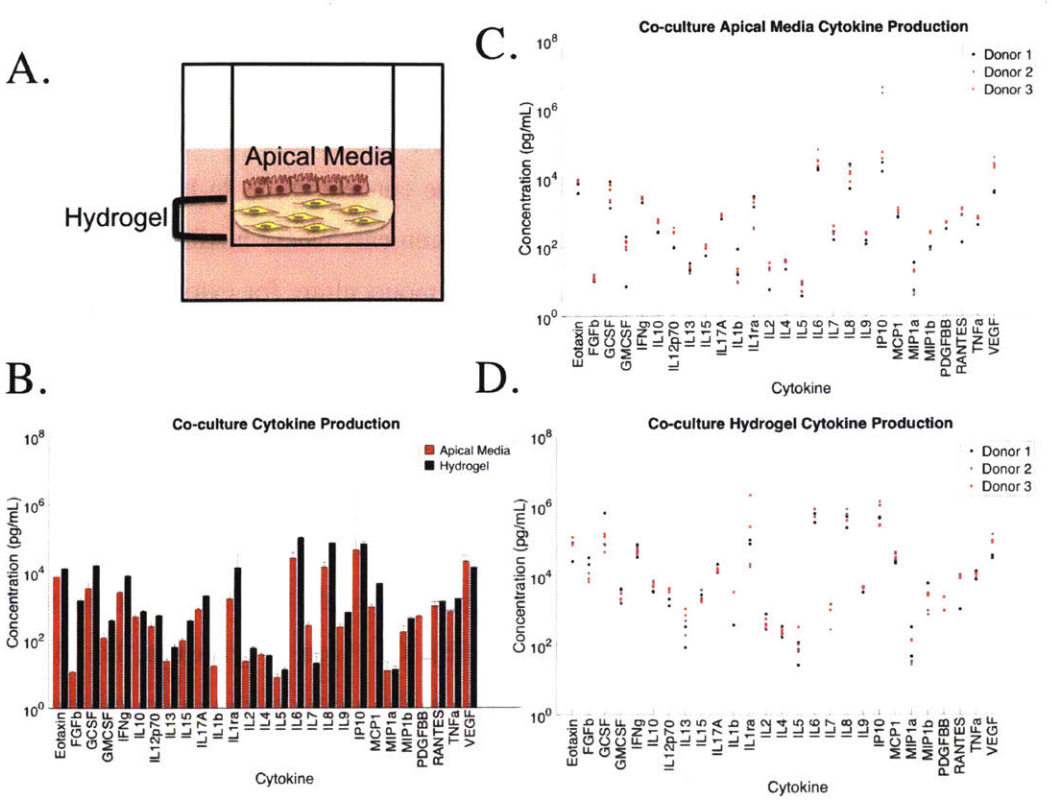

Figure 4-6. Cytokine production in apical media and hydrogel for epithelial-stromal co-culture. (A) Schematic of epithelial-stromal co-culture showing the cytokine measurement locations, apical media and hydrogel. (B) Day 15 median cytokine concentration (pg/mL) (48 hr) in the apical media (red) and hydrogel (black). Data shown are the median and median absolute deviation for 3 donors (including both proliferative and secretory hormone conditions). Individual donor data are represented in dot plots for cytokines measured in the (C) apical media and (D) hydrogel. Each of the two dots per donor represents the mean of 2-3 biological replicates under proliferative or secretory hormone stimulation. Plot (B) represents the median across all donors and hormone conditions with biological replicates represented in plots (C) and (D).

Primary epithelial-stromal co-cultures produce a wider variety and higher abundance of cytokines compared to stromal monocultures

Next, we evaluated which cytokines were differentially produced in monoculture and co-culture. Overall, co-cultures showed greater cytokine concentrations in both the gel and the media compared to stromal monoculture measurements where median fold-changes (n=3 donors) are shown for co-culture compared to monoculture for cytokines measured in the media and the gel (Fig. 4-7). Only one cytokine, FGF basic in the hydrogel, had a higher median measurement in monoculture compared to co-culture, whereas all other cytokines showed similar or greater production in co-culture independent of gel or media localization.

Additionally, some cytokines (GM-CSF, IL-1β, IL-2, MIP-1α, and PDGF-BB) were not detected in monoculture or were just slightly above the detection limit, but were detectible in co-culture (Fig. 4-5B and Fig. 4-6B). Of those 5 cytokines, IL-1β and PDGF-BB were the only two consistently present in the apical media in co-culture and variably present in the hydrogel. While IL-1β was present close to the detection limit in the apical compartment, and thus likely below in hydrogels during measurement, the relatively high concentration of PDGF-BB in the apical compartment and its absence in the hydrogel suggests that epithelial cells in co-culture primarily secrete PDGF-BB apically or that it is rapidly consumed in the stromal compartment. Thus, *SrtA*-mediated dissolution allowed for separate measurement of gel and media cytokines enhancing our understanding of compartmentalization of cytokines.

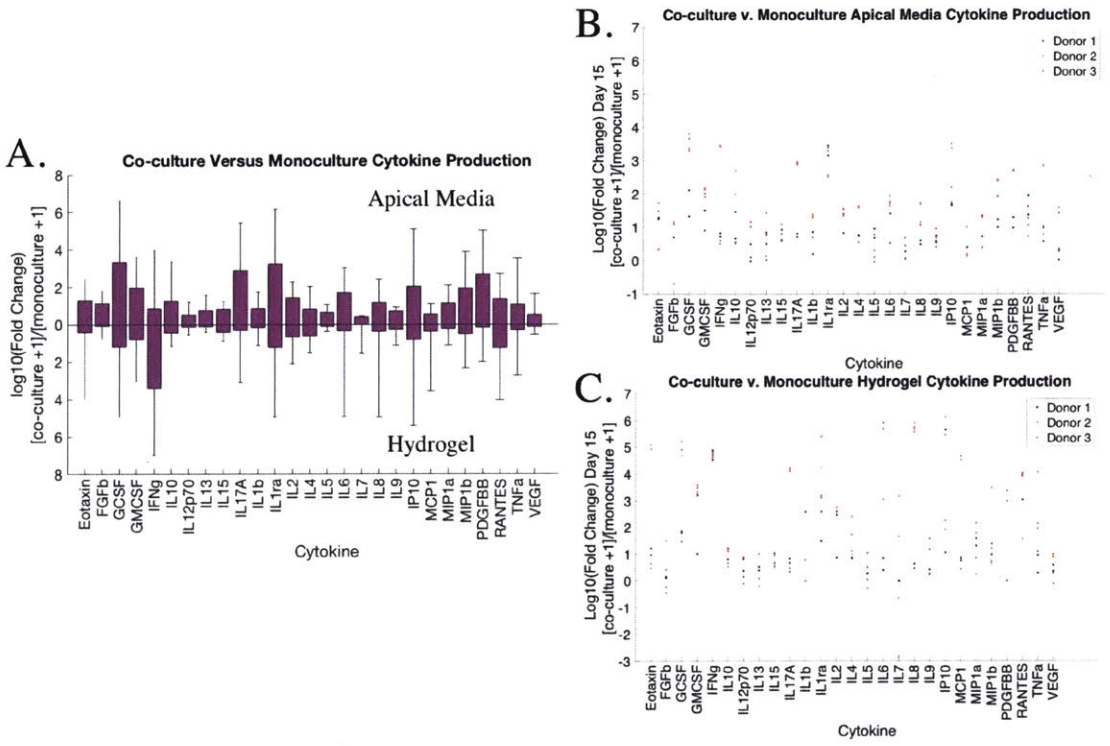

Figure 4-7. Cytokine secretion is higher in co-culture compared to monoculture. (A) Day 15 fold-changes for co-culture relative to monoculture median cytokine concentrations in the media (above X-axis) and gel (below X-axis). Data shown are the log-transformed median fold-changes and median absolute deviation for 3 donors, proliferative or secretory hormone conditions. Individual values are plotted for (B) the apical media and (C) hydrogel for each of the 3 donors with n=2 dots representing the mean of the proliferative or secretory hormone conditions (n=2-3 biological replicates).

4.2.4 Principal component analysis reveals cytokine variation is mainly due to the presence of epithelial cells and donor heterogeneity

Although primary cell co-cultures exhibited cytokine secretion profiles more similar to one another than endometrial cell lines, some heterogeneity in hormone-responsive cytokine secretion was previously observed (Section 4.2.2). Thus, we were interested in understanding what aspects of the cell cultures contributed most to observed variations in cytokine production. Possible factors included which cell types are present during culture (stromal monocultures versus epithelial-stromal co-cultures), inherent donor variability or the impact of hormone treatment (proliferative versus secretory hormone stimulation).

The goal of these experiments was to span a range of endometrial phenotypes—including estrogen v. estrogen and progesterone, clinically healthy v. adenomyosis, and stromal v. epithelial-stromal cells—to better understand what factors most contribute to variation in cytokine production by the endometrial mucosal barrier. Three different primary donors cultured as either stromal monocultures or epithelial-stromal co-cultures were hormone-stimulated to mimic either the proliferative or secretory phases of the menstrual cycle (see Methods).

Principal component analysis (PCA) is a useful method to gain insight into the variation that exists amongst samples for which we have multivariate data that cannot be intuitively understood in a univariate manner.[40] PCA was performed on the 27 cytokines measured in the apical media and hydrogel revealing that 75% of the observed cytokine variation could be explained by principal component (PC) 1, or the effect of having epithelial cells present in culture with stromal cells versus when stromal cells were cultured alone (Fig. 4-8A). All cytokines measured in the hydrogel and in the media contributed positively to explaining when epithelial cells were present (PC 1 loadings, Fig. 4-8C) suggesting that epithelial cells and/or epithelial-stromal interactions contribute to a cytokine rich milieu that modulates the local immune microenvironment within the endometrium.

Furthermore, this suggests cytokine signaling between stromal and epithelial cells superseded any donor variability and hormone treatments. In fact, within a given donor, cytokine secretion was similar despite either proliferative (estradiol) or secretory (estradiol and progesterone) hormone stimulation. This result is not surprising given our

previous results showing only 2 of the 27 cytokines exhibited consistent hormone responsive behavior in primary cells. Monocultures exhibited more heterogeneous cytokine secretion profiles between donors compared to donor co-cultures. Addition of multiple cell types in culture may result in a convergence of phenotypic behaviors, which minimizes individual donor differences and more closely resembles physiologic tissue signaling. Alternatively, this could indicate that endometrial epithelial cells contribute more or behave more homogeneously to one another in terms of cytokine secretion thus minimizing any donor specific stromal influences in co-culture.

An additional 16% of the cytokine variation was captured along PCs 2 and 3, and explained the differences observed between stromal monoculture donors (Fig. 4-8B). PCA also revealed stromal monoculture donor differences as follows: donor 1 was distinguished by higher levels of IL-6, IL-8 and G-CSF (cytokines positively contributing to PCs 2 and 3), donor 2 was distinguished by higher levels of IL-10, IL-12p70, IL-13, IL-15, IL-7, IP10 and RANTES (cytokines negatively contributing to PCs 2 and 3), and donor 3 was distinguished by higher levels of Eotaxin, IL-1β, IL-1ra and MCP-1 (cytokines contributing positively to PC2 and negatively to PC3) (Fig. 4-8D,E; data for PCA analysis contained in Appendix Tables 4A5-4A7). For these initial studies, we were encouraged to see that our culture matrix and experimental conditions supported heterogeneous donor behaviors; however, to understand clinical and biological significance of these findings, future studies evaluating many additional donors exhibiting various clinical pathologies will need to be conducted. For further discussion of donor specific differences see Section 4.2.6.

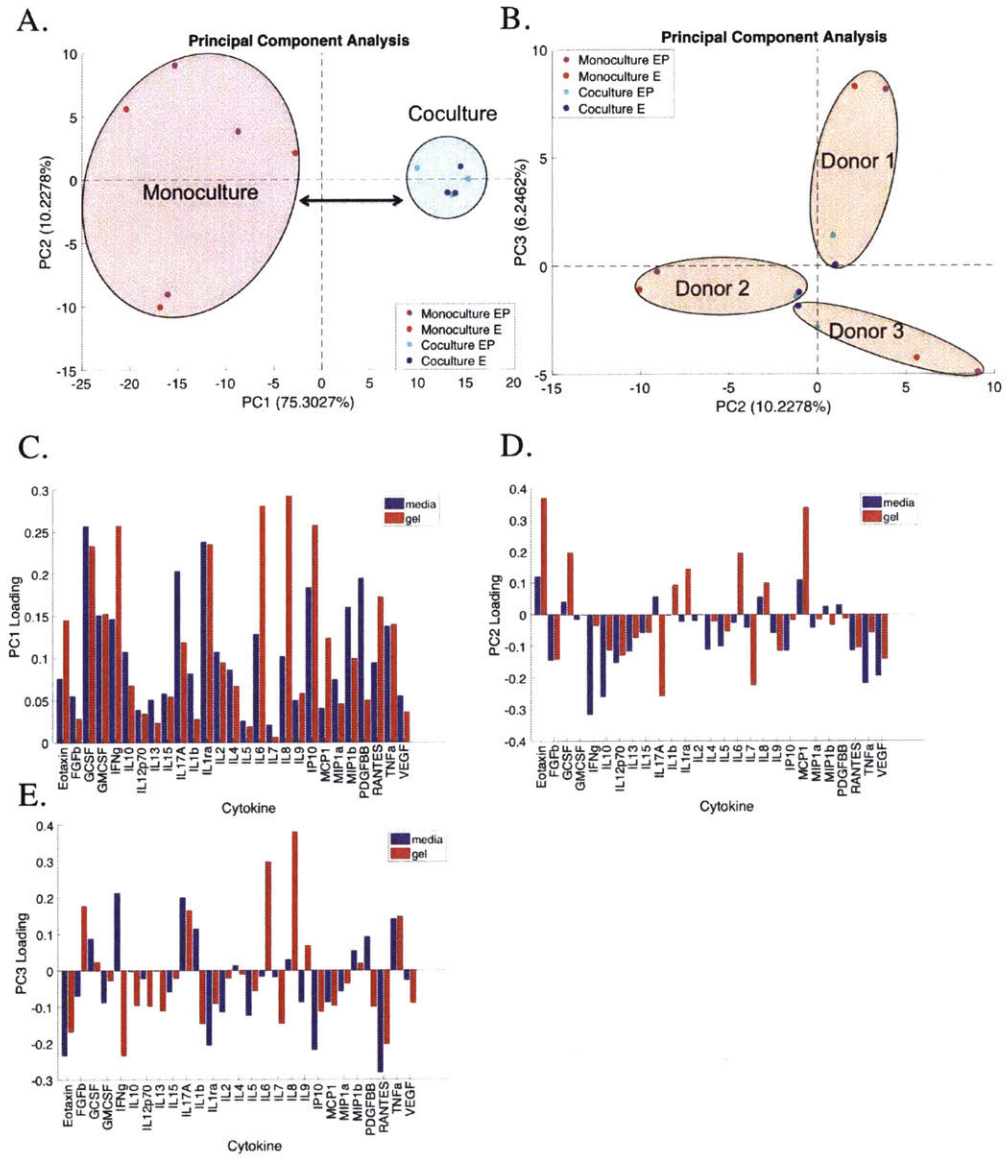

Figure 4-8. Principal component analysis reveals media and gel cytokine variation is greatest between epithelial-stromal co-cultures and stromal monocultures. (A) Principal component (PC) 1 explains 75% of the variation in primary culture cytokine secretion and separates stromal monocultures from epithelial-stromal co-cultures. (B) An additional 16% of cytokine variation occurs along PC2 and PC3 separating stromal monoculture donors. Loadings values show the contributions of each cytokine measured in the media (blue) or gel (red) for (C) PC1, (D) PC2, and (E) PC3.

We observed some cytokines whose contributions to donor variability along PCs 2 and 3 varied depending on whether they were measured in the cell media or within the hydrogel. For example, PC2 cytokines (IL-17A, IL-1ra, IL-6, MIP-1b, and PDGF-BB), and PC3 cytokines (FGF basic, IFN-g, IL-1β, IL-4, IL-6, IL-9, and PDGF-BB) contributed oppositely, as evidenced by the positive versus negative coefficient of the loading values, depending on whether the measurement occurred in the gel or the culture media (Fig. 4-8D,E).

4.2.5 An endometrial co-culture cytokine IL-1β increases cytokine expression in stromal monoculture

We have previously shown that IL-1β upregulates cytokine secretion in the Ishikawa-tHESC epithelial-stromal cell line co-culture model, but we were unable to specifically attribute cytokine changes to the stromal compartment, as both epithelial and stromal cells were present.[20] In general, we observed that co-cultures exhibited greater cytokine secretion in the media *and* in the gel than monocultures (Fig. 4-7), where increases in gel cytokine concentrations could be due to either basal cytokine secretion by the barrier epithelial cells or to changes in stromal produced cytokines in response to epithelial factors. Thus, to highlight the importance of intercellular cytokine signaling in epithelial-stromal co-culture, we examined how a primarily epithelial-produced cytokine, IL-1β, influenced cytokine secretion by stromal cells in monoculture.

Both stromal cells in monoculture and epithelial-stromal cells in co-culture respond to apical and basal stimulation of IL-1β in the culture media (Fig. 4-9 monoculture and Fig. 4-10 co-culture). In fact, compared to unstimulated monocultures, IL-1β enhanced detection of cytokines in both the apical and hydrogel compartments. Specifically, there was at least one donor monoculture that had undetectable levels of 16 cytokines in the apical media and 19 cytokines in the hydrogel in unstimulated conditions, whereas only 2 cytokines in the apical media and 3 cytokines in the hydrogel were undetectable after IL-1β stimulation (Fig. 4-5C,D and Fig. 4-9C,D).

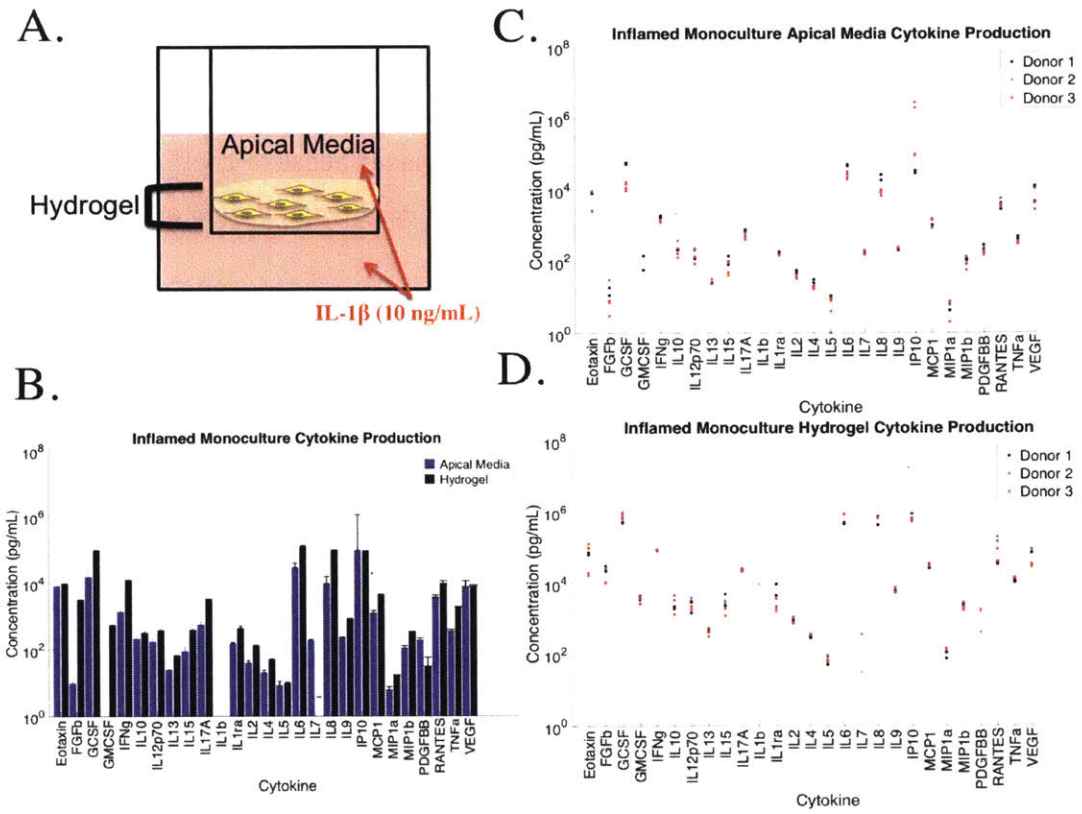

Figure 4-9. Cytokine production in apical media and gel for IL-1 inflamed stromal monoculture. (A) Schematic of stromal monoculture showing the cytokine measurement locations, apical media and hydrogel following IL-1β (10 ng/mL) stimulation on Day 13. (B) Day 15 median cytokine concentration (pg/mL) in the apical media (blue) and gel (black). Data shown are the median and median absolute deviation for 3 donors (including both proliferative and secretory hormone conditions). Individual donor data are represented in dot plots for cytokines measured in the (C) apical media and (D) hydrogel. Each of the two dots per donor represents the mean of 2-3 biological replicates under proliferative or secretory hormone stimulation. Plot (B) represents the median across all donors and hormone conditions with biological replicates represented in plots (C) and (D).

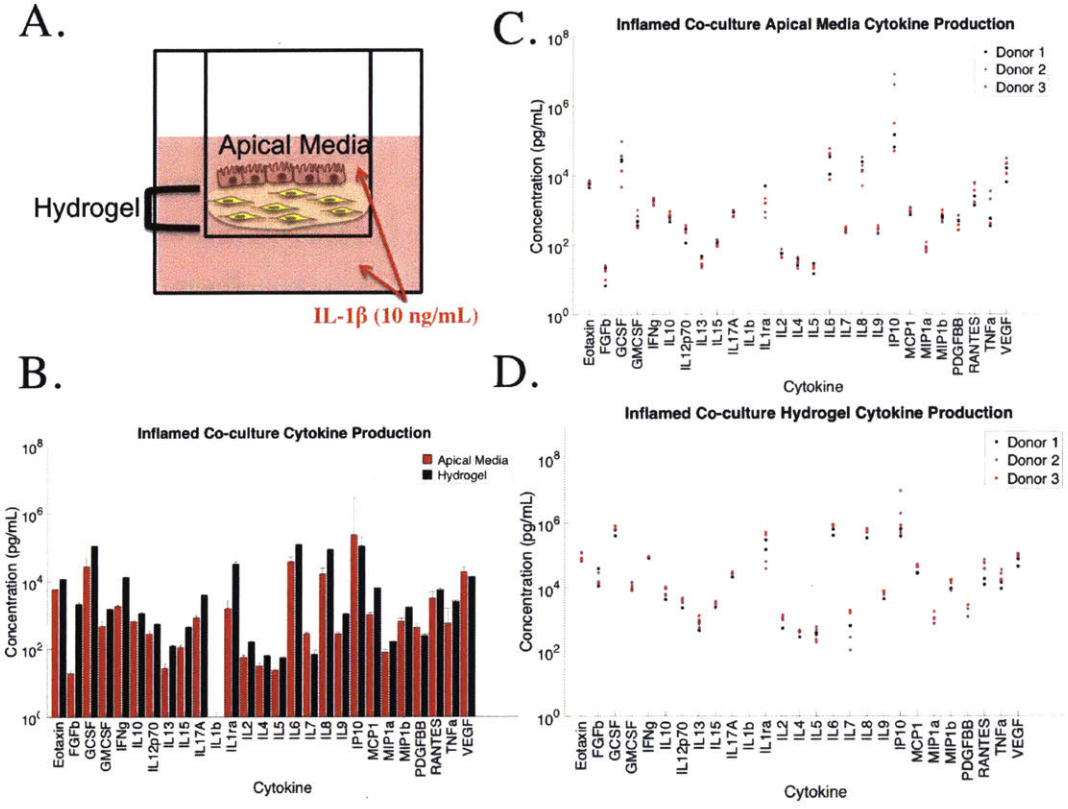

Figure 4-10. Cytokine production in apical media and gel for IL-1 inflamed epithelial-stromal co-culture. (A) Schematic of epithelial-stromal coculture showing the cytokine measurement locations, apical media and hydrogel following IL-1β (10 ng/mL) stimulation on Day 13. (B) Day 15 median cytokine concentration (pg/mL) in the apical media (red) and gel (black). Data shown are the median and median absolute deviation for 3 donors (including both proliferative and secretory hormone conditions). Individual donor data are represented in dot plots for cytokines measured in the (C) apical media and (D) hydrogel. Each of the two dots per donor represents the mean of 2-3 biological replicates under proliferative or secretory hormone stimulation. Plot (B) represents the median across all donors and hormone conditions with biological replicates represented in plots (C) and (D).

Comparison of IL-1β stimulation versus unstimulated cultures showed increased cytokine fold-changes in both the media and gel for both mono- and co-cultures (Fig. 4-11A,B; see Appendix Tables 4A8-4A10 for IL-1β stimulated cytokine measurements). Cytokine secretion by co-cultures was less affected by IL-1β treatment than in monocultures as evidenced by the lower fold-changes when comparing IL-1β stimulated to unstimulated cultures. Across all cytokines, median fold-changes were 1.4-fold and 1.9-fold in the apical media and gel, respectively for co-cultures, whereas median fold-changes were 2-fold and 15-fold in the apical media and gel for monocultures (Fig. 4-11). This suggests that the presence of IL-1β already in the co-cultures likely contributes to a cytokine-rich milieu and that further addition of IL-1β is superfluous for cytokine induction as evidenced by the lower median cytokine changes compared to monoculture.

Furthermore, previously undetected or low abundance cytokines in monoculture, GM-CSF, IL-2, MIP-1α, and PDGF-BB, became detectible after IL-1β stimulation, suggesting that under conditions mimicking inflammation, stromal cells can be induced to produce a wider variety of cytokines (Fig. 4-11A). Although we show an example of how a cytokine that is produced in co-culture, IL-1β, changes stromal cell cytokine production, future studies comparing epithelial cells alone, stromal cells alone, and epithelial-stromal cells in co-culture are necessary to determine which cell-signaling changes are specifically due to intercellular interactions.

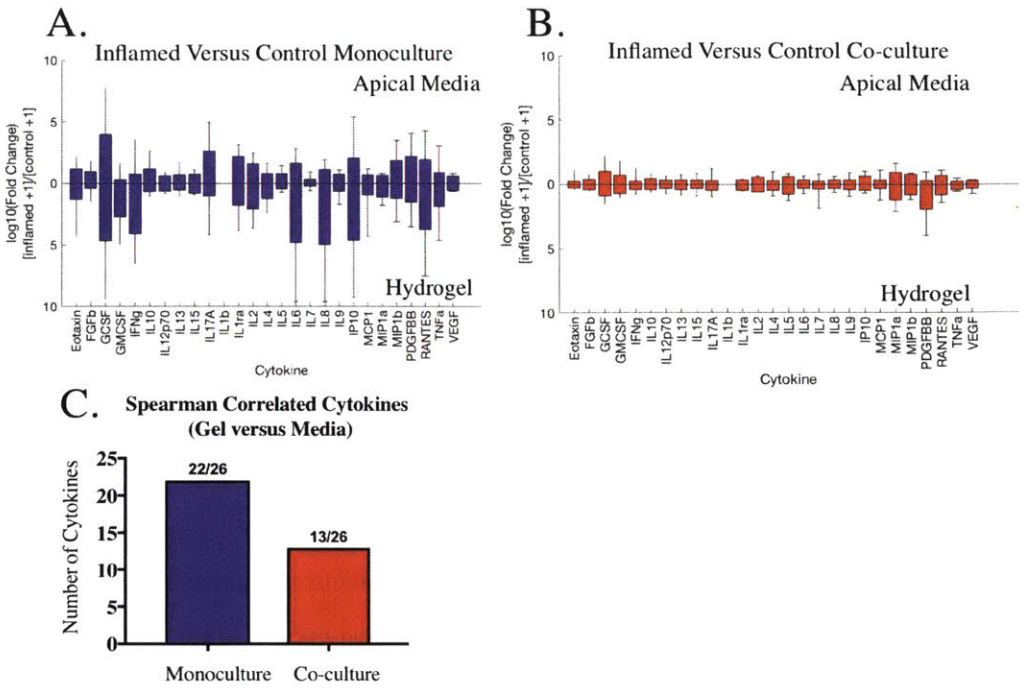

Figure 4-11. Inflammation increases cytokine secretion in primary monoculture and co-culture. Day 15 fold-changes of median cytokine concentrations in the apical media (above X-axis) and hydrogel (below X-axis) for inflamed versus control (A) stromal monocultures and (B) epithelial-stromal co-cultures. Inflamed cultures were stimulated with 10 ng/mL IL-1β on Day 13 of culture. Data shown are the log-transformed median fold-changes and median absolute deviation for 3 donors (including both proliferative and secretory hormone conditions). (C) Number of cytokines significantly correlated (Spearman) between gel and media in monoculture and co-culture including control and IL-1β inflamed conditions.

A barrier epithelial-stromal co-culture displays spatially heterogeneous cytokine secretion compared to stromal monoculture

Given the observed media and gel cytokine secretion heterogeneities, we were interested in how an epithelial barrier affected whether cytokine concentrations in the apical media were informative for understanding cytokine levels inside the hydrogel. While it is technically easier to measure cytokines in the apical media compared to the hydrogel, we expect an epithelial barrier to exhibit polarized cytokine secretion preventing free diffusion of cytokines between the apical media and hydrogel. Using Spearman's rank correlation analysis of control and inflamed (IL-1β stimulated) cultures, we determined that 85% (22 of 26) of cytokines measured in stromal monoculture were correlated between the media and the gel, whereas only 50% (13 of 26) were correlated in co-culture after Benjamini-Hochberg multiple hypothesis correction (Fig. 4-11C). Cytokine IL-1β was excluded from analysis due to exogenous addition precluding quantification in the inflamed conditions (see Appendix Table 4A11 for specific correlated cytokines).

As expected, an epithelial barrier on top of the stromal compartment established distinct apical and basal cytokine signaling microenvironments. There are several features of an epithelial barrier that could cause spatial heterogeneity in cytokine secretion including: directional cytokine secretion by the epithelial cells, physical blocking or uptake of stromal-produced cytokines by the epithelial cells, or variations in cell signaling due to intercellular communication between epithelial and stromal cells.

4.2.6 Primary cell co-cultures exhibit dynamic inflammatory cytokine induced intercellular protease signaling responses

Epithelial cells contribute directly and indirectly via IL-1 intercellular signaling to promote higher matrix metalloproteinase production

The interleukin-1 family, consisting of IL-1α and IL-1β, has previously been found to increase production of matrix metalloproteinases, MMPs, with endometrial expression increasing just prior to menstruation upon progesterone withdrawal.[11,17,28] An increase in MMPs in response to an inflammatory cue is likely important for dissemination of cytokines and chemokines to recruit and mature immune cells. Thus, we measured MMP concentrations in the media on day 15 of culture to assess proteases associated with

inflamed and control co-cultures and monocultures (Fig. 4-12; Appendix Table 4A12).

We observed all MMPs showed higher expression in co-culture compared to monoculture (Fig. 4-12A,B). Specifically, MMPs -7, -8, -9, and -13 were mainly present only in co-culture, but not monoculture, suggesting these proteases are produced primarily by epithelial cells. Furthermore, IL-1β stimulation increased MMPs -1, -3, -7 and -12 expression in monoculture and co-culture, with MMP-12 only observed in stromal monoculture upon IL-1β stimulation (Fig. 4-12C,D). Thus, we show epithelial cells contribute directly to MMP production, but also could contribute indirectly via secretion of IL-1β, which we demonstrate can upregulate MMP production by stromal cells in monoculture.

Taken together, IL-1β stimulation of monocultures increases cytokine and matrix metalloproteinase secretion, recapitulating facets of intercellular cytokine production in epithelial-stromal co-cultures. Furthermore, this study shows that consideration of intercellular signaling is warranted for immune signaling at the epithelial barrier as stromal cells are capable of responding to epithelial produced inflammatory cues by further producing additional cytokines and proteases. Because stromal cells may be able to respond to various epithelial secreted factors, future studies using inhibitors and blocking antibodies are necessary to specifically attribute which pathways may be regulated by intercellular epithelial-stromal signaling changes in co-culture and in particular which factors are primarily responsible for enhancing MMP production.

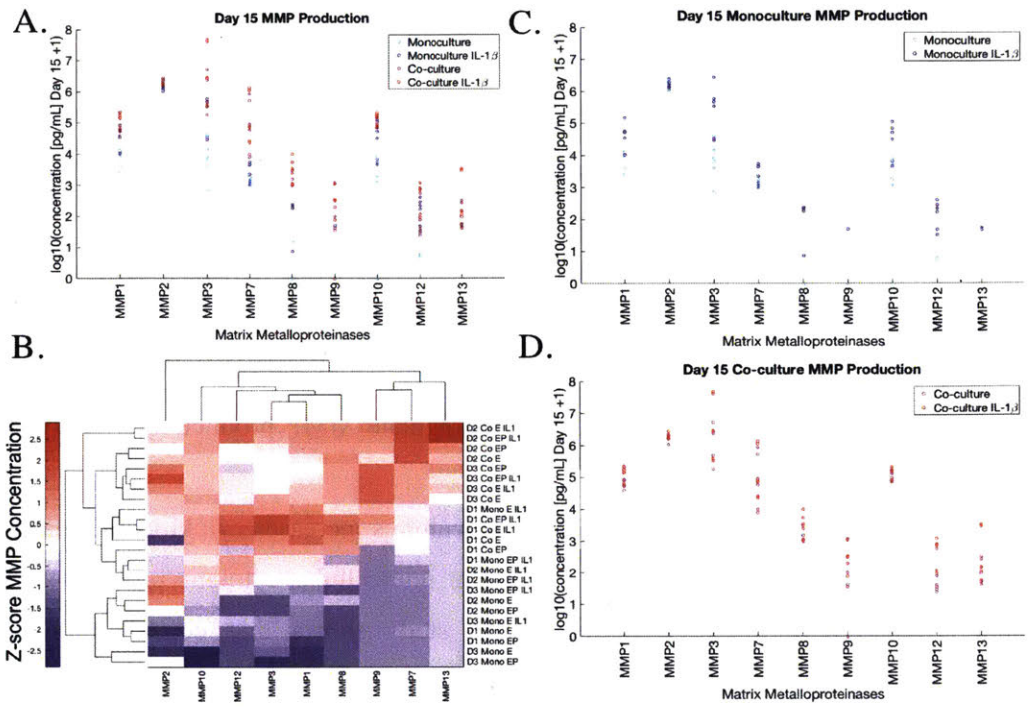

Figure 4-12. Matrix metalloproteinase production in day 15 apical medium shows enhanced production in co-culture and during inflammation. (A) Day 15 apical media MMP concentrations shows co-cultures (magenta) secrete greater amounts of all MMPs compared to monocultures (cyan), where IL-1β stimulated monocultures (blue) produce more MMPs than IL-1β stimulated co-cultures (red) compared to their respective unstimulated controls. Additionally, MMPs -1, -3, -7 and -12 are increased in response to IL-1β stimulation. (B) Unsupervised hierarchical clustering analysis (Z-scored and log-transformed) show unstimulated monocultures form their own cluster with IL-1β stimulated monocultures appearing more like co-cultures with or without IL-1β. (C) Monoculture and (D) co-culture MMP concentrations data are from N=3 primary donors (D1, D2 and D3) stimulated with 1 nM estradiol (E) or 1 nM estradiol and 100 nM progesterone (EP) +/- 10 ng/mL IL-1β. See Appendix Table 4A12 for MMP concentrations.

Synthetic matrix supports primary donors that exhibit variable progesterone hormone responsiveness

In order to evaluate progesterone responsiveness in primary mono- or co-cultures, we measured proteins from two different pathways that are differentially expressed by stromal cells in response to progesterone. Previous studies (sections 4.2.1 and 4.2.2) used a more potent co-stimulation of medroxy progesterone acetate and 8-Br-cAMP to induce decidualization. However, we were interested in more nuanced signaling that may be obscured by use of the second messenger cAMP, which can signal independently from the progesterone receptor.[6] Thus, we used the physiologic hormone, progesterone (P4) that stimulates decidualization of endometrial stromal cells *in vivo* causing secretion of characteristic proteins such as prolactin.[41] Prolactin was measured in the apical media on day 13 of culture after 8 days of estradiol and progesterone (EP) stimulation or estradiol (E) stimulation alone.

Progesterone, but not estradiol alone, significantly increases prolactin production by endometrial co-cultures for all three donors (Fig. 4-13A). Interestingly, only donor 1 exhibited significantly increased levels of prolactin in monoculture when comparing estradiol and progesterone to estradiol stimulation alone. Furthermore, donor 2 showed minimal (insignificant) prolactin production in response to P4 and prolactin production by donor 3 was undetectable in monoculture. Thus, as we have previously observed for cytokine secretion, the donor monocultures also exhibited greater culture heterogeneity in response to progesterone compared to the co-cultures. Previous studies have shown uterine glandular secretions including factors such as leukemia inhibitory factor (LIF) are indispensible for blastocyst implantation and stromal cell decidualization.[42–44] Our results also suggest that epithelial cells likely contribute to the decidual response as stromal monocultures variably produce prolactin in response to P4, however the decidual response was more robust for all donors when stromal cells were co-cultured with epithelial cells.

Next, we were interested in how progesterone modulated matrix metalloproteinase (MMP) expression within primary cultures. Progesterone suppresses global MMP expression in the endometrium during the secretory phase in preparation for embryo implantation. It is only after progesterone withdrawal, just prior to menstruation,

that MMPs are upregulated resulting in focal menstrual tissue breakdown. Previous studies have shown that progesterone is protective against inflammation (IL-1) induced expression of MMP-3 by stromal cells.[11] Thus, we measured MMP-3 in the apical supernate of day 15 cultures to assess whether EP limited MMP-3 expression in response to IL-1β stimulation (10 ng/mL added apically and basally on day 13) compared to E alone.

Similar to previous work by Osteen and colleagues,[11] we observed that stromal monocultures that were progesterone responsive, i.e., produced prolactin in response to P4, were also protected against induction of MMP-3 in response to IL-1 stimulation (Fig. 4-13B). In general, prolactin and MMP-3 levels were anti-correlated in monoculture with the most P4 responsive donor, donor 1, secreting the most prolactin and displaying the least MMP-3 induction compared to E2 alone. In addition, donor 3 showed no prolactin production in response to progesterone and equivalent stimulation of MMP-3 in EP versus E alone. Donor 2 exhibited a phenotype between donors 1 and 3. We note that donor 1 was considered a healthy control (myoma) whereas donor 2 had clinical adenomyosis and a myoma, whereas clinical data was unavailable for donor 3 (Appendix Table 4A13). Donor stromal cells from endometriosis and adenomyosis patients have been observed to be less P4 responsive overall and exhibit more MMP expression.[36,37] Excitingly, our culture model enabled known clinical phenotypes to be observed *in vitro,* where future studies using more donors are necessary to draw any further meaningful insight between biological differences in endometriosis and healthy donors.

Next, we assessed whether donor co-cultures were also protected by progesterone from IL-1 induced MMP-3 expression. All of the donor co-cultures exhibited P4 responsiveness by producing significantly more prolactin compared to estradiol stimulation alone. Interestingly, when co-cultures were challenged with 10 ng/mL IL-1β, all donors exhibited nearly equivalent amounts of MMP-3 production as compared to IL-1β stimulated estradiol treated cultures (Fig. 4-13C). This suggests that in co-culture progesterone does not protect against IL-1β induced MMP-3 production, in concordance with failure of P4 to protect against IL-1 in endometrial biopsy explant cultures.[11]

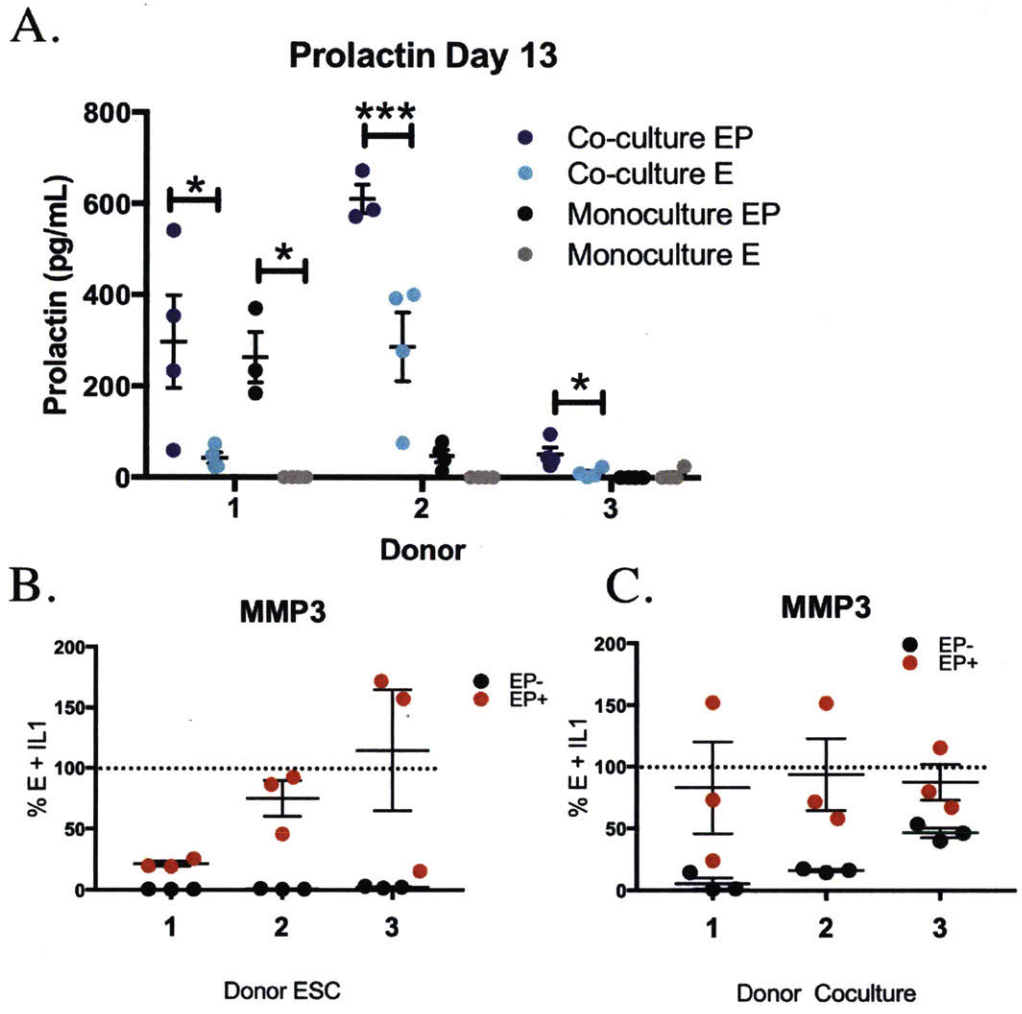

Figure 4-13. Progesterone protects against inflammation (IL-1) induced MMP3 expression in monoculture, but not co-culture. (A) Prolactin concentration, a marker of decidualization, is enhanced upon progesterone stimulation (EP) compared to estradiol alone (E) in monoculture and co-culture with epithelial-stromal co-cultures showing enhanced production of prolactin compared to stromal monocultures. Day 15 apical media measurements from (B) stromal monoculture and (C) epithelial-stromal co-culture showing mean values of MMP3 for EP and EP + IL-1β (10 ng/mL) stimulated cultures expressed as a percentage of estradiol + IL-1β (10 ng/mL) stimulated cultures. E = 1 nM estradiol and EP = 1 nM estradiol, 100 nM progesterone (see methods for timing). Data are the mean and SEM for each donor (n=3-4 biological replicates per condition).

The level of IL-1β in this study likely represents an extreme, as endogenous production observed in the apical co-culture medium was 1000-fold lower (9-85 pg/mL). Previous endometrial IL-1β stimulation studies have used between 0.05-50 ng/mL,[45–48] and we acknowledge that our study likely represents supraphysiological levels as serum levels in sepsis patients are ~10 pg/mL and levels measured in seminal plasma are 15-50 pg/mL.[49–51] The concentration of IL-1β present at the site of local embryo implantation may be higher, but it is challenging to estimate expected uterine levels, thus future dose-response studies evaluating concentrations spanning pico- to nano- grams are necessary.

Prolactin production was no longer predictive of MMP-3 production as was the case in monoculture. One hypothesis is that the signaling environment (cytokine milieu) in co-culture is more complex than in monoculture and that these cytokine-signaling cues may override any hormone-responsive donor heterogeneity that was observed in stromal monocultures. Thus, further investigation into the variable cytokines that may underlie differences in stromal monoculture and epithelial-stromal co-culture responses to hormones and inflammation may yield insights into clinically relevant biological heterogeneity.

4.2.7 Partial least squares regression reveals cytokines predictive of endometrial hormone and proteolytic remodeling responses

We have shown that cytokine signaling is heterogeneous with respect to mono- versus co-cultures, donor identity, and compartmental accumulation (gel v. media). Furthermore, hormone responsiveness of the *in vitro* cultures also depends on the initial culture state, e.g., donor identity and the cell culture composition—stromal monoculture versus epithelial-stromal co-culture. Thus, in order to ascertain which cytokines may contribute to altered hormone responsiveness, we can construct a model using partial least squares regression (PLSR) analysis to identify cytokine signals and their location that differentially predict prolactin and MMP-3 levels.

Two different PLSR models were constructed using 27-plex cytokine measurements taken from the apical media and dissolved hydrogels on day 15 of culture and regressed against apical media prolactin measured on day 13 or MMP-3 measured on day 15 of culture. Although sample volume limitations prevented measurement of all

analytes on day 15, we have previously observed prolactin levels display monotonic increases over time in response to progesterone, so we expect levels on day 13 to be informative of the trends that we would have seen on day 15. Therefore, we used PLSR to reveal which cytokines were most informative to predicting prolactin and MMP-3 concentrations, respectively (Fig. 4-14A,B).

PLSR model validation and the number of latent variables were determined via four-fold cross-validation, where both models showed prediction error (mean squared error) was not improved for models constructed using greater than two latent variables. We therefore evaluated which cytokines contributed most prominently to the predictive models using the first two latent variables. One method to extract a cytokines importance to the model is through computation of a variable importance in projection (VIP) score for each cytokine measured along the constructed latent variables.[52] A VIP score is a method of feature selection that enables identification of important predictive variables within multivariate datasets. Because the average of the squared values of all VIP scores in a model is 1, we chose an individual VIP score greater than 1 to be used as a threshold for selection of important cytokines predictive of prolactin or MMP-3.[53]

We identified some cytokines that had VIP scores greater than 1 in both models, suggesting that prediction of both prolactin and MMP-3 levels show dependence on some of the same cytokines (Appendix Table 4A14). These cytokines and their measurement location included G-CSF, IFN-γ, IL1-ra, and IP-10 (in both gel and media), IL-6 and IL-8 (in gel) and PDGF-BB and IL-17A (in media) (Fig. 4-14C,D). Interestingly, IL-6, IL-8 and G-CSF were also distinguishing of Donor 1 stromal monocultures in PCA, where donor 1 was also the only significantly progesterone responsive (prolactin producing) donor in monoculture. Thus, these cytokines may represent a local signaling environment for stromal cells that is conducive to prolactin and MMP-3 expression, as was observed for all donor co-cultures.

We also observed that VIP cytokines and chemokines were both canonical pro-inflammatory M1/TH1 (IFN-γ, IP-10, IL-6, and IL-8) and anti-inflammatory M2/TH2 (IL1-ra and PDGF-BB) suggesting that a balance in signaling between pro- and anti-inflammatory cytokines may underlie differences observed in mono- and co-cultures. Although inflammation is thought to compromise tissue integrity due to increased

proteolytic remodeling, previous animal studies have shown that local mechanical trauma can induce a decidual response, and a review of more recent clinical studies suggests that mechanical manipulation of the endometrium (e.g., taking a biopsy, curettage or hysteroscopy) in the cycle prior to *in vitro* fertilization (IVF) treatment may improve rates of implantation and pregnancy.[54] Increased implantation rates were associated with enhanced production of pro-inflammatory cytokines TNF-α, growth regulated oncogene GRO-α, IL-15, MIP-1β, and osteopontin, as well as increased influx of dendritic cells and macrophages after mechanical injury.[55]

Of the cytokines that were measured, we also identified TNF-α, MIP-1β, and IL-15 as predictive of either MMP-3 or prolactin, respectively. Thus, this inflammation signature was captured in our *in vitro* model of epithelial-stromal communication and was predictive of both proteolytic remodeling and decidualization. Additional cytokines specific only to MMP-3 prediction included GM-CSF (in gel and media), RANTES and Eotaxin (in gel) and MIP-1β and TNF-α (in media) (Fig. 4-14C). Endometrial remodeling becomes prominent during blastocyst implantation where factors secreted by the blastocyst modulate MMPs allowing invasion and tissue growth.[56,57] Thus, implantation represents a physiological wound-like process requiring proteolytic remodeling and immune cell recruitment and occurs concomitant with decidualization. Taken together, the construction of endometrial epithelial-stromal co-cultures from isolated primary cells might resemble a more wound-like state that could be informative for understanding endometrial regeneration as well as implantation.

Next, we identified VIP cytokines that were specific to prolactin prediction, which included IL-15 (in gel and media) and IL-17A, IL-1β, PDGF-BB and MIP-1β (in gel) (Fig. 4-14D). Interestingly, we observed IL-15 to be produced in response to decidualizing cues, cAMP and MPA, in a different subset of primary patients *in vitro* (See section 4.2.2). This result was replicated here as being correlated to prolactin production in an entirely different cohort of primary donors stimulated with the more physiologic decidualization cues, estradiol and progesterone, further suggesting IL-15 may be a general marker of decidualization. Interestingly, all other cytokines predictive of prolactin, but not MMP-3, were found in the gel suggesting that local in gel cytokine measurements are most predictive for distinguishing between prolactin and MMP-3.

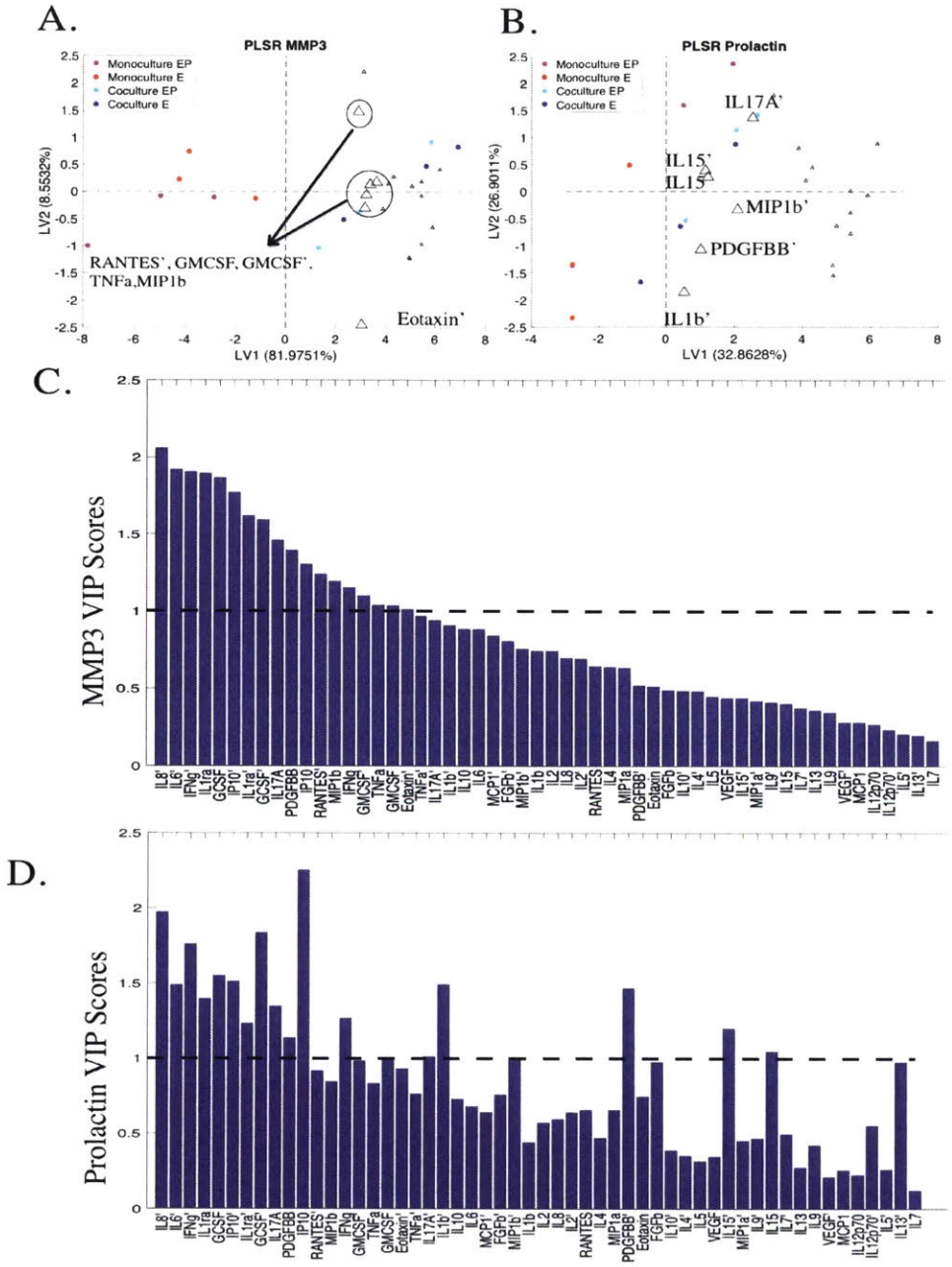

Figure 4-14. Partial least squares regression (PLSR) reveals cytokines and their localization important to predicting MMP3 and prolactin. Day 15 cytokines measured in the apical media and within the gel were used to construct PLSR models to predict (A) MMP3 measured on day 15 in apical media and (B) prolactin measured on day 13 in the apical media. Variable importance in projection scores were calculated for cytokines in the apical media or gel (') for (C) MMP3 and (D) prolactin where a threshold of 1 (dashed line) was used to determine importance. VIP cytokine loadings are plotted where small triangles represent VIP cytokines in common between MMP3 and prolactin models and large triangles represent model specific VIP cytokines. Data are from N=3 primary donors (D1, D2 and D3) stimulated with 1 nM estradiol (E) or 1 nM estradiol and 100 nM progesterone (EP).

Both MMP-3 and prolactin are produced primarily by endometrial stromal cells. However, we observed some cytokines (IL17A, MIP-1β, PDGF-BB, and TNF-α) to be predictive of MMP-3 that were present in the apical media but not in the hydrogel where the stromal cells were locally encapsulated. IL17A and TNF-α were slightly below the VIP threshold in the hydrogel suggesting they simply were just below the significance threshold possibly due to assay noise. However, MIP-1β and PDGF-BB appeared to be of importance only in the apical media. This observation was odd given that we would not expect cytokines detected primarily in the apical media, but not in the hydrogel, to influence stromal MMP-3 secretion. In our lab, it is well known that matrix effects influence immunoassays.

Specifically, the protein content in the measurement media can influence non-specific protein interactions, which change assay detection limits for antibody assays. Thus, we were interested in whether cytokine detection may be obscured in the gel measurements, which contained additional proteins sortase A (SrtA) (50 μM) and GGG (18 mM). Thus, in order to assess matrix effects due to sortase dissolution, 27-plex protein standard curves were generated in apical media and apical media with SrtA and GGG. Fitted curves were generated as previously described,[58] where a lower asymptote parameter was computed and represents the background response value of 0 standard concentration for the assay. Addition of SrtA and GGG increased the lower asymptote by greater than 3-fold for four cytokines including IFN-γ, IL-1β, IP-10 and PDGF-BB.

The cytokine INF-γ, especially in monoculture, was detectible in the apical medium, but not the hydrogel for 2 out of 3 donors (Appendix Table 4A5-7). This suggests that increased background due to SrtA and GGG likely obscures detection of INF-γ within the hydrogel. Further, both IL-1β and PDGF-BB, which were primarily detected in the apical medium in co-culture, also showed minimal detection in the hydrogel in mono- or co-culture. Thus, caution should be exercised when interpreting the VIP score for low abundance cytokines measured in different locations as assay detection limits increased after SrtA and GGG addition for hydrogel measurements (Appendix Table 4A15). Specifically, PDGF-BB shows up as important in the apical medium, but not the gel. The ability to detect this cytokine in the gel, especially at the low levels observed in our co-culture model, is further hindered in the presence of SrtA and GGG as

the detection limit shifted from 43 pg/mL without SrtA and GGG to 135 pg/mL after addition. One possible solution to overcome direct comparison of the apical media and the hydrogel is to add SrtA and GGG to all samples to enable measurements to be performed in the same protein matrix. We chose not to do this for these studies as this would have further diluted and obscured detection of apical media cytokines. Future studies investigating matrix effects for the Luminex assay are warranted for compartmental comparisons to identify how the PEG polymer from the dissolved gel also affects cytokine measurements.

Interleukin-1 family cytokines are predictive of protease expression and progesterone responsiveness

Interestingly, IL-1β levels in the gel was the only cytokine that was negatively correlated with prolactin production, and IL-1β and the IL-1 receptor antagonist, IL-1ra, were both distinguishing of donor 3 (PCA, Fig. 4-8) who showed the lowest prolactin levels in response to progesterone stimulation in both mono- and co-culture (Fig. 4-13A). Previous studies demonstrated that progesterone blocks IL-1α secretion by epithelial cells, and upon progesterone withdrawal, epithelial-produced IL-1α acts in a paracrine manner to stimulate IL-1α production by endometrial stromal cells, leading to menstruation.[17] Therefore, investigation into the mechanisms responsible for production of IL-1 by stromal cells (as observed for Donor 3) may inform why some patients fail to respond to progesterone treatment.

Both infection and embryo implantation are known to impact the local inflammatory cytokine milieu where changes in cytokine secretion modulate immune cell recruitment and activation. Specifically, the cytokine IL-1β is secreted by classically activated macrophages in response to infection, the implanting blastocyst, and is upregulated just prior to menstruation.[59–61] Elevated levels of IL-1β have been associated with recurrent pregnancy loss and preeclampsia suggesting IL-1β signaling must be tightly regulated as it contributes to both normal and pathological inflammatory events within the endometrium.

Furthermore, IL-1ra was predictive of both MMP-3 and prolactin suggesting that the balance of the IL-1 cytokine signaling family may be crucial to endometrial function.

Thus, altered ratios of IL-1ra/ IL-1β may result in pathological consequences underlying dysregulated tissue remodeling present in endometriosis, adenomyosis, or recurrent pregnancy loss.[8,62] Interestingly, IL-1β modulates embryo implantation via upregulation of cellular integrin adhesion receptors, whereas IL-1ra injection at the time of embryo implantation in a mouse model prevents implantation.[63,64] However, IL-1β knockout mice exhibit normal reproduction which may suggest there are other factors that mediate compensatory signaling to enable implantation in its absence.[65]

IL-1β is further implicated in inflammation associated with endometriosis, where IL-1β was secreted at higher levels by peritoneal macrophages in endometriosis patients compared to controls,[66,67] and intraperitoneal injection of IL-1ra was shown to be protective against endometriosis formation in a murine model of surgical related adhesions.[8] Notably, this may mean that the same signaling necessary to enable blastocyst attachment and invasion, may be altered in shed endometrial tissue where estrogen receptor ER-β has been shown to increase IL-1β activity leading to increased survival, attachment and proliferation of displaced menstrual tissue.[68] This provides a mechanism by which enhanced estrogen signaling which occurs due to both increased estradiol synthesis and ER-β expression in endometriotic implants, may contribute to lesion formation.[69,70]

Finally, our data suggests that endometrial epithelial cells enhanced stromal cell decidualization as co-cultures exhibited higher levels of prolactin and IL-15 than stromal monocultures. Although not measured in our current system, leukemia inhibitory factor (LIF) is a protein localized in luminal and glandular epithelium during the secretory phase and was previously identified as indispensible for decidualization and implantation.[71–73] Specifically, estrogen stimulation of epithelial ER-α has been shown to induce LIF production as endometrial epithelial ER-$\alpha^{-/-}$ mice failed to decidualize and thus were infertile.[42] Furthermore, IL-1β stimulates production of the IL-6 family cytokines, including LIF, by endometrial stromal cells.[74] Interestingly, decidualization cues, estradiol and medroxyprogesterone acetate, sensitize stromal cells to LIF via increases in LIF receptor gene expression.[43] Thus, there appears to be two mechanisms in the endometrium that increase LIF production whereby estrogen may initially prime the endometrium and IL-1β, secreted by the epithelium or blastocyst, may synergize during

the window of implantation to fully induce endometrial decidualization via epithelial-stromal paracrine signaling. Future investigation into this hypothesis, including understanding how the balance of LIF and IL-1 family cytokines contribute to decidualization, could offer insight into the critical balance of inflammatory signals important to endometrial function.

In conclusion, our model captures complex facets of cytokine signaling that are known to be important to both decidualization and matrix remodeling, and these are revealed through altering model complexity to parse cytokine localization and cell-specific cytokine signaling that may not be obvious from clinically obtained donor tissue samples. In fact, previous studies from our lab suggest dynamic, rather than static donor cytokine heterogeneity is most informative for differentiating endometriosis donors from controls when looking at peritoneal fluid and peritoneal fluid cells.[67] Thus, future investigation into the regulation of the IL-1 family in the context of endometrial pathologies is warranted, and this *in vitro* model provides opportunity to dynamically perturb cytokine signaling to unravel the complex interplay of epithelial-stromal communication using primary patients samples where inherent cellular states and inflammation-induced signaling changes may synergize to alter hormone responses and proteolytic tissue remodeling.

4.3 Materials and Methods

4.3.1 Materials

Hydrogel Reagents

PEG macromers (40 kDa, 8-arm) functionalized with vinyl sulfone (PEG-VS) were obtained from JenKem Technology (Beijing). All peptides were custom synthesized and purified (>95%) by Boston Open Labs (Cambridge, MA) or CPC Scientific (Sunnyvale, CA). Peptides used in these studies include the following: *"MMP-CL,"* a dithiol crosslinking peptide containing a matrix metalloproteinase (MMP)-sensitive substrate (Ac)GCRD-GPQGIAGQ-DRCG(Am); or *"SrtA-MMP-CL,"* a dithiol crosslinking peptide containing both a SrtA recognition sequence and matrix metalloproteinase (MMP)-sensitive substrate in tandem (Ac)GCRD-LPRTG-GPQGIAGQ-DRCG(Am);[75] *"PHSRN-K-RGD,"* a fibronectin-derived adhesion peptide containing both the RGD motif and the PHSRN synergy site from the 9,10 FN Type III repeat in a branched configuration to mimic features of the biophysical presentation in FN, (Ac)PHSRNGGGK-(Ac)GGGERCG-GGRGDSPY(Am);[76,77] *"FN-binder,"* a peptide with affinity for FN, (NH2-)GCRE-TLQPVYEYMVGV(-COOH);[78] and *"BM-binder,"* a peptide with affinity for basement membrane proteins type IV collagen and laminin, NH_2-GCRE-ISAFLGIPFAEPPMGPRRFLPPEPKKP(Am).[79] For reactions, peptides were reconstituted in Milli-Q water (Millipore) at a concentration of 10 mM for adhesion and matrix binding peptides and 45 mM for *MMP-CL* and *SrtA-MMP-CL*.

Cell Culture Reagents

Primary endometrial stromal cells, tert-immortalized human endometrial stromal cells (tHESCs) (ATCC), and Ishikawa human endometrial adenocarcinoma cells (Sigma-Aldrich) were routinely cultured in a humidified atmosphere at 37 °C and 5% CO_2 in DMEM/F12/FBS comprising phenol red-free DMEM/F12 (1:1 mixture of Dulbecco's Modified Eagle's Medium and Ham's F-12 (Gibco) media) supplemented with 1% penicillin/streptomycin (P/S) (Gibco) and 10% *v/v* dextran/charcoal treated fetal bovine serum (DC-FBS) (Atlanta Biologicals). Primary endometrial epithelial cells were expanded in F growth media comprising 3:1 mixture of DMEM/F12 supplemented with 5% *v/v* DC-FBS, 25 ng/mL hydrocortisone (Sigma H0888), 5 μg/mL insulin (Sigma

I9278), 10 ng/ml EGF (PeproTech AF-100-15), 10 μM Y-27632 (Tocris 1254), 8.5 ng/mL cholera toxin (Sigma C8052), and 1% P/S. 3T3-J2 embryonic mouse fibroblast cells (Kerafast) were cultured in DMEM/BCS comprising DMEM (Thermofisher 21063029) supplemented with 10% *v/v* iron-supplemented fetal calf serum (GE Healthcare/Hyclone SH30072.03) and 1% P/S.

Apical co-culture media (Apical DMEM/F12) comprised DMEM/F12 supplemented with 1% DC-FBS, 1% P/S, and 2% Cell Maintenance Supplement (Cocktail B) (LifeTechnologies CM4000). Basolateral co-culture media (WEM) comprised Williams E Medium (LifeTechnologies A1217601) supplemented with 1% P/S, 4% Cell Maintenance Supplement (Cocktail B) (LifeTechnologies CM4000) and 100 nM hydrocortisone (Sigma 50-23-7). Hormones 17β-estradiol (Sigma E2758) (E2) and progesterone (Millipore 5341-25GM) (P4) were prepared in 100% ethanol yielding 0.02% *v/v* of ethanol in the final culture media.

4.3.2 Primary Endometrial Biopsy Isolation and Cell Expansion

Purified endometrial glandular epithelium and stromal fibroblasts were isolated from eutopic endometrial biopsies using established protocols.[1,80] Pipelle biopsies (2 or 3 biopsies per donor) were obtained from women undergoing laparoscopic surgery for non-malignant gynecologic indications in accordance with a protocol approved by the Partners Human Research Committee and the Massachusetts Institute of Technology Committee on the Use of Humans as Experimental Subjects. Study enrollment was limited to pre-menopausal women with regular cycles (26-35 days) and excluded women with a history of hormone use in the prior 3 months. Donor specimens were from the proliferative or secretory phases according to histopathological assessment. Five out of 6 donors used in these studies were isolated from donor biopsies with known clinical data, whereas the one commercially sourced donor (Lifeline® FC-0078 donor 03839 and Lifeline® FC-0076 donor 02615, for matched epithelial and stromal cells, respectively) did not have accompanying clinical information (See Appendix Table 4A13).

Primary isolated endometrial stromal and epithelial cells were routinely cultured in a humidified atmosphere at 37°C and 5% CO_2. Stromal cells were expanded in culture

by seeding initial isolates (typical yield 1-5 x 10^6 cells per patient) into a T-25 or T-75 flask (Falcon) at a cell density of 2-5 x 10^4 cells/cm^2 in 4 mL or 8 mL of DMEM/F12/FBS, respectively. Cultures were grown to 70% confluency then subcultured 1:2 up to passage 6 prior to use.

Primary epithelial cells were both plated and used (passage 1) within one week of isolation for co-cultures (Section 4.2.1 and 4.2.2 experiments) or expanded and cryopreserved prior to use (Section 4.2.3, 4.2.4 and 4.2.5 experiments). We adapted previously established methods for primary epithelial expansion.[81] Briefly, isolated epithelial glandular fragments were initially seeded and subsequently passaged onto irradiated 3T3-J2 feeder cells. 3T3-J2 cells were cultured to 70% confluency in DMEM/BCS media, then trypsinized and irradiated (30 Gy) using a Cobalt-60 Irradiator (Gammacell 220 Excel), and cryopreserved in DMEM/BCS with 10% *v/v* DMSO. Irradiated feeders were seeded 1-2 days at 4 x 10^4 cells/cm^2 in DMEM/BCS media in advance of epithelial seeding. Epithelial cells were seeded onto feeders in F growth medium at 6 x 10^4 cells/cm^2 density, then split 1:4 once they reached 70% confluence (4-5 days), and medium was replaced every 2 days thereafter. Epithelial cells were passaged using serial trypsinization where flasks were rinsed with 1x PBS, incubated with RT trypsin for 1 minute to remove irradiated feeders, then incubated with pre-warmed 37 °C trypsin for 5 minutes to detach epithelial cells. Expanded primary epithelial cells were cryopreserved prior to passage 6 in F growth medium with 10% v/v DMSO.

4.3.3 Endometrial Cell Co-culture

PEG hydrogels (5 wt%) were fabricated on top of the membrane of Transwell® inserts (Corning #3470, 6.5 mm diameter, 0.4 um pores, 0.33 cm^2 culture area, polyester membrane) using Michael-type reaction chemistry as previously described.[1] For these experiments, PEG macromers were prepared by reacting 8-arm PEG vinyl sulfone with free thiols (-SH) on adhesion and/or matrix stabilization peptides in 1x PBS with 0.1 M HEPES (pH 7.8) for 30 minutes. Immediately after the functionalization reaction, the PEG macromer solution was mixed with a cell suspension (4.2 x 10^7 cells/mL in serum-free DMEM/F12, 1% penicillin/streptomycin) and then reacted with the cysteine thiol (-SH) groups on the bifunctional *MMP-CL* or *SrtA-MMP-CL* crosslinker to yield a final

(40% crosslinked hydrogel) solution comprising 4.2-6.3 X 10^6 tHESC or primary stromal cells/mL (~50,000-75,000 cells in 12 μL). Nominal peptide concentrations in the final gel were 1 mM *PHSRN-K-RGD*, 0.5 mM *FN-binder* and 0.5 mM *BM-binder*.

Hydrogel gelation, as determined by the point at which the solution could no longer be pipetted, occurred approximately 8 minutes (pH 7.8) after crosslinker addition at 25 °C. The hydrogel solution was pipetted for 2 minutes to keep stromal cells in suspension, allowed to sit in tube for 3 minutes, was transferred to inserts (12 μL/insert), manually spread with a pipette tip, then was centrifuged for 4 minutes at (330 RCF in an Eppendorf centrifuge 5810) to create a flat, meniscus-free hydrogel on the cell culture inserts. Plates were then incubated an additional 10 minutes at 25 °C prior to DMEM/F12/FBS addition on the apical (100 μL) and basolateral (600 μL) sides of the Transwell® to achieve hydrostatic equilibrium.

Endometrial epithelial cell cultures on synthetic hydrogels with encapsulated stroma

Methods for Sections 4.2.1 and 4.2.2

Endometrial epithelial cells were seeded on top of gel-encapsulated stromal cells 24 h after initiation of stromal cultures. Ishikawa cells were harvested via trypsinization, resuspended in DMEM/F12/FBS, and seeded at a density of 75,000 cells/Transwell® (225,000 cells/cm^2). Primary epithelial cells were harvested via trypsinization, resuspended in DMEM/F12/FBS and seeded at 50,000-75,000 cells/Transwell® (150,000-225,000 cells/cm^2). Apical and basal media were changed 24 hr after seeding to remove non-adherent epithelial cells. On day 3 of co-culture, medium was changed to maintenance media comprising Apical DMEM/F12 on the apical side (100 μL) and WEM on the basolateral side (600 μL), with changes every 2-3 days thereafter.

Methods for Sections 4.2.3, 4.2.4 and 4.2.5

Cryopreserved epithelial cells were thawed and seeded in F growth medium at 10^4 cells/cm^2 three days prior to use. For co-cultures, primary epithelial cells were harvested via trypsinization, resuspended in Apical DMEM/F12 supplemented with 1 nM E2 (100 μL/well), and seeded at a density of 75,000-100,000 cells/Transwell® (2-3 x 10^5

cells/cm^2) on top of gel-encapsulated stromal cells 24-48 h after initiation of stromal cultures. Basal media was replaced with WEM supplemented with 1 nM E2 (600 μL) when epithelial cells were seeded. Stromal monocultures had apical and basal media changed at the same time.

4.3.4 Hormone Treatment

Secretory phase hormone stimulation using cAMP and MPA (sections 4.2.1 and 4.2.2)

Endometrial co-culture decidualization was assessed by stimulation with 0.5 mM 8-bromoadenosine 3′,5′-cyclic monophosphate (Sigma B5386) and 1 μM medroxyprogesterone 17-acetate (MPA) (Sigma M1629) in the apical and basal medium starting on days 9 and 12 of co-culture, respectively, according to common protocols previously described.[82,83] Apical medium (100 μL) was collected on days 5, 7, 9, 12, and 15 of co-culture and stored at -80 °C.

Secretory and proliferative hormone and IL-1β stimulation (sections 4.2.3 and 4.2.4)

Beginning on day 5, secretory differentiation was simulated by supplementing apical media and basal media with 1 nM E2 and 100 nM P4 for 10 days. Proliferative phase cultures were treated with 1 nM E2 and an ethanol vehicle control (0.02% *v/v* media) for 10 days. Media (2/3 volume) was replaced every two days thereafter on days 7, 9, 11, and 13. Mono- and co-cultures were stimulated with 10 ng/mL interleukin-1β (PeproTech, 200-01B) on day 13. Apical media samples were collected and frozen at -80 °C on days 7, 9, 11, 13, and 15 of culture.

4.3.5 Sortase A Hydrogel Dissolution

On day 15, the hydrogel was removed from the culture insert by cutting around the membrane with a scalpel and gently placed in a pre-weighed 1.5 mL eppendorf tube. Sortase A penta-mutant P94R/D160N/D165A/K190E/K196T (SrtA), expressed and purified as previously reported,[20] was diluted in media and added to the hydrogel in an Eppendorf tube (50 μM in final 60 μL dissolving solution). SrtA was added (52.4 μL) for 10 minutes and incubated at 37 °C shaking at 400rpm on a thermal shaker prior to adding 18 mM Gly-Gly-Gly (GGG) (Sigma-Aldrich). GGG was added (7.6 μL) to the tubes and the solution was mixed at 400rpm during gel dissolution (10-20min). The membrane was

removed from the tube and the tubes were weighed. The dissolved hydrogel was separated from the cells by centrifugation at 0.3K rcf for 5 min. Supernatant (~85 ul, comprising 60 μL dissolution buffer and 25 μL gel) was transferred to a new tube and frozen at -80 °C until further use.

4.3.6 Biochemical Assays

ELISA for prolactin

Conditioned apical media from culture day 13 was analyzed by ELISA for prolactin (R&D systems DY682), indicative of secretory differentiation. Protocols provided by the manufacturer were adapted to allow ELISAs to be performed in a 384-well plate (ThermoFisher 464718) to minimize medium (sample) volume needed. Reported values are the mean of 2-4 (apical samples) biological replicates (different gels) minus mean concentration of no-cell gel controls.

Luminex immunoassay measurements

MMPs and TIMPs in 48-hour conditioned apical medium from day 13 during the co-culture period were measured using the magnetic Luminex Performance Assay, MMP 9-plex (MMP-1, -2, -3, -7, -8, -9, -10, -12, -13) (R&D LMPM000) and TIMP 4-plex (TIMP-1, -2, -3, -4) assays (R&D LKTM0003). Measurements of MMPs and TIMPs occurred using the following dilutions prepared in apical media: MMPs -1, -2, -3, and -10 and TIMPs were run diluted 1:150, MMP-7 was run diluted 1:25, and MMPs -8, -9, -12, and -13 were run undiluted.

Cytokines in undiluted conditioned apical medium or from sortase-dissolved hydrogels on days 7 and 15 of the co-culture period were measured by Luminex assay using the magnetic Bio-Plex Pro Human Cytokine 27-plex assay (BioRad, M500KCAF0Y). Protocols provided by the manufacturer were adapted to allow the assays to be performed in a 384 well plate to avoid introducing batch effects. Ten-point standard curves plus blanks (apical medium or sortase and GGG dissolution buffer) were included for quantification. For each cytokine, MMP or TIMP, 5-parameter logistic curves were fitted to the standards, excluding the blanks, using the L5P function in MATLAB (MathWorks)[58] Curve fits were used to calculate concentrations for each sample replicate.

Median fluorescence intensities (MFI) for the samples below the lower asymptote or above the upper asymptote of the fit were imputed to be either the MFI of the minimum asymptote or 99% of the MFI of the maximum asymptote, respectively. Values reported are the median of the number of gel replicates (n) specified in figures/tables corrected by the dilution factor. Concentrations that fell above the highest standard but below the maximum asymptote (due to incomplete coverage of the quantifiable range by the standard curve) were judged to be unreliable; these values are given as greater than the concentration of the highest standard and excluded from statistical testing.

4.3.7 Data-driven Models

Data Processing

Data processing of cytokine and protease measurements was performed prior to all subsequent analyses as follows: computed analyte concentrations were log-transformed to obtain $[analyte]_{log}$, where $[analyte]_{log} = \log([analyte] + 1)$. It was necessary to add 1 to all computed analyte concentrations in order to log-transform concentrations that were below the assay detection limit. Cytokine concentrations from the hydrogel were scaled 4-fold prior to all analyses to account for dilution due to the Sortase A dissolution buffer. Data processing and subsequent data-driven models were performed using MATLAB_R2016a (MathWorks, Natick, MA).

Principal Component Analysis

Principal component analysis was performed using the 'pca' function with singular value decomposition on the log-transformed day 15 apical media and gel cytokine measurements. Samples included epithelial-stromal co-cultures and stromal monocultures for n=3 donors stimulated with proliferative or secretory hormones.

Partial Least Squares Regression

Two different partial least squares regression (PLSR) models were constructed by regressing log-transformed cytokine concentrations measured from day 15 in the apical media and hydrogel against MMP3 measured on day 15 or prolactin measured on day 15 in the apical media. PLSR models were implemented using the SIMPLS 'plsregress'

algorithm in MATLAB and validated via four-fold cross-validation.[84] The number of latent variables was selected based on the minimization of mean squared error for model prediction after cross-validation. Samples included epithelial-stromal co-cultures and stromal monocultures for n=3 donors stimulated with proliferative or secretory hormones. Variable importance in projection scores were computed using the first two latent variables for each cytokine measured in either the apical media or in the hydrogel as previously described.[53]

Unsupervised Hierarchical Clustering Analysis

Unsupervised hierarchical clustering analysis was performed on the Z-scored log-transformed day 15 MMP concentrations measured in the apical media. Cluster analysis was performed using the function 'clustergram' with Euclidean distance metric and average linkage method.

4.3.8 Statistical Analysis

Data are expressed as mean ± SEM or median ± median absolute deviation as indicated in figures. Statistical analyses were performed using MATLAB (MathWorks) or GraphPad Prism v.5 for Mac OS X. Unpaired t-tests assuming unequal variances with appropriate post-tests were performed as indicated in the results. Statistical significance was defined as * $p < 0.05$, ** $p < 0.01$, *** $p < 0.0001$. Spearman's rank correlation analysis (two-tailed) was performed for cytokine concentrations measured in the media versus in the hydrogel using the 'Corr' function in MATLAB (MathWorks). Benjamini-Hochberg multiple hypothesis correction was performed to determine significance for cytokine analyses.

4.4 Conclusions

We demonstrate a framework for studying epithelial-stromal mucosal barrier biology using novel cell culture matrices and data-driven computational models to uncover complex cellular interactions *in vitro* from which understandings of intercellular hormone and matrix remodeling in the endometrium can be locally interrogated. Using this synthetic ECM, we illustrated profound differences in co-cultures constructed from standard endometrial cell lines compared to co-cultures constructed from patient-derived primary endometrial cells with respect to production of cytokines and growth factors that regulate tissue growth, maturation, and function. Interestingly, donor monocultures behaved more heterogeneous in terms of cytokine production compared to donor epithelial-stromal co-cultures possibly suggesting that stromal phenotypes may underlie clinical features associated with patient differences in hormone response or tissue remodeling. Moreover, we show that an epithelial barrier contributes to greater cytokine secretion and heterogeneous accumulation in co-culture warranting study of cytokines in the local microenvironment. Finally, we use this model to illustrate how dynamic intercellular signaling could influence cytokine and proteolytic remodeling by stimulating stromal monocultures with an inflammatory cytokine, interleukin-1, present primarily in co-culture, recapitulating facets of the more complex cytokine milieu and protease expression observed in co-culture.

4.5 References

1. Cook CD, Hill AS, Guo M, et al. Local remodeling of synthetic extracellular matrix microenvironments by co-cultured endometrial epithelial and stromal cells enables long-term dynamic physiological function. *Integr Biol (Camb).* 2017;9(4):271-289. doi:10.1039/c6ib00245e.
2. Liu H, Dowdle JA, Khurshid S, et al. Discovery of Stromal Regulatory Networks that Suppress Ras-Sensitized Epithelial Cell Proliferation. *Dev Cell.* 2017;41(4):392-407.e6. doi:10.1016/j.devcel.2017.04.024.
3. Mohammed J, Beura LK, Bobr A, et al. Stromal cells control the epithelial residence of DCs and memory T cells by regulated activation of TGF-β. *Nat Immunol.* 2016;17(4):414-421. doi:10.1038/ni.3396.
4. Broekman W, Amatngalim GD, de Mooij-Eijk Y, et al. TNF-α and IL-1β-activated human mesenchymal stromal cells increase airway epithelial wound healing in vitro via activation of the epidermal growth factor receptor. *Respir Res.* 2016;17(1):3. doi:10.1186/s12931-015-0316-1.
5. Tape CJ, Ling S, Dimitriadi M, et al. Oncogenic KRAS Regulates Tumor Cell Signaling via Stromal Reciprocation. *Cell.* 2016;165(4):910-920. doi:10.1016/j.cell.2016.03.029.
6. Aghajanova L, Hamilton A, Kwintkiewicz J, Vo KC, Giudice LC. Steroidogenic Enzyme and Key Decidualization Marker Dysregulation in Endometrial Stromal Cells from Women with Versus Without Endometriosis1. *Biol Reprod.* 2009;80(1):105-114. doi:10.1095/biolreprod.108.070300.
7. Igarashi TM, Bruner-Tran KL, Yeaman GR, et al. Reduced expression of progesterone receptor-B in the endometrium of women with endometriosis and in cocultures of endometrial cells exposed to 2,3,7,8-tetrachlorodibenzo-p-dioxin. *Fertil Steril.* 2005;84(1):67-74. doi:10.1016/j.fertnstert.2005.01.113.
8. Stocks MM, Crispens MA, Ding T, Mokshagundam S, Bruner-Tran KL, Osteen KG. Therapeutically Targeting the Inflammasome Product in a Chimeric Model of Endometriosis-Related Surgical Adhesions. *Reprod Sci.* 2017;24(8):1121-1128. doi:10.1177/1933719117698584.
9. Dyson MT, Roqueiro D, Monsivais D, et al. Genome-Wide DNA Methylation Analysis Predicts an Epigenetic Switch for GATA Factor Expression in Endometriosis. Barsh GS, ed. *PLoS Genet.* 2014;10(3):e1004158. doi:10.1371/journal.pgen.1004158.
10. Jichan Nie, Xishi Liu, Guo S-W. Promoter Hypermethylation of Progesterone Receptor Isoform B (PR-B) in Adenomyosis and Its Rectification by a Histone Deacetylase Inhibitor and a Demethylation Agent. *Reprod Sci.* 2010;17(11):995-1005. doi:10.1177/1933719110377118.
11. Keller NR, Sierra-Rivera E, Eisenberg E, Osteen KG. Progesterone Exposure Prevents Matrix Metalloproteinase-3 (MMP-3) Stimulation by Interleukin-1α in Human Endometrial Stromal Cells 1. *J Clin Endocrinol Metab.* 2000;85(4):1611-1619. doi:10.1210/jcem.85.4.6502.
12. Maybin JA, Critchley HOD. Menstrual physiology: implications for endometrial pathology and beyond. *Hum Reprod Update.* 2015;21(6):748-761. doi:10.1093/humupd/dmv038.
13. Maybin JA, Critchley HOD, Jabbour HN. Inflammatory pathways in endometrial

disorders. *Mol Cell Endocrinol.* 2011;335(1):42-51. doi:10.1016/j.mce.2010.08.006.
14. Seok J, Warren HS, Cuenca AG, et al. Genomic responses in mouse models poorly mimic human inflammatory diseases. *Proc Natl Acad Sci.* 2013;110(9):3507-3512. doi:10.1073/pnas.1222878110.
15. Osteen KG, Rodgers WH, Gaire M, Hargrove JT, Gorstein F, Matrisian LM. Stromal-epithelial interaction mediates steroidal regulation of metalloproteinase expression in human endometrium. *Proc Natl Acad Sci U S A.* 1994;91(21):10129-10133. doi:10.1073/pnas.91.21.10129.
16. Bruner KL, Rodgers WH, Gold LI, et al. Transforming growth factor beta mediates the progesterone suppression of an epithelial metalloproteinase by adjacent stroma in the human endometrium. *Proc Natl Acad Sci U S A.* 1995;92(16):7362-7366. http://www.pnas.org/content/92/16/7362.short. Accessed September 16, 2013.
17. Singer CF, Marbaix E, Kokorine I, et al. Paracrine stimulation of interstitial collagenase (MMP-1) in the human endometrium by interleukin 1α and its dual block by ovarian steroids. *Proc Natl Acad Sci U S A.* 1997;94(19):10341-10345. doi:10.1073/pnas.94.19.10341.
18. Wetendorf M, DeMayo FJ. The progesterone receptor regulates implantation, decidualization, and glandular development via a complex paracrine signaling network. *Mol Cell Endocrinol.* 2012;357(1-2):108-118. doi:10.1016/j.mce.2011.10.028.
19. Chen JC, Erikson DW, Piltonen TT, et al. Coculturing human endometrial epithelial cells and stromal fibroblasts alters cell-specific gene expression and cytokine production. *Fertil Steril.* 2013;100(4):1132-1143. doi:10.1016/j.fertnstert.2013.06.007.
20. Valdez J, Cook CD, Ahrens CC, et al. On-demand dissolution of modular, synthetic extracellular matrix reveals local epithelial-stromal communication networks. *Biomaterials.* 2017;130:90-103. doi:10.1016/j.biomaterials.2017.03.030.
21. Evans J, Salamonsen LA. Inflammation, leukocytes and menstruation. *Rev Endocr Metab Disord.* 2012;13(4):277-288. doi:10.1007/s11154-012-9223-7.
22. Krikun G, Mor G, Alvero A, et al. A novel immortalized human endometrial stromal cell line with normal progestational response. *Endocrinology.* 2004;145(5):2291-2296. doi:10.1210/en.2003-1606.
23. Nishida M, Kasahara K, Kaneko M, Iwasaki H, Hayashi K. [Establishment of a new human endometrial adenocarcinoma cell line, Ishikawa cells, containing estrogen and progesterone receptors]. *Nihon Sanka Fujinka Gakkai Zasshi.* 1985;37(7):1103-1111. http://www.ncbi.nlm.nih.gov/pubmed/4031568. Accessed August 13, 2013.
24. Leemasawatdigul K, Gappa-Fahlenkamp H. Development of a mathematical model to describe the transport of monocyte chemoattractant protein-1 through a three-dimensional collagen matrix. *Cardiovasc Pathol.* 2012;21(3):219-228. doi:10.1016/j.carpath.2011.09.002.
25. Meng C-X, Andersson KL, Bentin-Ley U, Gemzell-Danielsson K, Lalitkumar PGL. Effect of levonorgestrel and mifepristone on endometrial receptivity markers in a three-dimensional human endometrial cell culture model. *Fertil Steril.*

2009;91(1):256-264. doi:10.1016/j.fertnstert.2007.11.007.
26. Wang H, Pilla F, Anderson S, et al. A novel model of human implantation: 3D endometrium-like culture system to study attachment of human trophoblast (Jar) cell spheroids. *Mol Hum Reprod*. 2012;18:33-43. doi:10.1093/molehr/gar064.
27. Schutte SC, James CO, Sidell N, Taylor RN. Tissue-engineered endometrial model for the study of cell-cell interactions. *Reprod Sci*. 2015;22(3):308-315. doi:10.1177/1933719114542008.
28. Pretto CM, Gaide Chevronnay HP, Cornet PB, et al. Production of Interleukin-1α by Human Endometrial Stromal Cells Is Triggered during Menses and Dysfunctional Bleeding and Is Induced in Culture by Epithelial Interleukin-1α Released upon Ovarian Steroids Withdrawal. *J Clin Endocrinol Metab*. 2008;93(10):4126-4134. doi:10.1210/jc.2007-2636.
29. Bodnar RJ, Wells A. Differential regulation of pericyte function by the CXC receptor 3. *Wound Repair Regen*. 2015;23(6):785-796. doi:10.1111/wrr.12346.
30. Pence JC, Clancy KBH, Harley BAC. The induction of pro-angiogenic processes within a collagen scaffold via exogenous estradiol and endometrial epithelial cells. *Biotechnol Bioeng*. 2015;112(10):2185-2194. doi:10.1002/bit.25622.
31. Vinketova K, Mourdjeva M, Oreshkova T. Human Decidual Stromal Cells as a Component of the Implantation Niche and a Modulator of Maternal Immunity. *J Pregnancy*. 2016;2016:1-17. doi:10.1155/2016/8689436.
32. Okada S, Okada H, Sanezumi M, Nakajima T, Yasuda K, Kanzaki H. Expression of interleukin-15 in human endometrium and decidua. *Mol Hum Reprod*. 2000;6(1):75-80. doi:10.1093/molehr/6.1.75.
33. Pineda-Torres M, Flores-Espinosa P, Espejel-Nunez A, et al. Evidence of an immunosuppressive effect of progesterone upon in vitro secretion of proinflammatory and prodegradative factors in a model of choriodecidual infection. *BJOG An Int J Obstet Gynaecol*. 2015;122(13):1798-1807. doi:10.1111/1471-0528.13113.
34. Banerjee P, Ghosh S, Dutta M, et al. Identification of key contributory factors responsible for vascular dysfunction in idiopathic recurrent spontaneous miscarriage. *PLoS One*. 2013;8(11):1-9. doi:10.1371/journal.pone.0080940.
35. Singh B, Coffey RJ. Trafficking of epidermal growth factor receptor ligands in polarized epithelial cells. *Annu Rev Physiol*. 2014;76:275-300. doi:10.1146/annurev-physiol-021113-170406.
36. Bruner-Tran KL, Zhang Z, Eisenberg E, Winneker RC, Osteen KG. Down-Regulation of Endometrial Matrix Metalloproteinase-3 and -7 Expression in Vitro and Therapeutic Regression of Experimental Endometriosis in Vivo by a Novel Nonsteroidal Progesterone Receptor Agonist, Tanaproget. *J Clin Endocrinol Metab*. 2006;91(4):1554-1560. doi:10.1210/jc.2005-2024.
37. Bruner-Tran KL, Eisenberg E, Yeaman GR, Anderson TA, McBean J, Osteen KG. Steroid and Cytokine Regulation of Matrix Metalloproteinase Expression in Endometriosis and the Establishment of Experimental Endometriosis in Nude Mice. *J Clin Endocrinol Metab*. 2002;87(10):4782-4791. doi:10.1210/jc.2002-020418.
38. Mortier E, Quéméner A, Vusio P, et al. Soluble Interleukin-15 Receptor α (IL-15Rα)-sushi as a Selective and Potent Agonist of IL-15 Action through IL-15Rβ/γ.

J Biol Chem. 2006;281(3):1612-1619. doi:10.1074/jbc.M508624200.
39. Vlodavsky I, Miao HQ, Medalion B, Danagher P, Ron D. Involvement of heparan sulfate and related molecules in sequestration and growth promoting activity of fibroblast growth factor. *Cancer Metastasis Rev*. 1996;15(2):177-186. http://www.ncbi.nlm.nih.gov/pubmed/8842489.
40. Janes KA, Yaffe MB. Data-driven modelling of signal-transduction networks. *Nat Rev Mol Cell Biol*. 2006;7(11):820-828. doi:10.1038/nrm2041.
41. BRAVERMAN MB, BAGNI A, ZIEGLER D DE, DEN T, GURPIDE E. Isolation of Prolactin-Producing Cells from First and Second Trimester Decidua*. *J Clin Endocrinol Metab*. 1984;58(3):521-525. doi:10.1210/jcem-58-3-521.
42. Pawar S, Laws MJ, Bagchi IC, Bagchi MK. Uterine Epithelial Estrogen Receptor-α Controls Decidualization via a Paracrine Mechanism. *Mol Endocrinol*. 2015;29(9):1362-1374. doi:10.1210/me.2015-1142.
43. Shuya LL, Menkhorst EM, Yap J, Li P, Lane N, Dimitriadis E. Leukemia Inhibitory Factor Enhances Endometrial Stromal Cell Decidualization in Humans and Mice. Wutz A, ed. *PLoS One*. 2011;6(9):e25288. doi:10.1371/journal.pone.0025288.
44. Filant J, Spencer TE. Uterine glands: biological roles in conceptus implantation, uterine receptivity and decidualization. *Int J Dev Biol*. 2014;58(2-3-4):107-116. doi:10.1387/ijdb.130344ts.
45. Bersinger NA, Günthert AR, McKinnon B, Johann S, Mueller MD. Dose–response effect of interleukin (IL)-1β, tumour necrosis factor (TNF)-α, and interferon-γ on the in vitro production of epithelial neutrophil activating peptide-78 (ENA-78), IL-8, and IL-6 by human endometrial stromal cells. *Arch Gynecol Obstet*. 2011;283(6):1291-1296. doi:10.1007/s00404-010-1520-3.
46. Friebe-Hoffmann U, Baston DM, Hoffmann TK, Chiao JP, Rauk PN. The influence of interleukin-1β on oxytocin signalling in primary cells of human decidua. *Regul Pept*. 2007;142(3):78-85. doi:10.1016/j.regpep.2007.01.012.
47. Rossi M, Sharkey AM, Vigano P, et al. Identification of genes regulated by interleukin-1 in human endometrial stromal cells. *Reproduction*. 2005;130(5):721-729. doi:10.1530/rep.1.00688.
48. Braundmeier AG, Nowak RA. Cytokines Regulate Matrix Metalloproteinases in Human Uterine Endometrial Fibroblast Cells Through a Mechanism That Does Not Involve Increases in Extracellular Matrix Metalloproteinase Inducer. *Am J Reprod Immunol*. 2006;56(3):201-214. doi:10.1111/j.1600-0897.2006.00418.x.
49. Eidt M V., Nunes FB, Pedrazza L, et al. Biochemical and inflammatory aspects in patients with severe sepsis and septic shock: The predictive role of IL-18 in mortality. *Clin Chim Acta*. 2016;453:100-106. doi:10.1016/j.cca.2015.12.009.
50. Zhang X, Ibrahim E, de Rivero Vaccari JP, et al. Involvement of the inflammasome in abnormal semen quality of men with spinal cord injury. *Fertil Steril*. 2013;99(1):118-124.e2. doi:10.1016/j.fertnstert.2012.09.004.
51. Liu Z, Shi X, Wang L, Yang Y, Fu Q, Tao M. Associations between male reproductive characteristics and the outcome of assisted reproductive technology (ART). *Biosci Rep*. 2017;37(3):BSR20170095. doi:10.1042/BSR20170095.
52. Wold S, Sjöström M, Eriksson L. PLS-regression: a basic tool of chemometrics. *Chemom Intell Lab Syst*. 2001;58(2):109-130. doi:10.1016/S0169-7439(01)00155-

1.
53. Chong I-G, Jun C-H. Performance of some variable selection methods when multicollinearity is present. *Chemom Intell Lab Syst*. 2005;78(1-2):103-112. doi:10.1016/j.chemolab.2004.12.011.
54. Granot I, Gnainsky Y, Dekel N. Endometrial inflammation and effect on implantation improvement and pregnancy outcome. *Reproduction*. 2012;144(6):661-668. doi:10.1530/REP-12-0217.
55. Gnainsky Y, Granot I, Aldo PB, et al. Local injury of the endometrium induces an inflammatory response that promotes successful implantation. *Fertil Steril*. 2010;94(6):2030-2036. doi:10.1016/j.fertnstert.2010.02.022.
56. Guzeloglu-Kayisli O, Kayisli U, Taylor H. The Role of Growth Factors and Cytokines during Implantation: Endocrine and Paracrine Interactions. *Semin Reprod Med*. 2009;27(1):062-079. doi:10.1055/s-0028-1108011.
57. Chaouat G, Dubanchet S, Ledée N. Cytokines: Important for implantation? *J Assist Reprod Genet*. 2007;24(11):491-505. doi:10.1007/s10815-007-9142-9.
58. Cardillo G. Five parameters logistic regression - There and back again. http://www.mathworks.com/matlabcentral/fileexchange/38043. Published 2012. Accessed January 1, 2016.
59. Sequeira K, Espejel-Núñez A, Vega-Hernández E, Molina-Hernández A, Grether-González P. An increase in IL-1β concentrations in embryo culture-conditioned media obtained by in vitro fertilization on day 3 is related to successful implantation. *J Assist Reprod Genet*. 2015;32(11):1623-1627. doi:10.1007/s10815-015-0573-4.
60. Geisert R, Fazleabas A, Lucy M, Mathew D. Interaction of the conceptus and endometrium to establish pregnancy in mammals: role of interleukin 1β. *Cell Tissue Res*. 2012;349(3):825-838. doi:10.1007/s00441-012-1356-1.
61. Kauma S, Matt D, Strom S, Eierman D, Turner T. Interleukin-1β, human leukocyte antigen HLA-DRα, and transforming growth factor-β expression in endom trium, placenta, and placental membranes. *Am J Obstet Gynecol*. 1990;163(5):1430-1437. doi:10.1016/0002-9378(90)90601-3.
62. Krieg SA, Fan X, Hong Y, et al. Global alteration in gene expression profiles of deciduas from women with idiopathic recurrent pregnancy loss. *MHR Basic Sci Reprod Med*. 2012;18(9):442-450. doi:10.1093/molehr/gas017.
63. Simón C, Valbuena D, Krüssel J, et al. Interleukin-1 receptor antagonist prevents embryonic implantation by a direct effect on the endometrial epithelium. *Fertil Steril*. 1998;70(5):896-906. http://www.ncbi.nlm.nih.gov/pubmed/9806573.
64. Simón C, Gimeno MJ, Mercader A, et al. Embryonic Regulation of Integrins β 3 ,α 4 , and α 1 in Human Endometrial Epithelial Cells in Vitro 1. *J Clin Endocrinol Metab*. 1997;82(8):2607-2616. doi:10.1210/jcem.82.8.4153.
65. Zheng H, Fletcher D, Kozak W, et al. Resistance to fever induction and impaired acute-phase response in interleukin-1 beta-deficient mice. *Immunity*. 1995;3(1):9-19. http://www.ncbi.nlm.nih.gov/pubmed/7621081.
66. Keenan JA, Chen TT, Chadwell NL, Torry DS, Caudle MR. IL-1 beta, TNF-alpha, and IL-2 in peritoneal fluid and macrophage-conditioned media of women with endometriosis. *Am J Reprod Immunol*. 1995;34(6):381-385. http://www.ncbi.nlm.nih.gov/pubmed/8607944.

67. Beste MT, Pfaffle-Doyle N, Prentice EA, et al. Molecular Network Analysis of Endometriosis Reveals a Role for c-Jun-Regulated Macrophage Activation. *Sci Transl Med*. 2014;6(222):222ra16-222ra16. doi:10.1126/scitranslmed.3007988.
68. Han SJ, Jung SY, Wu S-P, et al. Estrogen Receptor β Modulates Apoptosis Complexes and the Inflammasome to Drive the Pathogenesis of Endometriosis. *Cell*. 2015;163(4):960-974. doi:10.1016/j.cell.2015.10.034.
69. Delvoux B, Groothuis P, D'Hooghe T, Kyama C, Dunselman G, Romano A. Increased Production of 17β-Estradiol in Endometriosis Lesions Is the Result of Impaired Metabolism. *J Clin Endocrinol Metab*. 2009;94(3):876-883. doi:10.1210/jc.2008-2218.
70. Bulun S, Monsavais D, Pavone M, et al. Role of Estrogen Receptor-β in Endometriosis. *Semin Reprod Med*. 2012;30(1):39-45. doi:10.1055/s-0031-1299596.
71. Stewart CL, Kaspar P, Brunet LJ, et al. Blastocyst implantation depends on maternal expression of leukaemia inhibitory factor. *Nature*. 1992;359(6390):76-79. doi:10.1038/359076a0.
72. Cullinan EB, Abbondanzo SJ, Anderson PS, Pollard JW, Lessey BA, Stewart CL. Leukemia inhibitory factor (LIF) and LIF receptor expression in human endometrium suggests a potential autocrine/paracrine function in regulating embryo implantation. *Proc Natl Acad Sci U S A*. 1996;93(7):3115-3120. http://www.ncbi.nlm.nih.gov/pubmed/8610178.
73. Chen JR, Cheng J-G, Shatzer T, Sewell L, Hernandez L, Stewart CL. Leukemia Inhibitory Factor Can Substitute for Nidatory Estrogen and Is Essential to Inducing a Receptive Uterus for Implantation But Is Not Essential for Subsequent Embryogenesis 1. *Endocrinology*. 2000;141(12):4365-4372. doi:10.1210/endo.141.12.7855.
74. Spratte J, Bornkessel F, Schütz F, Zygmunt M, Fluhr H. The presence of heparins during decidualization modulates the response of human endometrial stromal cells to IL-1β in vitro. *J Assist Reprod Genet*. 2016;33(7):949-957. doi:10.1007/s10815-016-0703-7.
75. Patterson J, Hubbell JA. Enhanced proteolytic degradation of molecularly engineered PEG hydrogels in response to MMP-1 and MMP-2. *Biomaterials*. 2010;31(30):7836-7845. doi:10.1016/j.biomaterials.2010.06.061.
76. Kuhlman W, Taniguchi I, Griffith LG, Mayes AM. Interplay between PEO tether length and ligand spacing governs cell spreading on RGD-modified PMMA-g-PEO comb copolymers. *Biomacromolecules*. 2007;8(10):3206-3213. doi:10.1021/bm070237o.
77. Cambria E, Renggli K, Ahrens CC, et al. Covalent Modification of Synthetic Hydrogels with Bioactive Proteins via Sortase-Mediated Ligation. *Biomacromolecules*. 2015;16(8):2316-2326. doi:10.1021/acs.biomac.5b00549.
78. Gao X, Groves MJ. Fibronectin-binding peptides. I. Isolation and characterization of two unique fibronectin-binding peptides from gelatin. *Eur J Pharm Biopharm*. 1998;45(3):275-284. http://www.ncbi.nlm.nih.gov/pubmed/9653632. Accessed September 14, 2013.
79. Johnson G, Moore SW. Identification of a structural site on acetylcholinesterase that promotes neurite outgrowth and binds laminin-1 and collagen IV. *Biochem*

Biophys Res Commun. 2004;319(2):448-455. doi:10.1016/j.bbrc.2004.05.018.
80. Osteen KG, Hill GA, Hargrove JT, Gorstein F. Development of a method to isolate and culture highly purified populations of stromal and epithelial cells from human endometrial biopsy specimens. *Fertil Steril*. 1989;52(6):965-972. http://www.ncbi.nlm.nih.gov/pubmed/2687030. Accessed September 17, 2013.
81. Liu X, Krawczyk E, Suprynowicz FA, et al. Conditional reprogramming and long-term expansion of normal and tumor cells from human biospecimens. *Nat Protoc*. 2017;12(2):439-451. doi:10.1038/nprot.2016.174.
82. Brosens JJ, Hayashi N, White JO. Progesterone receptor regulates decidual prolactin expression in differentiating human endometrial stromal cells. *Endocrinology*. 1999;140(10):4809-4820. doi:10.1210/endo.140.10.7070.
83. Gellersen B, Brosens J. Cyclic AMP and progesterone receptor cross-talk in human endometrium: a decidualizing affair. *J Endocrinol*. 2003;178(3):357-372. http://www.ncbi.nlm.nih.gov/pubmed/12967329. Accessed September 6, 2013.
84. de Jong S. SIMPLS: An alternative approach to partial least squares regression. *Chemom Intell Lab Syst*. 1993;18(3):251-263. doi:10.1016/0169-7439(93)85002-X.
85. PharmaCompass. Top drugs by sales revenue in 2015: Who sold the biggest blockbuster drugs? https://www.pharmacompass.com/radio-compass-blog/top-drugs-by-sales-revenue-in-2015-who-sold-the-biggest-blockbuster-drugs. Published 2017. Accessed October 8, 2017.
86. Kaiser J. Modified T cells that attack leukemia become first gene therapy approved in the United States. *Science (80-)*. August 2017. doi:10.1126/science.aap8293.
87. Shanks N, Greek R, Greek J. Are animal models predictive for humans? *Philos Ethics, Humanit Med*. 2009;4(1):2. doi:10.1186/1747-5341-4-2.
88. Gnecco JS, Pensabene V, Li DJ, et al. Compartmentalized Culture of Perivascular Stroma and Endothelial Cells in a Microfluidic Model of the Human Endometrium. *Ann Biomed Eng*. January 2017. doi:10.1007/s10439-017-1797-5.
89. Lee SK, Kim CJ, Kim D-J, Kang J. Immune Cells in the Female Reproductive Tract. *Immune Netw*. 2015;15(1):16. doi:10.4110/in.2015.15.1.16.
90. Cousins FL, Kirkwood PM, Saunders PTK, Gibson DA. Evidence for a dynamic role for mononuclear phagocytes during endometrial repair and remodelling. *Sci Rep*. 2016;6(1):36748. doi:10.1038/srep36748.
91. Bacci M, Capobianco A, Monno A, et al. Macrophages Are Alternatively Activated in Patients with Endometriosis and Required for Growth and Vascularization of Lesions in a Mouse Model of Disease. *Am J Pathol*. 2009;175(2):547-556. doi:10.2353/ajpath.2009.081011.
92. Tsamandouras N, Chen WLK, Edington CD, Stokes CL, Griffith LG, Cirit M. Integrated Gut and Liver Microphysiological Systems for Quantitative In Vitro Pharmacokinetic Studies. *AAPS J*. 2017;19(5):1499-1512. doi:10.1208/s12248-017-0122-4.
93. Chen WLK, Edington C, Suter E, et al. Integrated gut/liver microphysiological systems elucidates inflammatory inter-tissue crosstalk. *Biotechnol Bioeng*. 2017;114(11):2648-2659. doi:10.1002/bit.26370.
94. Stricker R, Eberhart R, Chevailler M-C, Quinn FA, Bischof P, Stricker R. Establishment of detailed reference values for luteinizing hormone, follicle

stimulating hormone, estradiol, and progesterone during different phases of the menstrual cycle on the Abbott ARCHITECT® analyzer. *Clin Chem Lab Med.* 2006;44(7). doi:10.1515/CCLM.2006.160.

95. Gargett CE, Schwab KE, Deane JA. Endometrial stem/progenitor cells: the first 10 years. *Hum Reprod Update.* November 2015:dmv051. doi:10.1093/humupd/dmv051.
96. Fayazi M, Salehnia M, Ziaei S. In-vitro construction of endometrial-like epithelium using CD146 + mesenchymal cells derived from human endometrium. *Reprod Biomed Online.* 2017;35(3):241-252. doi:10.1016/j.rbmo.2017.05.020.
97. Garry R, Hart R, Karthigasu K, Burke C. Structural changes in endometrial basal glands during menstruation. *BJOG An Int J Obstet Gynaecol.* 2010;117(10):1175-1185. doi:10.1111/j.1471-0528.2010.02630.x.
98. Boretto M, Cox B, Noben M, et al. Development of organoids from mouse and human endometrium showing endometrial epithelium physiology and long-term expandability. *Development.* 2017;144(10):1775-1786. doi:10.1242/dev.148478.
99. Turco MY, Gardner L, Hughes J, et al. Long-term, hormone-responsive organoid cultures of human endometrium in a chemically defined medium. *Nat Cell Biol.* 2017;19(5):568-577. doi:10.1038/ncb3516.
100. Garry R, Hart R, Karthigasu KA, Burke C. A re-appraisal of the morphological changes within the endometrium during menstruation: a hysteroscopic, histological and scanning electron microscopic study. *Hum Reprod.* 2009;24(6):1393-1401. doi:10.1093/humrep/dep036.

4.6 Appendix

Tables

Table 4A1: Cytokine concentrations (pg/mL) in apical medium collected on days 7 and 15 from monoculture (Ishikawa (75K cells) or tHESC (50K cells)) or co-culture gels (125K cells), with medium conditioned for 48 hours. In gels made with the cell lines, Ishikawa cells are the primary secretors of most cytokines, with the exception of Eotaxin, IL-15, and MCP-1.

	Day 7 (pg/mL)			Day 15 (pg/mL)		
	tHESC	Ishikawa	Co-culture	tHESC	Ishikawa	Co-culture
Eotaxin	136.6	77.5	80.6	76.7	42.2	79.9
FGF Basic (FGF-2)	6.7	0.0	0.0	0.0	0.0	0.0
G-CSF (CSF-3)	12.0	0.1	0.0	0.0	0.0	0.0
GM-CSF (CSF-2)	1.5[&]	2.5[&]	0.0	0.0	0.4[&]	0.0
IFN-γ	330.1	284.5	290.5	2.1[&]	268.8	259.6
IL-10	10.8	97.0	91.5	0.0	81.3	76.5
IL-12p70	29.3	577.0	566.6	0.0	579.9	514.2
IL-13	6.8	23.2	23.1	0.0	21.3	21.2
IL-15	0.9[&]	0.1[&]	0.1[&]	0.5[&]	0.0[&]	0.1[&]
IL-17A	78.4	22.9	5.8	0.0	3.5	12.3
IL-1β	1.5	0.0	0.0	0.0	0.0	0.0
IL-1ra	79.5	49.9	51.0	0.8[&]	43.0	45.1
IL-2	4.1	2.0[&]	1.6[&]	0.8[&]	1.3[&]	1.8[&]
IL-4	3.8	1.9	2.1	0.0	1.6	1.6
IL-5	14.9	0.0	0.0	0.0	0.0	0.0
IL-6	7.7	4.0	6.1	3.0[&]	4.1	10.7
IL-7	72.9	123.9	127.7	0.0	100.6	128.5
IL-8	19.1	8.8	28.4	16.6	11.3	26.9
IL-9	18.8	27.9	24.0	0.0	22.9	22.2
IP-10	259.5	253.1	290.2	17.3	211.6	270.8
MCP-1 (CCL2)	165.2	1.2	6.9	189.6	1.0	28.4
MIP-1α (CCL3)	1.6	0.2	0.1	0.0	0.0	0.3
MIP-1β (CCL4)	12.0	14.1	14.0	0.0	12.7	12.0
PDGF-BB	87.7	377.4	253.2	0.0	341.2	68.5
RANTES (CCL5)	9.2	0.0	0.0	0.0	0.0	0.0
TNF-α	81.5	0.0	0.0	0.0	0.0	0.0
VEGF	15.2	10231.4	13081.2	0.0	11545.8	7344.5

[&]Below the assay detection limit (blank + 2 standard deviations).

Table 4A2: Cytokine concentrations (pg/mL) in apical medium collected at 1 week for cell lines (Ishikawa and tHESC) and 1 and 2 weeks for primary endometrial cells.

	Week 1, 48 hr medium (pg/mL)				Week 2, 72 hr medium (pg/mL)		
	Cell Lines (n=8)	0188 (n=12)	0190 (n=4)	0191 (n=10)	0188 (n=6)	0190 (n=1)	0191 (n=5)
Eotaxin	274.1	1445.8	5291.7	10971.0	15636.3	10496.2	6449.7
FGF Basic (FGF-2)	0.0	12.7	0.0	21.7	19.5	NaN	3.0
G-CSF (CSF-3)	8.5	2130.5	1338.1	2268.2	1492.2	1523.5	1542.6
GM-CSF (CSF-2)	0.0	87.3	98.7	157.7	63.1	36.7	66.4
IFN-γ	101.1	303.8	215.0	360.7	244.0	301.8	235.4
IL-10	78.7	134.8	0.0	74.6	161.9	0.0	32.4
IL-12p70	239.4	38.6	0.0	100.2	49.7	0.0	8.3
IL-13	8.7	0.0	0.0	4.1[&]	0.0	0.0	0.0
IL-15	0.1[&]	21.5	19.5	34.2	24.3	56.0	34.7
IL-17A	95.8	172.4	112.2	233.0	126.6	152.7	119.3
IL-1β	0.0	11.9	4.5	20.2	5.0	7.3	5.8
IL-1ra	0.0	156.7	109.1	266.2	135.5	197.2	131.3
IL-2	0.0	1.6	0.0	5.2	0.1	0.0	1.7
IL-4	7.6	19.8	14.8	23.0	15.9	15.1	15.3
IL-5	0.0	0.5	0.0	1.5	0.0	0.0	0.0
IL-6	58.5	2131.1	1787.8	1977.8	2131.1	2131.1	1563.2
IL-7	79.1	71.4	58.1	85.0	97.0	88.1	75.1
IL-8	107.4	2690.7	2316.9	2523.1	2690.7	2690.7	2152.6
IL-9	9.0	9.7	5.1	30.9	9.3	0.0	7.4
IP-10^	245.2	21311.0	21311.0	21311.0	21311.0	21311.0	21311.0
MCP-1 (CCL2)	29.9	601.1	396.6	486.1	603.2	859.4	431.4
MIP-1α (CCL3)	0.7	17.0	6.4	60.8	9.2	6.3	16.2
MIP-1β (CCL4)	14.0	74.7	120.4	130.3	45.2	109.8	71.1
PDGF-BB	1666.6	380.5	151.5	1129.1	214.4	147.3	187.4
RANTES (CCL5)	0.7	96.3	253.0	90.7	453.3	1180.2	244.4
TNF-α	38.6[&]	945.4	928.9	2123.6	831.8	548.8	578.9
VEGF	7584.1	1391.1	27.9	4035.9	2164.0	46.3	617.7

[&]Concentration below the assay detection limit (blank + 2 standard deviations). ^Concentrations outside the range of the standard curve. NaN represents cytokines not quantified because of low bead counts. Total DNA from hydrogels (n=1-2 per condition) lysed on day 15 for cell line co-cultures was 1944±470 ng and primary cell hydrogels were 559±292 ng, 1255±110 ng, and 1212±82 ng for donors 0188, 0190 and 0191, respectively.

Table 4A3: Cytokine concentrations (pg/mL) in apical medium collected on day 15 from cAMP+MPA-stimulated and unstimulated primary endometrial cells and conditioned for 72 hours. Reported p-values were Benjamini-Hochberg adjusted for each subject. Four cytokines were significantly different for subject 0188 (Eotaxin, IL-10, IL-15, and MIP-1β), of which two (IL-10 and IL-15) behaved consistently across all three subjects.

	Subject 0188			Subject 0190			Subject 0191		
Cytokine (pg/mL)	Unstim (n=6)	Stim (n=6)	BH-adj. P-value	Unstim (n=2)	Stim (n=1)	BH-adj. P-value	Unstim (n=5)	Stim (n=5)	BH-adj. P-value
Eotaxin	15636	1892	**0.003**	10496	13960	NaN	6450	4976	0.685
FGF-b (FGF-2)	19.5	11.8	0.722	NaN	NaN	NaN	3.0	0.8	0.685
G-CSF (CSF-3)	1492	2238	0.317	1524	1025	NaN	1543	1965	0.685
GM-CSF (CSF-2)	63.1	72.6	0.684	36.7	0.0	NaN	66.4	69.1	0.897
IFN-γ	244.0	291.1	0.317	301.8	239.8	NaN	235.4	270.3	0.685
IL-10	161.9	482.0	**0.006**	0.0	206.9	NaN	32.4	310.5	0.224
IL-12p70	49.7	134.8	0.129	0.0	0.0	NaN	8.3	5.5	0.710
IL-13	0.0	5.8[&]	0.143	0.0	0.0	NaN	0.0	0.0	NaN
IL-15	24.3	115.6	**0.009**	56.0	70.8	NaN	34.7	54.7	0.685
IL-17A	126.6	146.6	0.426	152.7	119.6	NaN	119.3	143.6	0.685
IL-1β	5.0	7.2	0.302	7.3	3.9	NaN	5.8	7.2	0.685
IL-1ra	135.5	198.4	0.256	197.2	121.7	NaN	131.3	228.2	0.685
IL-2	0.1	3.7	0.317	0.0	0.0	NaN	1.7	0.0	0.685
IL-4	15.9	17.8	0.446	15.1	12.8	NaN	15.3	18.4	0.685
IL-5	0.0	1.5	0.446	0.0	0.0	NaN	0.0	1.4	0.685
IL-6	2131	1954	0.446	2131	2131	NaN	1563	1886	0.685
IL-7	97.0	90.4	0.722	88.1	112.1	NaN	75.1	88.0	0.685
IL-8	2690	2467	0.446	2691	2480	NaN	2153	2584	0.685
IL-9	9.3	16.3	0.325	0.0	0.0	NaN	7.4	1.7	0.685
IP-10[^]	21311	21311	NaN	21311	21311	NaN	21311	21311	NaN
MCP-1 (CCL2)	603.2	612.7	0.921	859.4	582.9	NaN	431.4	356.3	0.685
MIP-1α (CCL3)	9.2	15.7	0.256	6.3	3.0	NaN	16.2	31.4	0.685
MIP-1β (CCL4)	45.2	118.5	**0.026**	109.8	52.3	NaN	71.1	90.1	0.685
PDGF-BB	214.4	297.7	0.302	147.3	106.6	NaN	187.4	246.4	0.685
RANTES (CCL5)	453.3	475.3	0.921	1180	575.0	NaN	244.4	410.4	0.685
TNF-α	831.8	968.8	0.446	548.8	NaN	NaN	578.9	664.5	0.685
VEGF	2164	6032	0.134	46.3	81.5	NaN	617.7	691.0	0.816

[&]Below the assay detection limit (blank + 2 standard deviations).

[^]Concentrations outside the range of the standard curve; no statistics were calculated. NaN also represents p-values not calculable due to sample size (subject 0190) or comparisons for which both means and standard were 0.

Table 4A4: Cytokine concentrations (pg/mL) in apical medium collected on day 15 from cAMP+MPA-stimulated and unstimulated Ishikawa and tHESC endometrial cell line cultures conditioned for 72 hours. Cytokine data are the mean (n=4 hydrogels) background subtracted using mean of no cell hydrogels (n=2). Reported p-values were Benjamini-Hochberg adjusted.

	Ishikawa and tHESC		
Cytokine (pg/mL)	Unstim (n=4)	Stim (n=4)	BH-adj. P-value
Eotaxin	228.9	126.1	**0.001**
FGF-b (FGF-2)	48.8	46.7	**0.003**
G-CSF (CSF-3)	78.8	6.8	**0.001**
GM-CSF (CSF-2)	25.5	10.9	**0.0003**
IFN-γ	201.3	121.8	**0.002**
IL-10	138.2	138.8	0.641
IL-12p70	147.1	160.4	0.118
IL-13	20.5	20.2	0.081
IL-15	18.7	0	**0.002**
IL-17A	161.0	88.3	**0.003**
IL-1 β	0.9	0.5	**0.003**
IL-1ra	47.8	26.4	**0.002**
IL-2	19.9	20.1	0.828
IL-4	10.5	8.2	**0.002**
IL-5	15.8	5.7	0.180
IL-6	>229597.1	65.7	**1E-14**
IL-7	119.6	95.0	0.081
IL-8	535533.6	68.7	0.088
IL-9	53.2	48.9	**0.002**
IP-10	840.6	233.3	**2E-5**
MCP-1 (CCL2)	377.1	167.2	**0.002**
MIP-1 α (CCL3)	3.5	3.4	**0.0007**
MIP-1 β (CCL4)	10.6	7.9	**0.002**
PDGF-BB	4917.3	2683.9	**0.040**
RANTES (CCL5)	28.3	17.4	**0.0002**
TNF-α	192.9	127.2	**0.0009**
VEGF^	NaN	NaN	NaN

&Below the assay detection limit (blank + 2 standard deviations).
^Concentrations outside the range of the standard curve are reported as > highest standard concentration. VEGF concentration was too high to quantify.

Table 4A5: Primary endometrial monoculture (mono) and co-culture (co) (Donor 1) mean cytokine concentrations (pg/mL) in 48 hour conditioned media measured in the local hydrogel and in apical medium collected on day 15 for proliferative (E) and secretory (EP) hormone stimulated cultures. Hydrogel values are not corrected for four-fold dilution associated with gel dissolution.

Donor 1	Hydrogel				Apical Media			
Cytokine (pg/mL)	Mono E (n=3)	Mono EP (n=2)	Co E (n=3)	Co EP (n=3)	Mono E (n=3)	Mono EP (n=3)	Co E (n=3)	Co EP (n=3)
Eotaxin	199.2	100.6	3287.8	935.0	377.5	184.3	6679.5	3578.1
FGF-b (FGF-2)	911.2	537.7	1194.1	771.5	1.2	0.0	10.1	11.7
G-CSF (CSF-3)	317.0	45.3	22806.6	2839.8	59.4	61.6	7781.4	1328.4
GM-CSF (CSF-2)	14.7	0.0	151.7	58.0	5.1	0.0	193.3	7.0
IFN-γ	0.0	0.0	2818.8	1228.0	513.6	282.9	2727.6	1868.6
IL-10	20.3	7.4	130.0	123.6	58.2	7.7	270.8	252.6
IL-12p70	33.7	7.6	78.2	49.9	94.2	29.6	91.4	95.3
IL-13	5.1	0.9	12.5	3.2	5.8	3.8	20.6	32.7
IL-15	9.6	31.4	103.5	143.9	5.6	24.1	54.4	100.2
IL-17A	166.7	65.2	769.4	441.3	161.0	97.3	827.7	630.0
IL-1β	0.0	0.0	13.8	0.0	10.9	9.7	85.0	15.7
IL-1ra	9.9	95.5	3811.0	2924.9	0.0	0.0	1410.0	2822.8
IL-2	3.9	0.0	28.6	10.4	0.0	0.0	24.2	5.7
IL-4	1.8	0.8	12.7	6.1	6.3	3.2	39.6	22.3
IL-5	1.3	0.5	4.3	1.0	0.0	0.0	8.0	3.8
IL-6	8901.4	1717.9	21732.2	11882.0	4847.3	730.3	16347.2	18776.5
IL-7	0.0	0.0	0.0	0.0	136.6	145.8	157.9	275.5
IL-8	6064.9	1935.6	17617.1	8340.5	6166.2	1555.7	24321.9	4777.3
IL-9	65.4	66.8	169.6	118.2	42.8	21.3	153.0	120.0
IP-10	1460.0	0.0	16822.5	15792.6	596.7	306.8	27000.1	14800.3
MCP-1 (CCL2)	143.9	129.6	811.8	915.8	282.8	288.4	702.0	732.8
MIP-1α (CCL3)	0.3	0.1	12.0	1.7	0.6	0.2	34.3	5.4
MIP-1β (CCL4)	22.9	4.6	217.3	110.6	15.1	8.9	272.1	97.4
PDGF-BB	0.0	0.0	0.0	0.0	50.9	15.5	493.1	323.4
RANTES (CCL5)	0.0	0.0	379.4	39.2	8.1	4.6	811.5	130.3
TNF-α	251.0	30.9	482.4	279.3	169.3	42.3	636.8	416.4
VEGF	615.0	297.6	1359.0	1142.6	3748.1	1765.9	3965.6	3526.5

Table 4A6: Primary endometrial monoculture (mono) and co-culture (co) (Donor 2) mean cytokine concentrations (pg/mL) in 48 hour conditioned media measured in the local hydrogel and in apical medium collected on day 15 for proliferative (E) and secretory (EP) hormone stimulated cultures. Hydrogel values are not corrected for four-fold dilution associated with gel dissolution.

Donor 2	Hydrogel				Apical Media			
Cytokine (pg/mL)	Mono E (n=3)	Mono EP (n=3)	Co E (n=1)	Co EP (n=2)	Mono E (n=3)	Mono EP (n=3)	Co E (n=2)	Co EP (n=3)
Eotaxin	0.0	0.0	3133.6	4603.6	283.0	130.0	8650.0	6962.0
FGF-b (FGF-2)	663.3	736.7	242.0	431.7	78.0	0.0	15.0	14.0
G-CSF (CSF-3)	0.0	0.0	1746.2	2984.7	0.0	0.0	1965.0	2299.0
GM-CSF (CSF-2)	0.0	0.0	63.0	111.7	0.0	0.0	81.0	133.0
IFN-γ	0.0	0.0	1539.6	2115.8	776.0	589.0	2489.0	2366.0
IL-10	67.2	56.3	225.3	259.9	173.0	174.0	633.0	575.0
IL-12p70	156.7	109.3	121.8	158.0	285.0	204.0	353.0	265.0
IL-13	15.1	11.4	18.6	7.0	18.0	16.0	25.0	17.0
IL-15	25.3	39.1	82.4	141.4	25.0	26.0	100.0	115.0
IL-17A	164.8	239.1	483.6	523.7	0.0	0.0	777.0	758.0
IL-1β	0.0	0.0	0.0	0.0	1.0	1.0	9.0	9.0
IL-1ra	0.0	0.5	640.7	772.7	0.0	0.0	322.0	361.0
IL-2	0.0	0.0	11.3	14.9	0.0	0.0	24.0	21.0
IL-4	0.5	0.8	7.4	8.2	9.0	5.0	35.0	35.0
IL-5	2.2	5.4	2.4	2.8	10.0	4.0	9.0	9.0
IL-6	0.0	0.0	29290.1	29290.1	716.0	675.0	64165.0	29720.0
IL-7	26.2	46.4	0.0	10.2	230.0	209.0	261.0	231.0
IL-8	0.0	0.0	20810.4	29259.9	406.0	306.0	21551.0	14841.0
IL-9	83.8	90.5	154.5	157.0	102.0	60.0	262.0	233.0
IP-10	0.0	206.9	47422.8	37166.5	1267.0	1197.0	4082830.0	2735378.0
MCP-1 (CCL2)	0.0	0.0	1204.7	1678.4	93.0	88.0	936.0	912.0
MIP-1α (CCL3)	0.1	0.7	1.0	1.2	1.0	1.0	4.0	4.0
MIP-1β (CCL4)	5.9	6.6	27.4	36.2	0.0	0.0	80.0	85.0
PDGF-BB	0.0	0.0	0.0	0.0	0.0	0.0	510.0	526.0
RANTES (CCL5)	8.9	0.0	324.8	324.4	159.0	100.0	855.0	1143.0
TNF-α	3.5	31.8	323.8	395.9	102.0	70.0	622.0	746.0
VEGF	4035.2	2909.3	3157.4	5483.9	19744.0	10923.0	37612.0	24892.0

Table 4A7: Primary endometrial monoculture (mono) and co-culture (co) (Donor 3) mean cytokine concentrations (pg/mL) in 48 hour conditioned media measured in the local hydrogel and in apical medium collected on day 15 for proliferative (E) and secretory (EP) hormone stimulated cultures. Hydrogel values are not corrected for four-fold dilution associated with gel dissolution.

Donor 3	Hydrogel				Apical Media			
Cytokine (pg/mL)	Mono E (n=3)	Mono EP (n=3)	Co E (n=3)	Co EP (n=3)	Mono E (n=3)	Mono EP (n=3)	Co E (n=3)	Co EP (n=3)
Eotaxin	637.1	1580.1	2789.3	4652.2	3668.0	3987.0	7700.0	8968.0
FGF-b (FGF-2)	114.4	9.3	302.1	300.9	0.0	0.0	11.0	12.0
G-CSF (CSF-3)	0.0	159.9	5852.0	4809.1	0.0	0.0	4538.0	6201.0
GM-CSF (CSF-2)	0.0	0.0	78.7	140.4	0.0	0.0	101.0	147.0
IFN-γ	0.0	0.0	1795.4	2491.0	0.0	0.0	2676.0	2786.0
IL-10	13.2	11.6	172.3	184.6	4.0	0.0	491.0	501.0
IL-12p70	21.5	20.5	159.4	146.5	25.0	16.0	269.0	249.0
IL-13	7.5	4.0	26.5	40.9	0.0	3.0	26.0	23.0
IL-15	8.0	13.2	72.6	63.9	7.0	13.0	98.0	89.0
IL-17A	0.0	0.0	467.9	584.7	0.0	0.0	825.0	888.0
IL-1β	0.0	19.9	0.0	120.8	0.0	0.0	23.0	19.0
IL-1ra	0.0	56.1	9190.8	72502.8	0.0	0.0	1910.0	2424.0
IL-2	0.0	0.0	13.8	20.8	0.0	0.0	35.0	34.0
IL-4	0.0	0.2	9.2	10.5	0.0	0.0	39.0	42.0
IL-5	1.1	1.1	3.8	12.0	6.0	0.0	8.0	5.0
IL-6	0.0	26.5	17430.2	29290.1	409.0	526.0	21703.0	31302.0
IL-7	0.8	0.0	36.7	53.9	81.0	140.0	397.0	396.0
IL-8	0.0	0.0	13528.6	17457.0	656.0	902.0	7556.0	12844.0
IL-9	4.5	10.5	174.0	158.5	27.0	53.0	252.0	256.0
IP-10	0.0	117.4	10261.8	9660.4	344.0	653.0	54021.0	35034.0
MCP-1 (CCL2)	374.9	568.2	1032.8	1543.3	821.0	861.0	1119.0	1344.0
MIP-1α (CCL3)	0.0	0.0	5.3	4.9	0.0	0.0	21.0	19.0
MIP-1β (CCL4)	0.0	5.9	112.4	96.7	0.0	0.0	264.0	243.0
PDGF-BB	0.0	0.0	35.5	87.3	0.0	0.0	480.0	496.0
RANTES (CCL5)	0.0	0.0	362.9	302.8	30.0	70.0	1305.0	1319.0
TNF-α	0.0	2.9	425.7	402.4	0.0	0.0	709.0	698.0
VEGF	361.9	480.6	3540.4	3748.0	693.0	559.0	18479.0	21707.0

Table 4A8: Primary endometrial monoculture (mono) and co-culture (co) (Donor 1) mean cytokine concentrations (pg/mL) in 48 hour conditioned media measured in the local hydrogel and in apical medium collected on day 15 after IL-1β (10 ng/mL) stimulation on day 13 for proliferative (E) and secretory (EP) hormone stimulated cultures. Hydrogel values are not corrected for four-fold dilution associated with gel dissolution.

Donor 1 IL-1β stim	Hydrogel				Apical Media			
Cytokine (pg/mL)	Mono E (n=3)	Mono EP (n=3)	Co E (n=3)	Co EP (n=3)	Mono E (n=3)	Mono EP (n=3)	Co E (n=3)	Co EP (n=3)
Eotaxin	2266.7	2656.3	2496.2	2878.2	7902.3	8310.1	5907.0	4557.0
FGF-b (FGF-2)	825.1	1086.1	411.7	1430.1	18.3	11.3	23.0	6.8
G-CSF (CSF-3)	18662.4	17609.6	14926.6	22460.4	51430.1	56850.4	29490.0	25875.3
GM-CSF (CSF-2)	163.4	126.1	306.3	534.4	143.2	57.3	473.0	363.0
IFN-γ	3073.9	2980.4	3012.5	3237.5	1883.8	1690.9	2165.0	1456.6
IL-10	81.4	70.2	156.6	353.3	209.3	215.2	467.0	639.8
IL-12p70	107.7	54.3	86.4	125.1	225.4	119.5	290.0	114.3
IL-13	17.6	15.5	17.3	31.8	24.7	23.8	48.0	25.0
IL-15	86.6	181.1	89.2	118.4	82.0	140.6	118.0	101.8
IL-17A	853.5	810.0	756.0	971.3	757.8	654.2	899.0	660.2
IL-1β*	N/A	N/A	N/A	N/A	N/A	N/A	N/A	N/A
IL-1ra	165.2	343.4	5409.6	10741.8	184.6	159.4	5014.0	1608.8
IL-2	33.2	27.9	19.9	36.2	56.2	47.8	57.0	43.7
IL-4	11.7	10.6	10.4	15.0	31.1	24.7	40.0	25.8
IL-5	3.3	1.9	12.5	14.2	10.6	8.2	29.0	14.7
IL-6	18190.9	16235.2	14623.5	22605.1	48936.2	44974.9	34200.0	10761.9
IL-7	0.0	0.0	0.0	23.5	185.0	183.3	301.0	237.7
IL-8	25925.9	15378.2	12177.1	18527.1	25552.4	18040.4	24404.0	13847.0
IL-9	212.0	199.6	157.6	266.4	220.5	202.9	285.0	212.2
IP-10	32158.5	22661.0	13903.0	23112.0	33140.8	28318.9	146770.0	64489.9
MCP-1 (CCL2)	928.2	1245.4	966.9	1027.1	1024.9	1409.9	893.0	736.7
MIP-1α (CCL3)	4.1	2.8	27.6	39.9	7.2	4.2	85.0	61.7
MIP-1β (CCL4)	91.6	83.7	333.2	589.5	111.6	102.9	695.0	604.1
PDGF-BB	0.0	0.0	0.0	43.9	274.1	214.1	482.0	268.4
RANTES (CCL5)	1229.8	1362.5	438.3	659.3	2763.0	4095.5	2495.0	1377.7
TNF-α	415.8	381.2	327.0	508.9	481.9	398.5	575.0	347.8
VEGF	2539.0	1083.6	1585.5	2712.6	12424.9	4454.2	16034.0	6405.7

* Cytokine IL-1β was excluded from analysis due to exogenous addition precluding detection in the inflamed conditions.

Table 4A9: Primary endometrial monoculture (mono) and co-culture (co) (Donor 2) mean cytokine concentrations (pg/mL) in 48 hour conditioned media measured in the local hydrogel and in apical medium collected on day 15 after IL-1β (10 ng/mL) stimulation on day 13 for proliferative (E) and secretory (EP) hormone stimulated cultures. Hydrogel values are not corrected for four-fold dilution associated with gel dissolution.

Donor 2 IL-1β stim	Hydrogel				Apical Media			
Cytokine (pg/mL)	Mono E (n=3)	Mono EP (n=3)	Co E (n=1)	Co EP (n=2)	Mono E (n=3)	Mono EP (n=3)	Co E (n=2)	Co EP (n=3)
Eotaxin	712.3	598.3	4600.9	4287.2	2482.0	2607.0	7447.0	5983.0
FGF-b (FGF-2)	979.2	762.0	1081.6	570.5	8.0	30.0	26.0	20.0
G-CSF (CSF-3)	30502.2	26106.6	30502.2	30502.2	9391.0	16050.0	96845.0	37108.0
GM-CSF (CSF-2)	152.0	137.1	418.2	532.9	0.0	0.0	1019.0	688.0
IFN-γ	3242.5	3178.2	3406.0	3255.6	1232.0	1352.0	2241.0	1977.0
IL-10	122.6	168.0	210.8	233.4	231.0	380.0	547.0	689.0
IL-12p70	145.3	120.7	173.1	129.0	222.0	210.0	374.0	278.0
IL-13	19.7	20.6	20.9	28.0	23.0	24.0	25.0	22.0
IL-15	107.5	116.9	128.2	135.6	93.0	103.0	143.0	136.0
IL-17A	944.9	888.3	1031.5	956.4	522.0	613.0	1006.0	864.0
IL-1β*	N/A	N/A	N/A	N/A	N/A	N/A	N/A	N/A
IL-1ra	83.1	71.7	1397.8	2299.9	148.0	152.0	884.0	610.0
IL-2	41.7	35.4	50.7	36.3	33.0	41.0	76.0	57.0
IL-4	13.8	13.0	15.4	15.7	20.0	20.0	44.0	33.0
IL-5	3.4	2.3	17.2	21.2	4.0	1.0	22.0	25.0
IL-6	31891.7	31891.7	31891.7	31891.7	19431.0	30989.0	59881.0	40451.0
IL-7	1.2	13.7	10.2	4.1	194.0	196.0	220.0	266.0
IL-8	23507.1	23507.1	23507.1	23507.1	6640.0	9759.0	33485.0	19044.0
IL-9	271.4	241.4	275.2	216.6	227.0	240.0	302.0	226.0
IP-10	20965.0	18831.1	356382.9	70724.5	1902961.0	95416.0	8075385.0	4085009.0
MCP-1 (CCL2)	1133.7	1203.4	1534.3	1844.8	830.0	946.0	1179.0	1128.0
MIP-1α (CCL3)	4.6	4.1	27.4	40.9	6.0	6.0	88.0	62.0
MIP-1β (CCL4)	103.4	85.1	288.3	328.6	132.0	110.0	488.0	438.0
PDGF-BB	59.6	15.4	44.9	78.0	164.0	181.0	697.0	532.0
RANTES (CCL5)	7113.4	5244.9	2032.6	2616.4	3208.0	5574.0	6347.0	5641.0
TNF-α	509.8	457.7	955.2	1255.0	324.0	337.0	3523.0	2082.0
VEGF	3180.3	2528.9	4019.8	3150.1	10528.0	11200.0	31316.0	21683.0

* Cytokine IL-1β was excluded from analysis due to exogenous addition precluding detection in the inflamed conditions.

Table 4A10: Primary endometrial monoculture (mono) and co-cultures (co) (Donor 3) mean cytokine concentrations (pg/mL) in 48 hour conditioned media measured in the local hydrogel and in apical medium collected on day 15 after IL-1β (10 ng/mL) stimulation on day 13 for proliferative (E) and secretory (EP) hormone stimulated cultures. Hydrogel values are not corrected for four-fold dilution associated with gel dissolution.

Donor 3 IL-1β stim	Hydrogel				Apical Media			
Cytokine (pg/mL)	Mono E (n=3)	Mono EP (n=3)	Co E (n=3)	Co EP (n=3)	Mono E (n=3)	Mono EP (n=3)	Co E (n=3)	Co EP (n=3)
Eotaxin	4600.9	3505.9	2666.0	3067.0	9003.0	8519.0	5294.0	6797.6
FGF-b (FGF-2)	374.6	382.7	517.7	500.7	7.0	3.0	10.0	18.0
G-CSF (CSF-3)	22820.2	35705.1	30502.2	24702.0	14467.0	11106.0	4713.0	13637.9
GM-CSF (CSF-2)	98.2	141.7	291.8	341.7	0.0	0.0	313.0	498.0
IFN-γ	3112.0	3127.7	3431.6	3357.8	1355.0	1255.0	1381.0	1798.9
IL-10	49.1	78.4	378.2	345.9	164.0	126.0	744.0	937.2
IL-12p70	82.5	66.8	151.3	172.7	133.0	86.0	229.0	355.9
IL-13	15.5	11.7	49.1	35.9	32.0	26.0	29.0	41.0
IL-15	44.9	71.7	105.2	88.7	41.0	49.0	92.0	99.5
IL-17A	768.6	800.8	1093.8	1070.4	446.0	405.0	645.0	843.7
IL-1β*	N/A	N/A	N/A	N/A	N/A	N/A	N/A	N/A
IL-1ra	60.6	133.8	15261.6	18462.5	156.0	151.0	1583.0	2183.7
IL-2	27.2	32.6	44.9	42.8	37.0	33.0	43.0	55.8
IL-4	13.6	11.9	17.2	16.1	18.0	17.0	21.0	30.3
IL-5	2.6	2.3	8.6	7.4	9.0	8.0	21.0	24.5
IL-6	30110.7	31891.7	31891.7	27902.8	26939.0	21854.0	7605.0	42889.3
IL-7	0.0	0.0	57.9	69.2	154.0	160.0	313.0	331.7
IL-8	23507.1	23507.1	23507.1	18518.0	9191.0	8039.0	5007.0	12778.0
IL-9	199.2	198.7	274.2	280.4	237.0	226.0	280.0	359.6
IP-10	23498.2	21205.0	18049.0	30437.4	2708723.0	88593.0	50462.0	314892.7
MCP-1 (CCL2)	1080.7	1004.3	1572.6	1673.4	1409.0	1528.0	930.0	1195.0
MIP-1α (CCL3)	5.4	4.2	64.4	38.2	7.0	2.0	72.0	118.1
MIP-1β (CCL4)	76.8	63.4	617.1	490.2	83.0	56.0	798.0	1007.3
PDGF-BB	66.1	0.0	101.9	102.6	190.0	147.0	268.0	372.7
RANTES (CCL5)	3238.2	1468.9	1356.6	1375.1	3822.0	3364.0	1709.0	3725.4
TNF-α	522.3	485.7	632.0	592.0	348.0	296.0	414.0	566.1
VEGF	1049.0	1249.6	3608.4	3428.9	4134.0	2690.0	11424.0	22567.9

* Cytokine IL-1β was excluded from analysis due to exogenous addition precluding detection in the inflamed conditions.

Table 4A11: Spearman rank correlation analysis of day 15 cytokine concentrations measured in the apical media versus in the hydrogel for primary endometrial monocultures and co-cultures in 48 hour conditioned media. N=12 for monoculture and co-culture; including 3 donors, 2 hormone treatments (proliferative and secretory) and +/- IL-1β (10 ng/mL) stimulation on day 13. P-values are the Benjamini-Hochberg adjusted values for multiple hypothesis correction at q = 0.05.

Cytokine (pg/mL)	Monoculture		Co-culture	
	Spearman's Rho	BH-adj P-value	Spearman's Rho	BH-adj P-value
Eotaxin	0.97	**4E-06**	0.66	**0.0395**
FGF-b (FGF-2)	0.51	0.1069	-0.27	0.5073
G-CSF (CSF-3)	0.72	**0.0117**	0.77	**0.0137**
GM-CSF (CSF-2)	0.43	0.1648	0.92	**0.0002**
IFN-γ	0.69	**0.0163**	-0.52	0.1271
IL-10	0.89	**0.0004**	0.94	**9E-05**
IL-12p70	0.92	**0.0002**	0.58	0.0861
IL-13	0.71	**0.0124**	0.12	0.7043
IL-15	0.99	**1E-07**	0.58	0.0861
IL-17A	0.85	**0.0011**	0.23	0.5293
IL-1β	N/A	N/A	N/A	N/A
IL-1ra	0.75	**0.0078**	0.68	**0.0376**
IL-2	0.81	**0.0026**	0.74	**0.0191**
IL-4	0.77	**0.0063**	-0.16	0.6326
IL-5	0.48	0.1270	0.66	**0.0395**
IL-6	0.76	**0.0071**	0.29	0.5073
IL-7	0.67	**0.0209**	0.54	0.1133
IL-8	0.89	**0.0004**	0.26	0.5073
IL-9	0.85	**0.0011**	0.48	0.1773
IP-10	0.75	**0.0074**	0.82	**0.0062**
MCP-1 (CCL2)	0.82	**0.0023**	0.68	**0.0376**
MIP-1α (CCL3)	0.90	**0.0004**	0.80	**0.0076**
MIP-1β (CCL4)	0.93	**0.0001**	0.95	**6E-05**
PDGF-BB	0.43	0.1648	-0.17	0.6326
RANTES (CCL5)	0.87	**0.0008**	0.85	**0.0028**
TNF-α	0.79	**0.0045**	0.24	0.5293
VEGF	0.87	**0.0008**	0.70	**0.0341**

Table 4A12: Primary endometrial monoculture (mono) and co-culture (co) matrix metalloproteinase (MMP) and tissue inhibitor of matrix metalloproteinase (TIMP) concentrations (pg/mL) in 48 hr conditioned apical medium collected on day 15 +/- IL-1β (10 ng/mL) stimulation on day 13 for proliferative (E) and secretory (EP) hormone-stimulated cultures. Data are the mean of n=2-3 biological replicates per condition.

Sample	MMP1	MMP2	MMP3	MMP7	MMP8	MMP9	MMP10	MMP12	MMP13	TIMP1	TIMP2	TIMP4
D1 Mono EP	4166	1107332	14103	1390	0	0	1786	4	45	54892	226163	479
D2 Mono EP	10672	1618396	3940	1168	0	0	1166	4	45	136676	989631	589
D3 Mono EP	2498	1672230	714	1152	0	0	0	4	45	376677	541648	864
D1 Mono E	8937	979223	38294	1765	0	0	7469	5	44	53035	229370	509
D2 Mono E	12604	2093974	6243	1393	15	0	5192	4	44	103949	898791	626
D3 Mono E	2490	965076	7836	1043	0	0	0	4	45	437986	352191	811
D1 Mono EP IL1	55864	1431439	583442	4370	6	0	50109	215	44	117588	622304	590
D2 Mono EP IL1	34526	1970348	344318	2199	177	0	30361	167	46	171422	656297	659
D3 Mono EP IL1	10072	2400548	33347	1117	0	0	4654	46	53	390934	423617	772
D1 Mono E IL1	148735	1834417	2714944	5422	237	48	105980	398	45	84485	217571	505
D2 Mono E IL1	51590	1450500	458929	1359	206	0	67848	281	45	138030	531006	567
D3 Mono E IL1	10398	1299584	29002	986	0	0	6344	31	47	624961	231410	879
D1 Co EP	86141	1746836	2743842	7891	1028	0	75652	23	48	118246	1808772	620
D2 Co EP	79922	1618399	470135	853312	1534	98	124960	74	265	163178	973684	697
D3 Co EP	38998	2208437	175462	56268	1042	1148	91740	28	314	489939	2080445	1065
D1 Co E	220815	1065028	5169823	9729	2444	35	139156	547	49	97924	470312	541
D2 Co E	52320	1937523	323009	522667	3063	40	92855	38	141	162739	1589074	897
D3 Co E	57965	1891615	2398959	89465	1038	1135	176659	33	92	233717	1034134	814
D1 Co EP IL1	209880	1730934	40259387	23092	5415	195	145487	785	55	138997	1048890	523
D2 Co EP IL1	144373	1875612	2709173	1329282	2385	312	178837	695	2937	148938	666248	659
D3 Co EP IL1	54624	2737008	329217	71370	1101	1113	70629	89	110	395583	1971315	1090
D1 Co E IL1	168691	1721220	48497875	25561	9817	75	208315	1171	40	118289	628828	615
D2 Co E IL1	140394	1572978	2890529	1103028	3334	331	158441	761	3201	157059	581834	362
D3 Co E IL1	62319	2153182	376029	77946	957	1071	80613	114	146	137435	444180	600

Table 4A13: Clinical data for primary donor samples.

Donors 0188, 0190, 0191, 0160 and 0197 were acquired from Newton Wellesley Hospital in accordance with an IRB protocol approved by the Partners Human Research Committee and the Massachusetts Institute of Technology Committee on the Use of Humans as Experimental Subjects. Lifeline (Donor 3) was commercially available.

Donor	Age	Cycle Day/Phase	Diagnoses
0188	41	12	adenomyosis
0190	49	7	leiomyoma
0191	33	14	bilateral, paratubal cyst
0160 (Donor 1)	34	luteal	myoma
0197 (Donor 2)	35	luteal	myoma, adenomyosis
Lifeline (Donor 3)	33	unknown	unknown

Table 4A14. Variable Importance in Projection (VIP) scores for cytokines identified using partial least squares regression against MMP3 and prolactin. A VIP cutoff of 1 was used to identify those cytokines that contributed significantly to MMP3 and prolactin prediction and is denoted by *.

	MMP3 VIP		Prolactin VIP	
Cytokine	Hydrogel	Apical Media	Hydrogel	Apical Media
Eotaxin	*1.01	0.52	0.93	0.75
FGFb	0.81	0.49	0.76	0.98
GCSF	*1.60	*1.87	*1.84	*1.55
GMCSF	*1.10	*1.03	0.99	*1.00
IFNg	*1.91	*1.15	*1.76	*1.27
IL10	0.49	0.89	0.39	0.73
IL12p70	0.24	0.27	0.56	0.23
IL13	0.20	0.36	0.98	0.28
IL15	0.44	0.41	*1.20	*1.05
IL17A	0.94	*1.46	*1.01	*1.35
IL1b	0.91	0.74	*1.49	0.44
IL1ra	*1.62	*1.90	*1.23	*1.40
IL2	0.69	0.74	0.64	0.57
IL4	0.49	0.64	0.35	0.47
IL5	0.21	0.45	0.26	0.32
IL6	*1.92	0.88	*1.49	0.68
IL7	0.38	0.16	0.50	0.12
IL8	*2.06	0.70	*1.97	0.60
IL9	0.41	0.35	0.47	0.42
IP10	*1.77	*1.30	*1.51	*2.25
MCP1	0.84	0.28	0.64	0.26
MIP1a	0.42	0.64	0.45	0.66
MIP1b	0.76	*1.19	*1.01	0.85
PDGFBB	0.52	*1.39	*1.47	*1.14
RANTES	*1.24	0.65	0.92	0.66
TNFa	0.97	*1.04	0.77	0.83
VEGF	0.28	0.44	0.21	0.35

Table 4A15. Matrix effects on cytokine detection using sortase A and GGG. Luminex protein standard curves prepared in Apical DMEM/F12 media with and without 50 μM sortase A (SrtA) and 18 mM GGG reveal assay matrix effects where addition of SrtA and GGG result in fitted standard curve lower asymptotes that are 3-fold higher for cytokines IFN-gamma, IL-1b, IP10 and PDGFBB suggesting the lower limit of detection is increased for these analytes.

Lower Asymptote of Standard Curve Fit (pg/mL)		
	SrtA + GGG	Media
Eotaxin	26.3	37.9
FGFb	0.8	92.3
GCSF	56.9	83.9
GMCSF	380.1	421.4
IFNg	**113.5**	**24.2**
IL10	27.7	116.3
IL12p70	73.3	55.8
IL13	16.8	15.2
IL15	95.0	218.3
IL17A	110.5	69.4
IL1b	**89.8**	**23.3**
IL1ra	0.0	136.6
IL2	107.6	198.1
IL4	20.3	23.6
IL5	0.0	10.8
IL6	0.0	80.9
IL7	51.8	26.9
IL8	0.0	0.0
IL9	106.1	109.4
IP10	**97.9**	**19.5**
MCP1	66.2	161.4
MIP1a	0.0	10.3
MIP1b	76.6	78.0
PDGFBB	**135.4**	**42.5**
RANTES	0.0	55.1
TNFa	39.0	36.0
VEGF	65.2	50.1

Chapter 5

5 Conclusions

Drug development increasingly includes biologics with therapeutic modalities spanning gene products, viruses, recombinant proteins, antibodies and engineered cell therapies. As of 2015, 7 of the top 10 selling drugs fell into the category of biologics with the remaining three being traditional small molecule therapeutics.[85] Excitingly in 2017, the first genetically engineered cell therapy using a patients own immune cells, chimeric antigen receptor T-cell therapy, became FDA approved for the treatment of acute lymphoblastic leukemia.[86] However, with the development of more costly biological drugs and the trend toward more personalized therapeutics, there is a need to overcome limitations in the traditional drug development pipeline. Specifically, simple preclinical cell assays and animal studies for assessment of drug toxicity and efficacy continue to display shortcomings that result in costly failed clinical trials mainly due to a lack of efficacy and idiopathic toxicity that was not previously detected during preclinical drug development.[14,87]

More complex human *in vitro* culture systems offer promise to augment preclinical drug studies in a moderate throughput, cost-effective manner. The goal of these models is to achieve complex cellular and matrix environments that more closely mimic *in vivo* physiology and importantly support primary patient cellular heterogeneity that may underlie disease pathology and inform drug responses. While the utility of prospective drug development studies using complex 3D cell culture models remains to be established, these models offer promise for many stages of the drug development pipeline including 1) prediction of toxicity where animal models fail, 2) support for personalized therapeutic development including a better understanding of patient heterogeneity and stratification prior to clinical trials initiation, 3) identification of novel disease biomarkers or therapeutic targets, and 4) earlier prediction and evaluation of drug efficacy prior to clinical trial initiation.

Importantly, the main utility and validation of these models will likely begin with retrospective studies involving failed drugs where simple cell assays or animal models failed to predict a lack of efficacy or toxicity observed in the clinic. These models offer

the opportunity to investigate the molecular underpinnings of these costly failures to inform future drug discovery efforts. Additionally, with new tools for genetic manipulation, such as CRISPR/Cas9, more cost effective whole genome sequencing efforts, and big data science initiatives, genomic variations can be used to inform drug discovery. For example, complex *in vitro* culture models allow genetic manipulation, which may inform development of preventative therapeutics prior to clinical disease presentation, explain how genetic donor predispositions influence disease presentation and drug toxicity, and may enable better prescreening for therapeutics that will be most efficacious.

Aside from the preclinical utility of more complex *in vitro* culture models, advances in cultures containing primary donor biopsies may aid in real-time appropriate selection of clinical treatments. For example, in cancer therapy where drug resistance is an enduring challenge, these models offer the opportunity to perform side-by-side treatment evaluation using *in vitro* screening of primary biopsy cells or tissues while the patient undergoes clinical therapy. This paradigm could augment earlier identification of clinical resistance or even allow for screening of appropriate therapies prior to treatment initiation.

5.1 Summary

In this thesis, we develop design principles to enable construction of primary 3D mucosal barrier cell cultures along with a data-driven modeling framework to parse heterotypic epithelial-stromal intercellular protein signaling. In particular, we show how a 'one-size-fits-all' modular, synthetic PEG hydrogel matrix can be engineered to culture both epithelial and stromal cells allowing characteristic epithelial polarization and stromal cell differentiation underlying endometrial physiology. Furthermore, both cell types locally remodeled this matrix as evidenced by proteolytic stromal cell migration and local capture of cell-secreted matrix proteins. This local remodeling may contribute to distinct epithelial and stromal signaling microenvironments as revealed by heterogeneities in compartmental cytokine analysis (apical media versus inside the hydrogel). The modular nature of the synthetic matrix, its ease of fabrication, and the delineation of design

principles, together provides a foundation for its adaptation for widespread application in mucosal barrier tissue engineering.

We have shown that primary donor cells offer greater signaling heterogeneity and more complex immune cytokine interactions compared to common cell line cultures.[1] However, studies have been limited to use of fresh donor tissues where the lack of methods to culture expand and cryopreserve primary endometrial epithelial cells has hampered *in vitro* studies of donor heterogeneity that may underlie molecular differences in complex endometrial disorders. We employ a previously established strategy for expansion of other epithelial cells, namely conditional reprogramming of epithelial cells by feeder fibroblasts and ROCK inhibition, that has not been previously explored for endometrial epithelium.[81] We show conditional reprogramming is a generalizable method that enables expansion of primary donors (8 out of 9 donors exhibited an average of 12 population doublings) from different endometrial states and clinical pathologies while retaining epithelial cell barrier and secretory function that is not fully observed in the Ishikawa cell line.

Finally, we evaluated donor heterogeneity in inflammatory cytokine signaling via construction of *in vitro* primary endometrial epithelial-stromal cultures using the synthetic, modular matrix established in Ch. 2 and expanded primary cells as in Ch. 3. We demonstrate using data-driven models including Principal Component Analysis that primary epithelial cells contribute to a complex cytokine milieu, and that cytokines produced by epithelial cells (IL-1) recapitulate facets of cytokine signaling in stromal monocultures alone. This suggests that epithelial cells directly contribute to cytokine secretion, but also participate in intercellular communication that can further stimulate stromal cells to secrete more abundant and heterogeneous cytokine signals.

Additionally, sortase A enabled hydrogel dissolution and measurement of cytokine localization in the apical media versus in the local hydrogel.[20] We observed distribution was more heterogeneous (lower correlation in apical media versus local hydrogel) with an epithelial barrier compared to encapsulated stromal monocultures warranting consideration of measurement location in complex culture models constructed to capture directional intercellular signaling. Altogether, we show how careful consideration of the design parameters governing the cell culture matrix environment,

selection of cell types and source, and dynamic hormonal or inflammatory perturbations reveal known endometrial biology *in vitro* and anticipate such models will hold promise for uncovering novel molecular targets for treating endometrial pathologies.

5.2 Future Work

While the focus of this thesis was establishing a framework for constructing and parsing *in vitro* models of epithelial-stromal intercellular communication in response to hormonal and inflammatory cues, future work should be directed at extension of the above-established models to include additional facets that contribute to dynamic endometrial physiology. For example, endothelial and immune cells also contribute to the dynamic hormonal remodeling observed throughout the menstrual cycle. Endothelial cells that make up uterine blood vessels are the sights of focal edema and decidualization initiation within the endometrium. A recent model of endometrial stromal-endothelial communication has been developed to investigate hormone signaling throughout the menstrual cycle[88] where future investigation into the intercellular crosstalk in endometrial models with endothelial cell networks could be informative for studies of abnormal uterine bleeding, endometriosis, and infertility.

Additionally, immune cells play a prominent role in the endometrium including during infection, menstruation, and tolerance at the maternal-fetal interface. Interestingly, we observed cytokine secretion that varied in response to inflammation and hormones suggesting that our model may capture dynamic signaling changes associated with immune cell recruitment, activation, and differentiation. Thus, extension to include immune cells will be important to fully understand endometrial repair and function as numerous immune cells are recruited premenstrually including neutrophils (6-15%), macrophages, uterine natural killer cells (30-40%), T-cells, and eosinophils (3-5%) where percentages are representative of the decidual cell proportion of each cell type.[12,21,89] Interestingly, macrophages have been shown to play an important role in endometrial repair following menstruation.[90] Further, macrophages in the peritoneal fluid of patients with endometriosis show alternative activation, and our lab has previously identified a macrophage cytokine signature indicative of more severe disease.[67,91] Thus, future

investigation into the macrophage polarization and signaling within the endometrium could offer insight into endometrial tissue clearance and lesion formation.

The advent of new platform technologies, that enable control over media circulation, are poised to advance studies of dynamic biology for organs-on-chips applications and drug discovery by more closely mimicking facets of *in vivo* biology for study of *in vitro* microtissues.[92,93] For example, the dynamic monthly profiles of sex steroid hormones have been extensively studied,[94] but scientist largely still rely on addition of bolus hormones during media changes every 2-3 days. Newer platform technologies with mixing chambers and drug holding reservoirs offer facile opportunity to closely mimic *in vivo* sex steroid profiles. Further, preliminary studies in our own lab suggest the microfluidic media circulation capabilities may allow immune cells, such as monocytes, to be circulated and recruited into the microtissues in a way that more physiologically mimics peripheral blood circulation. This exciting capability could also allow study of mesenchymal stem cell recruitment, which has been posited as a potential source of progenitor cells that repopulate the endometrium following menstruation.[95–97]

Additionally, development of primary cultures will depend on further exploration into new culture methods and sources of endometrial epithelial cells. Specifically, this year (2017) new culture methods have show the ability to generate endometrial epithelial organoids from both epithelial and mesenchymal cells.[96,98,99] Intriguingly, organoids derived from endometrial epithelial cells showed about the same growth potential that we observed using conditional reprogramming (~10 culture passages), although it should be noted the authors did not specifically comment that this was the expansion limit.[98,99] Some evidence suggests epithelial cells may be derived from mesenchymal progenitors and that reepithelialization following menstruation may occur from the stromal compartment.[96,97,100] It remains to be seen whether the mesenchymal compartment contains a long-lived progenitor that gives rise to the more differentiated epithelial cells, and whether this may explain why previous attempts at long-term endometrial epithelial expansion, in contrast to organoids generated for other epithelial tissues, have been unproductive when using epithelial cells as starting material.

Finally, these culture models could be extended to compare inflammatory cytokine production and hormone responsiveness in patients with varying clinical

conditions. For example, several *in vitro* studies have shown that donors with endometriosis and adenomyosis exhibit progesterone resistance, while numerous patients fail to respond to clinical hormone therapy. Of interest, would be to construct endometrial co-cultures using cells from the same donor and different donors from healthy and diseased states. The ability to mix and match primary cells may offer insight into whether the stromal cells, epithelial cells, or both contribute to aberrant hormone signaling in endometriosis/adenomyosis patients and potentially offer novel insights for therapeutic intervention.

The construction of epithelial-stromal cultures that can be later recovered and dissolved for analysis may also provide mechanistic insight into the early signaling events and immune cell recruitment that modulate endometrial cell attachment and invasion into the peritoneum. In pilot experiments in collaboration with Kevin Osteen's lab at Vanderbilt University, we have initial data suggesting our endometrial models hold promise for use in an *in vivo* murine model of endometriosis where endothelial vascular networks and immune cells were recruited into hydrogels containing primary endometrial cells. Thus, we provide a platform for new culture technologies that we anticipate will be useful to understand patient heterogeneity *in vitro* (with future extension to *in vivo* models) to drive personalized medicine approaches and to better understand the complex etiologies and molecular changes that underlie endometrial disease pathophysiology to inform therapeutic intervention.

5.3 References

1. Cook CD, Hill AS, Guo M, et al. Local remodeling of synthetic extracellular matrix microenvironments by co-cultured endometrial epithelial and stromal cells enables long-term dynamic physiological function. *Integr Biol (Camb).* 2017;9(4):271-289. doi:10.1039/c6ib00245e.
2. Liu H, Dowdle JA, Khurshid S, et al. Discovery of Stromal Regulatory Networks that Suppress Ras-Sensitized Epithelial Cell Proliferation. *Dev Cell.* 2017;41(4):392-407.e6. doi:10.1016/j.devcel.2017.04.024.
3. Mohammed J, Beura LK, Bobr A, et al. Stromal cells control the epithelial residence of DCs and memory T cells by regulated activation of TGF-β. *Nat Immunol.* 2016;17(4):414-421. doi:10.1038/ni.3396.
4. Broekman W, Amatngalim GD, de Mooij-Eijk Y, et al. TNF-α and IL-1β-activated human mesenchymal stromal cells increase airway epithelial wound healing in vitro via activation of the epidermal growth factor receptor. *Respir Res.* 2016;17(1):3. doi:10.1186/s12931-015-0316-1.
5. Tape CJ, Ling S, Dimitriadi M, et al. Oncogenic KRAS Regulates Tumor Cell Signaling via Stromal Reciprocation. *Cell.* 2016;165(4):910-920. doi:10.1016/j.cell.2016.03.029.
6. Aghajanova L, Hamilton A, Kwintkiewicz J, Vo KC, Giudice LC. Steroidogenic Enzyme and Key Decidualization Marker Dysregulation in Endometrial Stromal Cells from Women with Versus Without Endometriosis1. *Biol Reprod.* 2009;80(1):105-114. doi:10.1095/biolreprod.108.070300.
7. Igarashi TM, Bruner-Tran KL, Yeaman GR, et al. Reduced expression of progesterone receptor-B in the endometrium of women with endometriosis and in cocultures of endometrial cells exposed to 2,3,7,8-tetrachlorodibenzo-p-dioxin. *Fertil Steril.* 2005;84(1):67-74. doi:10.1016/j.fertnstert.2005.01.113.
8. Stocks MM, Crispens MA, Ding T, Mokshagundam S, Bruner-Tran KL, Osteen KG. Therapeutically Targeting the Inflammasome Product in a Chimeric Model of Endometriosis-Related Surgical Adhesions. *Reprod Sci.* 2017;24(8):1121-1128. doi:10.1177/1933719117698584.
9. Dyson MT, Roqueiro D, Monsivais D, et al. Genome-Wide DNA Methylation Analysis Predicts an Epigenetic Switch for GATA Factor Expression in Endometriosis. Barsh GS, ed. *PLoS Genet.* 2014;10(3):e1004158. doi:10.1371/journal.pgen.1004158.
10. Jichan Nie, Xishi Liu, Guo S-W. Promoter Hypermethylation of Progesterone Receptor Isoform B (PR-B) in Adenomyosis and Its Rectification by a Histone Deacetylase Inhibitor and a Demethylation Agent. *Reprod Sci.* 2010;17(11):995-1005. doi:10.1177/1933719110377118.
11. Keller NR, Sierra-Rivera E, Eisenberg E, Osteen KG. Progesterone Exposure Prevents Matrix Metalloproteinase-3 (MMP-3) Stimulation by Interleukin-1α in Human Endometrial Stromal Cells 1. *J Clin Endocrinol Metab.* 2000;85(4):1611-1619. doi:10.1210/jcem.85.4.6502.
12. Maybin JA, Critchley HOD. Menstrual physiology: implications for endometrial pathology and beyond. *Hum Reprod Update.* 2015;21(6):748-761. doi:10.1093/humupd/dmv038.
13. Maybin JA, Critchley HOD, Jabbour HN. Inflammatory pathways in endometrial

disorders. *Mol Cell Endocrinol.* 2011;335(1):42-51. doi:10.1016/j.mce.2010.08.006.
14. Seok J, Warren HS, Cuenca AG, et al. Genomic responses in mouse models poorly mimic human inflammatory diseases. *Proc Natl Acad Sci.* 2013;110(9):3507-3512. doi:10.1073/pnas.1222878110.
15. Osteen KG, Rodgers WH, Gaire M, Hargrove JT, Gorstein F, Matrisian LM. Stromal-epithelial interaction mediates steroidal regulation of metalloproteinase expression in human endometrium. *Proc Natl Acad Sci U S A.* 1994;91(21):10129-10133. doi:10.1073/pnas.91.21.10129.
16. Bruner KL, Rodgers WH, Gold LI, et al. Transforming growth factor beta mediates the progesterone suppression of an epithelial metalloproteinase by adjacent stroma in the human endometrium. *Proc Natl Acad Sci U S A.* 1995;92(16):7362-7366. http://www.pnas.org/content/92/16/7362.short. Accessed September 16, 2013.
17. Singer CF, Marbaix E, Kokorine I, et al. Paracrine stimulation of interstitial collagenase (MMP-1) in the human endometrium by interleukin 1α and its dual block by ovarian steroids. *Proc Natl Acad Sci U S A.* 1997;94(19):10341-10345. doi:10.1073/pnas.94.19.10341.
18. Wetendorf M, DeMayo FJ. The progesterone receptor regulates implantation, decidualization, and glandular development via a complex paracrine signaling network. *Mol Cell Endocrinol.* 2012;357(1-2):108-118. doi:10.1016/j.mce.2011.10.028.
19. Chen JC, Erikson DW, Piltonen TT, et al. Coculturing human endometrial epithelial cells and stromal fibroblasts alters cell-specific gene expression and cytokine production. *Fertil Steril.* 2013;100(4):1132-1143. doi:10.1016/j.fertnstert.2013.06.007.
20. Valdez J, Cook CD, Ahrens CC, et al. On-demand dissolution of modular, synthetic extracellular matrix reveals local epithelial-stromal communication networks. *Biomaterials.* 2017;130:90-103. doi:10.1016/j.biomaterials.2017.03.030.
21. Evans J, Salamonsen LA. Inflammation, leukocytes and menstruation. *Rev Endocr Metab Disord.* 2012;13(4):277-288. doi:10.1007/s11154-012-9223-7.
22. Krikun G, Mor G, Alvero A, et al. A novel immortalized human endometrial stromal cell line with normal progestational response. *Endocrinology.* 2004;145(5):2291-2296. doi:10.1210/en.2003-1606.
23. Nishida M, Kasahara K, Kaneko M, Iwasaki H, Hayashi K. [Establishment of a new human endometrial adenocarcinoma cell line, Ishikawa cells, containing estrogen and progesterone receptors]. *Nihon Sanka Fujinka Gakkai Zasshi.* 1985;37(7):1103-1111. http://www.ncbi.nlm.nih.gov/pubmed/4031568. Accessed August 13, 2013.
24. Leemasawatdigul K, Gappa-Fahlenkamp H. Development of a mathematical model to describe the transport of monocyte chemoattractant protein-1 through a three-dimensional collagen matrix. *Cardiovasc Pathol.* 2012;21(3):219-228. doi:10.1016/j.carpath.2011.09.002.
25. Meng C-X, Andersson KL, Bentin-Ley U, Gemzell-Danielsson K, Lalitkumar PGL. Effect of levonorgestrel and mifepristone on endometrial receptivity markers in a three-dimensional human endometrial cell culture model. *Fertil Steril.*

2009;91(1):256-264. doi:10.1016/j.fertnstert.2007.11.007.
26. Wang H, Pilla F, Anderson S, et al. A novel model of human implantation: 3D endometrium-like culture system to study attachment of human trophoblast (Jar) cell spheroids. *Mol Hum Reprod*. 2012;18:33-43. doi:10.1093/molehr/gar064.
27. Schutte SC, James CO, Sidell N, Taylor RN. Tissue-engineered endometrial model for the study of cell-cell interactions. *Reprod Sci*. 2015;22(3):308-315. doi:10.1177/1933719114542008.
28. Pretto CM, Gaide Chevronnay HP, Cornet PB, et al. Production of Interleukin-1α by Human Endometrial Stromal Cells Is Triggered during Menses and Dysfunctional Bleeding and Is Induced in Culture by Epithelial Interleukin-1α Released upon Ovarian Steroids Withdrawal. *J Clin Endocrinol Metab*. 2008;93(10):4126-4134. doi:10.1210/jc.2007-2636.
29. Bodnar RJ, Wells A. Differential regulation of pericyte function by the CXC receptor 3. *Wound Repair Regen*. 2015;23(6):785-796. doi:10.1111/wrr.12346.
30. Pence JC, Clancy KBH, Harley BAC. The induction of pro-angiogenic processes within a collagen scaffold via exogenous estradiol and endometrial epithelial cells. *Biotechnol Bioeng*. 2015;112(10):2185-2194. doi:10.1002/bit.25622.
31. Vinketova K, Mourdjeva M, Oreshkova T. Human Decidual Stromal Cells as a Component of the Implantation Niche and a Modulator of Maternal Immunity. *J Pregnancy*. 2016;2016:1-17. doi:10.1155/2016/8689436.
32. Okada S, Okada H, Sanezumi M, Nakajima T, Yasuda K, Kanzaki H. Expression of interleukin-15 in human endometrium and decidua. *Mol Hum Reprod*. 2000;6(1):75-80. doi:10.1093/molehr/6.1.75.
33. Pineda-Torres M, Flores-Espinosa P, Espejel-Nunez A, et al. Evidence of an immunosuppressive effect of progesterone upon in vitro secretion of proinflammatory and prodegradative factors in a model of choriodecidual infection. *BJOG An Int J Obstet Gynaecol*. 2015;122(13):1798-1807. doi:10.1111/1471-0528.13113.
34. Banerjee P, Ghosh S, Dutta M, et al. Identification of key contributory factors responsible for vascular dysfunction in idiopathic recurrent spontaneous miscarriage. *PLoS One*. 2013;8(11):1-9. doi:10.1371/journal.pone.0080940.
35. Singh B, Coffey RJ. Trafficking of epidermal growth factor receptor ligands in polarized epithelial cells. *Annu Rev Physiol*. 2014;76:275-300. doi:10.1146/annurev-physiol-021113-170406.
36. Bruner-Tran KL, Zhang Z, Eisenberg E, Winneker RC, Osteen KG. Down-Regulation of Endometrial Matrix Metalloproteinase-3 and -7 Expression in Vitro and Therapeutic Regression of Experimental Endometriosis in Vivo by a Novel Nonsteroidal Progesterone Receptor Agonist, Tanaproget. *J Clin Endocrinol Metab*. 2006;91(4):1554-1560. doi:10.1210/jc.2005-2024.
37. Bruner-Tran KL, Eisenberg E, Yeaman GR, Anderson TA, McBean J, Osteen KG. Steroid and Cytokine Regulation of Matrix Metalloproteinase Expression in Endometriosis and the Establishment of Experimental Endometriosis in Nude Mice. *J Clin Endocrinol Metab*. 2002;87(10):4782-4791. doi:10.1210/jc.2002-020418.
38. Mortier E, Quéméner A, Vusio P, et al. Soluble Interleukin-15 Receptor α (IL-15Rα)-sushi as a Selective and Potent Agonist of IL-15 Action through IL-15Rβ/γ.

J Biol Chem. 2006;281(3):1612-1619. doi:10.1074/jbc.M508624200.
39. Vlodavsky I, Miao HQ, Medalion B, Danagher P, Ron D. Involvement of heparan sulfate and related molecules in sequestration and growth promoting activity of fibroblast growth factor. *Cancer Metastasis Rev*. 1996;15(2):177-186. http://www.ncbi.nlm.nih.gov/pubmed/8842489.
40. Janes KA, Yaffe MB. Data-driven modelling of signal-transduction networks. *Nat Rev Mol Cell Biol*. 2006;7(11):820-828. doi:10.1038/nrm2041.
41. BRAVERMAN MB, BAGNI A, ZIEGLER D DE, DEN T, GURPIDE E. Isolation of Prolactin-Producing Cells from First and Second Trimester Decidua*. *J Clin Endocrinol Metab*. 1984;58(3):521-525. doi:10.1210/jcem-58-3-521.
42. Pawar S, Laws MJ, Bagchi IC, Bagchi MK. Uterine Epithelial Estrogen Receptor-α Controls Decidualization via a Paracrine Mechanism. *Mol Endocrinol*. 2015;29(9):1362-1374. doi:10.1210/me.2015-1142.
43. Shuya LL, Menkhorst EM, Yap J, Li P, Lane N, Dimitriadis E. Leukemia Inhibitory Factor Enhances Endometrial Stromal Cell Decidualization in Humans and Mice. Wutz A, ed. *PLoS One*. 2011;6(9):e25288. doi:10.1371/journal.pone.0025288.
44. Filant J, Spencer TE. Uterine glands: biological roles in conceptus implantation, uterine receptivity and decidualization. *Int J Dev Biol*. 2014;58(2-3-4):107-116. doi:10.1387/ijdb.130344ts.
45. Bersinger NA, Günthert AR, McKinnon B, Johann S, Mueller MD. Dose–response effect of interleukin (IL)-1β, tumour necrosis factor (TNF)-α, and interferon-γ on the in vitro production of epithelial neutrophil activating peptide-78 (ENA-78), IL-8, and IL-6 by human endometrial stromal cells. *Arch Gynecol Obstet*. 2011;283(6):1291-1296. doi:10.1007/s00404-010-1520-3.
46. Friebe-Hoffmann U, Baston DM, Hoffmann TK, Chiao JP, Rauk PN. The influence of interleukin-1β on oxytocin signalling in primary cells of human decidua. *Regul Pept*. 2007;142(3):78-85. doi:10.1016/j.regpep.2007.01.012.
47. Rossi M, Sharkey AM, Vigano P, et al. Identification of genes regulated by interleukin-1 in human endometrial stromal cells. *Reproduction*. 2005;130(5):721-729. doi:10.1530/rep.1.00688.
48. Braundmeier AG, Nowak RA. Cytokines Regulate Matrix Metalloproteinases in Human Uterine Endometrial Fibroblast Cells Through a Mechanism That Does Not Involve Increases in Extracellular Matrix Metalloproteinase Inducer. *Am J Reprod Immunol*. 2006;56(3):201-214. doi:10.1111/j.1600-0897.2006.00418.x.
49. Eidt M V., Nunes FB, Pedrazza L, et al. Biochemical and inflammatory aspects in patients with severe sepsis and septic shock: The predictive role of IL-18 in mortality. *Clin Chim Acta*. 2016;453:100-106. doi:10.1016/j.cca.2015.12.009.
50. Zhang X, Ibrahim E, de Rivero Vaccari JP, et al. Involvement of the inflammasome in abnormal semen quality of men with spinal cord injury. *Fertil Steril*. 2013;99(1):118-124.e2. doi:10.1016/j.fertnstert.2012.09.004.
51. Liu Z, Shi X, Wang L, Yang Y, Fu Q, Tao M. Associations between male reproductive characteristics and the outcome of assisted reproductive technology (ART). *Biosci Rep*. 2017;37(3):BSR20170095. doi:10.1042/BSR20170095.
52. Wold S, Sjöström M, Eriksson L. PLS-regression: a basic tool of chemometrics. *Chemom Intell Lab Syst*. 2001;58(2):109-130. doi:10.1016/S0169-7439(01)00155-

1.
53. Chong I-G, Jun C-H. Performance of some variable selection methods when multicollinearity is present. *Chemom Intell Lab Syst*. 2005;78(1-2):103-112. doi:10.1016/j.chemolab.2004.12.011.
54. Granot I, Gnainsky Y, Dekel N. Endometrial inflammation and effect on implantation improvement and pregnancy outcome. *Reproduction*. 2012;144(6):661-668. doi:10.1530/REP-12-0217.
55. Gnainsky Y, Granot I, Aldo PB, et al. Local injury of the endometrium induces an inflammatory response that promotes successful implantation. *Fertil Steril*. 2010;94(6):2030-2036. doi:10.1016/j.fertnstert.2010.02.022.
56. Guzeloglu-Kayisli O, Kayisli U, Taylor H. The Role of Growth Factors and Cytokines during Implantation: Endocrine and Paracrine Interactions. *Semin Reprod Med*. 2009;27(1):062-079. doi:10.1055/s-0028-1108011.
57. Chaouat G, Dubanchet S, Ledée N. Cytokines: Important for implantation? *J Assist Reprod Genet*. 2007;24(11):491-505. doi:10.1007/s10815-007-9142-9.
58. Cardillo G. Five parameters logistic regression - There and back again. http://www.mathworks.com/matlabcentral/fileexchange/38043. Published 2012. Accessed January 1, 2016.
59. Sequeira K, Espejel-Núñez A, Vega-Hernández E, Molina-Hernández A, Grether-González P. An increase in IL-1β concentrations in embryo culture-conditioned media obtained by in vitro fertilization on day 3 is related to successful implantation. *J Assist Reprod Genet*. 2015;32(11):1623-1627. doi:10.1007/s10815-015-0573-4.
60. Geisert R, Fazleabas A, Lucy M, Mathew D. Interaction of the conceptus and endometrium to establish pregnancy in mammals: role of interleukin 1β. *Cell Tissue Res*. 2012;349(3):825-838. doi:10.1007/s00441-012-1356-1.
61. Kauma S, Matt D, Strom S, Eierman D, Turner T. Interleukin-1β, human leukocyte antigen HLA-DRα, and transforming growth factor-β expression in endom trium, placenta, and placental membranes. *Am J Obstet Gynecol*. 1990;163(5):1430-1437. doi:10.1016/0002-9378(90)90601-3.
62. Krieg SA, Fan X, Hong Y, et al. Global alteration in gene expression profiles of deciduas from women with idiopathic recurrent pregnancy loss. *MHR Basic Sci Reprod Med*. 2012;18(9):442-450. doi:10.1093/molehr/gas017.
63. Simón C, Valbuena D, Krüssel J, et al. Interleukin-1 receptor antagonist prevents embryonic implantation by a direct effect on the endometrial epithelium. *Fertil Steril*. 1998;70(5):896-906. http://www.ncbi.nlm.nih.gov/pubmed/9806573.
64. Simón C, Gimeno MJ, Mercader A, et al. Embryonic Regulation of Integrins β 3 ,α 4 , and α 1 in Human Endometrial Epithelial Cells in Vitro 1. *J Clin Endocrinol Metab*. 1997;82(8):2607-2616. doi:10.1210/jcem.82.8.4153.
65. Zheng H, Fletcher D, Kozak W, et al. Resistance to fever induction and impaired acute-phase response in interleukin-1 beta-deficient mice. *Immunity*. 1995;3(1):9-19. http://www.ncbi.nlm.nih.gov/pubmed/7621081.
66. Keenan JA, Chen TT, Chadwell NL, Torry DS, Caudle MR. IL-1 beta, TNF-alpha, and IL-2 in peritoneal fluid and macrophage-conditioned media of women with endometriosis. *Am J Reprod Immunol*. 1995;34(6):381-385. http://www.ncbi.nlm.nih.gov/pubmed/8607944.

67. Beste MT, Pfaffle-Doyle N, Prentice EA, et al. Molecular Network Analysis of Endometriosis Reveals a Role for c-Jun-Regulated Macrophage Activation. *Sci Transl Med*. 2014;6(222):222ra16-222ra16. doi:10.1126/scitranslmed.3007988.
68. Han SJ, Jung SY, Wu S-P, et al. Estrogen Receptor β Modulates Apoptosis Complexes and the Inflammasome to Drive the Pathogenesis of Endometriosis. *Cell*. 2015;163(4):960-974. doi:10.1016/j.cell.2015.10.034.
69. Delvoux B, Groothuis P, D'Hooghe T, Kyama C, Dunselman G, Romano A. Increased Production of 17β-Estradiol in Endometriosis Lesions Is the Result of Impaired Metabolism. *J Clin Endocrinol Metab*. 2009;94(3):876-883. doi:10.1210/jc.2008-2218.
70. Bulun S, Monsavais D, Pavone M, et al. Role of Estrogen Receptor-β in Endometriosis. *Semin Reprod Med*. 2012;30(1):39-45. doi:10.1055/s-0031-1299596.
71. Stewart CL, Kaspar P, Brunet LJ, et al. Blastocyst implantation depends on maternal expression of leukaemia inhibitory factor. *Nature*. 1992;359(6390):76-79. doi:10.1038/359076a0.
72. Cullinan EB, Abbondanzo SJ, Anderson PS, Pollard JW, Lessey BA, Stewart CL. Leukemia inhibitory factor (LIF) and LIF receptor expression in human endometrium suggests a potential autocrine/paracrine function in regulating embryo implantation. *Proc Natl Acad Sci U S A*. 1996;93(7):3115-3120. http://www.ncbi.nlm.nih.gov/pubmed/8610178.
73. Chen JR, Cheng J-G, Shatzer T, Sewell L, Hernandez L, Stewart CL. Leukemia Inhibitory Factor Can Substitute for Nidatory Estrogen and Is Essential to Inducing a Receptive Uterus for Implantation But Is Not Essential for Subsequent Embryogenesis 1. *Endocrinology*. 2000;141(12):4365-4372. doi:10.1210/endo.141.12.7855.
74. Spratte J, Bornkessel F, Schütz F, Zygmunt M, Fluhr H. The presence of heparins during decidualization modulates the response of human endometrial stromal cells to IL-1β in vitro. *J Assist Reprod Genet*. 2016;33(7):949-957. doi:10.1007/s10815-016-0703-7.
75. Patterson J, Hubbell JA. Enhanced proteolytic degradation of molecularly engineered PEG hydrogels in response to MMP-1 and MMP-2. *Biomaterials*. 2010;31(30):7836-7845. doi:10.1016/j.biomaterials.2010.06.061.
76. Kuhlman W, Taniguchi I, Griffith LG, Mayes AM. Interplay between PEO tether length and ligand spacing governs cell spreading on RGD-modified PMMA-g-PEO comb copolymers. *Biomacromolecules*. 2007;8(10):3206-3213. doi:10.1021/bm070237o.
77. Cambria E, Renggli K, Ahrens CC, et al. Covalent Modification of Synthetic Hydrogels with Bioactive Proteins via Sortase-Mediated Ligation. *Biomacromolecules*. 2015;16(8):2316-2326. doi:10.1021/acs.biomac.5b00549.
78. Gao X, Groves MJ. Fibronectin-binding peptides. I. Isolation and characterization of two unique fibronectin-binding peptides from gelatin. *Eur J Pharm Biopharm*. 1998;45(3):275-284. http://www.ncbi.nlm.nih.gov/pubmed/9653632. Accessed September 14, 2013.
79. Johnson G, Moore SW. Identification of a structural site on acetylcholinesterase that promotes neurite outgrowth and binds laminin-1 and collagen IV. *Biochem*

Biophys Res Commun. 2004;319(2):448-455. doi:10.1016/j.bbrc.2004.05.018.
80. Osteen KG, Hill GA, Hargrove JT, Gorstein F. Development of a method to isolate and culture highly purified populations of stromal and epithelial cells from human endometrial biopsy specimens. *Fertil Steril*. 1989;52(6):965-972. http://www.ncbi.nlm.nih.gov/pubmed/2687030. Accessed September 17, 2013.
81. Liu X, Krawczyk E, Suprynowicz FA, et al. Conditional reprogramming and long-term expansion of normal and tumor cells from human biospecimens. *Nat Protoc*. 2017;12(2):439-451. doi:10.1038/nprot.2016.174.
82. Brosens JJ, Hayashi N, White JO. Progesterone receptor regulates decidual prolactin expression in differentiating human endometrial stromal cells. *Endocrinology*. 1999;140(10):4809-4820. doi:10.1210/endo.140.10.7070.
83. Gellersen B, Brosens J. Cyclic AMP and progesterone receptor cross-talk in human endometrium: a decidualizing affair. *J Endocrinol*. 2003;178(3):357-372. http://www.ncbi.nlm.nih.gov/pubmed/12967329. Accessed September 6, 2013.
84. de Jong S. SIMPLS: An alternative approach to partial least squares regression. *Chemom Intell Lab Syst*. 1993;18(3):251-263. doi:10.1016/0169-7439(93)85002-X.
85. PharmaCompass. Top drugs by sales revenue in 2015: Who sold the biggest blockbuster drugs? https://www.pharmacompass.com/radio-compass-blog/top-drugs-by-sales-revenue-in-2015-who-sold-the-biggest-blockbuster-drugs. Published 2017. Accessed October 8, 2017.
86. Kaiser J. Modified T cells that attack leukemia become first gene therapy approved in the United States. *Science (80-)*. August 2017. doi:10.1126/science.aap8293.
87. Shanks N, Greek R, Greek J. Are animal models predictive for humans? *Philos Ethics, Humanit Med*. 2009;4(1):2. doi:10.1186/1747-5341-4-2.
88. Gnecco JS, Pensabene V, Li DJ, et al. Compartmentalized Culture of Perivascular Stroma and Endothelial Cells in a Microfluidic Model of the Human Endometrium. *Ann Biomed Eng*. January 2017. doi:10.1007/s10439-017-1797-5.
89. Lee SK, Kim CJ, Kim D-J, Kang J. Immune Cells in the Female Reproductive Tract. *Immune Netw*. 2015;15(1):16. doi:10.4110/in.2015.15.1.16.
90. Cousins FL, Kirkwood PM, Saunders PTK, Gibson DA. Evidence for a dynamic role for mononuclear phagocytes during endometrial repair and remodelling. *Sci Rep*. 2016;6(1):36748. doi:10.1038/srep36748.
91. Bacci M, Capobianco A, Monno A, et al. Macrophages Are Alternatively Activated in Patients with Endometriosis and Required for Growth and Vascularization of Lesions in a Mouse Model of Disease. *Am J Pathol*. 2009;175(2):547-556. doi:10.2353/ajpath.2009.081011.
92. Tsamandouras N, Chen WLK, Edington CD, Stokes CL, Griffith LG, Cirit M. Integrated Gut and Liver Microphysiological Systems for Quantitative In Vitro Pharmacokinetic Studies. *AAPS J*. 2017;19(5):1499-1512. doi:10.1208/s12248-017-0122-4.
93. Chen WLK, Edington C, Suter E, et al. Integrated gut/liver microphysiological systems elucidates inflammatory inter-tissue crosstalk. *Biotechnol Bioeng*. 2017;114(11):2648-2659. doi:10.1002/bit.26370.
94. Stricker R, Eberhart R, Chevailler M-C, Quinn FA, Bischof P, Stricker R. Establishment of detailed reference values for luteinizing hormone, follicle

stimulating hormone, estradiol, and progesterone during different phases of the menstrual cycle on the Abbott ARCHITECT® analyzer. *Clin Chem Lab Med.* 2006;44(7). doi:10.1515/CCLM.2006.160.

95. Gargett CE, Schwab KE, Deane JA. Endometrial stem/progenitor cells: the first 10 years. *Hum Reprod Update.* November 2015:dmv051. doi:10.1093/humupd/dmv051.
96. Fayazi M, Salehnia M, Ziaei S. In-vitro construction of endometrial-like epithelium using CD146 + mesenchymal cells derived from human endometrium. *Reprod Biomed Online.* 2017;35(3):241-252. doi:10.1016/j.rbmo.2017.05.020.
97. Garry R, Hart R, Karthigasu K, Burke C. Structural changes in endometrial basal glands during menstruation. *BJOG An Int J Obstet Gynaecol.* 2010;117(10):1175-1185. doi:10.1111/j.1471-0528.2010.02630.x.
98. Boretto M, Cox B, Noben M, et al. Development of organoids from mouse and human endometrium showing endometrial epithelium physiology and long-term expandability. *Development.* 2017;144(10):1775-1786. doi:10.1242/dev.148478.
99. Turco MY, Gardner L, Hughes J, et al. Long-term, hormone-responsive organoid cultures of human endometrium in a chemically defined medium. *Nat Cell Biol.* 2017;19(5):568-577. doi:10.1038/ncb3516.
100. Garry R, Hart R, Karthigasu KA, Burke C. A re-appraisal of the morphological changes within the endometrium during menstruation: a hysteroscopic, histological and scanning electron microscopic study. *Hum Reprod.* 2009;24(6):1393-1401. doi:10.1093/humrep/dep036.